Ministry for Primary Industries
Manatū Ahu Matua

Characterisation and length-based population model for scampi (*Metanephrops challengeri*) on the Mernoo Bank (SCI 3)

New Zealand Fisheries Assessment Report 2013/24.

I. Tuck

ISSN 1179-5352 (online)
ISBN 978-0-478-41406-6 (online)

April 2013

New Zealand Government

Growing and Protecting New Zealand

Requests for further copies should be directed to:

Publications Logistics Officer
Ministry for Primary Industries
PO Box 2526
WELLINGTON 6140

Email: brand@mpi.govt.nz
Telephone: 0800 00 83 33
Facsimile: 04-894 0300

This publication is also available on the Ministry for Primary Industries websites at:
http://www.mpi.govt.nz/news-resources/publications.aspx
http://fs.fish.govt.nz go to Document library/Research reports

.

CONTENTS

EXECUTIVE SUMMARY

Tuck, I.D. (2013). Characterisation and length-based population model for scampi (*Metanephrops challengeri*) on the Mernoo Bank (SCI 3).

***New Zealand Fisheries Assessment Report 2013/24.* 161 p.**

The ongoing development of a Bayesian, length based population model for scampi has been continued through MFish project DEE201002SCIA. This work has applied the approach developed for scampi in the Bay of Plenty (SCI 1) and Wairarapa / Hawke Bay (SCI 2) to data for the Mernoo Bank (SCI 3) fishery.

A stock characterisation was undertaken, identifying marked spatial and temporal patterns in scampi targeted fishing activity in SCI 3, associated with changes to the management of the stocks in October 2004. Seasonal changes in scampi sex ratio and catchability (related to reproductive behaviour and moulting) were identified. On the basis of the seasonal and spatial patterns observed, and other information on scampi biology, a three stock, three timestep model structure was proposed. Core vessels were selected, and standardised CPUE indices were estimated for each subarea and timestep, modelling catch on an individual tow basis in relation to a range of explanatory variables.

Assessment models were fitted to abundance indices (standardised CPUE, trawl surveys and photographic surveys) and length frequency data (commercial catches, research trawl catches, size distributions from burrow counts). The models investigated a base case, and also sensitivity to assumptions on natural mortality and growth. The models provided similar stock trajectories, indicating a decline in biomass from a peak in the late 1990s, but varied in their estimated of SSB_0. MCMC simulations were conducted, but did not suggest the models had converged, and none of the models were accepted. Worst case options were examined, suggesting that on the basis of the models examined, SSB_{2011} was over 40% SSB_0 for each of the subareas.

1. INTRODUCTION

This report undertakes a fishery characterisation for the Mernoo Bank (SCI 3) scampi stock, and applies the previously described Bayesian, length-based, two-sex population model for Bay of Plenty (SCI 1) and Wairarapa / Hawke Bay (SCI 2) scampi (Cryer et al. 2005, Tuck & Dunn 2006, 2009, 2012) to the Mernoo Bank (SCI 3) fishery for the first time. Previous characterisations of scampi stocks are described by Tuck (2009). The first attempt at developing a length-based population model for any scampi stock was conducted for SCI 1 (Cryer et al. 2005), implemented using the general-purpose stock assessment program CASAL v2.06 (September 2004). This model for SCI 1 was developed further and the same model structure was also applied to SCI 2 in a later project (Tuck & Dunn 2006). The current study used CASAL v 2.22 (Bull et al. 2008) with a slightly modified selectivity option. Developments in the model implementation and structure have been largely based on suggestions raised at Shellfish Fisheries Assessment Working Group (SFAWG) meetings in 2007 and 2008 and the progress presented after the MFish funded Scampi Assessment Workshop (Tuck & Dunn 2009). Assessments for SCI 1 and SCI 2 using this model were accepted in 2011 (Tuck & Dunn 2012).

We describe the available data and how they were used, the parameterisation of the model, and model fits and sensitivity. This report fulfils Ministry of Fisheries project DEE201002SCIA "*Stock*

assessment of scampi", undertaking a first assessment of SCI 3. The objective of this project was to conduct a stock assessment, including estimating yield, for SCI 1 in 2011-12.

1.1. The Mernoo Bank (SCI 3) scampi fishery

Scampi is fished all around New Zealand, in nine fishery management areas (Figure 1).The SCI 3 fishery to the western end of the Chatham Rise is one of New Zealand's four main scampi fisheries (the others being SCI 1, SCI 2 and SCI 6A), and over the last five years (2006–07 to 2010–11) has contributed an average of 252 tonnes annually, the largest contribution of any management area. Over this period, the SCI 3 landings have made up 36% of the total average annual scampi landings of 706 tonnes. The TAC for SCI 3 is 340 tonnes, and the total TAC for all management areas is 1291 tonnes.

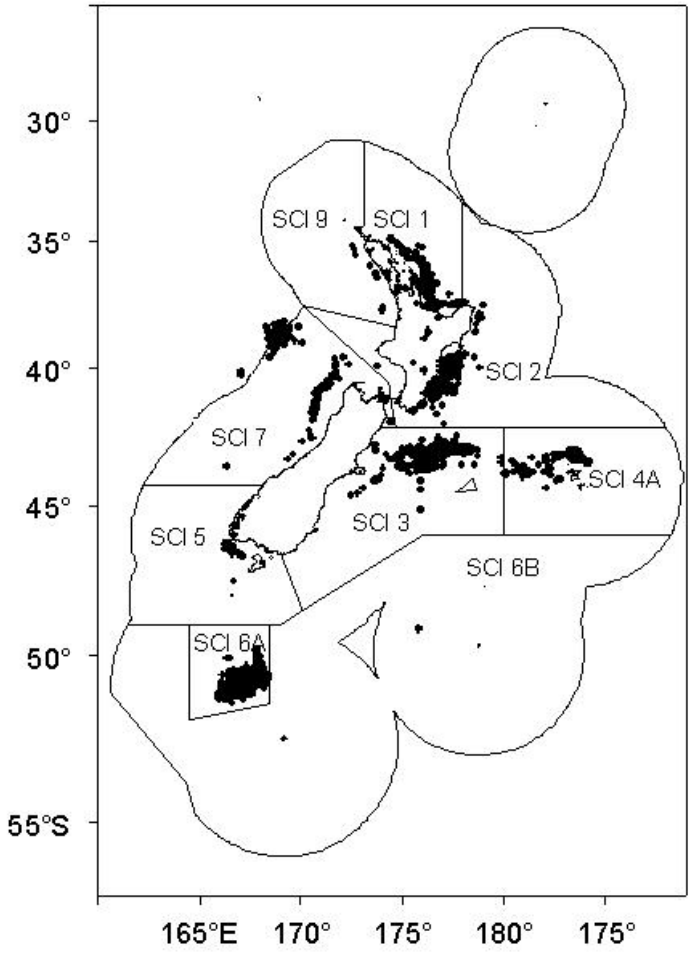

Figure 1: Spatial distribution of the scampi fishery since 1988–89. Each dot shows the mid-point of one or more tows recorded on TCEPR with scampi as the target species.

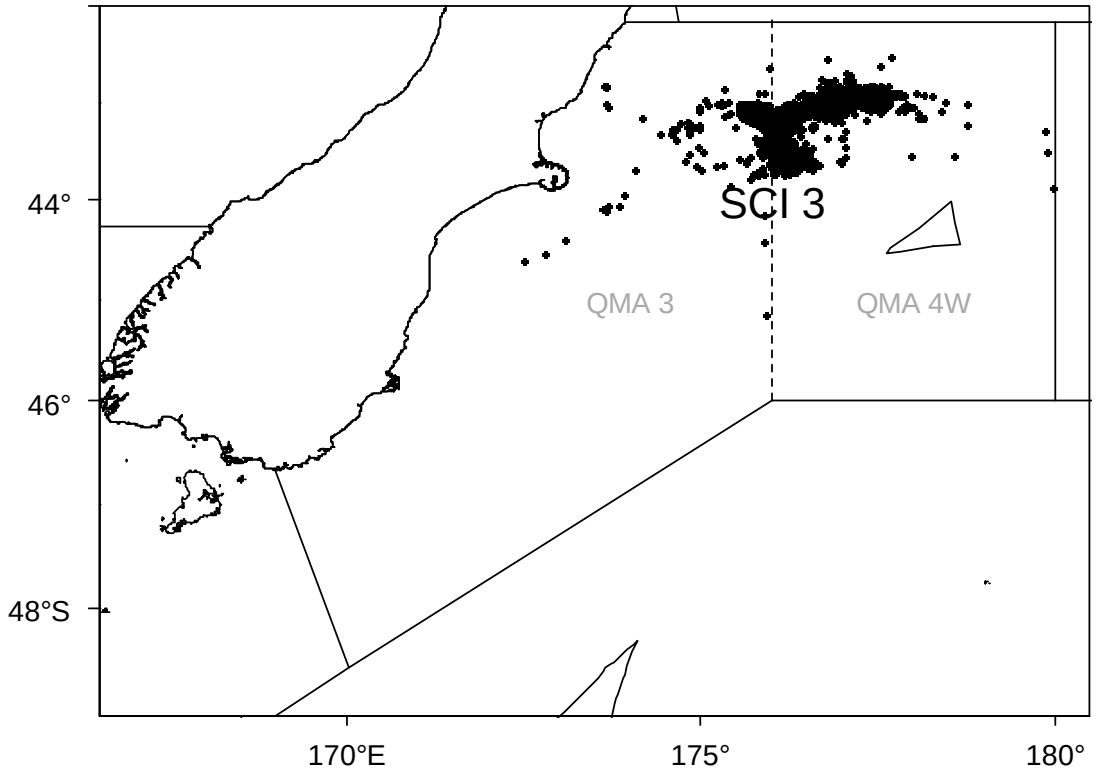

Figure 2: Spatial distribution of the scampi fishery within management area SCI 3 since 1988–89. Each dot shows the mid-point of one or more tows recorded on TCEPR with scampi as the target species. Previous (prior to the 2004–05 fishing year) scampi management areas QMA 3 and QMA 4W are also shown. The boundary between QMA 3 and QMA 4W was 176°E.

The spatial distribution of the targeted scampi fishing within SCI 3 is focussed in an area on the western end of the Chatham Rise, and straddles the boundary between the old QMA 3 and QMA 4W management areas (Figure 2). Prior to introduction into the QMS, the management area boundaries for the Mernoo Bank / Chatham Rise (QMA 3 and QMA 4) fisheries were reviewed on the basis of information on average catch rates, trends in CPUE, average size, sex ratio, bathymetry, and by-catch amount and composition (Cryer 2000), resulting in changes being introduced on 1st October 2004. The fishery parameters examined were generally similar between QMA 3 and 4W but less similar for QMA 4E, and hence the former two areas were combined into SCI 3. This study also suggested that it may be appropriate to separate the Mernoo Bank / western Chatham Rise fishery from the rest of QMA 3 (Canterbury and Otago coastline), since the deep water between the two areas is a natural break between the populations, although this was not adopted by managers. Minimal scampi fishing takes place outside the main Mernoo Bank / western Chatham Rise area.

The changes to the management area boundaries mean that different parts of the SCI 3 area have different management histories. Until entry into the QMS (1 October 2004), the QMA 3 area was managed under a competitive catch limit. Individual quotas were introduced for QMA 4 in 1992–93 (allocated on the basis of the permit holders catch in 1991–92), and maintained until October 2001, when all scampi fisheries were managed with competitive catch limits. Since October 2004, all scampi fisheries have been managed with individual quotas.

Previous fishery characterisations have been undertaken for this area; by Cryer & Coburn ((2000) as separate areas (QMA 3 and QMA 4W), and by Tuck (2009), as SCI 3. The more recent study identified two separate areas within the SCI 3 fishery, one of which showed a distinct spatial shift over time (Tuck 2009).

2. FISHERY CHARACTERISATION AND DATA

2.1. Commercial catch and effort data

Scampi fishers have consistently reported catches on the Trawl Catch, Effort, and Processing Returns (TCEPR) form since its introduction in 1989–90, providing a valuable record of catch and effort on a tow by tow basis.

Data were extracted from the Ministry of Fisheries (now Ministry for Primary Industries) TCEPR database, requesting all tows where scampi (SCI) was the nominated target species. Previous analyses using TECPR data have produced a groomed data set, and it was not considered necessary to repeat this grooming. Therefore, only an extraction of the most recent fishing years was conducted (2009–10 to 2010–11, 8 673 tow records). Errors in TCEPR records are reducing in frequency, but do occur, and the raw records were sorted by vessel and start time and screened for obvious errors in the following manner. For each record, the reported data was used to estimate the catch rate of scampi (kg h^{-1}), the duration of the trawl shot, the distance between the start and finish locations, the average speed at which the trawl shot was conducted, the non-fishing time (down-time) between the start of the shot and the end of the previous shot, and the average steaming speed necessary to get to the start position of the shot from the end position of the previous shot. Adjacent records were also checked to identify and exclude duplicates, i.e., records with the same time and location, but with different reported catches. This can occur where "SCI" is mistakenly written on the form or punched to the database instead of another code such as "SKI" (gemfish). Range checks were applied to these diagnostics as follows (Table 1).

Table 1: Diagnostic criteria applied to reported commercial trawl shots for scampi

Diagnostic	Criterion
Catch rate	>100 kg h^{-1}
Trawling speed for a given shot	>5 kn
Steaming speed between shots	>10 kn
Trawl duration	>8 h
Down-time between shots	<0.5 h
Trawl distance	> 35 n.mile

These same range checks have been applied in previous years to generate the groomed data set. Records which violate any one of the diagnostic criteria were briefly examined for obvious errors. Our experience with this process in previous analyses suggests that, in most instances, the field causing the error will be quite evident, and the cause of the violation clear. Most errors identified in the past have been mis-reported, mis-punched, or missing positions (e.g., a latitude of 37 within a series of shots at latitude 39), incorrect dates (wrong months or years being most common), or times (a.m. as opposed to p.m. and vice versa). Some records have been found with incorrect vessel identifiers. Data editing was undertaken to correct such obvious errors and, where the correction removed the diagnostic violations, the record was flagged as "corrected". Where the cause of the violation is not easily reconcilable, or diagnostic violations remained after the correction of obvious errors, then the record was flagged as "irreconcilable". In many instances, records with diagnostic violations were considered not to be errors (e.g., some unusually long shots have been found in the past, especially in SCI 6A).

Having completed the grooming of the most recent years, these were combined with the previously groomed data to produce a total data set including 98 268 individual tow records over the fishing

years 1988–89 to 2010–11. Subsequent analyses were conducted on a cleaned version of the data set, limited to records with a valid haul duration (greater than zero), a scampi catch greater than zero and excluding any records with irreconcilable errors (identified from the grooming process). This cleaned data set represents roughly 95% of total scampi landings (94 716 records), and is considered to be the most appropriate to investigate patterns in the fishery, given that it represents the targeted scampi fishery and latitude and longitude data are available for spatial aspects of the analysis.

Total annual landings for the fishery and the percentage taken by the target scampi fishery are presented in Table 2. The main activity in the fishery has focussed on the Mernoo Bank and western Chatham Rise areas, rather than the Canterbury and Otago coastline, and the distribution of fishing activity within this main (Mernoo) area over time is presented in Figure 3 and Figure 4. Over 98% of the targeted scampi catch has been reported from this main area in all years (Table 2). On the basis of the patterns observed within the fishery in this main area, three sub-areas have been identified (Figure 5), each of which show different historical fishing patterns (Table 2). Boxplots of the unstandardized CPUE (Figure 6) show reasonably similar patterns over time between areas, with catch rates initially increasing to the late 1990s or early 2000s, declining to about 2008, and then showing an increase in the most recent years (where data is available).

The MN subarea consistently contributed over 50% of catches until 2003–04 (and over 70% in the early years of the fishery), with the MO area consistently contributing about 20%. Since 2004–05, there has been minimal fishing activity within the MO subarea, and while overall catches from SCI 3 have declined slightly, average catches from MW exceed those from MN. Although levels of effort and removals were low in MN prior to 2004–05, catch rates appear to have been reasonably similar to MO over this period (Figure 6). In characterising the fishery, and estimating standardised CPUE indices, these three areas are considered separately. Given the adjacent locations of the subareas, data for examination of maturity and seasonal patterns in sex ratio have been pooled for all three areas.

Monthly patterns of effort and catch are presented by subarea in Figure 7 to Figure 12. Subarea MN was previously managed within QMA 4W, and was only managed with competitive catch limits between 2001–02 and 2003–04. During this period, catches only took place in October, but prior to and since this time, fishing has been distributed throughout the year. Subarea MN was also previously managed within QMA 4W, and only had competitive catch limits between 2001–02 and 2003–04. Fishing was relatively sporadic prior to the competitive catch limit period, focussed in October during this period, and has been spread throughout the year since 2004–05 (with some indication of increased activity towards the end of the fishing year). Subarea MO was managed with competitive catch limits until 2004–05. Fishing was consistently focussed in October throughout this period, and there has been minimal activity in this subarea since 2004–05.

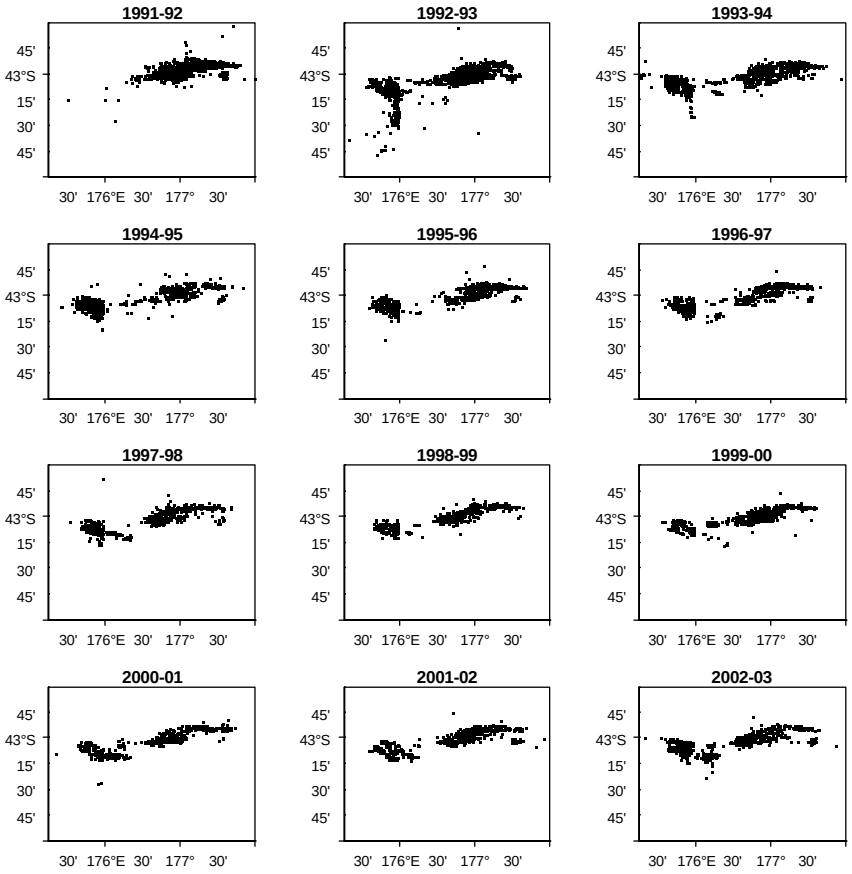

Figure 3: Spatial distribution of the main area of the SCI 3 scampi trawl fishery from 1991–92 to 2002–03. Each dot represents the mid-point of one or more tows reported on a TCEPR. General area covered by plots is indicated within Figure 4.

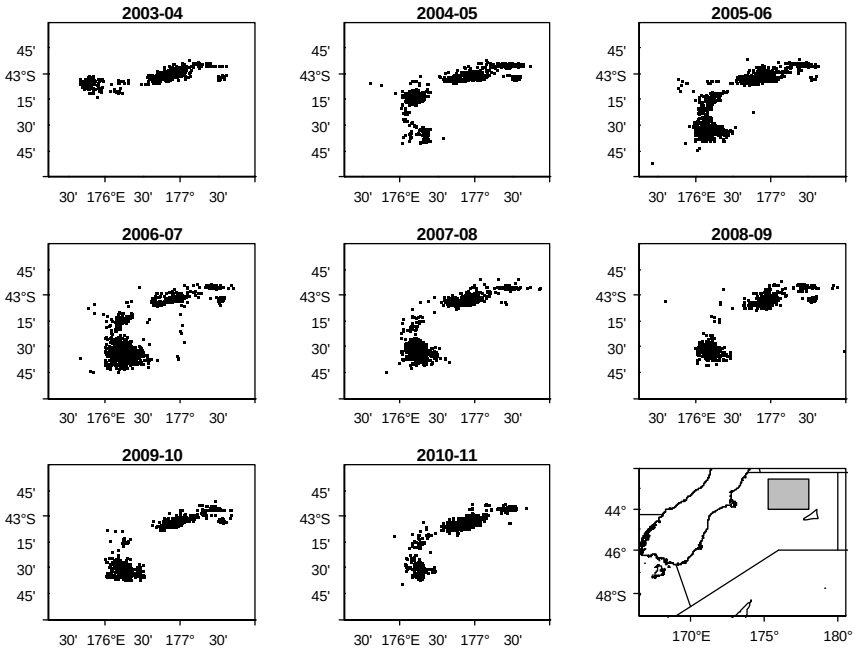

Figure 4: Spatial distribution of the main area of the SCI 3 scampi trawl fishery from 2003–04 to 2010–11. Each dot represents the mid-point of one or more tows reported on a TCEPR. General area covered by plots is indicated by shaded box in bottom right plot.

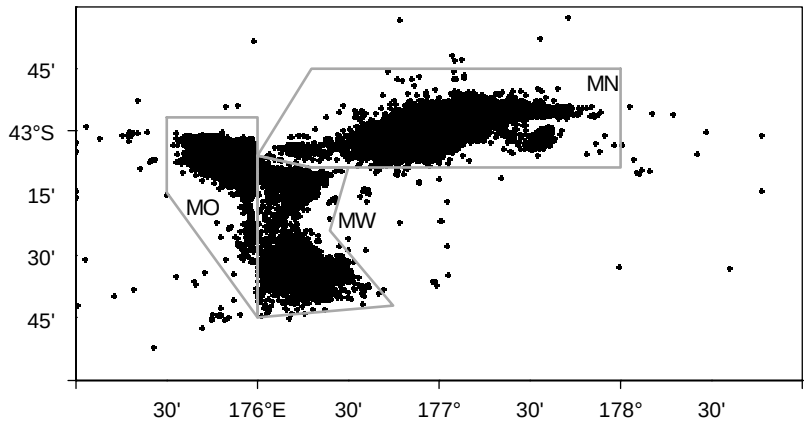

Figure 5: Sub-areas of SCI 3 used for fine scale analysis of catch and effort. Each dot represents the mid-point of one or more tows reported on a TCEPR.

Table 2: Reported commercial landings (tonnes) from the 1990–91 to 2010–11 fishing years for SCI 3 (based on management area in force since introduction to the QMS in October 2004), catch estimated from scampi target fishery, and breakdown by spatial areas identified in Figure 5.

		Target	%	Catch			% of total			
	Landings (MHR)	catch (TCEPR)	SCI target	MN	MO	MW	MN	MO	MW	% of target catch in main areas
1990–91	0	0								
1991–92	153	153	100%	151	0	0	99%	0%	0%	99%
1992–93	296	297	100%	210	80	2	71%	27%	1%	98%
1993–94	324	313	97%	251	59	2	77%	18%	1%	100%
1994–95	292	291	100%	224	65	1	77%	22%	0%	100%
1995–96	306	305	100%	226	76	2	74%	25%	1%	100%
1996–97	304	304	100%	217	72	15	72%	24%	5%	100%
1997–98	296	297	100%	211	60	25	71%	20%	9%	100%
1998–99	292	271	93%	209	58	4	72%	20%	1%	100%
1999–00	322	291	90%	215	67	5	67%	21%	2%	99%
2000–01	333	313	94%	200	71	42	60%	21%	13%	100%
2001–02	304	264	87%	181	63	20	60%	21%	6%	100%
2002–03	264	220	83%	128	59	32	49%	22%	12%	100%
2003–04	277	228	82%	174	50	3	63%	18%	1%	100%
2004–05	335	311	93%	184	0	127	55%	0%	38%	100%
2005–06	319	291	91%	106	2	182	33%	1%	57%	100%
2006–07	307	278	90%	51	0	224	17%	0%	73%	99%
2007–08	209	176	84%	75	0	101	36%	0%	48%	100%
2008–09	190	170	90%	70	0	100	37%	0%	53%	100%
2009–10	302	278	92%	82	0	196	27%	0%	65%	100%
2010–11	256	236	92%	181	0	55	71%	0%	22%	100%

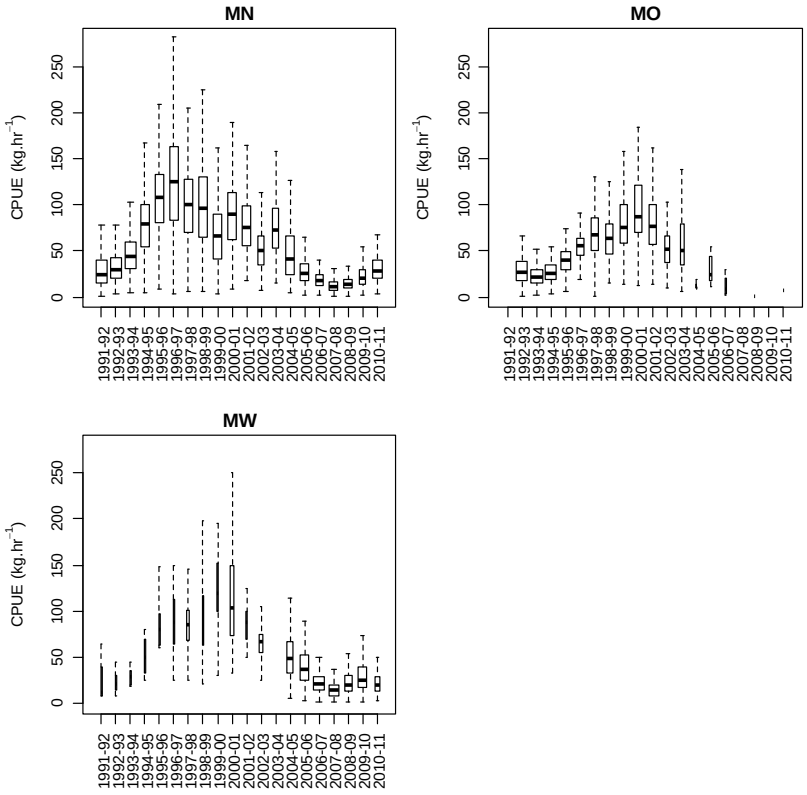

Figure 6: Boxplots (with outliers removed) of individual observations from TCEPR of unstandardized catch rate (catch (kg) divided by tow effort (hours)) with tows of zero scampi catch excluded, by fishing year for the SCI 3 subarea. Box width is proportional to square root of number of observations.

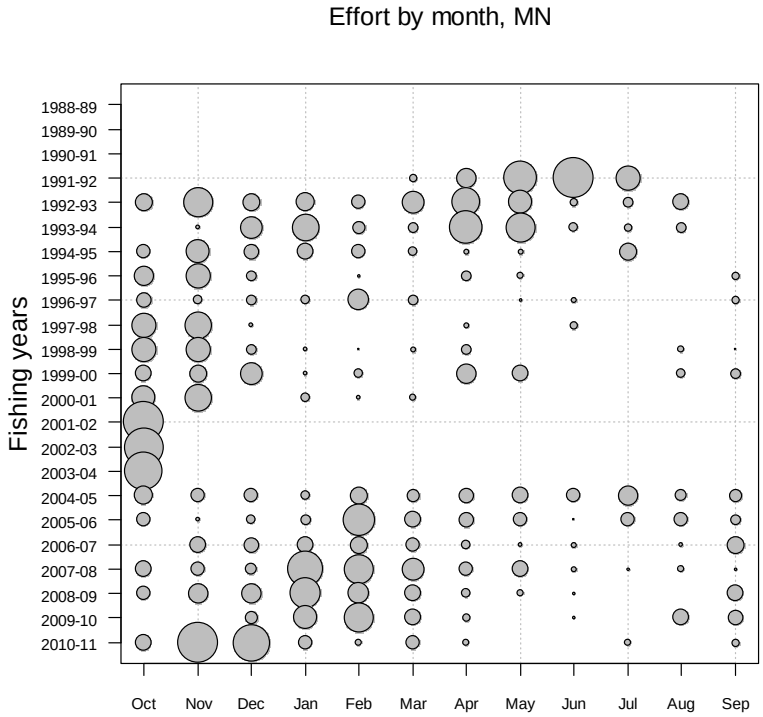

Figure 7: Monthly pattern of fishing effort in the scampi targeted fishery by fishing year for the MN subarea of SCI 3. The area of the circles is proportional to the hours fishing; the largest circle represents 2438 hours.

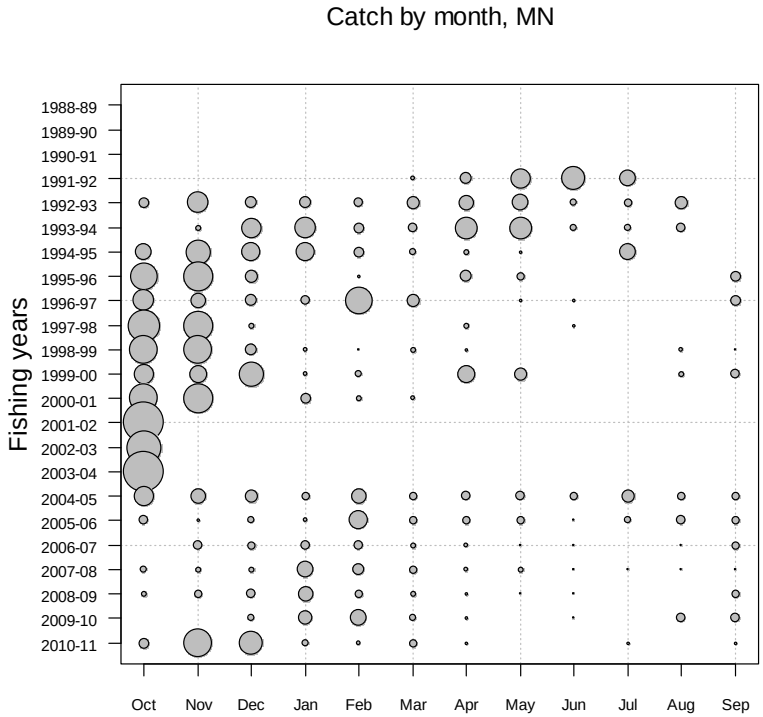

Figure 8: Monthly pattern of scampi catches in the scampi targeted fishery by fishing year for the MN subarea of SCI 3. The area of the circles is proportional to the catch weight; the largest circle represents 181 tonnes.

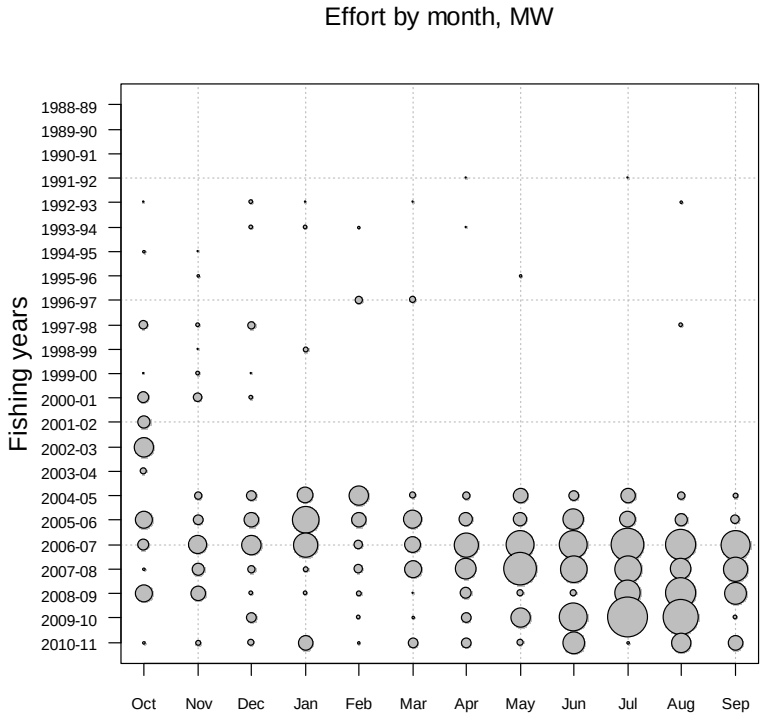

Figure 9: Monthly pattern of fishing effort in the scampi targeted fishery by fishing year for the MW subarea of SCI 3. The area of the circles is proportional to the hours fishing; the largest circle represents 2418 hours.

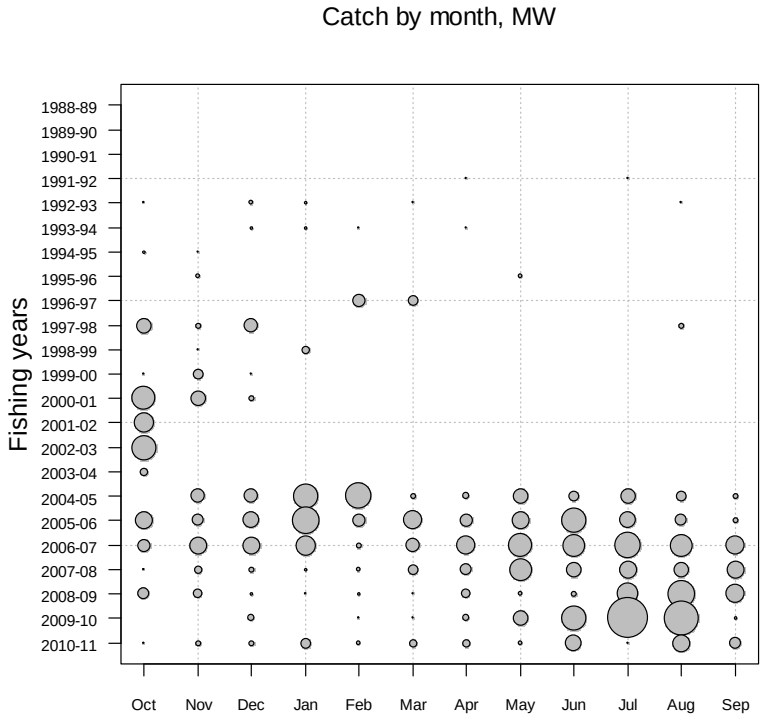

Figure 10: Monthly pattern of scampi catches in the scampi targeted fishery by fishing year for the MW subarea of SCI 3. The area of the circles is proportional to the catch weight; the largest circle represents 84.6 tonnes.

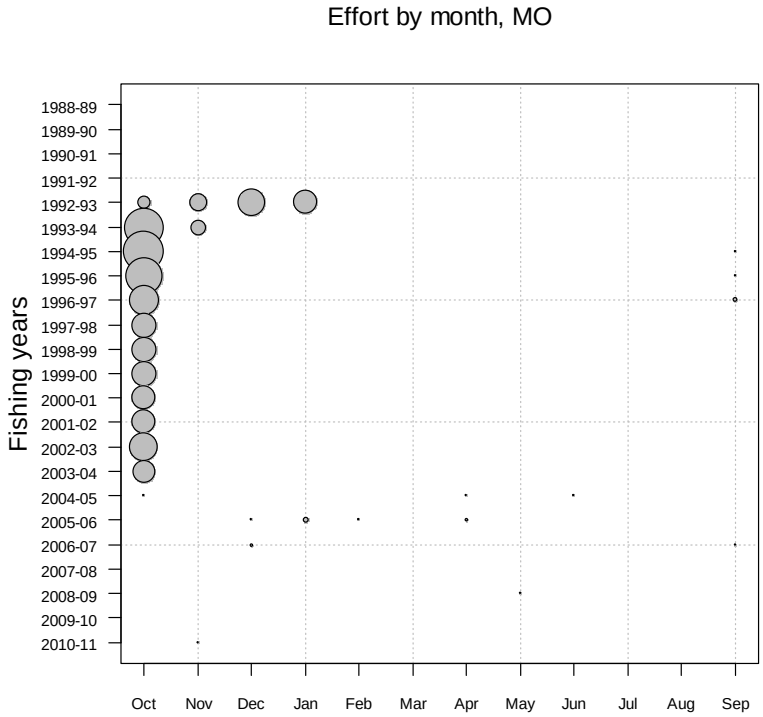

Figure 11: Monthly pattern of fishing effort in the scampi targeted fishery by fishing year for the MO subarea of SCI 3. The area of the circles is proportional to the hours fishing; the largest circle represents 2413 hours.

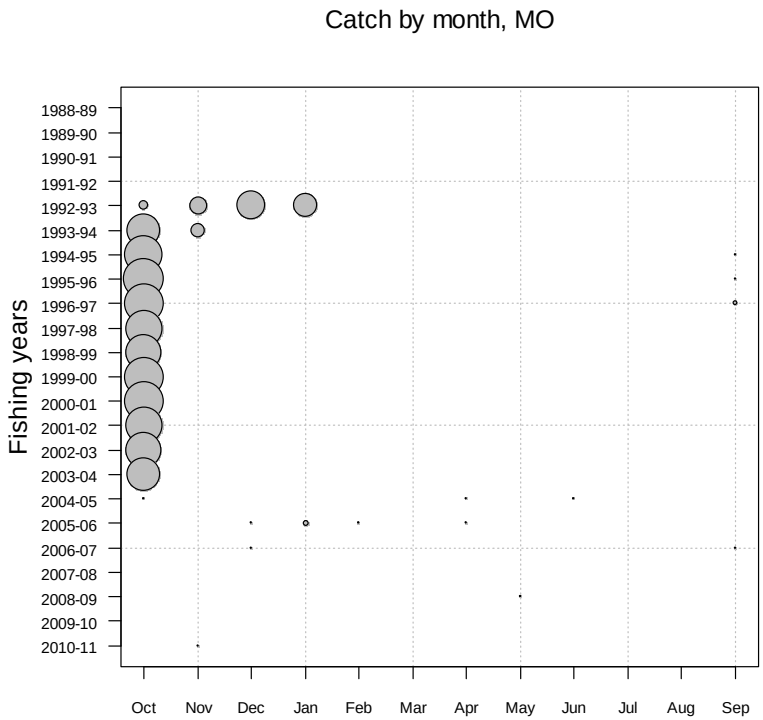

Figure 12: Monthly pattern of scampi catches in the scampi targeted fishery by fishing year for the MO subarea of SCI 3. The area of the circles is proportional to the catch weight; the largest circle represents 75.9 tonnes.

2.2. Seasonal patterns in scampi biology

Previous development of the length based model for scampi has shown that determination of appropriate time steps for the model is important in fitting it to length and sex ratio data in particular (Tuck & Dunn 2006, 2009, 2012). Scampi inhabit burrows, and are not available to trawling when within a burrow. Catchability varies between the sexes on a seasonal basis in relation to moulting and reproductive behaviour, and leads to seasonal changes in sex ratio in catches.

2.2.1. Sex ratio

Current knowledge of the timing of scampi biological processes in SCI 3 is summarised in Table 3 (Tuck 2010). The combination of differing biological processes for males and females lead to different relative availabilities of the two sexes through the year, resulting in the pattern of sex ratios (displayed as proportion males) shown in Figure 13. Females predominate in the catch from January to July, with males more prevalent between August and December.

The timing of the reproductive cycle can be inferred from observations of ovigerous females and the moult cycle. Ovary development occurs through the winter, and mating occurs in October and November, just after the female moult, while the carapace is still soft. Eggs are them spawned onto the pleopods, and carried until the following August or September, when they hatch, and the female moults. The proportion of mature females carrying eggs (ovigerous) reaches a minimum in September (Figure 14), suggesting that most spawning has occurred by this time, so females would be ready to moult and mate. Observer sampling also records the incidence of soft post-moult scampi. Female moulting peaks around October (Figure 15), but continues into December.

Table 3: Summary of scampi biological processes for SCI 3. Source; Tuck (2010) and more recent survey data.

	Jan	Feb	Mar	Apr	May	Jun	Jul	Aug	Sep	Oct	Nov	Dec
Male moult		X	?	X								
Female moult										X	X	
Mating										X	X	
Eggs spawn											X	X
Eggs hatch								X	X			

2.2.2. Time steps in assessment model

On the basis of our understanding of the timing of biological processes for scampi in this area, and the seasonal pattern in sex ratio, three time steps are proposed for the assessment model, as defined in Table 4. Catch data, stock abundance indices and length frequency distributions have been collated and estimated in relation to these time steps, for inclusion in the assessment model.

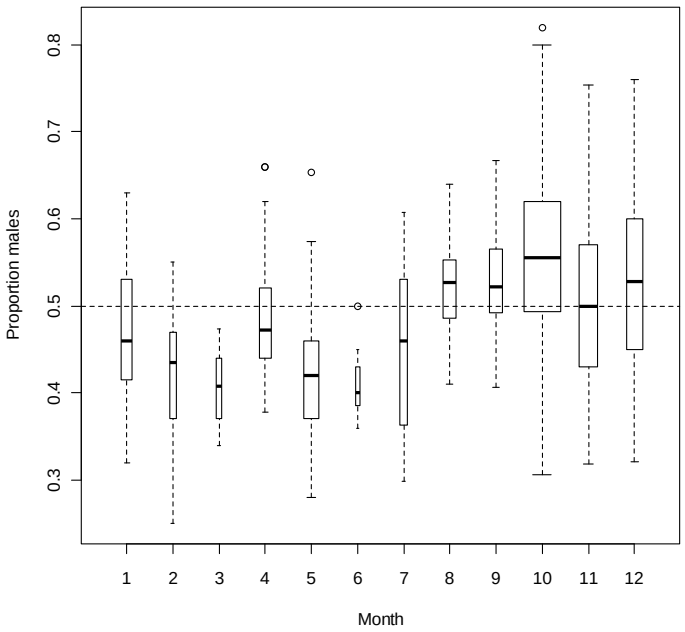

Figure 13: Boxplots of proportion of males in catches by month from observer sampling in SCI 3. Box widths are proportional to square root of number of observations.

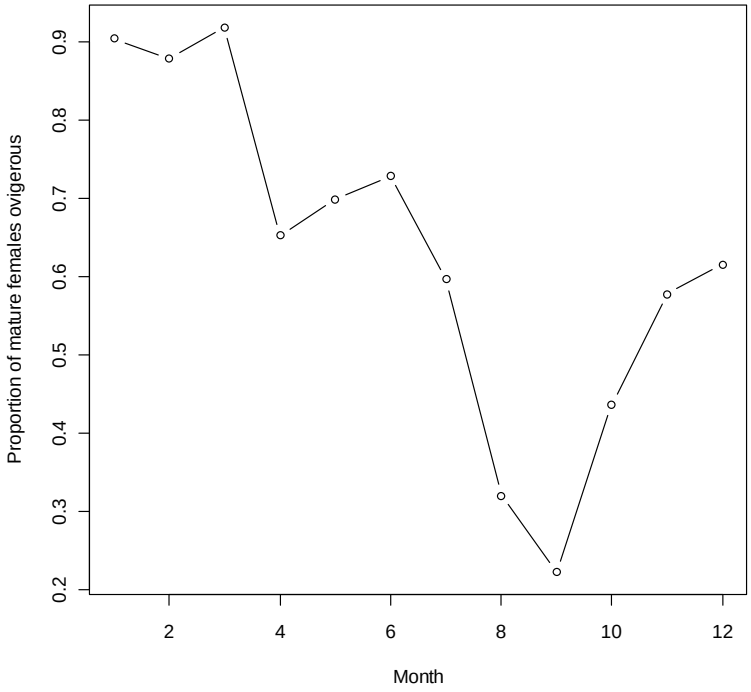

Figure 14: Proportion of mature (greater than 43mm, from section 3.2.2) females carrying eggs by month from observer sampling in the SCI 3.

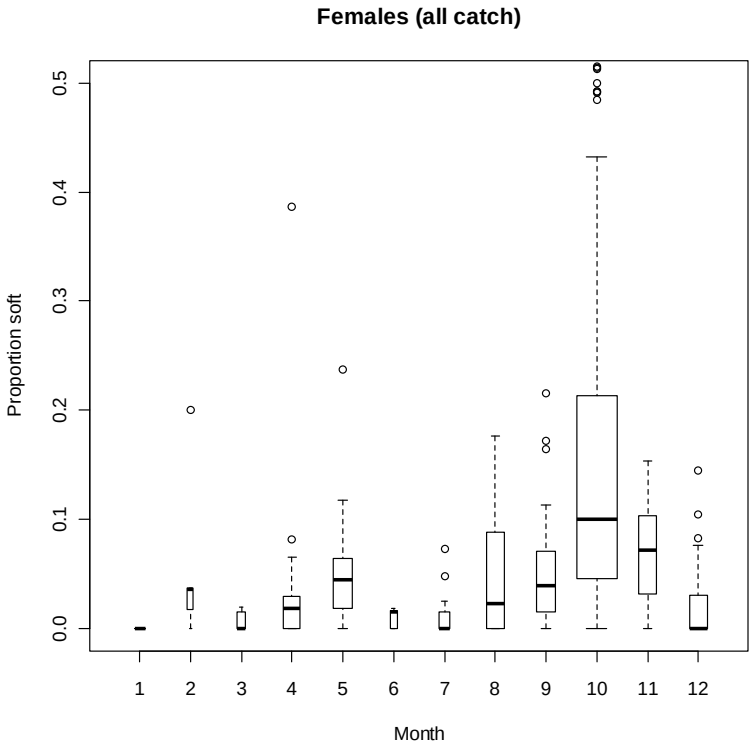

Figure 15: Proportion of females with soft carapace by month, from observer sampling in SCI 3. Box widths proportional to square root of number of observations.

Table 4: Annual cycle of the population model for SCI 3, showing the processes taking place at each time step and their sequence within each time step. Fishing and natural mortality that occur together within a time step occur after all other processes, with 50% of the natural mortality for that time step occurring before and 50% after the fishing mortality. Natural mortality is apportioned to time steps in relation to their duration (as a fraction of the year). Fishing mortality is apportioned to time steps according to reported landings.

Step	Period	Process
1	October – December	Growth (both sexes)
		Natural mortality
		Fishing mortality
2	January – July	Recruitment
		Maturation
		Natural mortality
		Fishing mortality
3	August - September	Natural mortality
		Fishing mortality

2.3. Standardised CPUE indices

2.3.1. Core vessels

A plot of vessel activity over time is presented in Figure 16. Within this plot, vessels are coded by the combination of a single letter, 2 or 3 (for twin or triple rig) and 1 or 2 (to indicate where engine power has changed), so that changes in gear configuration or engine power result in a new unique code. There are a number of vessels with long histories in the fishery, but of these, vessels I, K and Q have changes of gear configuration or engine power in recent years.

Figure 17 (upper plot) shows the proportion of the total catch landed in relation to the number of years vessels have been active in the fishery (ignoring gear and engine changes), and on the basis of this, a cut off of 10 years of activity has been selected to identify core vessels (vessels – E, F, G, H, I, J, K, M, P, and Q). The lower plot of Figure 17 shows the proportion of catch accounted for by vessels active for over 5 or 10 years. Other than in 2002–03 and 2003–04, the core vessels (active for over 10 years) have accounted for over 60% of targeted scampi catches, and often over 80%. Considering gear and engine changes as new vessels (Figure 18) provides a similar pattern (upper plot), and again, 10 years of activity has been selected to identify core vessels (vessels – E_2_1, F_2_2, G_3_1, H_2_1, I_2_1, J_2_1, K_2_1, M_3_1, P_2_1, Q_2_1). The lower plot of Figure 18 shows a similar pattern to Figure 17 until 2006–07, after which the proportion of annual catches accounted for by core vessels declines, to about 40% in the most recent years. Examining the subareas separately generated a similar list of core vessels (Appendix 1).

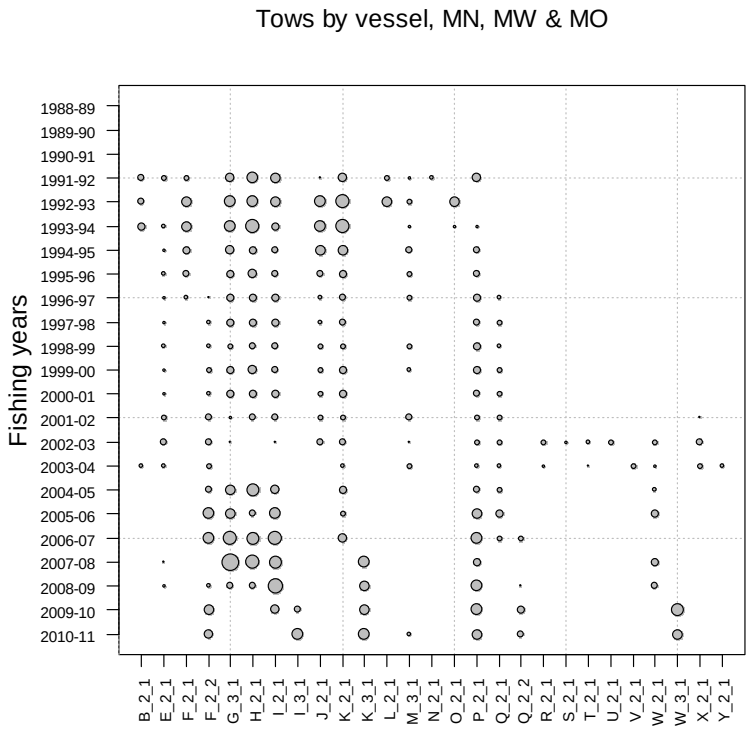

Figure 16: Pattern of fishing activity by vessel and fishing year for the main area (subareas MN, MW and MO) of SCI 3. Vessels labelled using the combination Vessel_gear configuration_engine. The area of the circles is proportional to the number of tows recorded; the largest circle represents 539 tows.

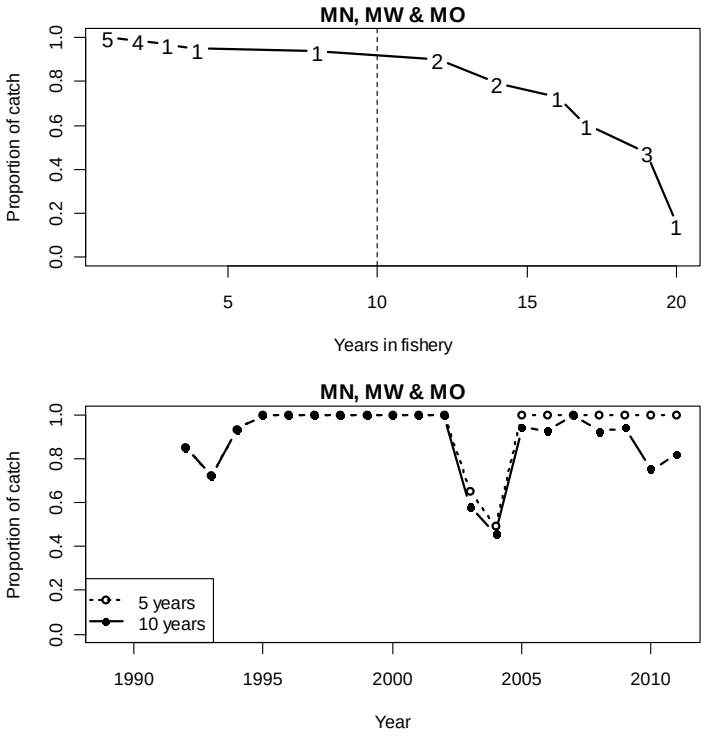

Figure 17: Catch breakdown by vessel.
Upper plot - Proportion of total scampi catch (all years) plotted against the number of years the vessels reporting that catch have been active in the fishery. Numbers indicate number of vessels active for that duration. Vertical dotted line represents cut off for core vessels.
Lower plot – Proportion of annual catch reported by vessels active in the fishery for 5 and 10 years.

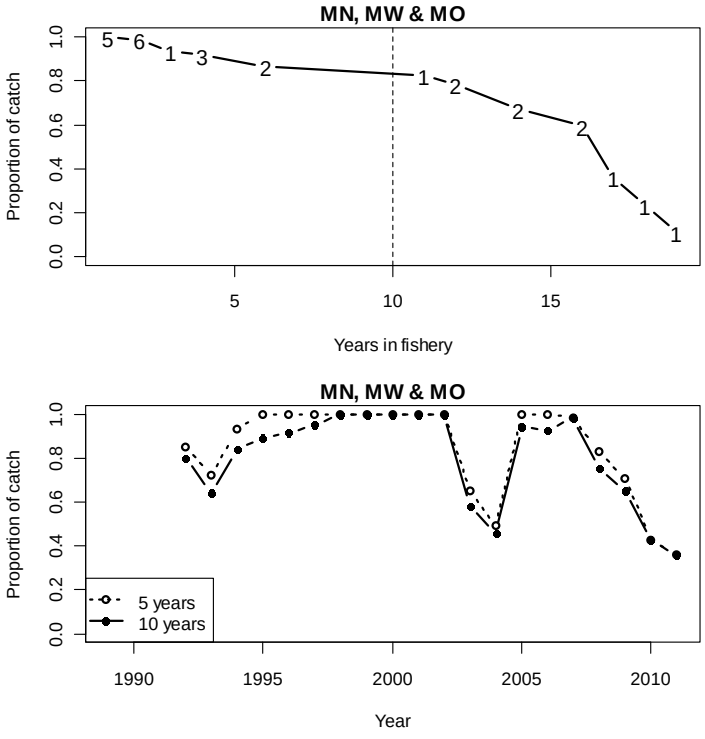

Figure 18: Catch breakdown by vessel_gear_engine.
Upper plot - Proportion of total scampi catch (all years) plotted against the number of years the vessels reporting that catch have been active in the fishery. Numbers indicate number of vessels active for that duration. Vertical dotted line represents cut off for core vessels.
Lower plot – Proportion of annual catch reported by vessels active in the fishery for 5 and 10 years.

2.3.2. Calculation of indices

Standardised indices of CPUE were estimated for each time step in each subarea. The scampi catch of core vessels within each subarea were modelled on an individual tow basis as log (scampi catch (kg)) with explanatory variables including fishing year_timestep, vessel, time of day, state of moon, depth, and fishing duration.

The time of day of each tow was calculated in relation to nautical dawn and dusk (the time when the sun is 12 degrees below the horizon in the morning and evening), as calculated by the *crepescule* function of the *maptools* package in R. Individual tows were characterised on the basis of whether they included dawn (shot before dawn, hauled after dawn and before dusk), day (shot after dawn, hauled before dusk), dusk (shot before dusk, hauled after dusk and before dawn) or night (shot after dusk and hauled before dawn). Longer tows including more than one period (i.e. shot before dusk and hauled after dawn were excluded from this part of the analysis (excluding six records from a total of over 23 000 for SCI 3).

Individual hauls were also categorised in terms of moon state, on the assumption that tidal current strength at the sea floor will be related to the lunar cycle. Tows were categorised by their date in relation to the lunar cycle, as Full moon (more than 26 days since full moon, or less than 3 days since full moon), Waning (4 – 11 days since full moon), New moon (12 – 18 days since full moon), and Waxing (19 – 26 days since full moon).

Core vessels were selected by examining the scampi fleet's activity over the history of the fishery in each subarea, and selecting vessels that had consistently contributed over a number of years, and together, had contributed a significant proportion of the overall catches over the whole fishery, and in each year.

A number of the vessels involved in the scampi fisheries have changed gear configuration (twin rig to triple rig) in recent years, and two have changed engine power over the history of the fishery. Two different approaches were considered in estimating the standardised indices,

1. Treating changes in gear configuration or engine power as a new vessel
2. Fitting engine power within the model (either as a continuous variable, or as a binned factor), and fitting gear configuration as a two level factor (with or without a vessel interaction).

In addition, preliminary examination of the data identified a distinct shift in trawl duration between 2002–03 and 2006–07 (Figure 19). This shift was fleet-wide, and associated with a modification to the top of the trawl to reduce the bycatch (John Finlayson, Sanford Ltd. *pers comm*.), enabling vessels to fish for longer on each tow. Boxplots of tow duration over time have been examined for each vessel to estimate when this change occurred.

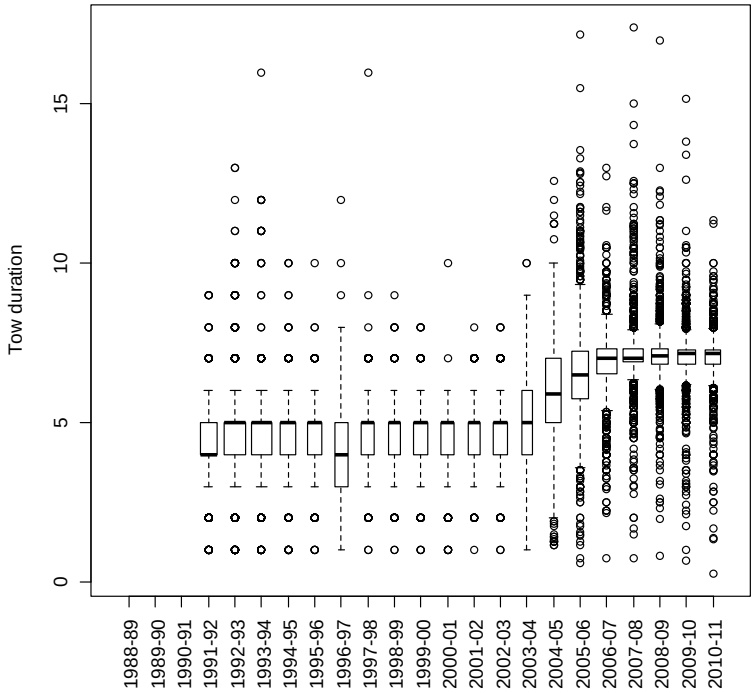

Figure 19: Boxplots of tow duration (hours) for scampi targeted fishery in main area of SCI 3. Box widths proportional to square root of number of observations.

Catch indices were derived using generalised linear modelling (GLM) procedures (Vignaux 1994, Francis 1999). Indices were calculated for the three subareas within a single model, with fishing-year_timestep_subarea as a forced term in the model. Catch is assumed to reflect scampi abundance, and there is no reason to suggest that the effects of vessel, depth, time of day, tide or effort would vary between subarea, and so this approach (modelling the indices for the three areas together) will provide more information on these effects. It is possible that the gear modification associated with the shift in tow duration (designed to reduce bycatch) may have changed the relationship between catch, abundance and effort, and so models were examined with and without an effort : binary modification factor interaction. The GLM's were conducted using the statistical software package R. The response variable in the GLM was log catch. Fishing-year was entered as a categorical covariate (explanatory) term on the right-hand side of the model. Standardised CPUE abundance indices (canonical) were derived from the exponential of the fishing-year_timestep_subarea covariate terms as described in Francis (1999).

In order to accommodate a non-linear relationship with the response variable (log catch), the continuous variables (effort and depth) were offered to the GLMs as third order polynomials. Vessel, time of day, state of tide, twin or triple rig, bycatch modification and vessel power were offered to the GLMs as factors. A forward fitting, stepwise, multiple-regression algorithm was used to fit GLMs to groomed catch, effort and characterisation data. The stepwise algorithm generates a final regression model iteratively and uses a simple model with a single predictor variable, fishing year, as the initial or base model. The reduction in residual deviance relative to the null deviance is calculated for each additional term added to the base model. The term that results in the greatest reduction in residual deviance is added to the base model if this results in an improvement in residual deviance of more than 1%. The algorithm repeats this process, updating the model, until no new terms can be added. Diagnostic plots for the final models are presented in Appendix 2 (Bentley et al. 2012).

Approach 1 (twin/triple rig or engine changes considered as new vessel).

Stepwise regression analysis of the dataset where changes from twin rig to triple rig, or changes in engine power were classed as a new vessel, selected a model explaining 62% of the variation in the data, using the terms yr_step_area (forced), time of day, effort and vessel (Table 5). Effort was the most influential variable, at 12%, with the other variables having influences of about 5%. The canonical indices for each subarea and time step estimated from this model are presented in Figure 20.

Approach 2 (twin/triple rig fitted as factor).

Stepwise regression analysis of the datasets fitting twin/triple rig and engine power factors (with or without a vessel gear interaction) resulted in the same final model, with vessel power, twin/triple rig, and effort:bycatch modification interaction not retained. The selected model explained 60% of the variation in the data, using the terms yr_step_area (forced), time of day, effort and vessel (Table 6). Effort was the most influential variable, at 13%, with the other variables having influences of about 6%. The canonical indices for each subarea and time step estimated from this model are presented in Figure 21. The respective indices from the model of the Approach 1 dataset are also plotted in these figures (in red). The Approach 1 dataset includes less data, and some yr_step_area combinations are not estimated, but the overall patterns in the indices from the two models are very similar.

The Shellfish Fisheries Assessment Working Group agreed that the use of Approach 2 was appropriate to calculate CPUE indices (using gear as a factor), but also recommended further investigation into the effect of removing subarea timestep combinations with low numbers of tows from the calculation of the index, and also the potential change in catchability in about 2005, in relation to the observed change in tow duration, related to gear modifications to reduce bycatch.

As described above, the patterns of fishing activity have changed considerably over the history of the fishery. Therefore, the amount of data (number of commercial tows) contributing to the indices varies considerably between areas and time steps over time. While each index value (for an area, year and time step) has a c.v. estimated, index values from low numbers of tows are unlikely to be representative of the overall subarea and time step, and it may be appropriate to exclude some points from the indices. The number of tows contributing to the core vessel dataset varied considerably between subarea and timestep (Figure 22), and an arbitrary cut off value of five per subarea and time step was examined. This approach potentially introduces a bias, in that low numbers of tows are more likely in areas or times of low catch rate. Subarea MN (Figure 22) has consistently been relatively well sampled by the core vessels, and no data were removed by the cut off limit. The shift in effort from subarea MO to subarea MW means that the number of tows by the core vessels was relatively low in MW in the early part of the time series, and more recently in MO, resulting in data points being removed from the indices in both areas by the cut off limits.

The distribution of standardised residuals (from Approach 2) over the period when the bycatch modification occurred are presented in Figure 23 and Figure 24. Standardised residuals within the year the vessels changed configuration were slightly higher without the modification to reduce bycatch (Figure 23), but the pattern was not consistent across subareas and time steps (Figure 24). When a term for the bycatch modification is forced in the standardisation model (without interaction), predicted catches are about 20% lower with the modification (Figure 25).

The Shellfish Fisheries Assessment Working Group proposed that the CPUE indices used within the assessment model should be estimated from the dataset excluding subarea timestep combinations with low effort, and with the standardisation forcing the inclusion of the bycatch modification term. This selected model explained 60% of the variation in the data, using the terms yr_step_area (forced), time of day, effort, vessel and bycatch modification (forced) (Table 7). Model diagnostic plots are presented in Appendix 2. Effort was the most influential variable, at 12.5%, with the bycatch modification having an influence of 9%, and the other variables having influences of about 5%. The

relative effects of the explanatory variables (excluding subarea_timestep) are shown in Figure 26. Expected catch rates are highest during the day, and lowest at night, being about two thirds of the daytime rate. Expected catch does not increase for tow durations greater than about 8 hours. The average effect of the gear modification is to reduce catch by about 20%. It was interesting to note that catch rate was not significantly affected by shifting from twin to triple rig trawls (term not retained within model). Swept width is generally not increased, but by using three small trawls rather than two larger ones, drag (and fuel consumption) is reduced, while fishing the same seabed area.

Revised indices from the final model are compared with the Approach 2 indices in Figure 27. Comparisons of the standardised indices from this model and the unstandardized CPUE data are provided in Figure 28. Within these plots the canonical indices values are scaled to the median CPUE (of the core fleet), to allow for comparison on the same axes.

Table 5: Analysis of deviance table and overall influence for standardisation model selected by stepwise regression for Approach 1.

	Df	Deviance explained	Additional deviance explained (%)	Overall influence (%)*
NULL				
yr_step_area	103	5840.7	54.24	
TOD	3	341.8	3.17	5.55
poly(effort, 3)	3	262.3	2.43	11.78
unique_vessel_code	9	206.3	1.91	5.05

*- Overall influence as in Table 1 of Bentley et al. (2012)

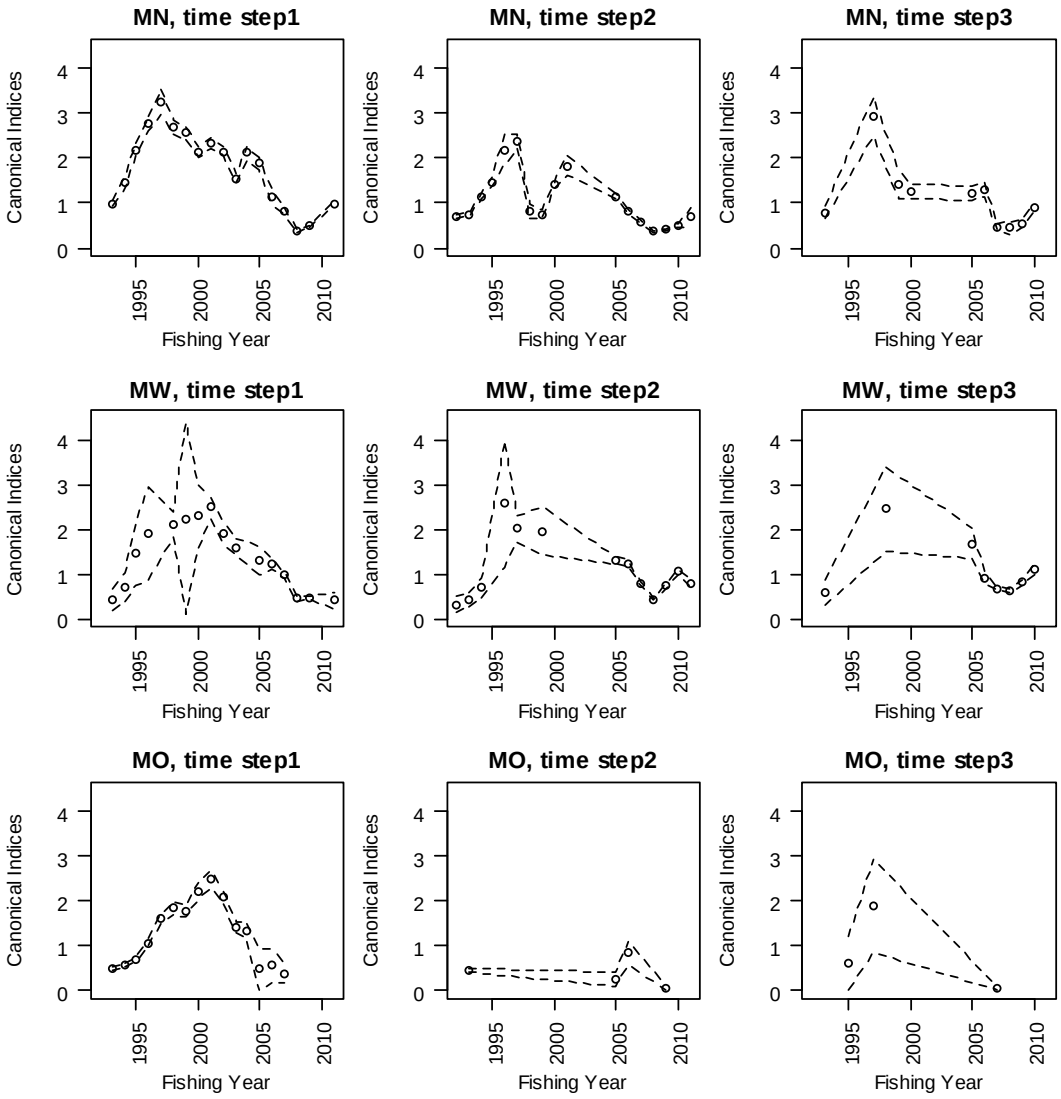

Figure 20: Canonical indices for each subarea and time step, from model fitted to Approach 1 dataset.

Table 6: Analysis of deviance table and overall influence for standardisation model selected by stepwise regression for Approach 2.

	Df	Deviance explained	Additional deviance explained (%)	Overall influence (%)*
NULL				
yr_step_area	111	6160.6	51.73	
TOD	3	403.8	3.39	5.63
poly(effort,3)	3	320.4	2.69	12.92
vessel_code	9	259.2	2.17	5.79

*- Overall influence as in Table 1 of Bentley et al. (2012)

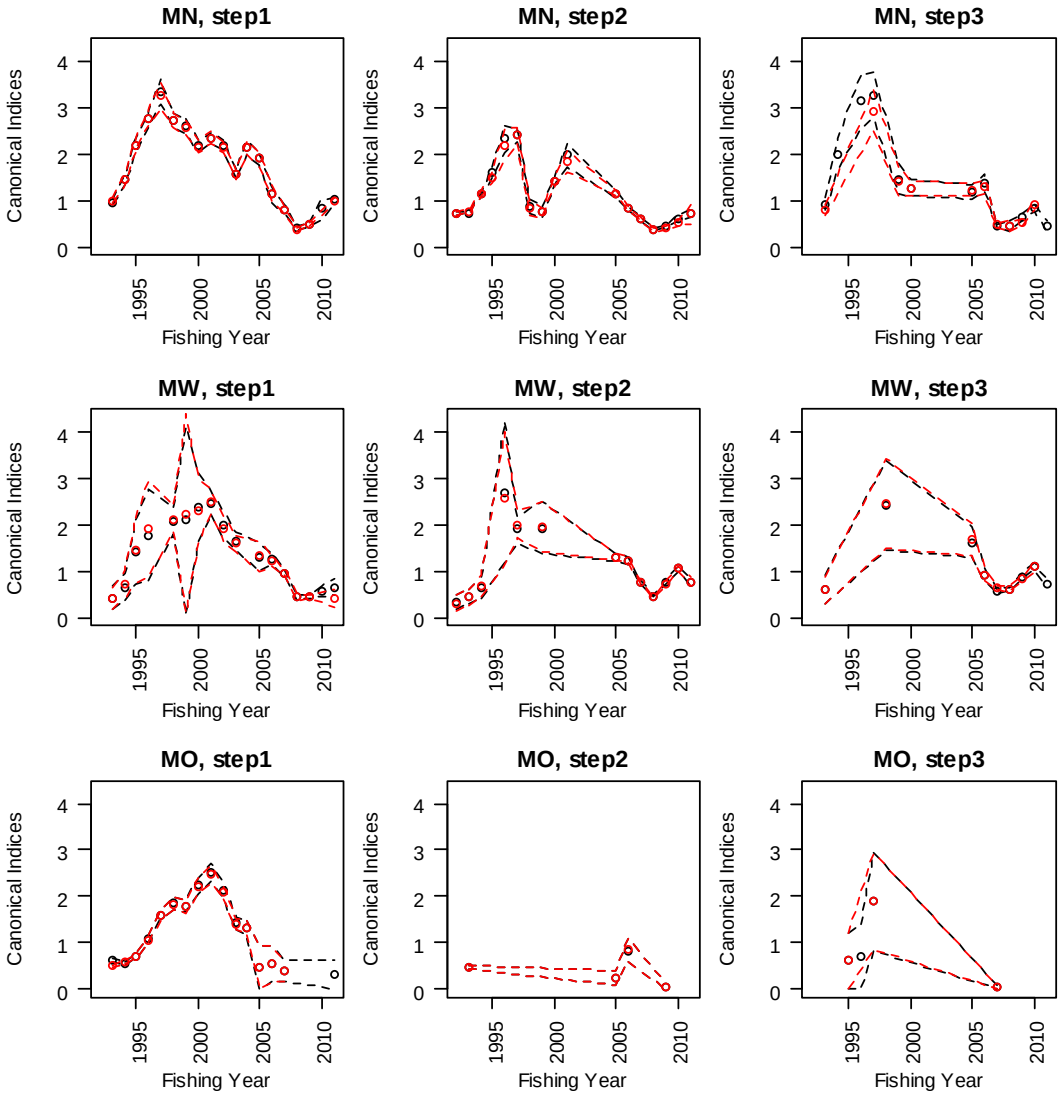

Figure 21: Canonical indices for each subarea and time step, from model fitted to Approach 2 (black) and Approach 1 datasets (red).

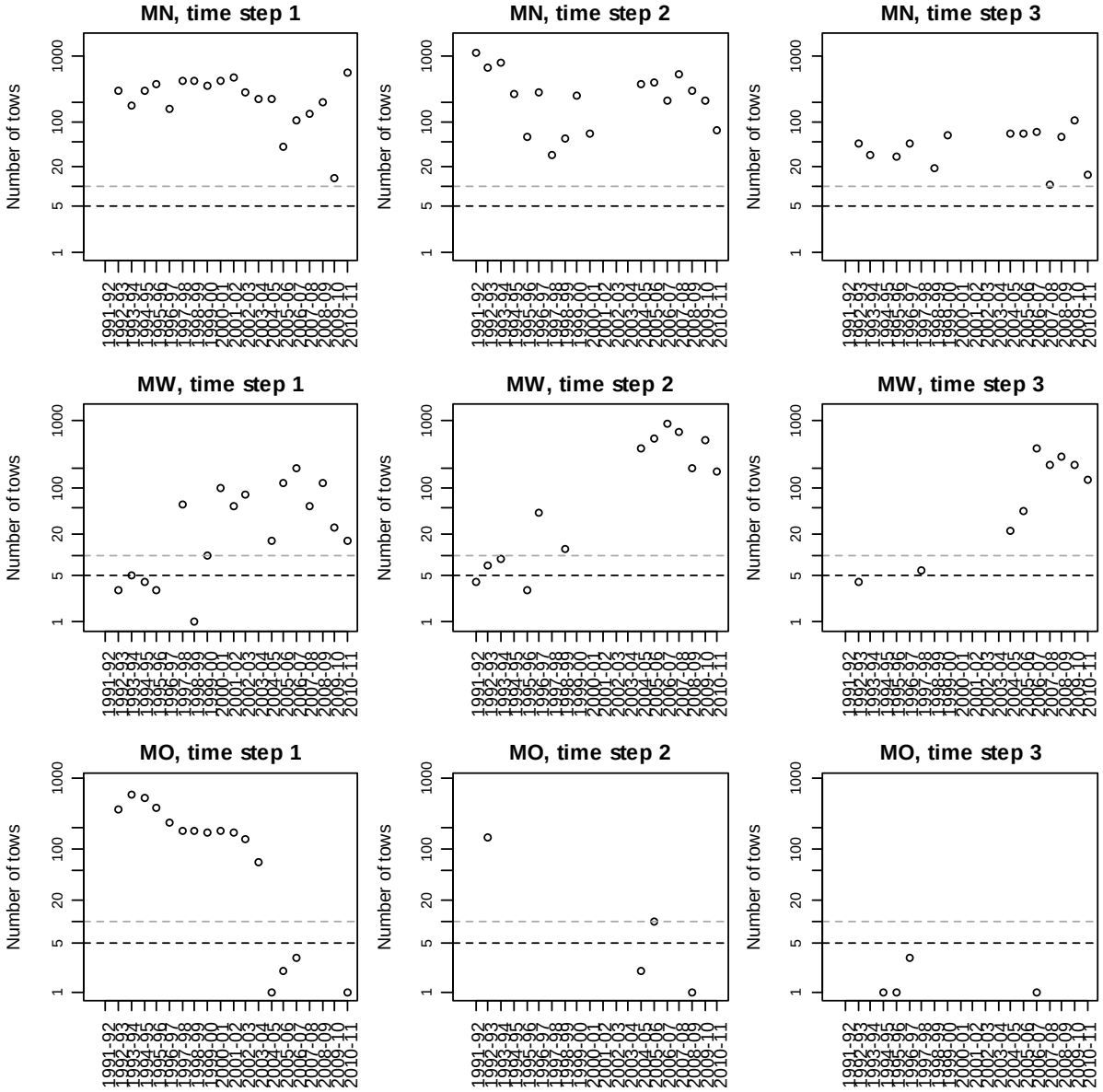

Figure 22: Numbers of commercial tows available within the core vessel dataset by time step and fishing year for each subarea. Dashed lines represent arbitrary cut offs at 5 and 10 tows.

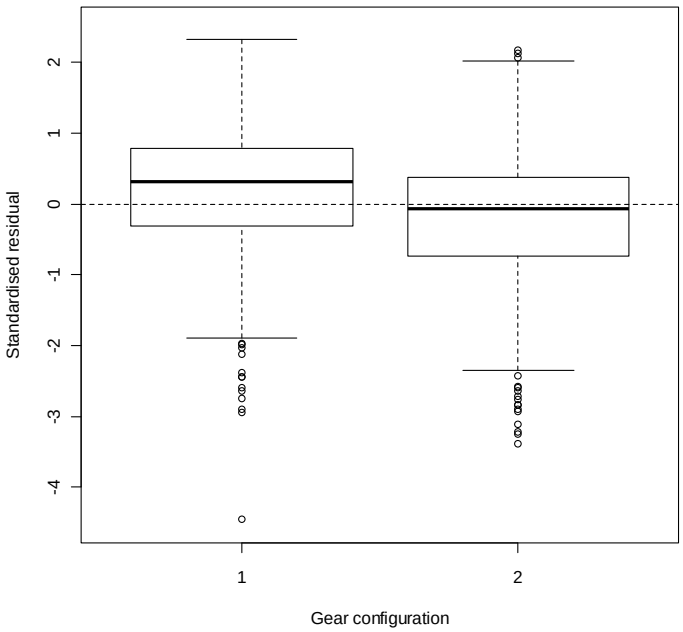

Figure 23: Boxplots of standardised residuals by gear bycatch configuration from standardised CPUE for fishing year in which vessels changed configuration (all core vessels). The year in which each vessel changed was identified individually from tow duration, and then data for years of change combined. Gear configuration 2 represents the modified gear to reduce bycatch and allow longer tows.

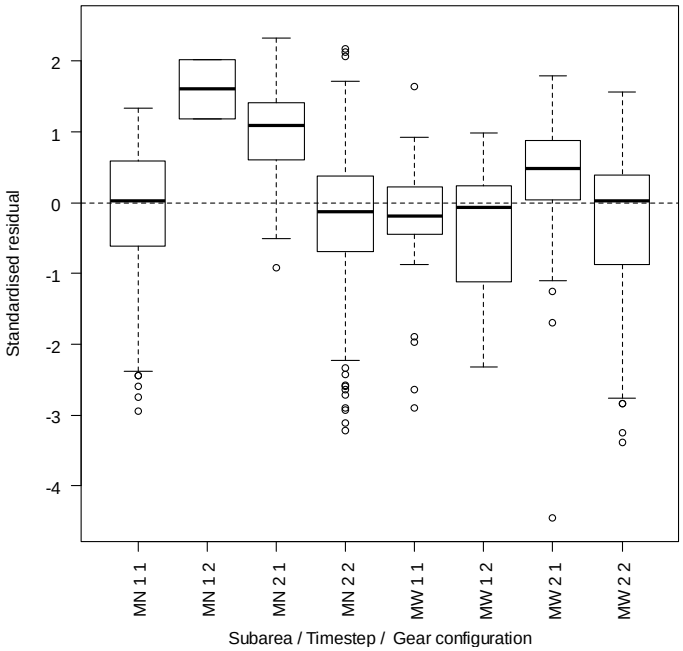

Figure 24: Boxplots of standardised residuals by subarea timestep gear bycatch configuration from standardised CPUE for fishing year in which vessels changed configuration (all core vessels). The year in which each vessel changed was identified individually from tow duration, and then data for years of change combined. Gear configuration 2 represents the modified gear to reduce bycatch and allow longer tows.

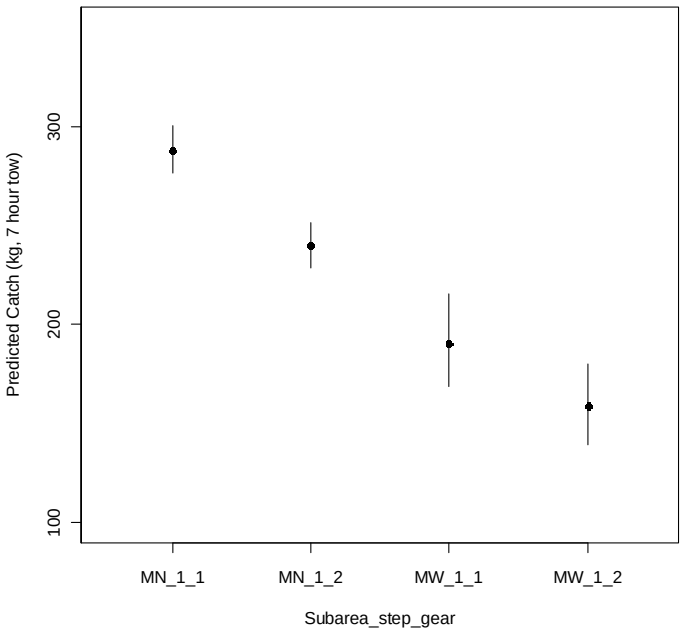

Figure 25: Predicted scampi catch for a 7 hour tow for the MN and MW subareas in time step 1, without (1) and with (2) bycatch modification.

Table 7: Analysis of deviance table and overall influence for final standardisation model (Approach 2, more than five tows, bycatch modification forced into the model).

	Df	Deviance explained	Additional deviance explained (%)	Overall influence (%)*
NULL				
yr_step_area	93	6110.6	51.55	
TOD	3	402.8	3.40	4.57
poly(effort,3)	3	320.8	2.71	12.46
vessel_code	9	258.5	2.18	4.76
Bycatch config	1	6.2	0.05	9.19

*- Overall influence as in Table 1 of Bentley et al. (2012)

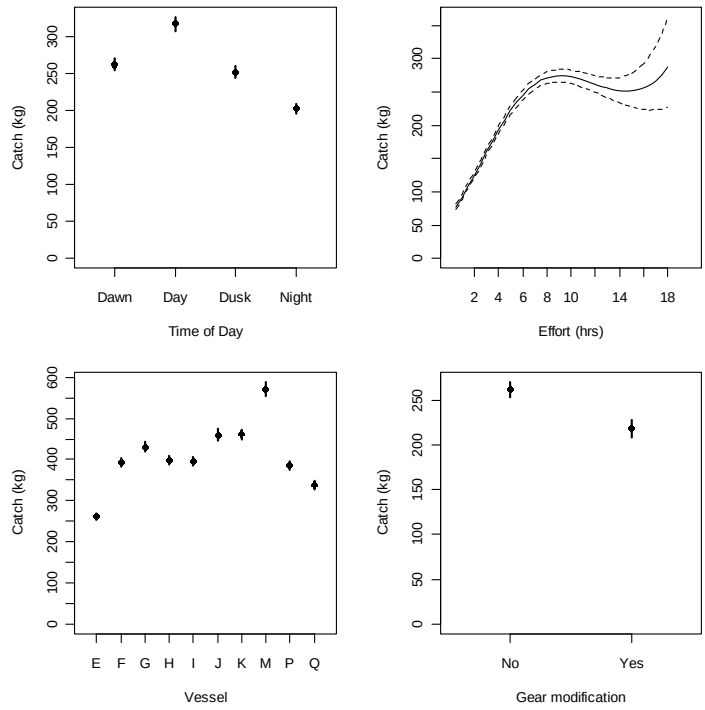

Figure 26: Termplot (in natural space) for final standardisation model (Table 7), showing relative effects of time of day, effort (tow duration), vessel and gear modification.

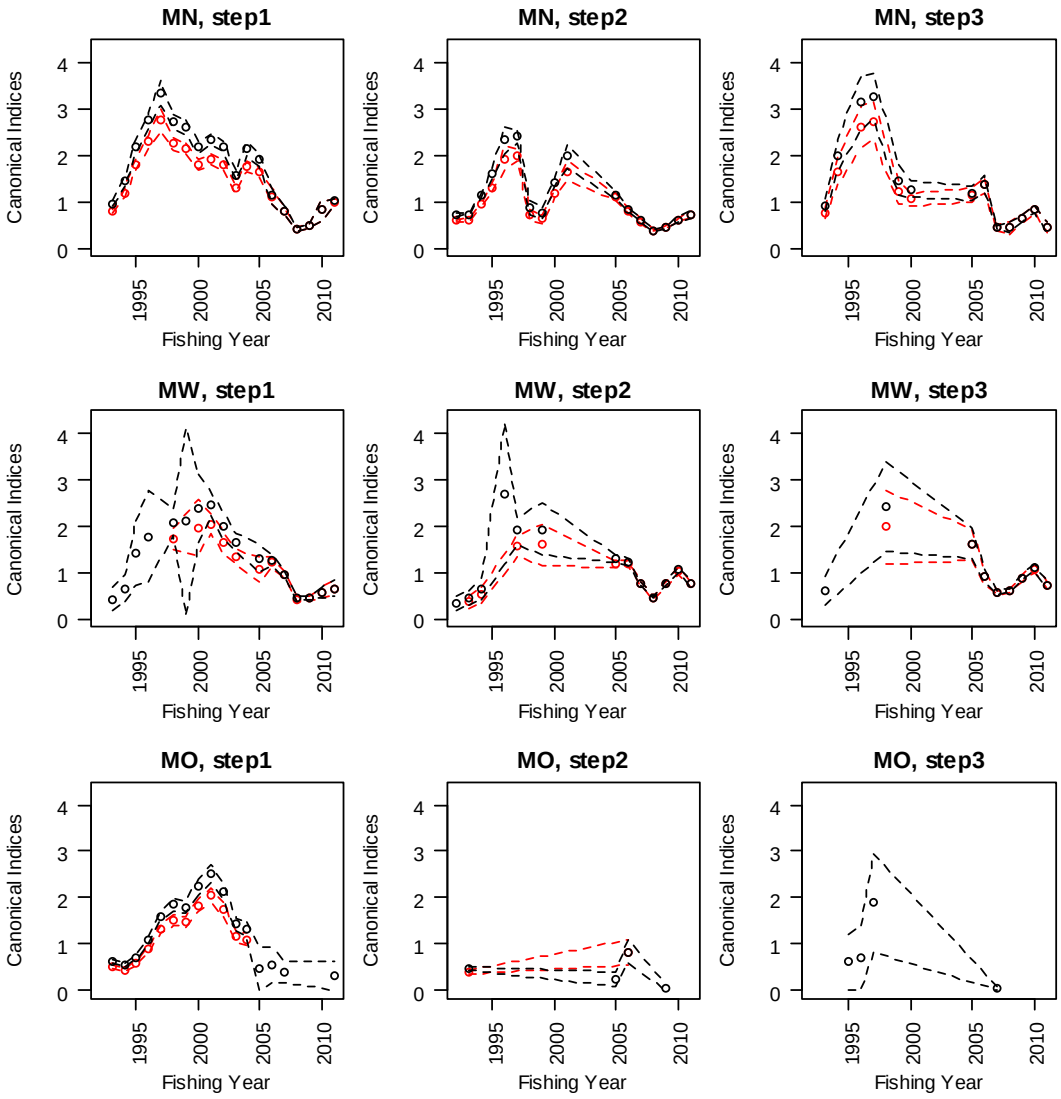

Figure 27: Canonical indices for each subarea and time step, from model fitted to Approach 2 (black) and excluding data with five or less tows by subarea timestep and bycatch modification forced (red) into the model.

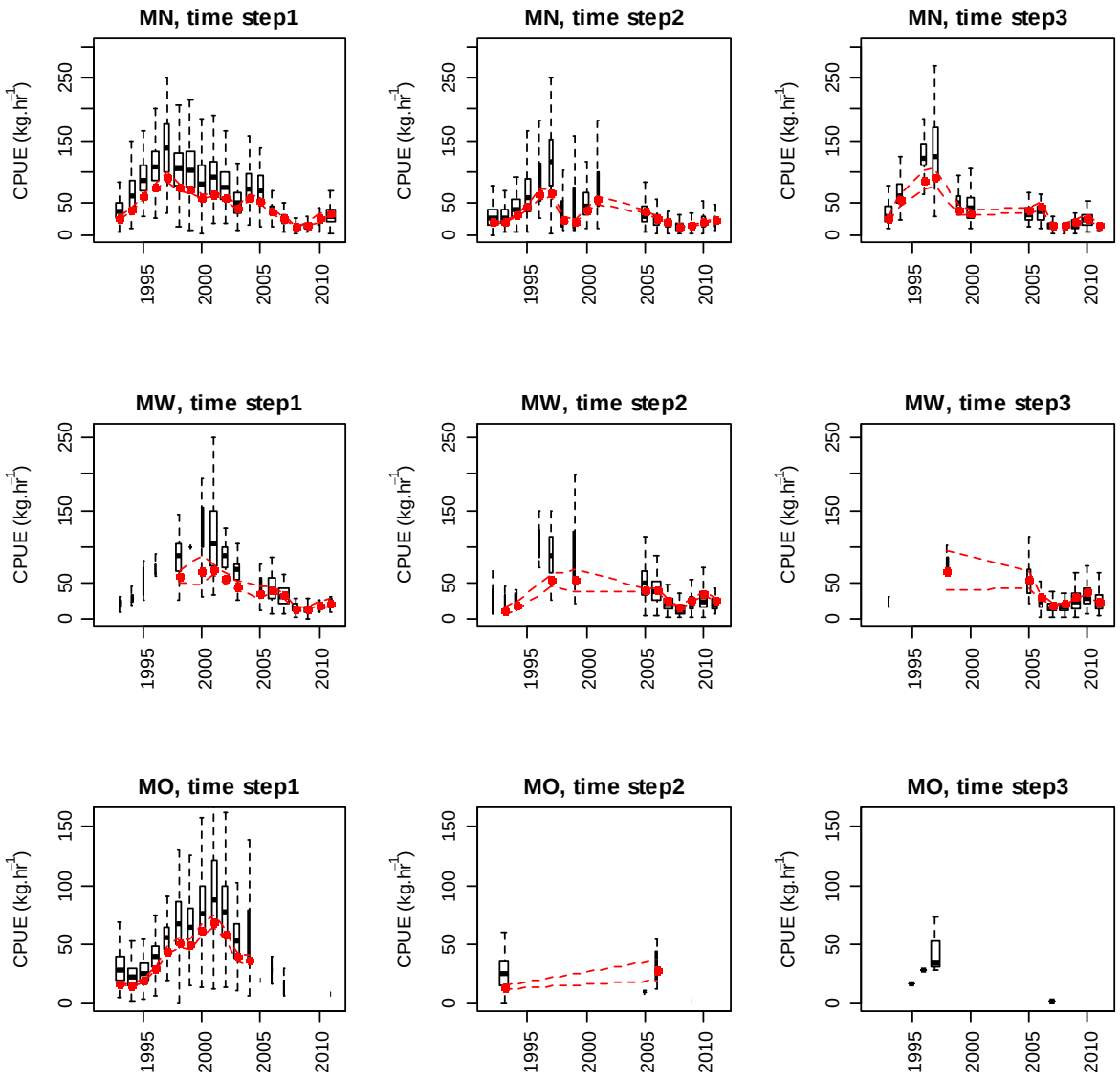

Figure 28: Comparisons of standardised CPUE indices (using Approach 2, more than five tows, bycatch modification forced into the model) for each subarea (red dots, dashed lines representing 95% confidence limits) and unstandardized data (boxplots). Box widths are proportional to square root of number of observations. Outliers from the boxplots have been removed.

3. MODEL STRUCTURE

3.1. Spatial and seasonal structure, and the model partition

The model partitions scampi by area (MN, MO, and MW), stock (one stock per area), sex, and length class. The model assumes that the three subareas are completely separate and that there is no movement, either by adults or recruitment, between them. No recaptures have been made from the tagged scampi released in SCI 3, but recaptures from other New Zealand stocks suggest very limited movement (Cryer & Stotter 1999, Tuck et al. 2009a), and this is supported by acoustic tracking of the European scampi *Nephrops norvegicus* (Chapman et al. 1974), albeit in shallower waters. Larval development of scampi appears to be partially abbreviated (compared to similar shallow water species), in that there only appears to be one larval stage, with a duration of three to four days (Wear 1976). The postlarvae appears to be benthic orientated (Wear 1976), and it has therefore been assumed that there is little potential for larval exchange between the subareas. By assessing the three areas within the same model, catches, survey indices and length distributions can be specific to each area, but other parameters (growth, natural mortality, selectivity, catchability) can be shared.

Growth between length classes are determined by sex-specific, length-based growth parameters. Individuals enter the partition by recruitment and are removed by natural mortality and fishing mortality. The model's annual cycle is based on the fishing year and is divided into the three time-steps described above for the respective stocks (Table 4). The choice of three time steps was based on current understanding of scampi biology and sex ratio in catches. Note that model references to year within this report refer to the modelled or fishing year, and are labelled as the most recent calendar year, i.e., the fishing year 1998–99 is referred to as 1999 throughout.

The model uses capped logistic length based selectivity curves for commercial fishing and research trawl surveys, assumed constant over years, but allowed to vary with sex and time step (where necessary). While the sex ratio data suggest that the relative catchability of the sexes vary through the year (hence the model time structure adopted), there is no reason to suggest that assuming equal availability, selectivity at size would be different between the sexes. Therefore the two sex selectivity implementation developed within CASAL for the SCI 1 and SCI 2 assessments (Tuck & Dunn 2012) was applied. This allows the L_{50} (size at which 50% of individuals are retained) and a_{95} (size at which 95% of individuals are retained) selectivity parameters to be estimated as single values shared by both sexes in a particular time step, but allows for different availability between the sexes through estimation of different a_{max} (maximum level of selectivity) values for each sex. Photographic survey abundance indices are not sex specific, and a standard logistic length based selectivity curve is applied.

3.2. Biological inputs

3.2.1. Growth

Recent scampi assessments have estimated growth within the model from tag recapture data (Tuck & Dunn 2012). Although surveys in 2009 and 2010 released over 5000 tagged scampi, returns have been very low, and there are insufficient data to estimate growth.

As an alternative to estimating growth with tag recapture data, growth parameters were initially taken as those estimated within a previous assessment model from 2011 (Tuck & Dunn 2012). From these starting values, growth was then estimated within a simple (one area) model, to provide the base growth parameters (more details of approach implemented are provided in section 4.1). Sensitivity to

faster, slower, and estimated growth is examined. Growth is estimated using the Francis (1988) parameterisation of the growth increment von-Bertalanffy curve. Within the model, growth is defined by sex specific expected annual increments at 20 mm (g_{20}) and 40 mm (g_{40}) OCL (orbital carapace length), and a standard deviation (min_sigma).

3.2.2. Maturity

Data on egg development stage are available from observer sampling (conducted throughout the year) and research trawl sampling associated with photographic surveys (conducted in October). The most appropriate time of year to examine maturity from ovigerous females is immediately after spawning, which occurs immediately after moulting. Female moulting peaks around October (based on observer data on the prevalence of scampi with soft carapaces; Figure 15), but continues into December. The data on the proportion of females that are ovigerous have been examined for the period from January to March. This assumes that all mature females will be ovigerous during this period.

Analysis of the proportion ovigerous data, modelled as a function of length, was conducted within a GLM framework, with a quasibinomial distribution of errors and a logit link (McCullagh & Nelder 1989),

$$P.mature = a + b * Length$$

which equates to the logistic model. The model was weighted by the number measured at each length. After obtaining estimates for the parameters *a* and *b*, the length at which 50% are mature (L_{50}) was calculated from:

$$L_{50} = -\frac{a}{b}$$

with selection range (SR) calculated from:

$$SR = \frac{(2.\ln(3))}{b}$$

The L_{50} estimate for the SCI 3 data was 43.2 mm, with a selection range a_{10} to a_{90} of 6.5 mm (Figure 29).

3.2.3. Natural mortality

The instantaneous rate of natural mortality, M, has not been estimated directly for any scampi species, but estimates have been made based on the estimate of the K parameter from a von Bertalanffy growth curve (Cryer & Stotter 1999) using a correlative method (Pauly 1980, Charnov et al. 1983). For the current model, M is fixed at 0.2. Sensitivity to this assumption is also examined.

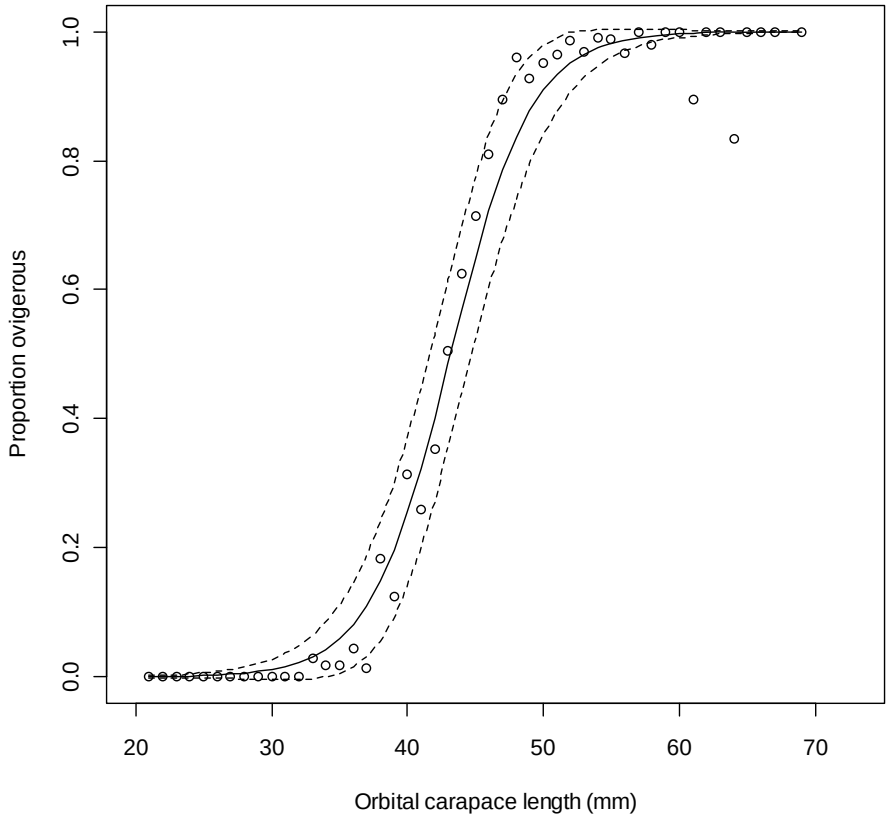

Figure 29: Proportions of female scampi carrying eggs (ovigerous) at length, from sampling in January to March period, just after spawning period. Solid line represents logistic curve fitted to the data (L_{50} 43.2 mm and selection range 6.5 mm). Dashed line represents plus or minus one Standard Error.

3.3. Catch data

Data for the model were collated over the spatial and temporal strata as defined in the model structure. Catches in these three sub-areas represent over 98% of scampi catches from SCI 3, and are presented in Table 8.

3.4. CPUE indices

The CPUE indices estimated within the standardisation including subarea timestep combinations with five or more tows, and with the bycatch modification forced (Figure 27) were fitted within the model as abundance indices. There has been considerable discussion on whether CPUE is proportional to abundance for scampi (Tuck 2009), with rapid increases in both CPUE and trawl survey catch rates for a number of stocks in the early to mid 1990s (and changes in sex ratio in trawl survey catches) initially being considered related to changes in catchability. Later analysis (Tuck & Dunn 2009) suggested that the observed changes in sex ratio were related to slight changes in the survey timing in relation to the moult cycle. Similar patterns in CPUE are observed over the same period for rock lobster (Starr 2009, Starr et al. 2009), which may suggest broad scale environmental drivers influencing crustacean recruitment. The increase in CPUE observed for SCI 3 is similar to that observed for SCI 1 and SCI 2 during the 1990s (Tuck & Dunn 2012). The CPUE trend for these areas is mirrored by trawl survey catch rates, suggesting that they do not reflect fisher learning, and although no trawl survey data are available for SCI 3 prior to 2001, the Working Group considered it

unlikely that it would take the fishing industry five to six years to find the best grounds on the Mernoo Bank. While not considered appropriate for use as an index in the model (section 3.5.2), the middle depths trawl survey scampi abundance index (not presented) shows a very similar temporal pattern to the standardised CPUE indices, supporting the suggestion that the increases during the 1990s reflect scampi abundance rather than fisher learning.

3.5. Research survey indices

Photographic surveys (with trawl survey components) have been undertaken from the RV *Kaharoa* in August and November 2001, and October 2009 and 2010. In 2001, pre and post fishery surveys were conducted in the MO subarea (the fishery occurring over a few weeks in October). This survey was for the QMA 3 management area, and did not cover the MN and MW subareas. The surveys in 2009 and 2010 were for the SCI 3 management area, and covered all three subareas.

Table 8: Estimated landed catch (t) from SCI 3, by sub-area and time-step.

Fishing year	MN_1	MN_2	MN_3	MW_1	MW_2	MW_3	MO_1	MO_2	MO_3
1991	0.00	0.00	0.00	0.00	0.00	0.00	0.00	0.00	0.00
1992	0.00	151.59	0.00	0.00	0.23	0.00	0.00	0.00	0.00
1993	77.16	114.21	17.95	1.00	0.63	0.41	54.84	25.27	0.00
1994	49.52	200.05	10.46	0.74	1.36	0.00	60.64	0.00	0.00
1995	130.91	93.32	0.00	1.00	0.00	0.00	65.26	0.00	0.17
1996	190.12	23.36	12.99	1.00	1.37	0.00	76.15	0.00	0.12
1997	90.08	113.54	13.60	0.00	14.60	0.00	71.22	0.00	0.96
1998	205.93	4.62	0.00	23.34	0.00	2.07	59.85	0.00	0.00
1999	211.27	10.08	4.17	0.43	3.96	0.00	62.09	0.00	0.00
2000	156.60	66.88	15.02	6.02	0.00	0.00	74.79	0.00	0.00
2001	192.04	19.96	0.00	44.51	0.00	0.00	75.82	0.00	0.00
2002	208.50	0.00	0.00	22.61	0.00	0.00	72.89	0.00	0.00
2003	153.93	0.00	0.00	38.88	0.00	0.00	70.85	0.00	0.00
2004	211.78	0.00	0.00	3.84	0.00	0.00	61.38	0.00	0.00
2005	90.11	91.48	16.55	22.58	105.92	8.17	0.09	0.09	0.00
2006	17.45	79.58	18.83	41.88	148.42	9.57	0.18	2.15	0.00
2007	19.55	29.59	7.59	46.57	151.39	49.36	0.25	0.00	0.01
2008	15.22	72.70	1.29	6.81	80.94	31.84	0.00	0.00	0.00
2009	25.21	44.27	8.78	13.59	35.57	62.53	0.00	0.01	0.00
2010	6.05	63.85	19.44	3.18	143.76	65.47	0.00	0.00	0.00
2011	174.00	20.34	1.62	3.91	32.50	23.46	0.05	0.00	0.00

3.5.1. Photographic surveys

Photographic surveys provide two indices of scampi abundance, one based on major burrow openings, and one based on visible scampi. Previous assessments of SCI 1 and SCI 2 have used the index of burrow openings as an index of scampi abundance, while concerns that larger scampi (in particular) in SCI 6A may not maintain burrows (Tuck et al. 2009b) led to the use of the index of visible scampi as an index of scampi abundance for the development of an assessment model in this area (Tuck & Dunn 2012).

Both indices are subject to uncertainty, either from burrow detection and occupancy rates (for burrow based indices) or emergence patterns (for visible scampi based indices). Scaled survey estimates (by survey strata and subarea) are provided for scampi burrows in Table 9 and visible scampi in Table 10.

3.5.2. Trawl surveys

Trawl catch rates from scampi surveys have been raised to strata to provide biomass estimates in Table 11. The raised biomass index was used in the assessment model. Research trawl data are also available from a Chatham Rise middle depths trawl survey time series, but this survey targets hoki, hake and ling across the whole region, with station coverage being low within the main scampi fishery areas, and the trawl gear used is not considered appropriate for sampling scampi.

3.6. Length distributions

3.6.1. Commercial catch at length data

Ministry of Fisheries (now Ministry for Primary Industries) observers have collected scampi length frequency data from scampi targeted fishing on commercial vessels in SCI 3 since 1991–92. The numbers of tows for which length data are available are presented by fishing year and month in Table 12 (subarea MN), Table 13 (subarea MW), and Table 14 (subarea MO). One trip has been excluded from 2002 where scampi were measured to the centimetre below the actual measurement rather than to the millimetre below.

Proportional length distributions (and associated c.v.s) were calculated using CALA (Francis & Bian 2011), using the approaches previously implemented in NIWA's *Catch-at-Age* software (Bull & Dunn 2002). Plots of the proportional length frequency distribution are shown by year for subarea MN, time step 1(Figure 30 to Figure 32), subarea MN, time step 2 (Figure 33), subarea MN, time step 3 (Figure 34), subarea MW, time step 1 (Figure 35 to Figure 36), subarea MW, time step 2 (Figure 37), subarea MW, time step 3 (Figure 38), and subarea MO, time step 1 (Figure 39 to Figure 40).

3.6.2. Trawl survey length distributions

Length frequency samples from research trawling have been taken by scientific staff since 2001 (Table 11). Estimates of the length frequency distributions (with associated c.v.s) were derived using the NIWA CALA software (Francis & Bian 2011), using 1 mm (OCL) length classes by sex, and are presented in Figure 41 and Figure 42. These were calculated separately for the sexes for each subarea-time step in the model.

Table 9: Scaled photo survey estimates of scampi burrow abundance in SCI 3 by survey strata and subarea.

Burrows		2000 step 3 (pre fishery)				2001 step 1 (post fishery)				2010 step 1				2011 step 1			
Subarea	Strata	N	Mean density (m^{-2})	c.v.	millions	N	Mean density (m^{-2})	c.v.	millions	N	Mean density (m^{-2})	c.v.	millions	N	Mean density (m^{-2})	c.v.	millions
MO	902	7	0.127	0.196	96.77	7	0.133	0.118	101.35	7	0.053	0.29	40.02	7	0.041	0.25	31.38
	903	9	0.182	0.199	97.01	9	0.333	0.092	177.49	10	0.044	0.14	23.49	9	0.081	0.08	43.41
	Combined	16	0.149	0.140	193.78	16	0.215	0.073	278.84	17	0.049	0.19	63.51	16	0.058	0.12	74.79
MW	902A									20	0.048	0.12	102.83	19	0.054	0.10	114.48
MN	902B									19	0.053	0.11	66.94	20	0.081	0.82	103.37
	902C									3	0.041	0.19	7.12	3	0.053	0.17	9.12
	903A									5	0.046	0.13	21.07	5	0.101	0.15	46.4
	Combined									27	0.050	0.03	95.12	28	0.084	0.03	158.89

Table 10: Scaled photo survey estimates of visible scampi abundance in SCI 3 by survey strata and subarea.

Visible scampi		2000 step 3 (pre fishery)				2001 step 1 (post fishery)				2010 step 1				2011 step 1			
Subarea	Strata	N	Mean density (m^{-2})	c.v.	millions	N	Mean density (m^{-2})	c.v.	millions	N	Mean density (m^{-2})	c.v.	millions	N	Mean density (m^{-2})	c.v.	millions
MO	902	7	0.036	0.387	27.58	7	0.020	0.408	15.75	7	0.018	0.279	13.95	7	0.009	0.364	6.92
	903	9	0.056	0.183	28.97	9	0.071	0.167	36.99	10	0.019	0.198	9.89	9	0.008	0.235	4.05
	Combined	16	0.042	0.208	57.28	16	0.041	0.167	53.08	17	0.018	0.171	23.65	16	0.008	0.232	10.88
MW	902A									20	0.029	0.175	61.96	19	0.016	0.179	34.76
MN	902B									19	0.025	0.146	32.00	20	0.027	0.149	34.22
	902C									3	0.017	0.387	2.95	3	0.018	0.537	3.02
	903A									5	0.009	0.246	4.08	5	0.019	0.393	8.57
	Combined									27	0.021	0.045	39.03	28	0.024	0.049	45.82

Table 11: Scaled trawl survey estimates of scampi biomass in SCI 3 by survey strata and subarea.

	Biomass	2000 step 3 (pre fishery)				2001 step 1 (post fishery)				2010 step 1				2011 step 1			
Subarea	Strata	N	Mean catches ($kg.hr^{-1}$)	c.v.	tonnes	N	Mean catches ($kg.hr^{-1}$)	c.v.	tonnes	N	Mean catches ($kg.hr^{-1}$)	c.v.	tonnes	N	Mean catches ($kg.hr^{-1}$)	c.v.	tonnes
MO	902	2	6.67	0.55	109.9					3	3.35	0.45	55.1	2	2.38	0.19	39.1
	903	3	17.53	0.27	201.8	2	13.73	0.01	158.1	3	0.71	0.49	8.1	2	2.22	0.14	25.5
	Combined	5	11.14	0.26	311.7					6	2.26	0.39	63.2	4	2.31	0.12	64.6
MW	902A									4	6.4	0.36	295.5	3	7.53	0.06	347.7
MN	902B									4	1.81	0.41	49.7	3	4.5	0.09	123.3
	902C									3	6.51	0.1	24.2	2	10.13	0.06	37.7
	903A									3	0.85	0.09	8.5	3	3.86	0.19	38.4
	Combined									10	2.00	0.25	82.3	8	4.85	0.07	199.4

3.6.3. Photo survey length distributions

Photographic surveys provide two indices of scampi abundance, one based on major burrow openings, and one based on visible scampi. Overall length frequency distributions (undifferentiated by sex) are estimated for each of these indices.

Length frequency distributions were estimated for the relative photographic abundance series, by measuring the widths of a large sample of major burrow openings in the images, and converting these to orbital carapace lengths using a regression of OCL on major opening width (Cryer et al. 2005), augmented with additional data collected from more recent surveys. To estimate the c.v.s at length for each year, we used a bootstrap procedure, resampling with replacement from the original observations of burrow width, converting each observation to an estimated scampi size (in OCL), using an error term sampled from a normal distribution fitted to the regression residuals. Compared with the length frequency distributions from trawl catches, this procedure gave very large c.v.s, but we think this is realistic given the uncertainties involved in generating a length frequency distribution from burrow sizes. Estimates of the length frequency distributions (with associated c.v.s) for scampi generating burrows are presented in Figure 43. The length frequency distributions for the "scampi out of burrows" index were estimated by measuring the OCL of all scampi out of burrows observed within each survey. To estimate the c.v.s at length for each year, we used a bootstrap procedure, resampling with replacement from the original observations. Estimates of the length frequency distributions (with associated c.v.s) for visible scampi are presented in Figure 44.

Table 12: Number of commercial tows for which length distributions are available for subarea MN, by fishing year. Dashed lines represent splits between model time steps.

	Month											
	1	2	3	4	5	6	7	8	9	10	11	12
1992												
1993	20	11					3	3		13	2	
1994		5		27	14						1	27
1995	18										4	19
1996										5		
1997												
1998										7	13	
1999										18	5	
2000										8	14	
2001										17		
2002										6		
2003										52		
2004										52		
2005											4	6
2006							15	6				
2007											4	
2008					7						10	
2009				2					9			
2010									14			
2011			9								19	5

Table 13: Number of commercial tows for which length distributions are available for subarea MW, by fishing year. Dashed lines represent splits between model time steps.

	Month											
	1	2	3	4	5	6	7	8	9	10	11	12
1992												1
1993												
1994												
1995												
1996												
1997												
1998										5	1	
1999												
2000											7	
2001										1		
2002												
2003										3		
2004												
2005											12	6
2006						7		2				
2007					20						5	10
2008				3	39						5	9
2009				11				24	24			
2010								16	1			
2011												

Table 14: Number of commercial tows for which length distributions are available for subarea MO, by fishing year. Dashed lines represent splits between model time steps.

	Month											
	1	2	3	4	5	6	7	8	9	10	11	12
1992												
1993												
1994										49	3	
1995										51		
1996										12		
1997												
1998									1	13		
1999										17		
2000										6		
2001										17		
2002										27		
2003										19		
2004										22		
2005												
2006												
2007												
2008												
2009												
2010												
2011												

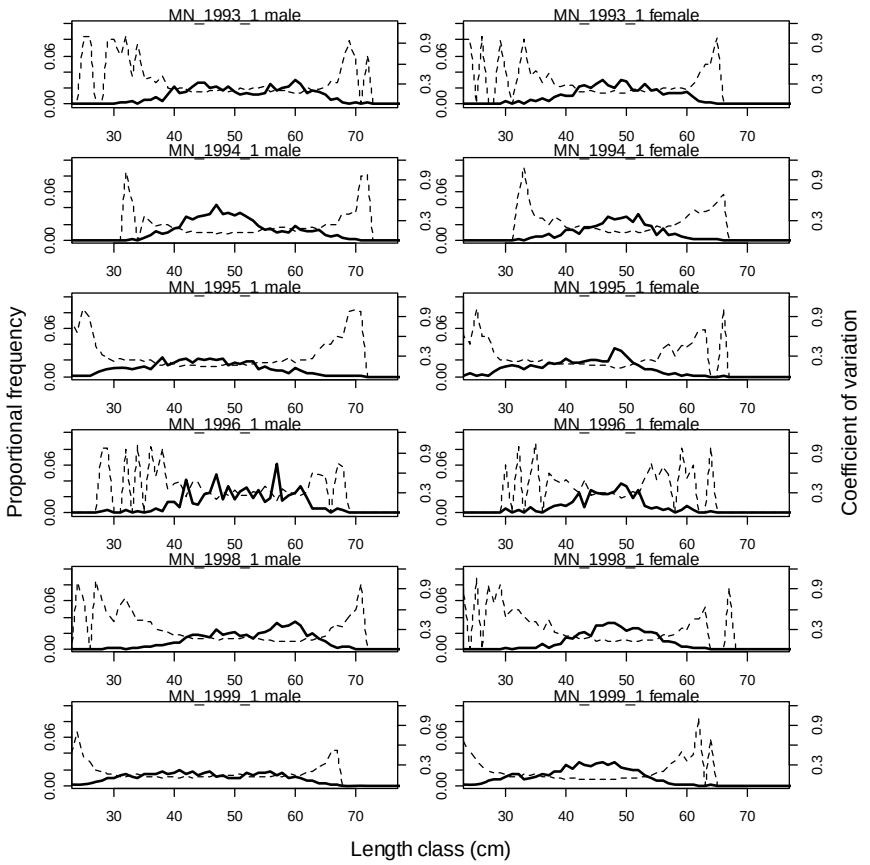

Figure 30: Proportional length frequencies and c.v.s for commercial catches by model year and time step 1 for subarea MN, 1993 to 1999.

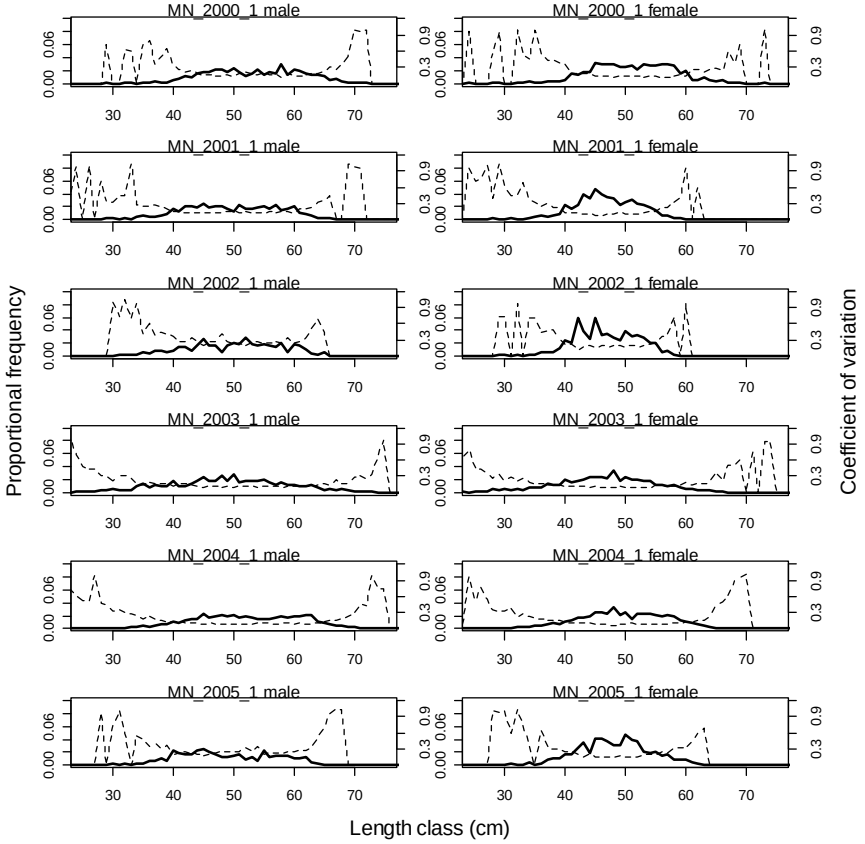

Figure 31: Proportional length frequencies and c.v.s for commercial catches by model year and time step 1 for subarea MN, 2000 to 2005.

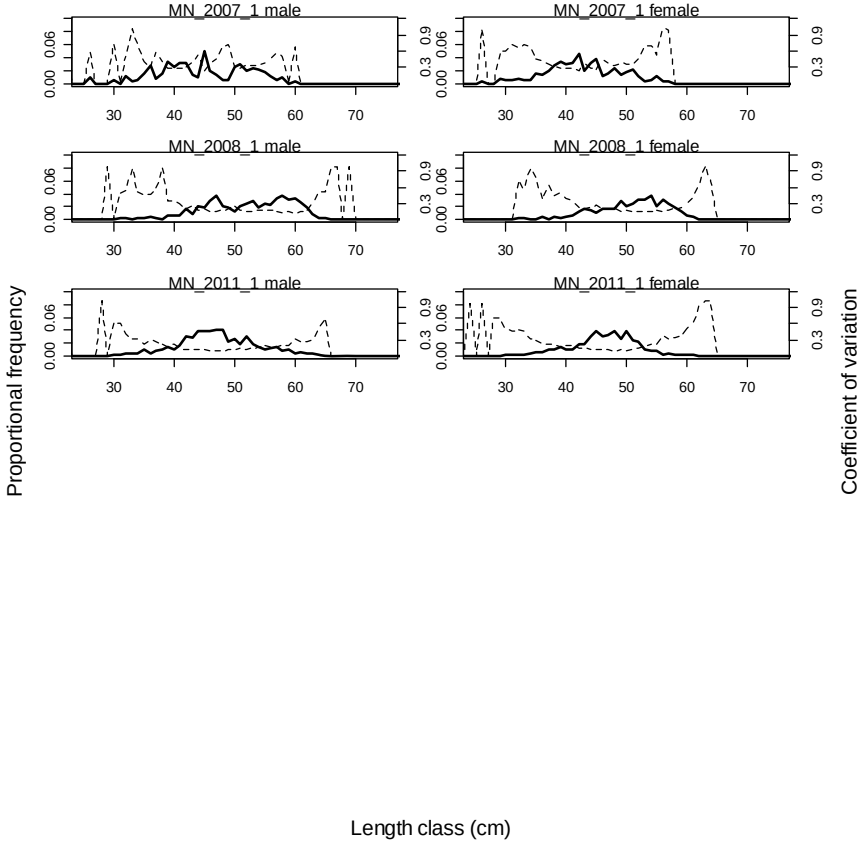

Figure 32: Proportional length frequencies and c.v.s for commercial catches by model year and time step 1 for subarea MN, 2007 to 2011.

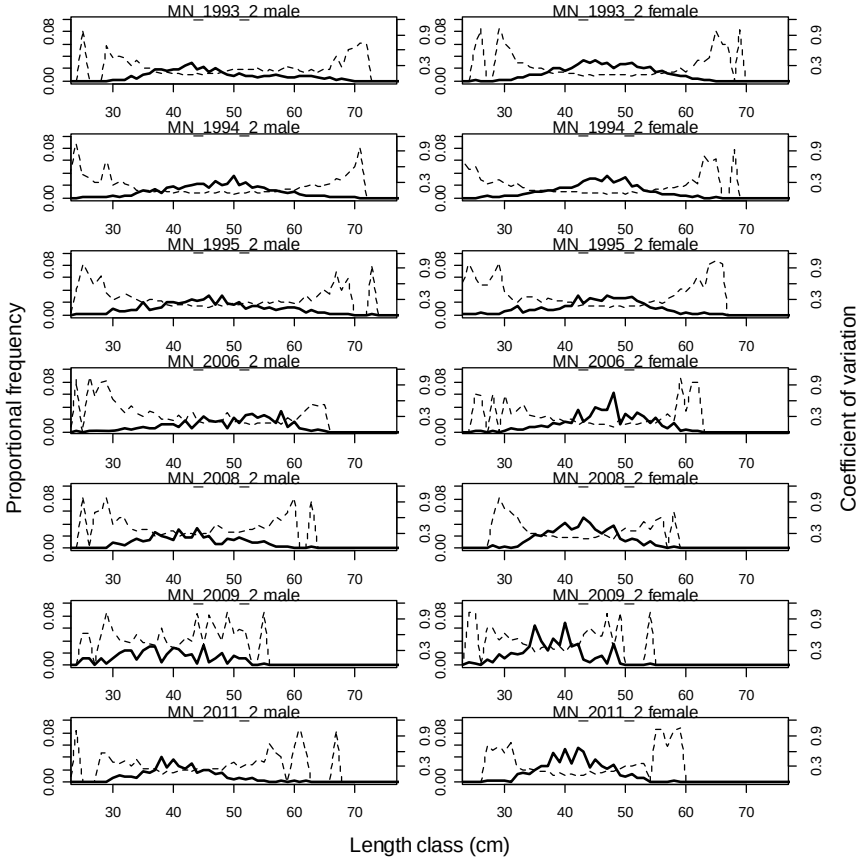

Figure 33: Proportional length frequencies and c.v.s for commercial catches by model year and time step 2 for subarea MN.

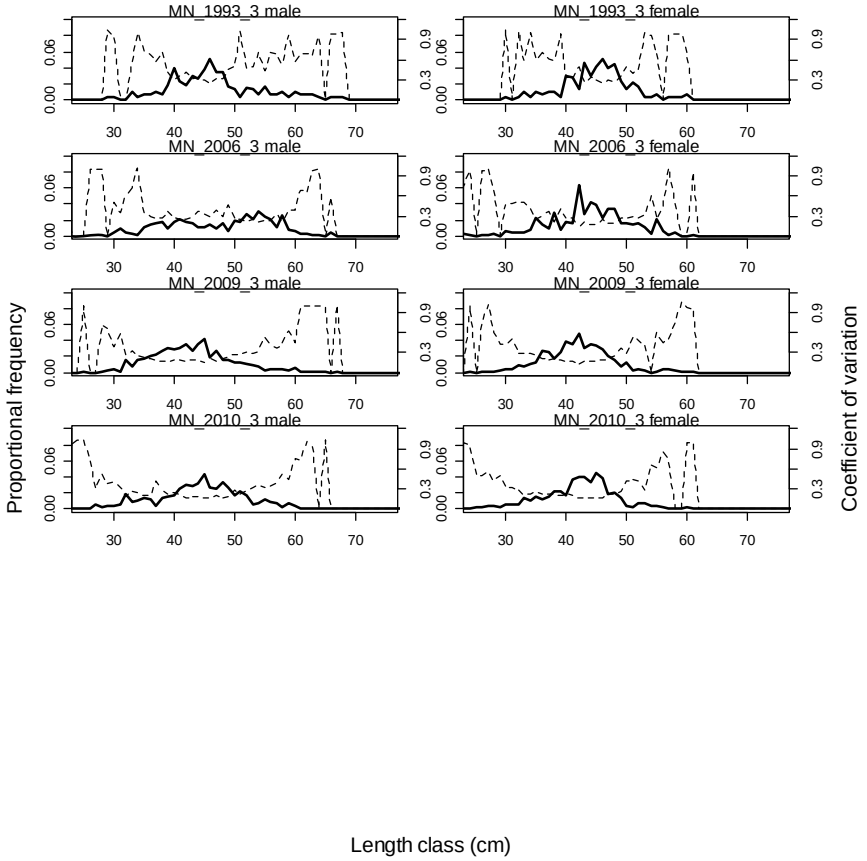

Figure 34: Proportional length frequencies and c.v.s for commercial catches by model year and time step 3 for subarea MN.

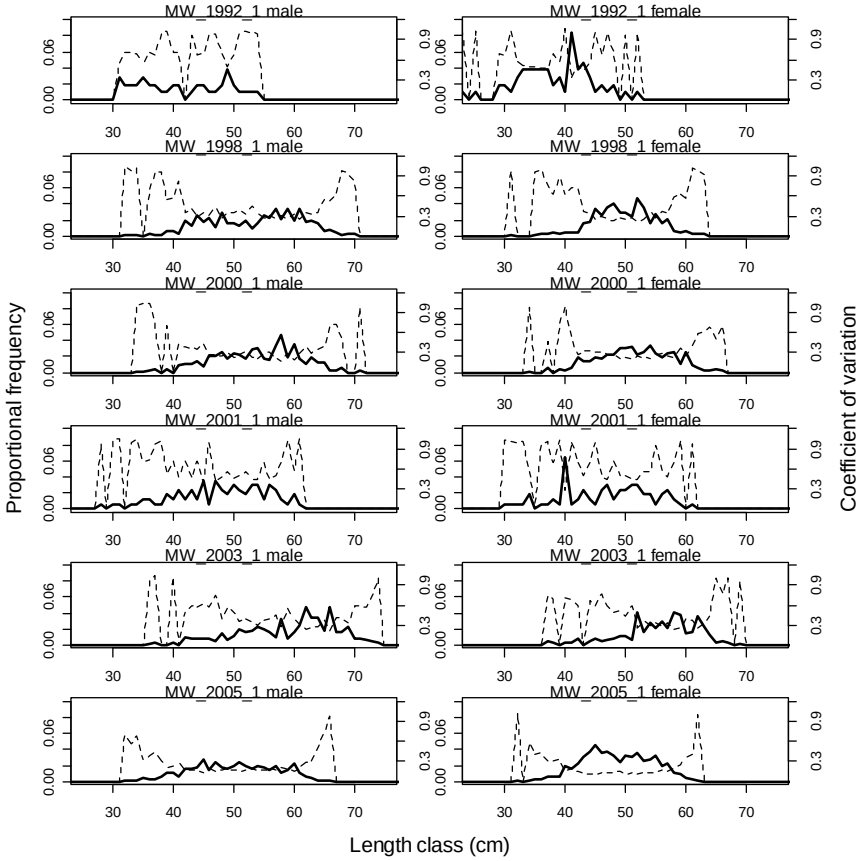

Figure 35: Proportional length frequencies and c.v.s for commercial catches by model year and time step 1 for subarea MW, 1992 to 2005.

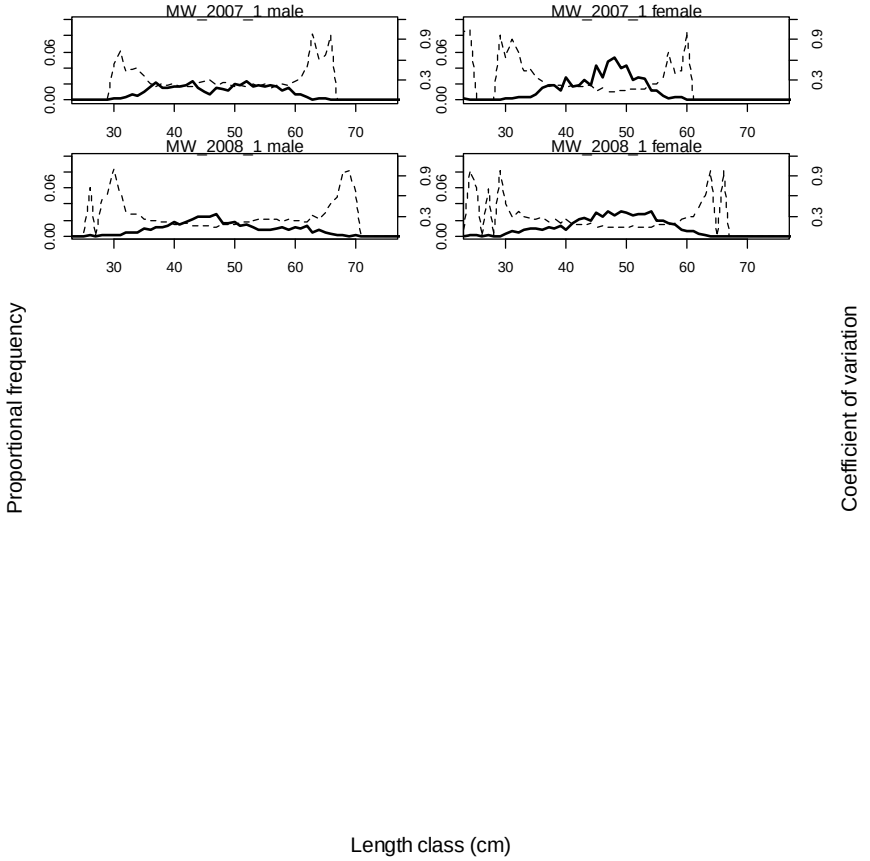

Figure 36: Proportional length frequencies and c.v.s for commercial catches by model year and time step 1 for subarea MW, 2007 to 2008.

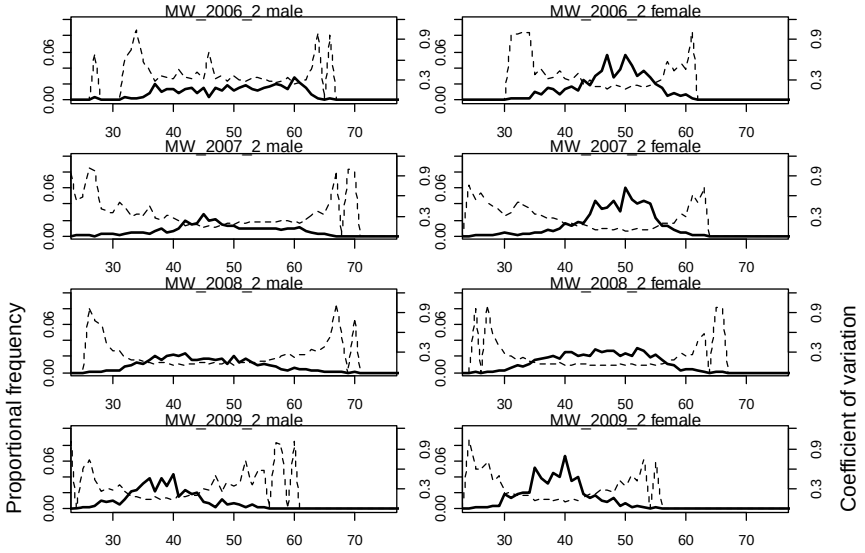

Figure 37: Proportional length frequencies and c.v.s for commercial catches by model year and time step 2 for subarea MW.

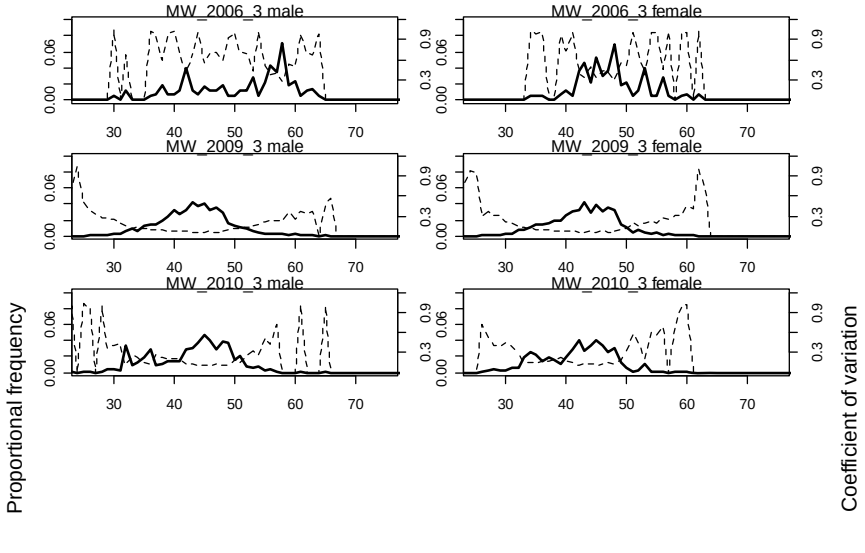

Figure 38: Proportional length frequencies and c.v.s for commercial catches by model year and time step 3 for subarea MW.

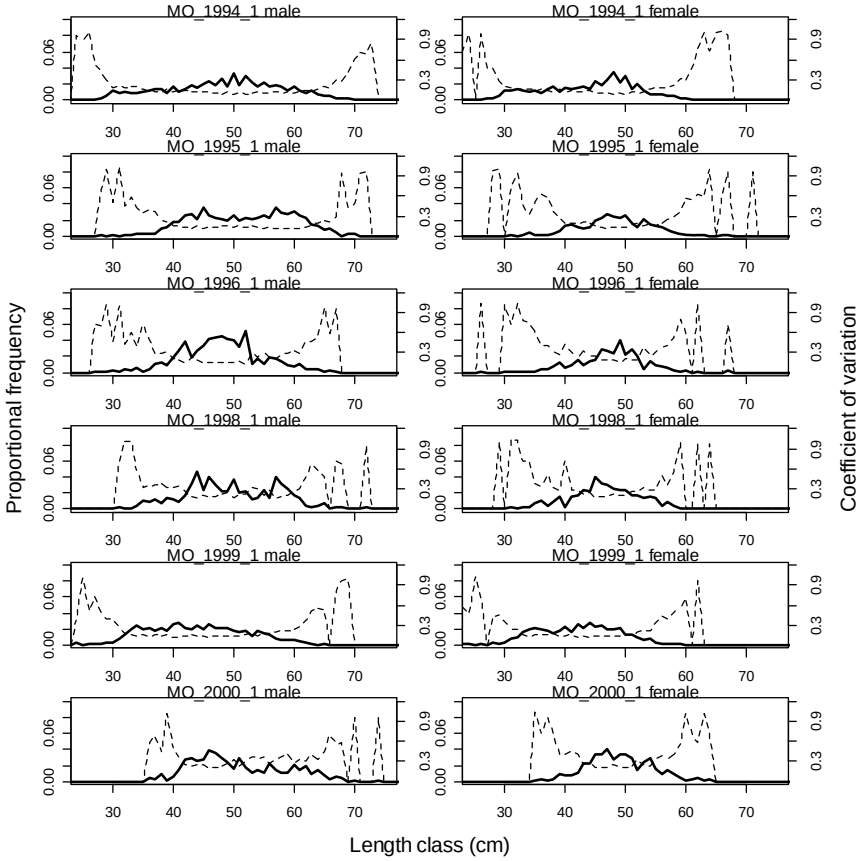

Figure 39: Proportional length frequencies and c.v.s for commercial catches by model year and time step 1 for subarea MO, 1994 to 2000.

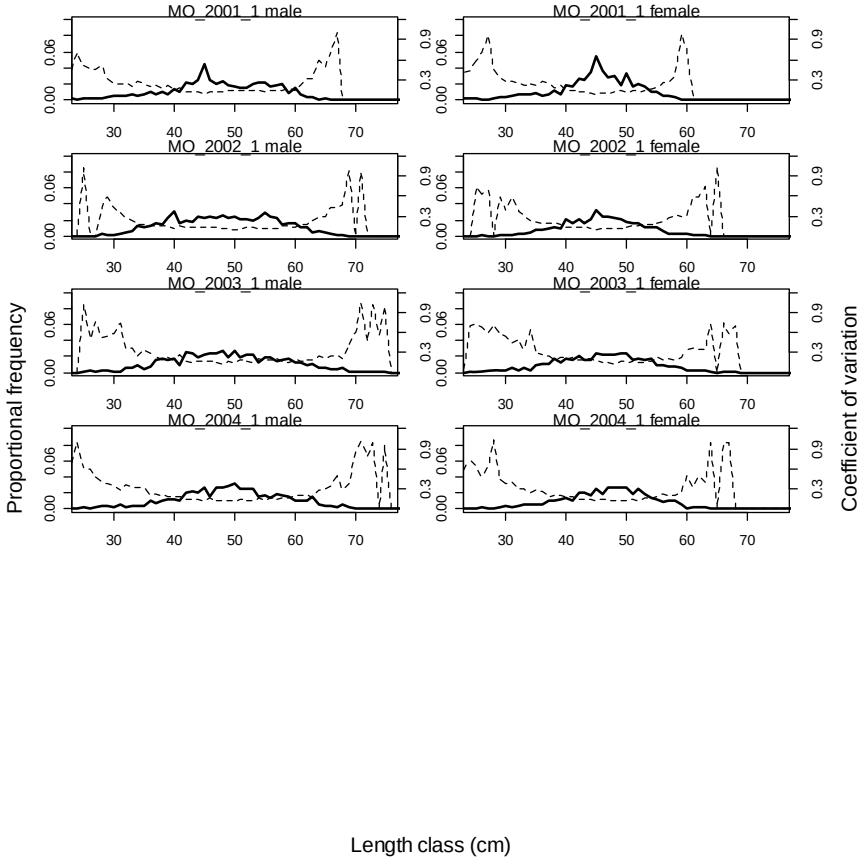

Figure 40: Proportional length frequencies and c.v.s for commercial catches by model year and time step 1 for subarea MO, 2001 to 2004.

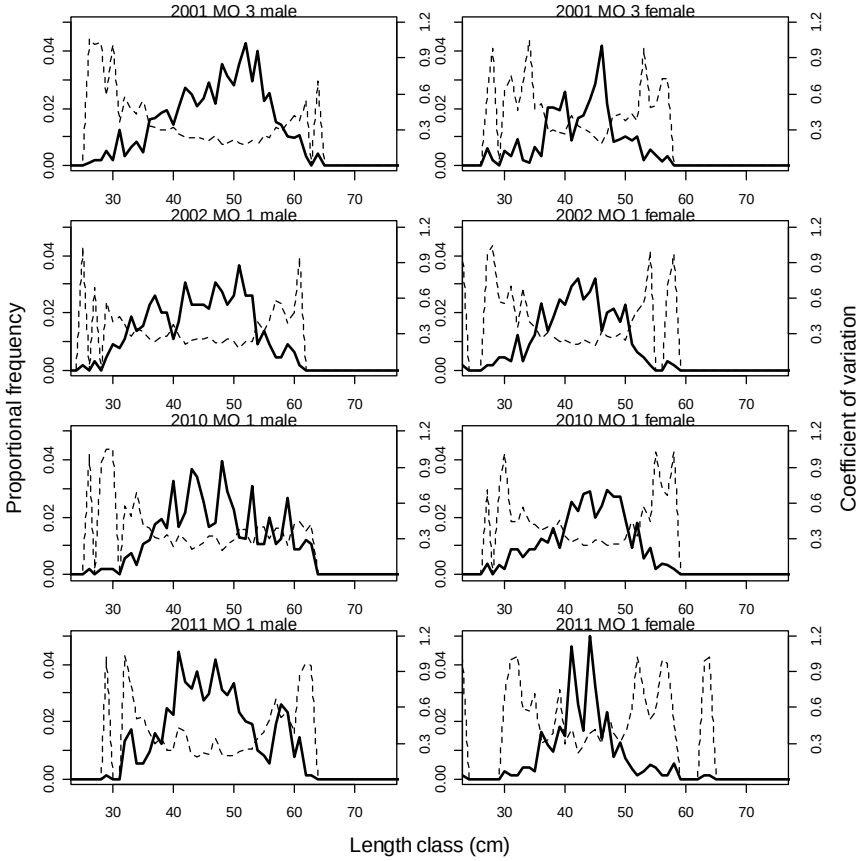

Figure 41: Proportional length frequencies and c.v.s for research trawling by model year and time step for subarea MO. Sampling in 2002 only occurred in survey strata 903.

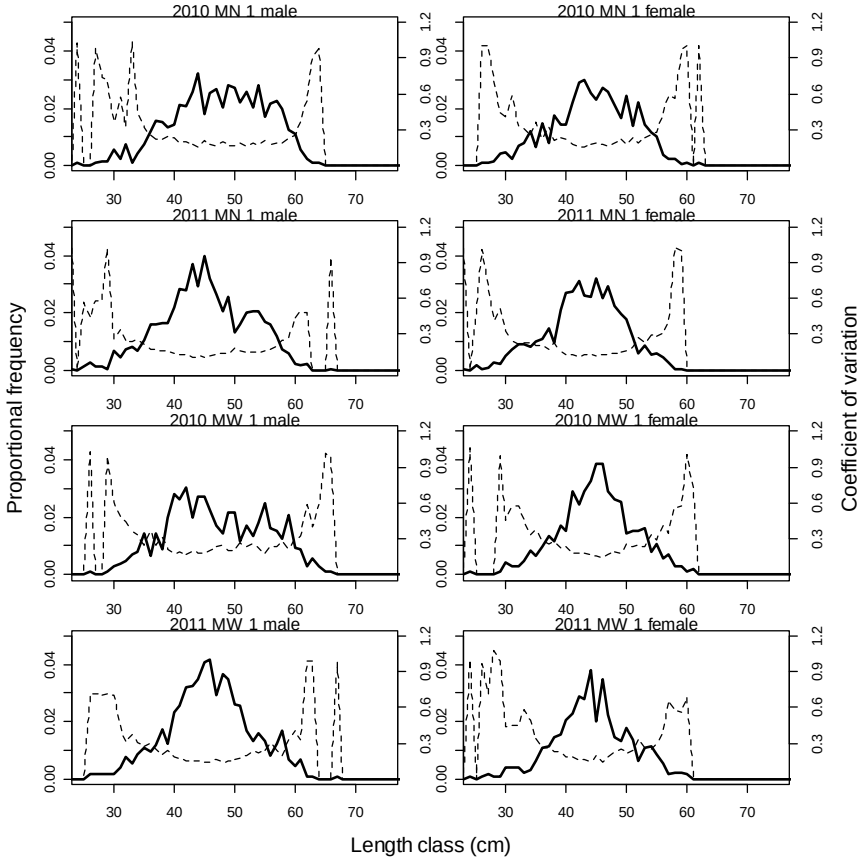

Figure 42: Proportional length frequencies and c.v.s for research trawling by model year and time step for subarea MN and subarea MW.

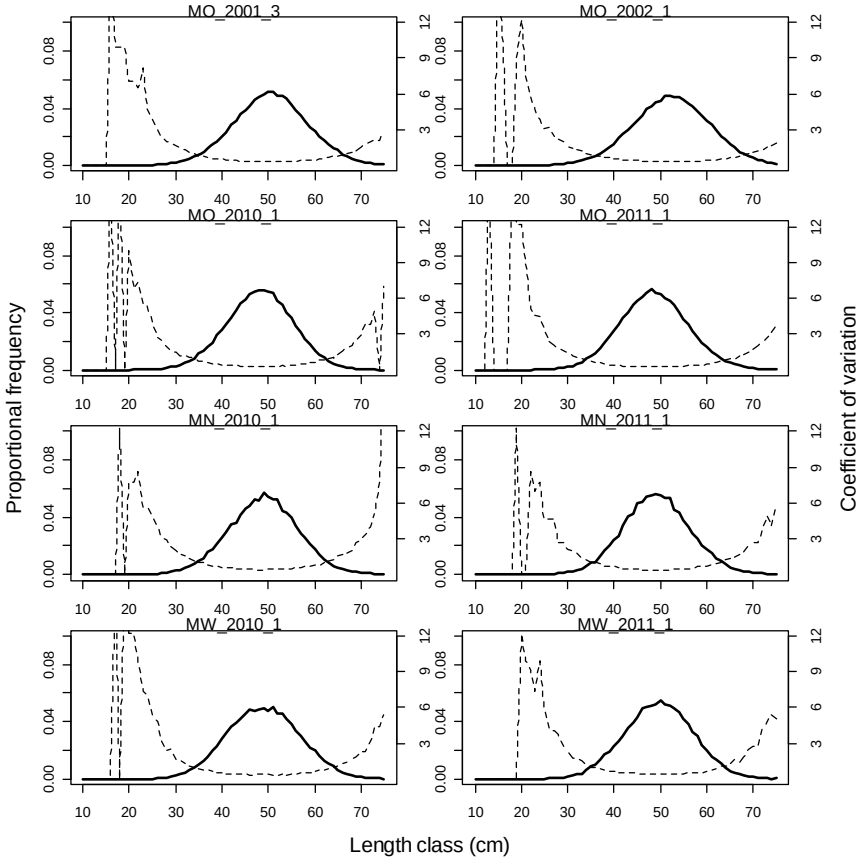

Figure 43: Proportional length frequencies and c.v.s for scampi responsible for burrows counted within photo surveys.

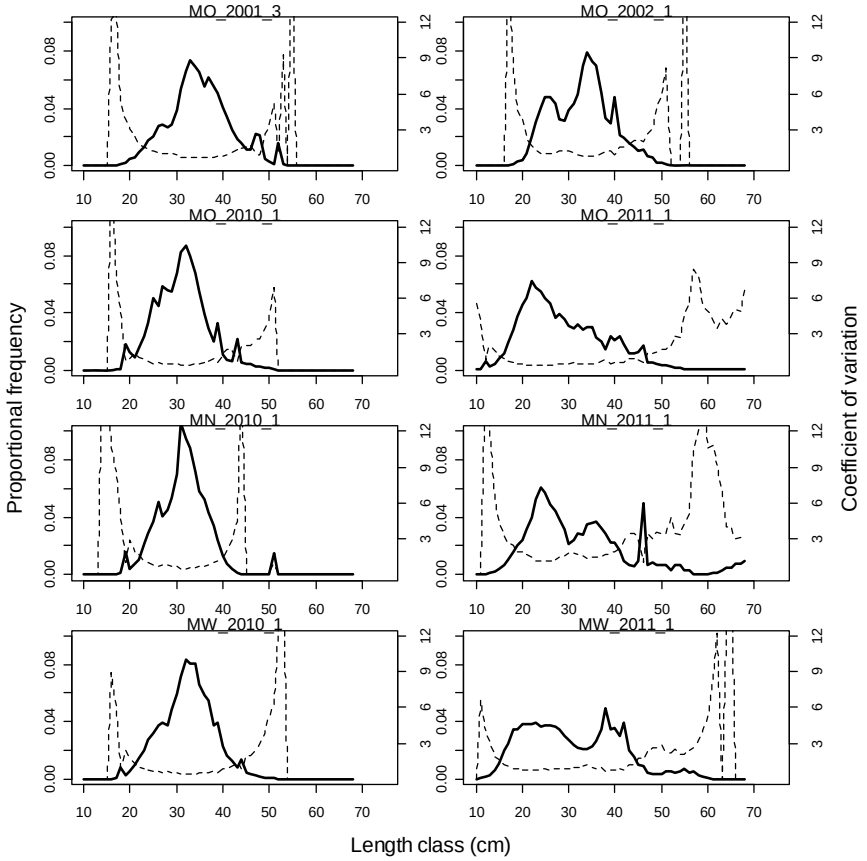

Figure 44: Proportional length frequencies and c.v.s for scampi counted within photo surveys.

3.7. Model assumptions and priors

Maximum Posterior Density (MPD) fits were found within CASAL using a quasi-Newton optimiser and the BETADIFF automatic differentiation package (Bull et al. 2008). Fitting was done inside the model except for the weighting of the length frequency data. For these, observation-error c.v.s were estimated using CALA, converted to equivalent observation-error multinomial *N*s, and used within the model. The appropriate multinomial *N*s to account for both observation and process error were then calculated from the model residuals, and these final *N*s were used in all models reported (Francis 2011). This generally resulted in small *N*s for the commercial length frequency data in particular, and therefore relatively low weighting within the model. CASAL was also used to run Monte-Carlo Markov Chains (MCMC) on the base models. MPD output was analysed using the extract and plot utilities in the CASAL library running under the general analytical package R.

The initial model was based on that described by Tuck & Dunn (2009, 2012). The model inputs include catch data, abundance indices (CPUE, trawl and photo surveys) and associated length frequency distributions. The parameters estimated by the base model include SSB_0 and R_0, and time series of SSB and year class strength for each subarea, selectivity parameters for commercial and research trawling, and the photo survey, and associated catchability coefficients. To reduce the number of fitted parameters, the catchability coefficients (*q*'s) for commercial fishing, research trawling, and photographic surveys were assumed to be nuisance rather than free parameters. The only informative priors used in the initial model were for *q-Photo* (or *q-Scampi* in some initial runs)*, q-Trawl*, and the YCS vector (which constrains the variability of recruitment).

Previous priors for scampi catchability have been largely based on information on *Nephrops* emergence and occupancy rates from European studies conducted in far shallower waters than *Metanephrops* populations inhabit (Tuck & Dunn 2012). The acoustic tagging study conducted at the Mernoo Bank in October 2010 offers an opportunity to estimate priors for occupancy and emergence from New Zealand data.

Acoustic tags were fitted to scampi, and released with a moored hydrophone which recorded tag detections, when animals were emerged from their burrows. Tag detections showed distinct cyclical patterns (with a 12.6 hour cycle), and detection over the duration of the study varied from 20–80%, with a daily median detection of 38.9%. On the basis of shallow water trials with the acoustic tags, and scampi observations, it is assumed that these detections include scampi in burrow entrances and scampi walking free on the seabed (all of which would be visible to the photographic survey). Estimates of the density of major burrow openings, all visible scampi, and scampi out of burrows are available from the survey conducted in October 2010 in SCI 3. An estimate of scampi density is provided by dividing the density of visible scampi by the rate of emergence.

Priors for three q terms have been estimated (Table 15).

3.7.1. q-Scampi

This is the proportion of the scampi population seen by the photo survey. The best estimate is 38.9% (emergence estimated by acoustic tags). Upper and lower estimates of emergence are arbitrarily set at 90% and 10%.

3.7.2. q-Photo

This is the proportion of the scampi population represented by the count of major burrow openings. The best estimate is 1.477 (major burrow openings divided by estimated scampi density). Upper and lower estimates are taken as the highest and lowest values calculated at the survey stratum level, assuming either 10% or 90% emergence.

3.7.3. q-Trawl

This is the proportion of the scampi population represented by the trawl survey catches. The best estimate is 0.094 (scampi out of burrows divided by estimated scampi density). Upper and lower estimates are taken as the highest and lowest values calculated at the survey stratum level, assuming either 10% or 90% emergence.

The bounds and best estimate were assumed to represent the 2.5^{th} 50^{th} and 97.5^{th} percentiles of the prior distribution. These values were fitted within a binomial GLM (probit link) to estimate the slope and intercept of the cumulative frequency distribution, which in turn were used to estimate the mean and standard deviation of the lognormal distribution of the prior (pers. comm. Murray Smith, NIWA.). The distributions of the priors are presented in Figure 45. The best estimates of the priors are quite similar to values used previously.

Table 15: Component factors for estimation of priors for *q-Scampi, q-Photo*, and *q-Trawl*.

	Lower	Best est.	Upper	Source
Major openings		$0.0653.m^{-2}$		Survey
Visible scampi		$0.0172.m^{-2}$		Survey
Scampi "out"		$0.0041.m^{-2}$		Survey
Scampi as % of openings	33%	26.29	9%	Visible/openings
% of scampi "out"	6%	24.13	31%	Out/visible
Median emergence	10%	38.9%	90%	Acoustic tags
Est. scampi density		$0.0442.m^{-2}$		Visible/emergence
Est. occupancy		67.73%		Est. density/major
q-Trawl	0.006	0.094	0.281	Out/Est. density
q-Scampi	0.10	0.389	0.90	Visible/Est. density
q-Photo	0.30	1.477	9.65	Major/Est. density

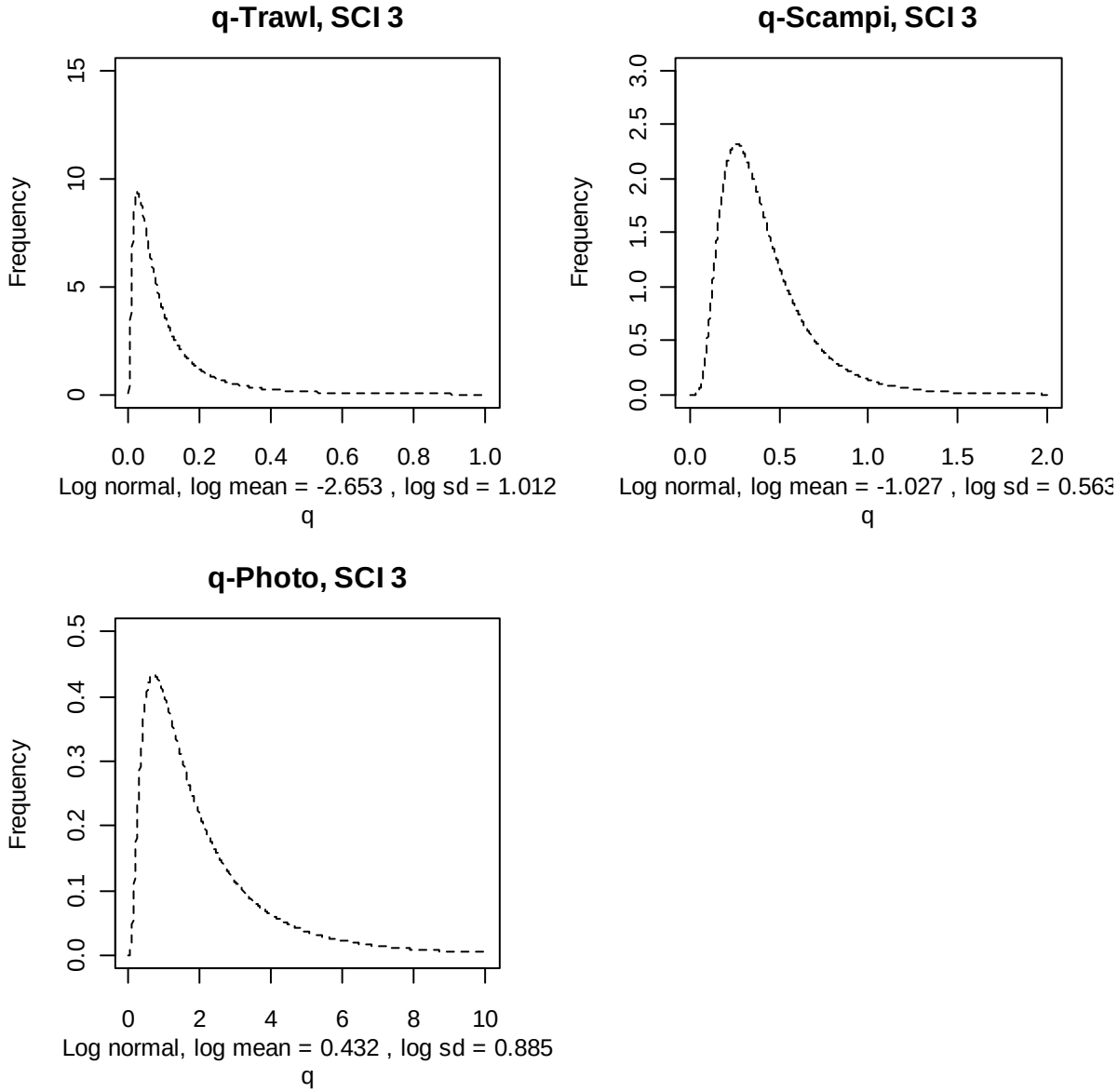

Figure 45: Estimated distribution of *q-Scampi*, *q-Photo*, and *q-Trawl*.

3.7.4. Recruitment

Few data are available on recruitment. Relative year class strengths were assumed to average 1.0 up to the last two years, and are fixed at 1 for these. In the initial model development (Cryer et al. 2005) lognormal priors on relative year class strengths were assumed, with mean 1.0 and c.v. 0.2, and the sensitivity of year class strength (YCS) variation was examined in further developments (Tuck & Dunn 2006). More recent model investigations, particularly those fitting the CPUE indices, suggest that the constraint on variability in YCS may be too severe, and the SFAWG suggested increasing the c.v (Tuck & Dunn 2012). In the current implementation, lognormal priors on relative year class strengths were assumed, with mean 1.0 and c.v. 1.0. The relationship between stock size and recruitment for scampi is unknown, and a Beverton Holt relationship with a steepness of 0.8 has been assumed. New Zealand scampi have very low fecundity (Wear 1976, Fenaughty 1989) (in the order of tens to hundreds of eggs carried by each female), so very successful recruitment is probably not plausible at low abundance. Recruitment enters the model partition as a year class, with a normally distributed OCL of mean 10 mm and c.v. 0.4.

4. ASSESSMENT MODEL RESULTS

4.1. Initial models

Initial models were developed in an iterative process, initially starting with only the MN data, and subsequently adding data from other areas. Initial runs with growth parameters from SCI 2 did not generate enough large scampi, and subsequent examination of the length frequencies from observer and research sampling suggested that growth parameters from SCI 6A would be more appropriate.

Model runs were conducted for SCI 6A in 2010 (Tuck & Dunn 2012), estimating growth parameters within the model from tag recapture data, but these model runs were not accepted by the Working Group as being sufficiently robust for use in management. In development of the starting models here, M was fixed at 0.2 (as in previous implementations), and growth was estimated (using the SCI 6A estimates as starting values) with selectivities fixed at previous estimates. Selectivities were then estimated with growth fixed, and the process repeated until stable values were reached. These new growth parameters were taken as the growth parameters for the base model. Sensitivity to faster and slower growth rates (Figure 46) was investigated. Parameters for these growth curves were generated by calculating equivalent von Bertalanffy parameters L_∞ and k from the base growth increments, multiplying the k term by 1.3 (fast growth) and 0.5 (slow growth), and then back calculating growth increments for the two new curves. A multiplier of 1.5 was initially examined for the fast growth option, but models with these growth parameters failed to converge.

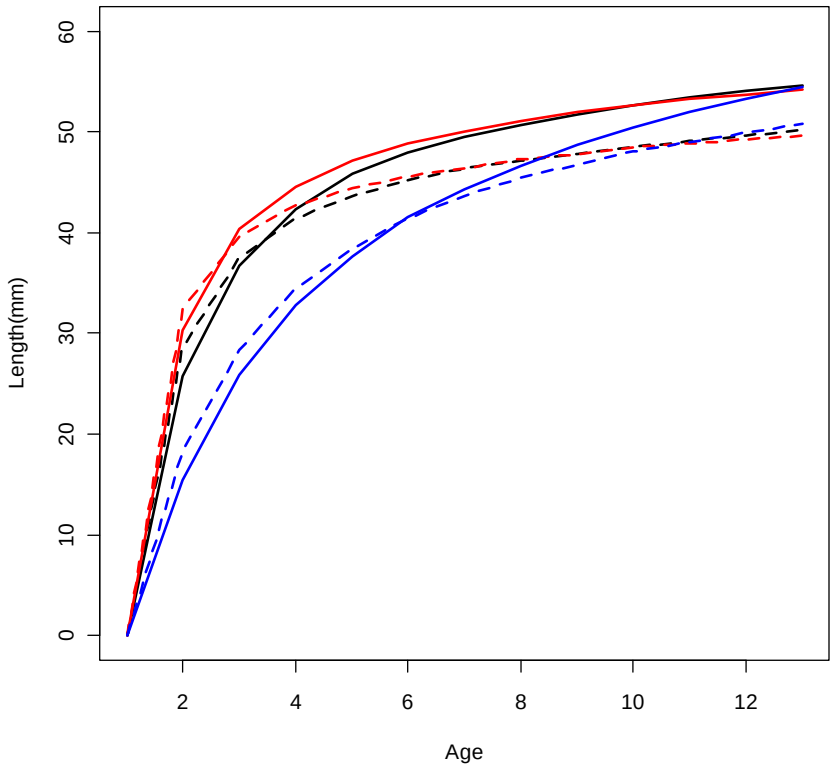

Figure 46: Growth curves for base case (black), fast (red), and slow (blue) sensitivity analyses. Male growth curve represented by solid line, female growth curve represented by dashed line.

A base model, and sensitivity to growth rate and natural mortality were investigated. Details of differences between models examined within sensitivity analysis are presented in Table 16. Key parameter and quantity estimates from the MPD fits for the models described in Table 17 are presented in Figure 47. In the model where growth was estimated, only the two increments for each sex were estimated, with the min_sigma term fixed (the Working Group did not consider it realistic to estimate all three parameters).

Table 16: General details of models examined within sensitivity analyses.

Model	M	Growth
Base	0.2	Fixed
Base-015	0.15	Fixed
Base-030	0.3	Fixed
Base-fast	0.2	Faster
Base-slow	0.2	Slower
Base-g-est	0.2	Estimated

Models attempting to estimate mortality (with or without estimating growth) failed to converge, and are not reported. Additionally, models using the visible scampi index (instead of the burrow index) estimated a *q-Scampi* of 1 (all scampi seen), which is considered very unlikely, and also suggested that the larger scampi were not seen. This has been interpreted as an issue related to measuring the carapace length of scampi when they are not horizontal, and these models are not reported.

Table 17: Estimated key parameters and quantities from MPD fits for SCI 3 models. M fixed in all models. Growth only estimated in Base-g-est model.

		Base	Base-015	Base-030	Base-fast	Base-slow	Base-g-est
MN	SSB_0	4 965	3 037	17 635	4 296	3 275	7 842
	$SSB_{current}$	2 548	1 115	10 863	2 288	1 401	4 425
	$SSB_{current}/SSB_0$	0.51	0.37	0.62	0.53	0.42	0.56
MO	SSB_0	3 081	1 615	11 862	2 664	1 838	5 081
	$SSB_{current}$	1 915	1 082	6520	1 809	1 332	3 529
	$SSB_{current}/SSB_0$	0.62	0.67	0.55	0.68	0.72	0.69
MW	SSB_0	4 668	2 442	17 608	4 112	2 778	7 671
	$SSB_{current}$	3 202	1 475	13 056	2 839	1 829	5 462
	$SSB_{current}/SSB_0$	0.69	0.60	0.74	0.69	0.66	0.71
	q-Photo	3.82	8.65	1.17	5.19	7.87	2.21
	q-Trawl	0.047	0.09	0.01	0.05	0.07	0.03
	M (fixed)*	*0.2*	*0.15*	*0.3*	*0.2*	*0.2*	*0.2*
	Male g20*	*14.44*	*14.44*	*14.44*	*16.90*	*8.71*	1 3.92
	Male g40*	*3.11*	*3.11*	*3.11*	*3.63*	*1.87*	2.56
	Female g20*	*14.72*	*14.72*	*14.72*	*16.70*	*9.44*	1 2.34
	Female g40*	*0.99*	*0.99*	*0.99*	*1.13*	*0.64*	-0.75
	min_sigma*	*5.55*	*5.55*	*5.55*	*5.55*	*5.55*	*5.55*

*- values in italics fixed within model.

Across the six models examined, the proportional breakdown of SSB_0 between areas was very consistent, with 33% in MN, 26% in MO and 41% in MW. Brief descriptions of the MPD fits for each model are provided below. Model stock trajectory plots and diagnostics are provided

in the appendices as indicated. Key plots are provided for the base model below, while others, and plots for other models are provided in the appendices.

Base model (standard growth, M=0.2)(Appendix 3)
MPD suggests SSB_0 estimates of about 5000 t, 3000 t and 4700 t for MN, MO and MW respectively (Figure 48). The trajectories of SSB all showed an initial decrease to about 1995, an increase to a peak biomass in 1999, and a steady decline thereafter to 2009, with evidence of an increase in the most recent year (2011) in MN and MW (Figure 48). A very strong year class was estimated for all areas in the early 1990s, with better than average YCS also estimated at the end of the series for MN and MW. The increase in abundance in the most recent years estimated by the model was observed in the CPUE (Figure 49), trawl (Figure 50) and photo survey data (Figure 48), but there was no evidence of a recent strong year class in the length frequency data either in the early 1990s or the most recent years (shown in Appendix 3). Fits to abundance indices were reasonable, and the seasonal patterns in sex ratio observed in the catch composition data were reflected in the estimated selectivities, with maximum availability higher for males in time step 1 for both the commercial and trawl survey data (when females are moulting), and lower for males in time step 2 (when males are moulting). Current SSB was estimated to be between 50 and 70% of respective SSB_0. Estimates for *q-Photo* and *q-Trawl* were 3.82 and 0.047 (Table 17). Fits to LFs for research surveys (trawl and photo) were better than those for commercial catches.

Likelihood profiles when SSB_0 is fixed in the model were relatively flat, indicating that a range of biomass values were equally plausible.

Natural mortality (Base-015 and Base-030) (Appendix 4 and Appendix 5)
The model was sensitive to the assumption on natural mortality, with SSB_0 estimates being lower when M=0.15, and substantially higher when M=0.3. The Base-015 model estimated a steeper decline in SSB for the MN subarea (SSB_{curr} 37% of SSB_0), but a similar stock trajectory for the other subareas (Figure 47). As with the base model, a very strong year class was estimated for all areas in the early 1990s, with better than average YCS also estimated at the end of the series (all areas). Estimates for *q-Photo* and *q-Trawl* were 8.65 and 0.09 (Table 17). Fits to abundance indices were reasonable, and the selectivities showed the same pattern with timestep as the base model, reflecting observed sex ratios in catches. Fits to LFs for research surveys (trawl and photo) were better than commercial catches. The Base-030 model estimated similar stock trajectory to the base model, although with a greater range of % SSB_0 for some areas. The recruitment pattern was similar to the Base model (although there was an additional good recruitment year in the late 1990s for MN). Estimates for *q-Photo* and *q-Trawl* were 1.17 and 0.01. Fits to LFs for research surveys (trawl and photo) are better than commercial catches.

Growth (Base-fast, Base-slow, Base-g-est)(Appendix 6 to 8)
The model appeared less sensitive to the changes in growth examined than to the changes in natural mortality (Table 17). Allowing the model to estimate the growth parameters resulted in a very similar growth curve to the base model for males, but a smaller maximum size for females (although a similar growth rate)(Figure 51**Error! Reference source not found.**). Both the faster and slower growth sensitivity analyses estimated lower SSB_0 values than the base model, but the model with growth estimated provided higher SSB_0 values. Both the fast and estimated growth sensitivity analyses estimated very similar stock trajectories to the base model, while the slow growth model estimated a smaller peak biomass in the late 1990s, but a relatively similar stock status (% SSB_0) by 2011 (Figure 47). Estimates for *q-Photo* ranged from 2.21 (estimated growth) to 7.87 (slow growth) while *q-Trawl* ranged from 0.03 (estimated growth) to 0.07 (slow growth)(Table 17). Fits to the abundance indices and LFs were comparable between models, as were estimated YCS patterns (although the good recruitment in recent years was estimated to be larger in the slow growth model).

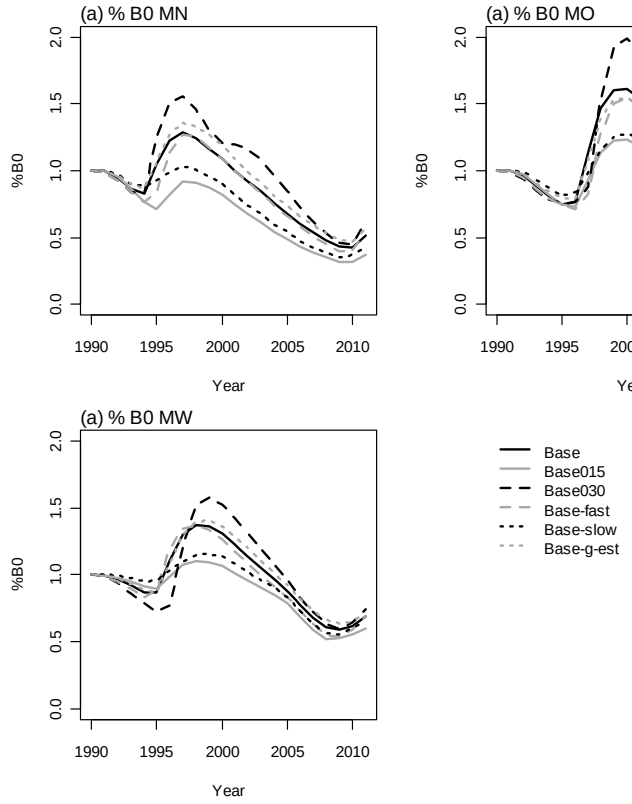

Figure 47: Comparison of trajectory of SSB as a percentage of B_0 for each subarea from the MPD fits to the sensitivity models. Model details provided in Table 16.

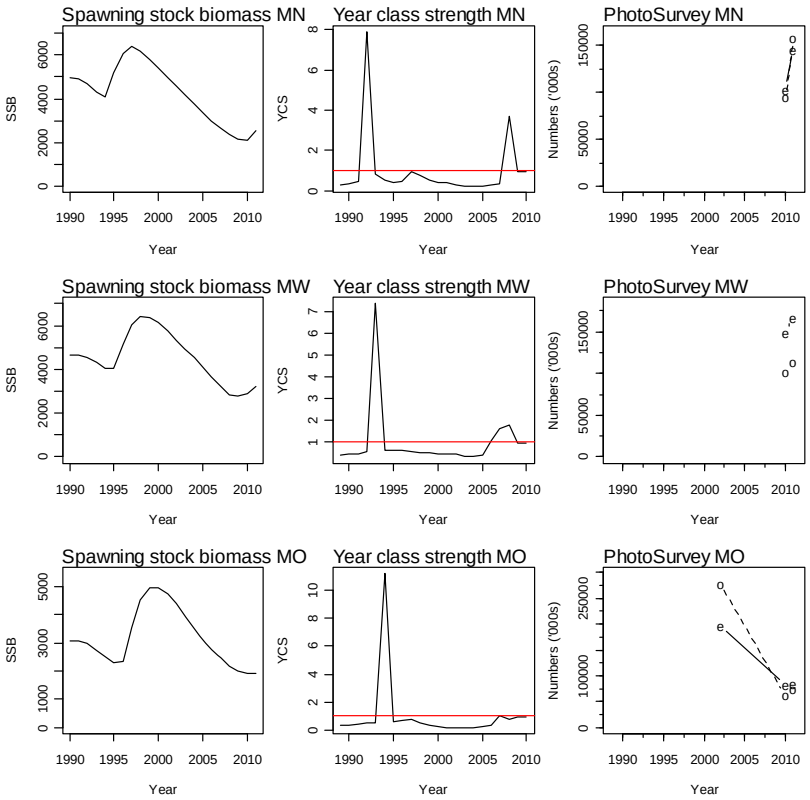

Figure 48: Spawning stock biomass trajectory (left column), year class strength (middle column) and fits to photo survey abundance index (right column) for each subarea of SCI 3 for base model.

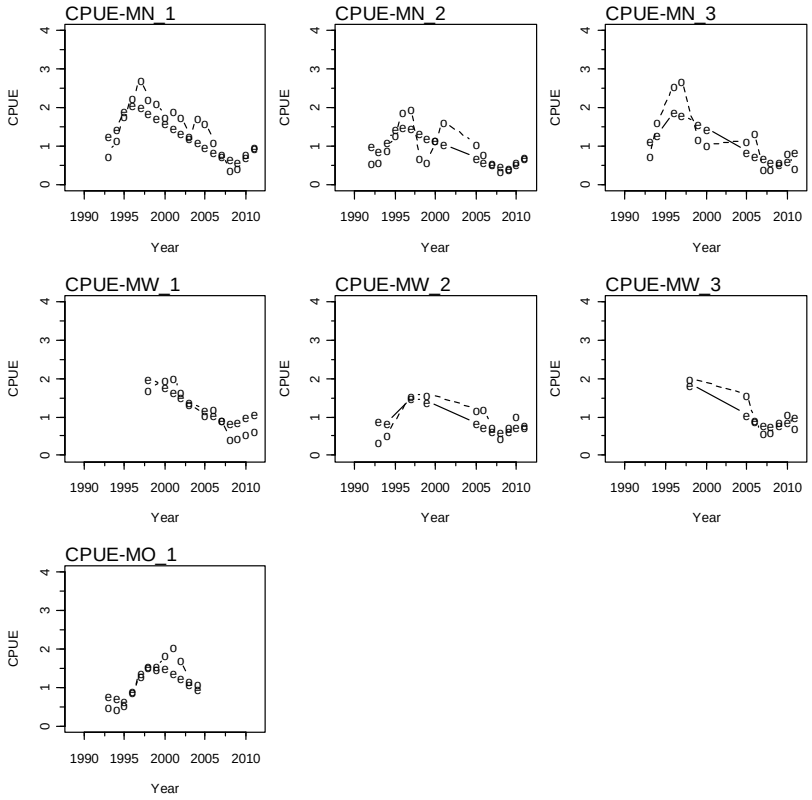

Figure 49: Fits to CPUE indices by subarea (row) and timestep (column) (o – observed value, e – expected value).

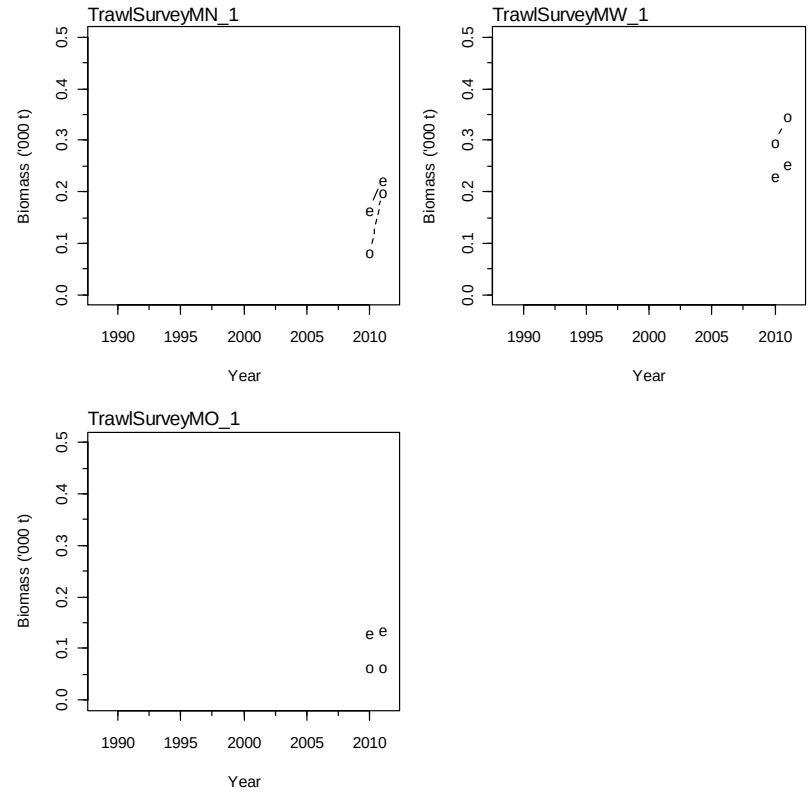

Figure 50: Fits to trawl survey indices (o – observed value, e – expected value).

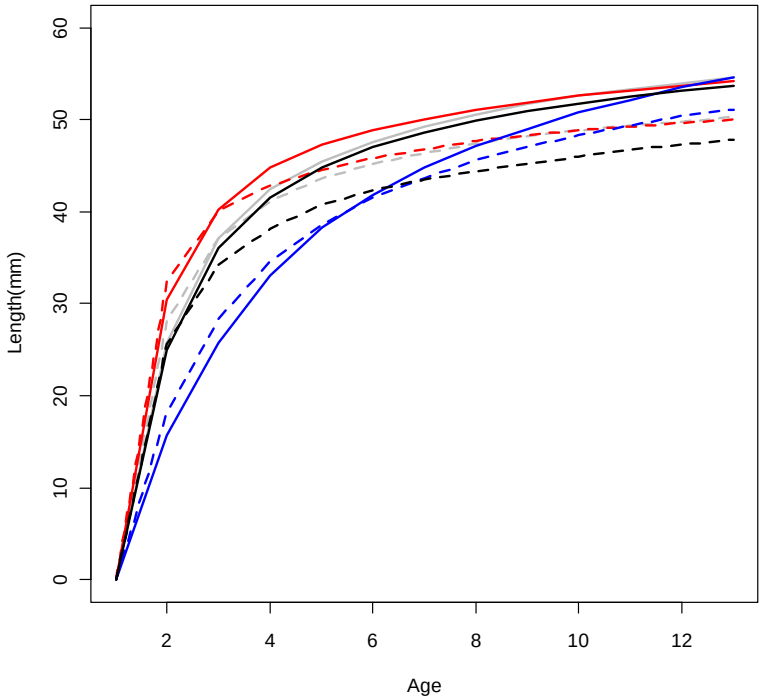

Figure 51: Growth curves for estimated growth (black), base case (grey), fast (red), and slow (blue) sensitivity analyses. Male growth curve represented by solid line, female growth curve represented by dashed line.

4.2. MCMC runs

MCMCs were started at the MPD for each model, and run for 5 million simulations, with every thousandth sample saved, giving a set of 5000 samples. MCMC runs were initially investigated with an upper limit of 30 000 tonnes biomass for each sub-area (limit set on the basis of MPD estimates). These runs had a small proportion of simulations (typically 2% or less) close to either SSB_0 or *q-Photo* bounds. Increasing the bounds led to a shift in the distribution of parameter estimates.

Further investigations were undertaken for the BASE and BASE-g-est models, relaxing the SSB_0 bounds, and trace plots are presented for key parameters within the relevant Appendix for each of these models. The Working Group agreed that none of the SCI 3 assessment models could be accepted. Although the MPD runs for the various sensitivity options appeared reasonably similar in their perception of stock status (SSB_{curr}/SSB_0), MCMCs were very variable, and showed little evidence of convergence.

4.3. Worst case options

The WG requested investigations into the worst case option from the MPD runs. This was investigated through examining stock status across a range of SSB_0 levels for the Base and growth estimated models, extracting the run outputs from a likelihood profile analysis.

Base case model (growth fixed, M=0.2)

B_0 for the MN subarea was fixed at values from 2000 to 15 000 t (500 t intervals), and all other parameters normally estimated within the model were estimated. The MPD estimate for the MN B_0 was 4965 tonnes with the base model.

Plots of *q-Photo*, *q-Trawl* and B_{2011}/B_0 across the range of fixed B_0 values are shown in Figure 52. For undertaking this likelihood analysis the bounds on the priors were relaxed, but within the original development of the distribution for the prior on *q-Photo*, the upper bound was set at an arbitrary level of 10 (one scampi maintains ten counted burrows). Our current best estimate of *q-Photo* is 1.47 (from acoustic tag emergence data and counts of visible animals and burrows). If we take 10 as a maximum possible *q-Photo* value, then the smallest B_0 values are not feasible.

Trajectories of $\%B_0$ and YCS are shown in Figure 53 and Figure 54. The B_0 trajectories show a very similar shape, but vary between cases in the magnitude of the change in SSB relative to B_0. The trajectories of YCS are all very similar. Excluding profile runs where *q-Photo* was estimated to be greater than 10 leaves the run with B_0 set to 3000 t as the most pessimistic option. This run has a *q-Photo* estimate of 7.9, and a $\%B_0$ trajectory that drops to a minimum of 34% B_0 for MN in 2010, increasing to 41% in 2011. The MO and MW subareas are estimated to be at 57% and 60% B_0, respectively.

Base-g-est model (growth estimated, M=0.2)

SSB_0 for the MN subarea was fixed at values from 2000 to 30 000 t (1000 t intervals), and all other parameters normally estimated within the model were estimated. The MPD estimate for the MN SSB_0 was 7 842 tonnes with the base-g-est model.

Plots of *q-Photo*, *q-Trawl* and SSB_{2011}/SSB_0 across the range of fixed SSB_0 values are shown in Figure 55. For undertaking this likelihood analysis the bounds on the priors were relaxed, but within the original development of the distribution for the prior on *q-Photo*, the upper bound was set at an arbitrary level of 10 (one scampi maintains ten counted burrows). Our current best estimate of *q-Photo* is 1.47 (from acoustic tag emergence data and counts of visible animals and burrows). If we take 10 as a maximum possible *q-Photo* value, then the smallest SSB_0 values are not feasible.

Trajectories of $\%SSB_0$ and YCS are shown in Figure 56 and Figure 57. The SSB_0 trajectories show a very similar shape, but vary between cases in the magnitude of the change in SSB relative to SSB_0. The trajectories of YCS are all quite similar, although one model estimates a slightly later recruitment peak than the other models. Growth is estimated within this model, and differences in growth parameters may also contribute to differences between estimated stock trajectories and YCSs. Excluding profile runs where *q-Photo* was estimated to be greater than 10 leaves the run with SSB_0 set to 3000 t as the most pessimistic option. As with the Base model, this run has a *q-Photo* estimate of 7.9, but the $\%SSB_0$ trajectory drops to a minimum of 35% SSB_0 for MN in 2009, increasing to 44% in 2011. The MO and MW subareas are estimated to be at 61% and 62% SSB_0, respectively.

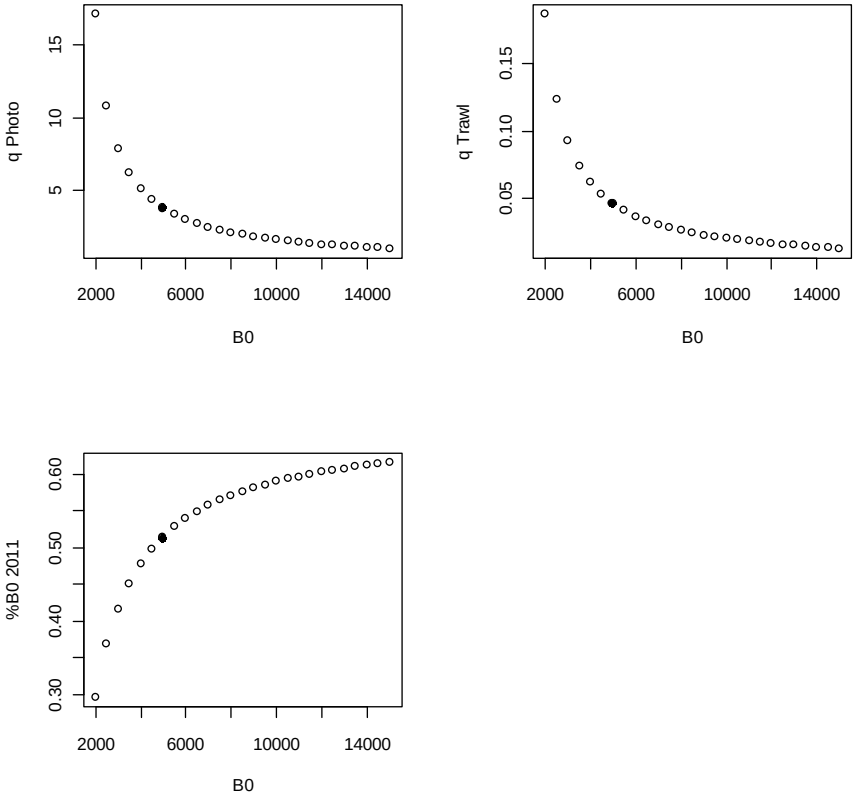

Figure 52: Plots of *q-Photo*, *q-Trawl* and SSB_{2011}/SSB_0 for Base case models across a range of fixed SSB_0 values for subarea MN. MPD estimate shown as solid symbol.

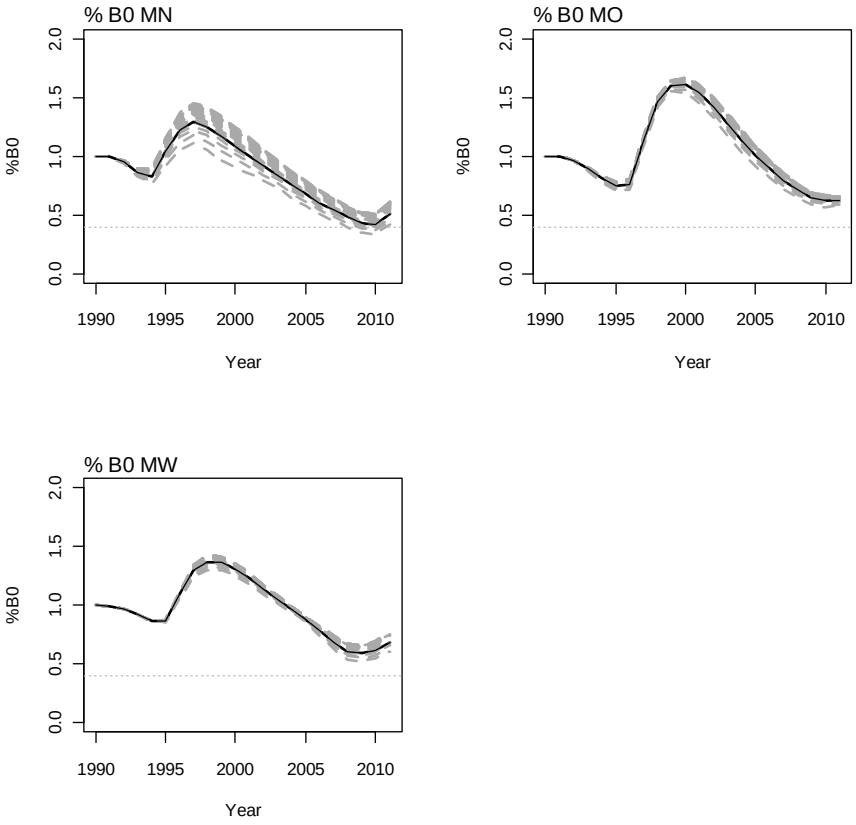

Figure 53: Plots of stock trajectory (%SSB_0) for Base case models across a range of fixed SSB_0 values for subarea MN. MPD estimate shown as solid black line.

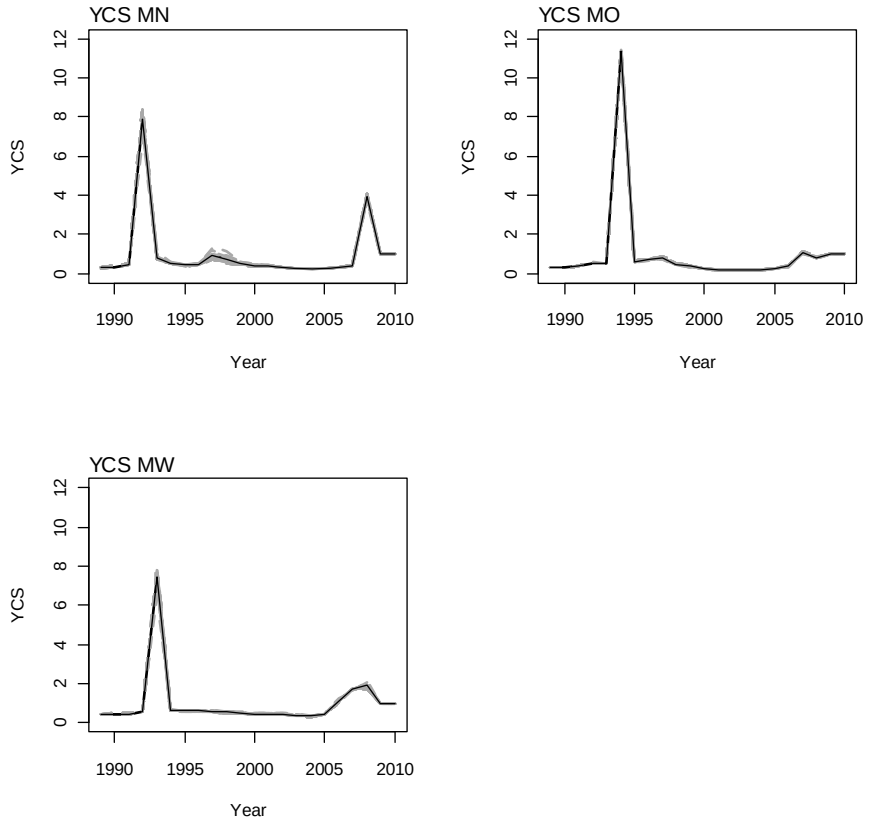

Figure 54: Plots of YCS for Base case models across a range of fixed SSB_0 values for subarea MN. MPD estimate shown as solid black line.

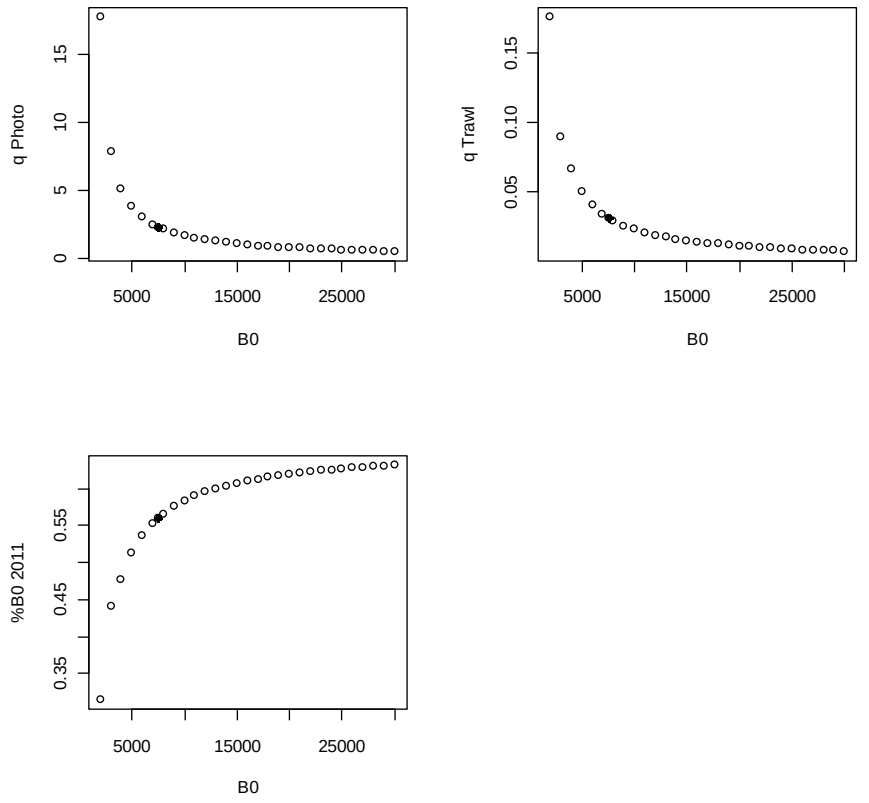

Figure 55: Plots of *q-Photo*, *q-Trawl* and SSB_{2011}/SSB_0 for Base-g-est case models across a range of fixed B_0 values for subarea MN. MPD estimate shown as solid symbol.

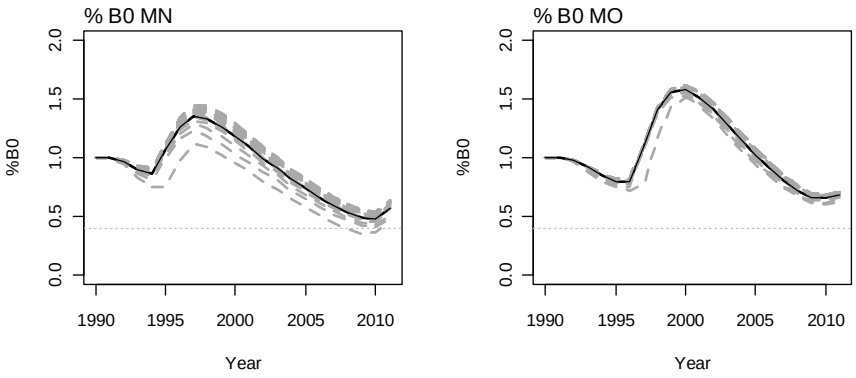

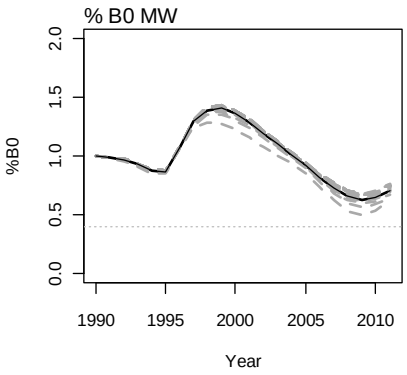

Figure 56: Plots of stock trajectory ($\%SSB_0$) for Base-g-est case models across a range of fixed SSB_0 values for subarea MN. MPD estimate shown as solid black line.

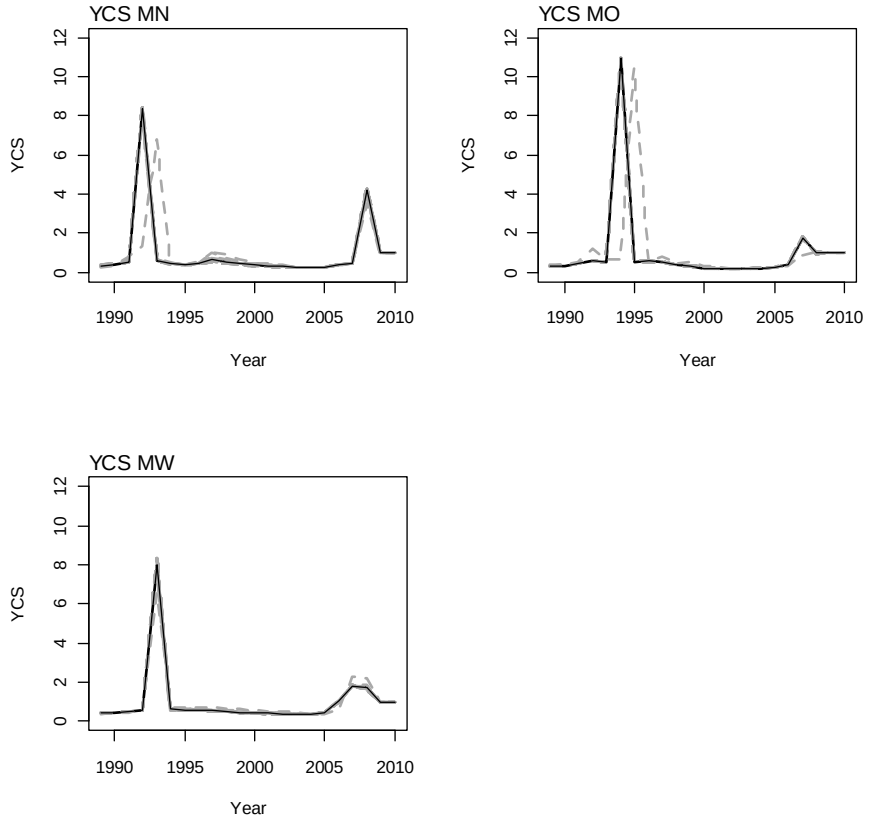

Figure 57: Plots of YCS for Base-g-est case models across a range of fixed SSB_0 values for subarea MN. MPD estimate shown as solid black line.

5. DISCUSSION

The management history of the SCI 3 fishery has led to a shift in the spatial and temporal pattern in activity, with the start of the fishing year focussed activity within the old QMA 3 area largely replaced by effort more evenly distributed through the year within areas formerly managed within QMA 4. Seasonal patterns in sex ratio of catches related to moulting have been identified, and a model time step structure proposed to account for this. Standardised CPUE indices were calculated by sub-area and time step, from TCEPR data recorded from a group of core vessels, taking into account for each time of day, fishing duration, vessel and gear modifications to reduce bycatch.

A three area, length-based assessment model was developed to allow for the spatial change in fishing pattern over time, with other parameters (growth, mortality, selectivity and catchability) shared across the three sub-areas. CPUE indices, trawl survey and photo survey data were fitted as abundance indices, with associated length frequency distributions.

A base model was developed, with sensitivity analyses examined to assumptions on natural mortality and growth. The different models estimated different levels of biomass, but generally similar stock trajectories, with biomass in all three sub-areas declining from a peak in the late 1990s to a minimum in the late 2000s, and stabilising or increasing in the most recent years. The model was sensitive to assumptions about natural mortality, but appeared less sensitive to growth. The models consistently estimated a very strong year class in the early 1990s (across all areas) and above average year class strength in 2009 for some areas. While the above average 2009 YCS is somewhat corroborated by subsequent increases in CPUE and the survey

indices, the very high YCS value in the early 1990s appears to be the model's interpretation of the increase in CPUE in the mid-1990s, no trawl survey data prior to 2001 being included in the model. Neither of these increases in YCS were supported by evidence of strong recruitment in the length frequency data. MCMCs did not suggest that the models had converged, and none of the models were accepted by the Shellfish Fisheries Assessment Working Group.

The Working Group did consider investigating worst case options from the models to be useful, and so the worst case (lowest % SSB_0) conditions were identified for the base case and growth estimated model (excluding options where *q-Photo* values were considered implausible). These worst case options suggested that the biomass in the MN sub-area fell to about 35% of SSB_0 in 2009, but was over 40% by 2011. Biomass in the other sub-areas was estimated to be about 60% in these worst case options.

6. ACKNOWLEDGEMENTS

This work was funded by the Ministry of Primary Industries under project DEE201002SCI, and builds on a series of scampi assessment projects funded by the Ministry. We thank the many NIWA and Ministry for Primary Industries staff who measured scampi over the years, and the members of the NIWA scampi image reading team. Development of the model structure benefitted greatly from discussions at a series of meetings of the Scampi Assessment Workshop. This report benefitted considerably from a review by Chris Francis.

7. REFERENCES

Bentley, N.; Kendrick, T.H.; Starr, P.J.; Breen, P.A. (2012). Influence plots and metrics: tools for better understanding fisheries catch-per-unit-effort standardisations. *ICES Journal of Marine Science 69*: 84-88.

Bull, B.; Dunn, A. (2002). Catch-at-age: User manual v 1.06.2002/09/12. *NIWA Internal Report 114*.

Bull, B.; Francis, R.I.C.C.; Dunn, A.; McKenzie, A.; Gilbert, D.J.; Smith, M.H.; Bian, R. (2008). CASAL (C++ algorithmic stock assessment laboratory). *NIWA technical Report 130*.

Chapman, C.J.; Johnstone, A.D.F.; Urquhart, G.G. (1974). Preliminary acoustic tracking studies on *Nephrops norvegicus*. Department of Agriculture and Fisheries for Scotland, Marine Laboratory Internal Report. 15 p. (Unpublished report held by FRS Marine Laboratory, Aberdeen.)

Charnov, E.L.; Berrigan, D.; Shine, R. (1983). The M/*k* ratio is the same for fish and reptiles. *Amer Naturalist 142*: 707-711.

Cryer, M. (2000). A consideration of current management areas for scampi in QMAs 3, 4, 6A and 6B. Final Research Report for Ministry of Fisheries Project MOF1999-04K. 52 p. (Unpublished report held by MFish, Wellington)

Cryer, M.; Coburn, R. (2000). Scampi stock assessment for 1999. *New Zealand Fisheries Assessment Report 2000/7*.

Cryer, M.; Dunn, A.; Hartill, B. (2005). Length-based population model for scampi (*Metanephrops challengeri*) in the Bay of Plenty (QMA 1). *New Zealand Fisheries Assessment Report 2005/27*: 55.

Cryer, M.; Stotter, D.R. (1999). Movement and growth rates of scampi inferred from tagging, Alderman Islands, western Bay of Plenty. *NIWA technical Report (49)*.

Fenaughty, C. (1989). Reproduction in *Metanephrops challengeri*. Unpubl. Rep. MAF Fisheries, Wellington. 46 p. (Unpublished report held by Ministry for Primary Industries, Wellington)

Francis, R.I.C.C. (1988). Maximum likelihood estimation of growth and growth variability from tagging data. *New Zealand journal of Marien and Freshwater Research 22*: 43–51.

Francis, R.I.C.C. (1999). The impact of correlations in standardised CPUE indices. New Zealand Fisheries Assessment Research Document 99/42. 30 p. (Unpublished report held by NIWA library, Wellington.)

Francis, R.I.C.C. (2011). Data weighting in statistical fisheries stock assessment models. *Canadian Journal Fisheries and Aquatic Science 68*: 1124-1138.

Francis, R.I.C.C.; Bian, R. (2011). Catch-at-length and -age (CALA) User Manual. 83 p. (NIWA Unpublished Report)

McCullagh, P.; Nelder, J.A. (1989). Generalised Linear Models. 2nd Ed. Chapman and Hall, London. 511

Pauly, D. (1980). On the interrelationships between natural mortality, growth parameters, and mean environmental temperature in 175 fish stocks. *Journal du Conseil International pour l'Exloration du Mer 39*: 175-192.

Starr, P.J. (2009). Rock lobster catch and effort data: summaries and CPUE standardisations, 1979–80 to 2007–08. *New Zealand Fisheries Assessment Report 2009/38*: 73p.

Starr, P.J.; Breen, P.A.; Kendrick, T.H.; Haist, V. (2009). Model and data used for the 2008 stock assessment of rock lobsters (*Jasus edwardsii*) in CRA 3. *New Zealand Fisheries Assessment Report 2009/22*: 62pp.

Tuck, I.D. (2009). Characterisation of scampi fisheries and the examination of catch at length and spatial distribution of scampi in SCI 1, 2, 3, 4A and 6A. *New Zealand Fisheries Assessment Report 2009/27*: 102.

Tuck, I.D. (2010) Scampi burrow occupancy, burrow emergence and catchability. *Final Research Report for Ministry of Fisheries research project 2010/13.* 58 p.

Tuck, I.D.; Dunn, A. (2006). Length based population model for scampi (*Metanephrops challengeri*) in the Bay of Plenty (SCI 1) and Wairarapa / Hawke Bay (SCI 2). Final Research Report for Ministry of Fisheries research project SCI2005-01. 93 p. (Unpublished report held by MFish, Wellington.)

Tuck, I.D.; Dunn, A. (2009). Length-based population model for scampi (*Metanephrops challengeri*) in the Bay of Plenty (SCI 1) and Wiararapa / Hawke Bay (SCI 2). Final Research Report for Ministry of Fisheries research projects SCI2006-01 & SCI2008-03W. 30 p. (Unpublished report held by MFish, Wellington.)

Tuck, I.D.; Dunn, A. (2012). Length-based population model for scampi (*Metanephrops challengeri*) in the Bay of Plenty (SCI 1), Wiararapa / Hawke Bay (SCI 2) and Auckland Islands (SCI 6A). *New Zealand Fisheries Assessment Report 2012/1*: 125pp.

Tuck, I.D.; Hartill, B.; Parkinson, D.; Drury, J.; Smith, M.; Armiger, H. (2009a). Estimating the abundance of scampi - Relative abundance of scampi, *Metanephrops challengeri*, from a photographic survey in SCI 6A (2009). Final Research Report for Ministry of Fisheries research project SCI2008-01. 26 p. (Unpublished report held by MFish, Wellington.)

Tuck, I.D.; Hartill, B.; Parkinson, D.; Harper, S.; Drury, J.; Smith, M.; Armiger, H. (2009b). Estimating the abundance of scampi - Relative abundance of scampi, *Metanephrops challengeri*, from a photographic survey in SCI 1 and SCI 6A (2008). Final Research Report for Ministry of Fisheries research project SCI2007-02. p. (Unpublished report held by MFish, Wellington.)

Vignaux, M. (1994). Catch per unit effort (CPUE) analysis of west coast South Island and Cook Strait spawning hoki fisheries, 1987–93. *New Zealand Fisheries Assessment Research Document 94/11*: 29p.

Wear, R.G. (1976). Studies on the larval development of *Metanephrops challengeri* (Balss, 1914) (Decapoda, Nephropidae). *Crustaceana 30*: 113-122.

8. APPENDIX 1. Fishing activity by vessel for each subarea.

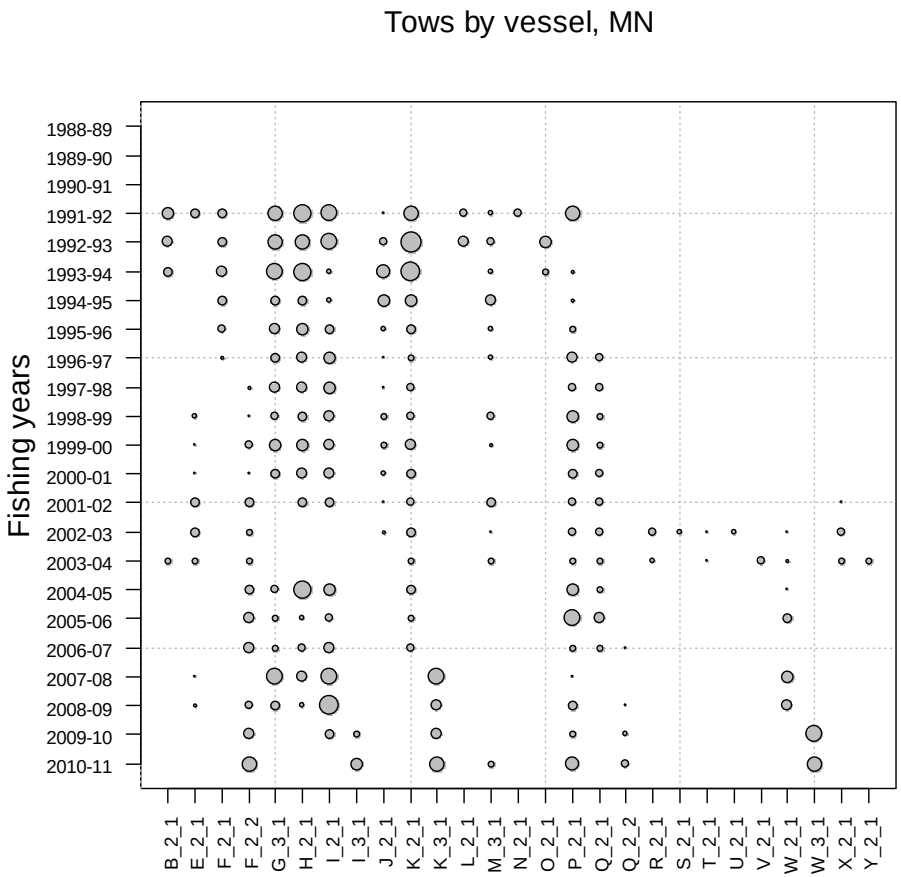

A1. 1: Pattern of fishing activity by vessel and fishing year for the subarea MN of SCI 3. Vessels labelled as Vessel_gear configuration_engine. The area of the circles is proportional to the number of tows recorded; the largest circle represents 292 tows.

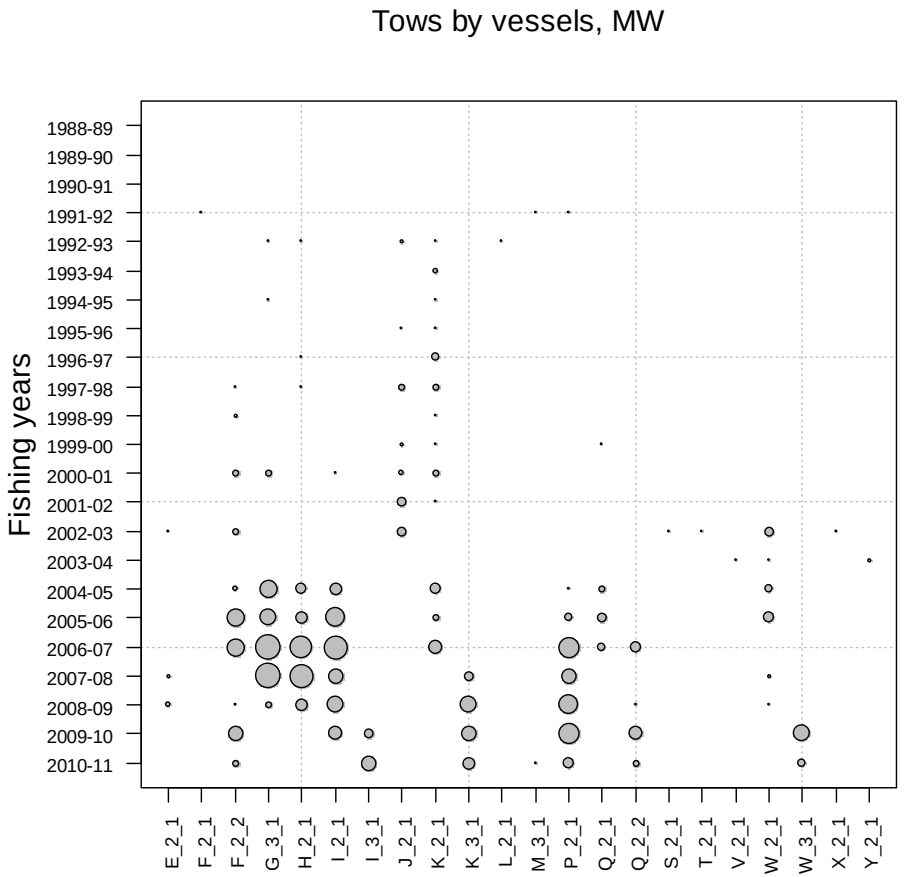

A1. 2: Pattern of fishing activity by vessel and fishing year for the subarea MW of SCI 3. Vessels labelled as Vessel_gear configuration_engine. The area of the circles is proportional to the number of tows recorded; the largest circle represents 327 tows.

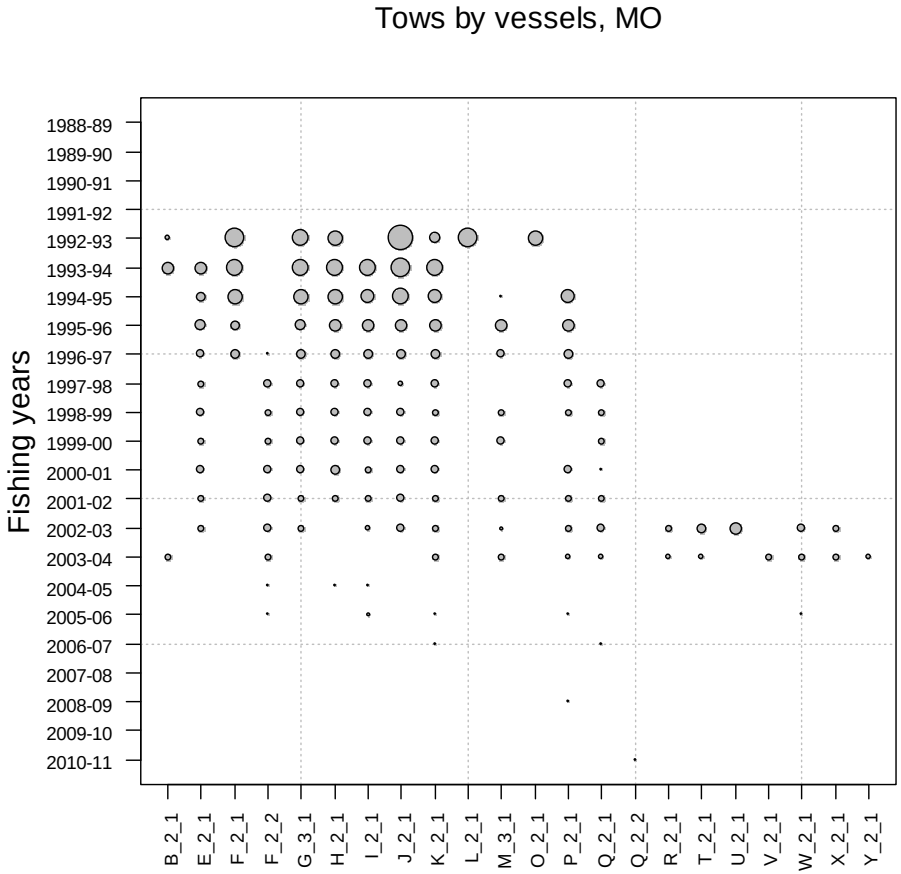

A1. 3: Pattern of fishing activity by vessel and fishing year for the subarea MO of SCI 3. Vessels labelled as Vessel_gear configuration_engine. The area of the circles is proportional to the number of tows recorded; the largest circle represents 197 tows.

9. APPENDIX 2. Diagnostic plots for final CPUE standardisation model.

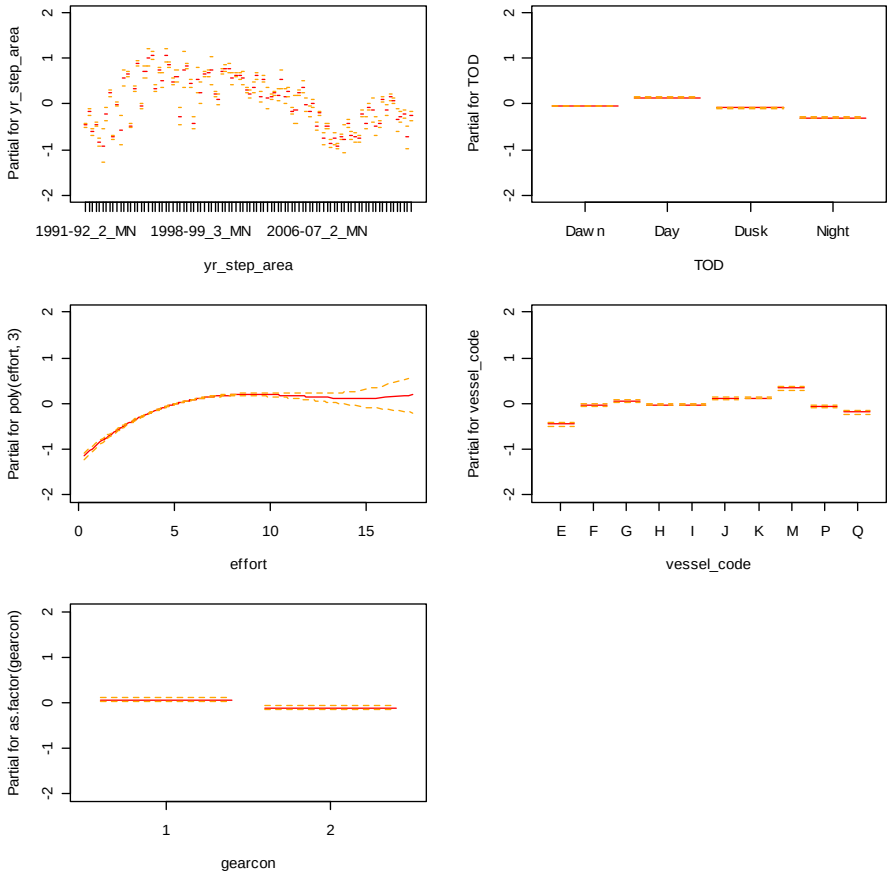

A2. 1: Termplot for final standardisation model (Table 7).

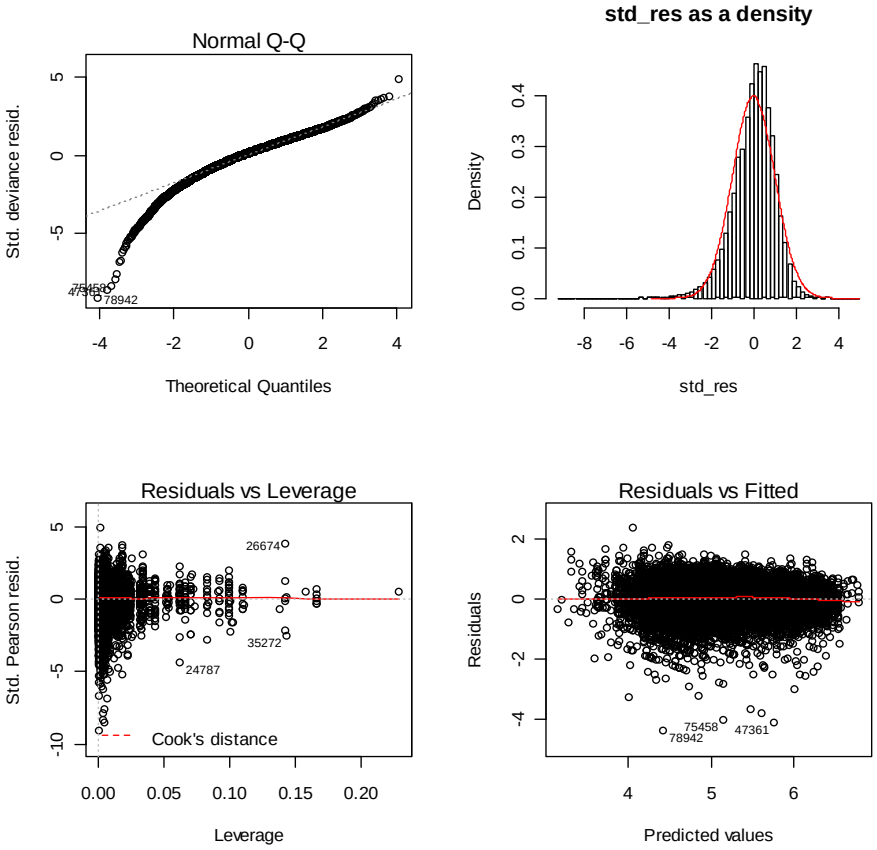

A2. 2. Diagnostic plots for final standardisation model (Table 7).

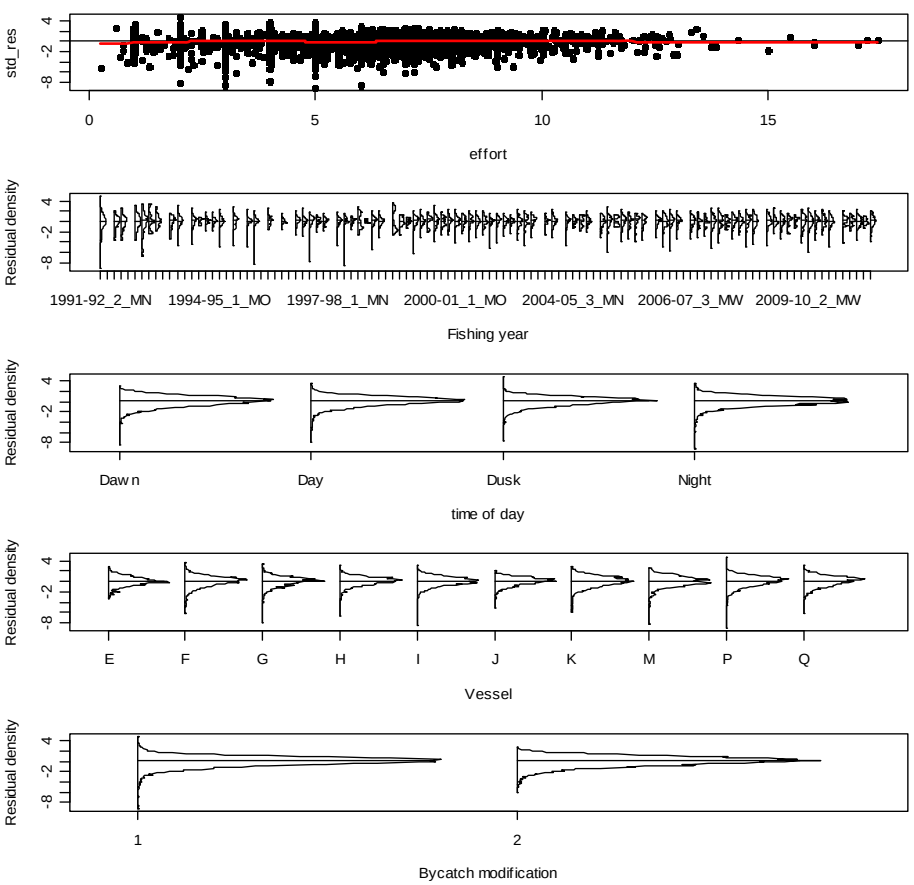

A2. 3: Distributions of residuals for final standardisation model (Table 7).

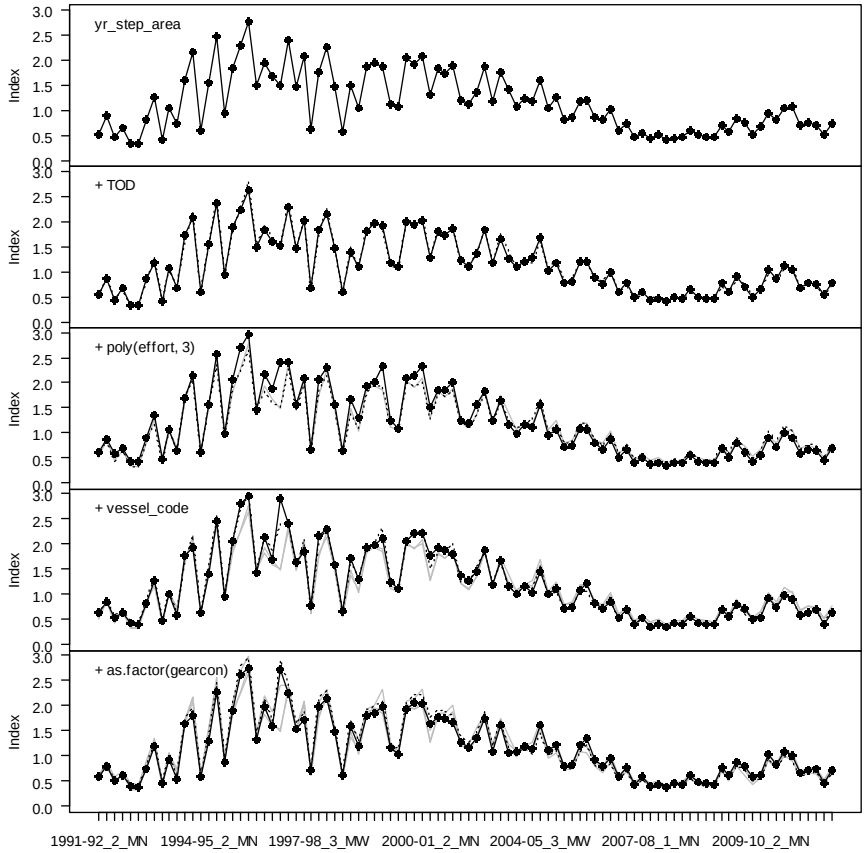

A2. 4: Step influence plot for final standardisation model (Table 7).

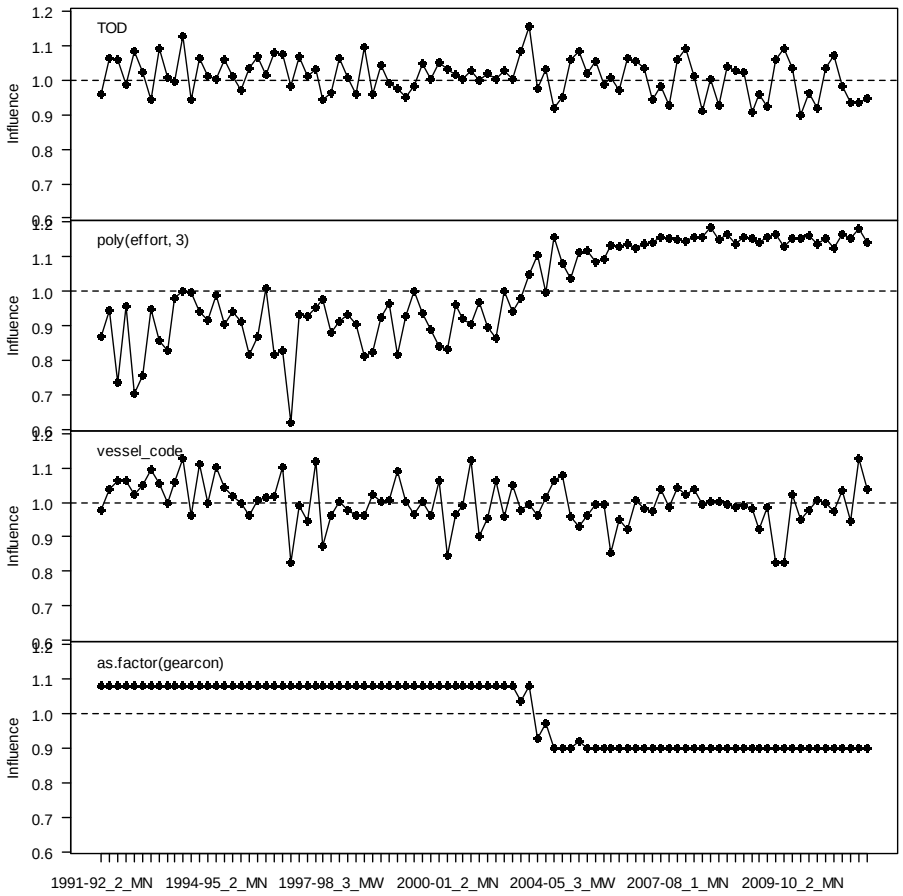

A2. 5: Year_timestep_sub-area inflence plots for each explanatory variable for final standardisation model (Table 7).

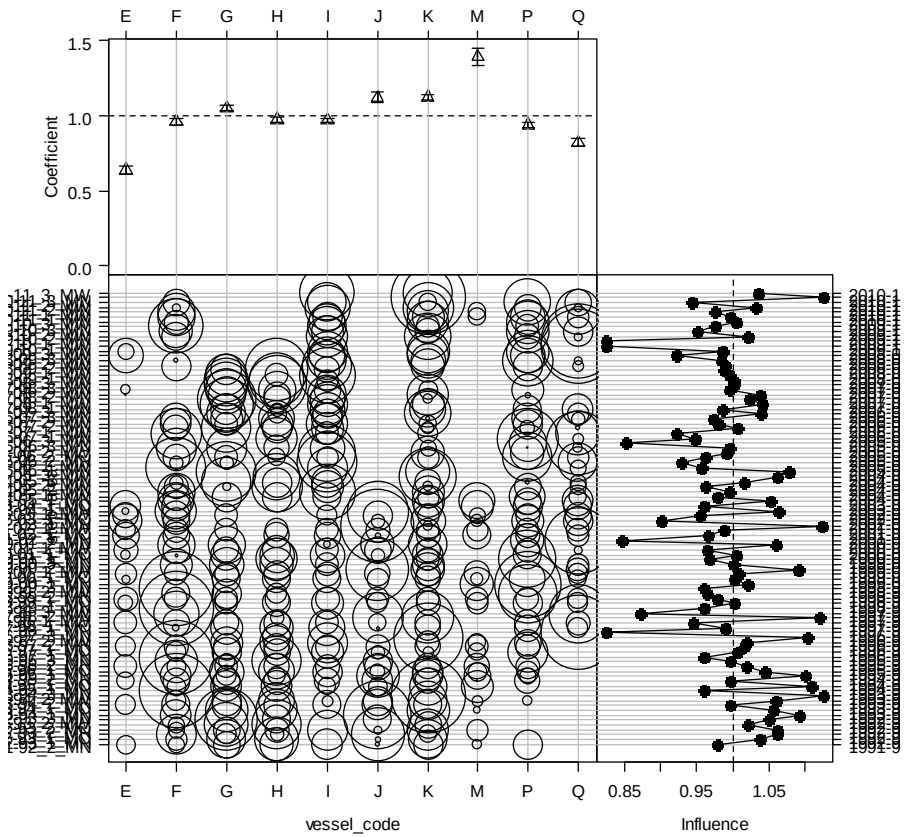

A2. 6: Coefficient-distribution_inflence plot for vessel for final standardisation model (Table 7).

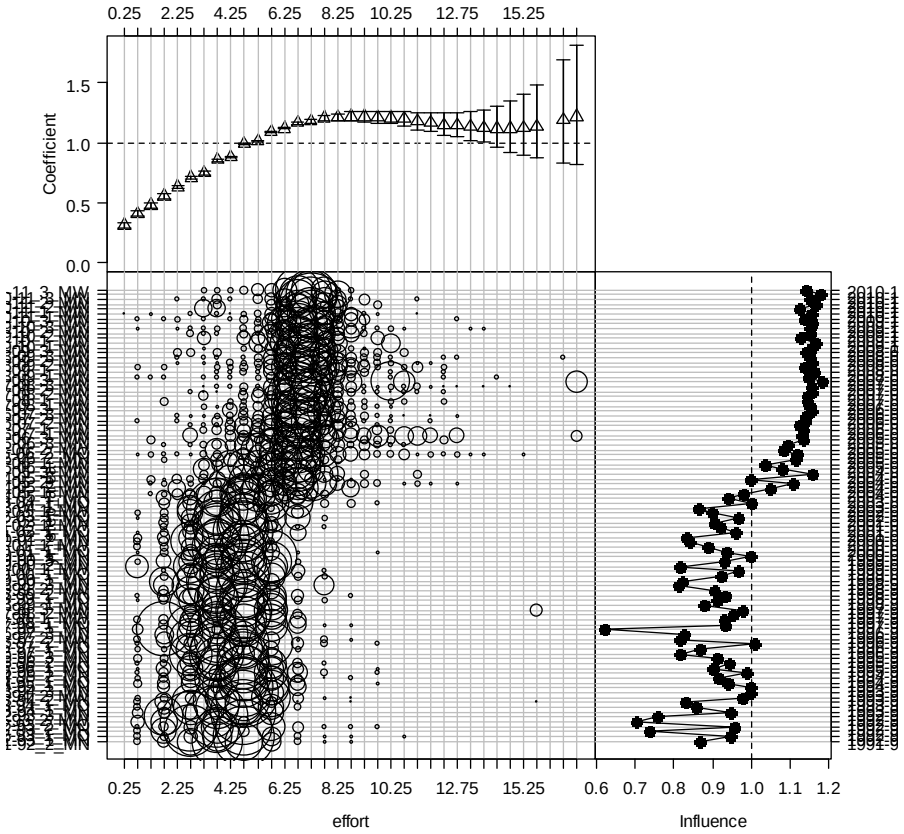

A2. 7: Coefficient-distribution_inflence plot for effort for final standardisation model (Table 7).

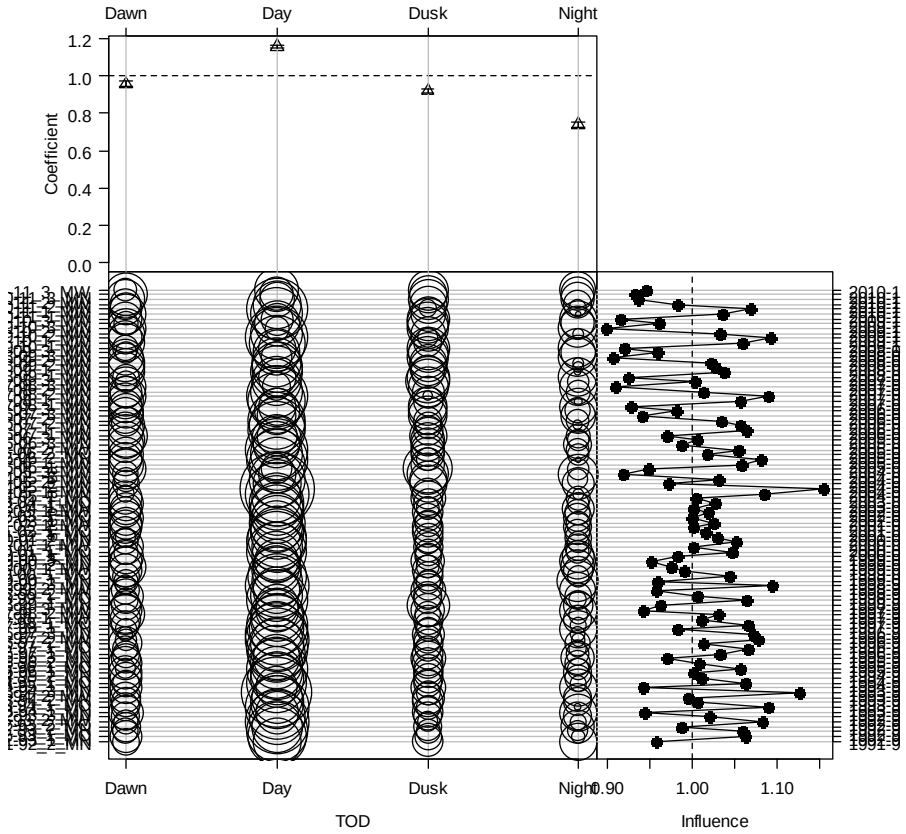

A2. 8: Coefficient-distribution_inflence plot for time of day for final standardisation model (Table 7).

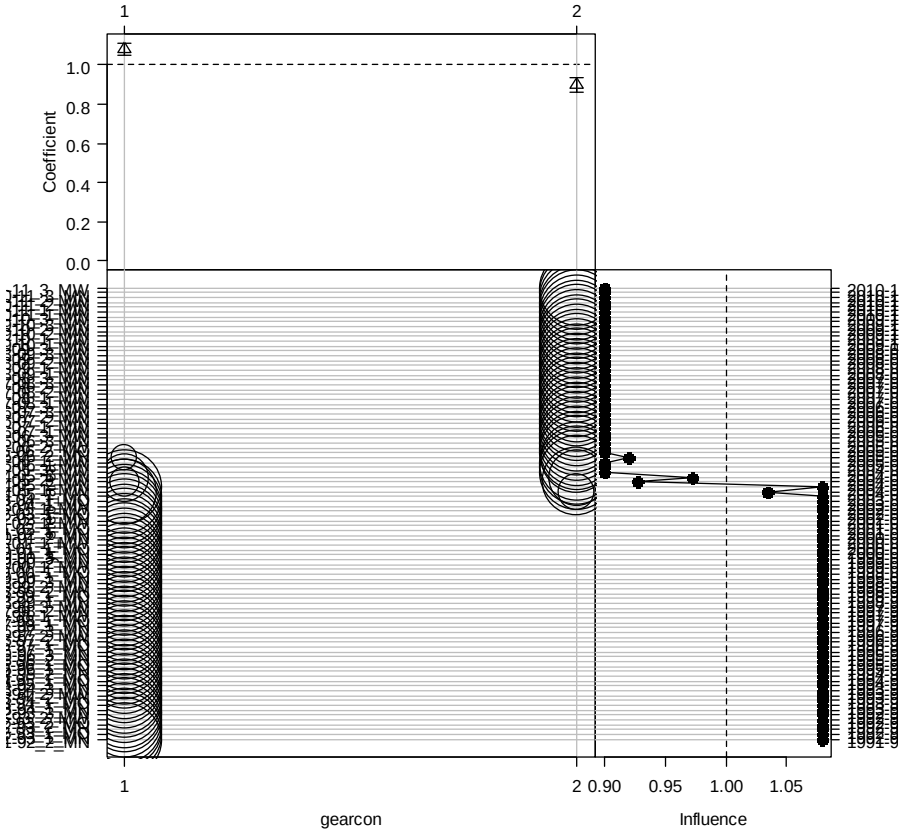

A2. 9: Coefficient-distribution_inflence plot for bycatch modification for final standardisation model (Table 7).

10. APPENDIX 3. BASE model plots

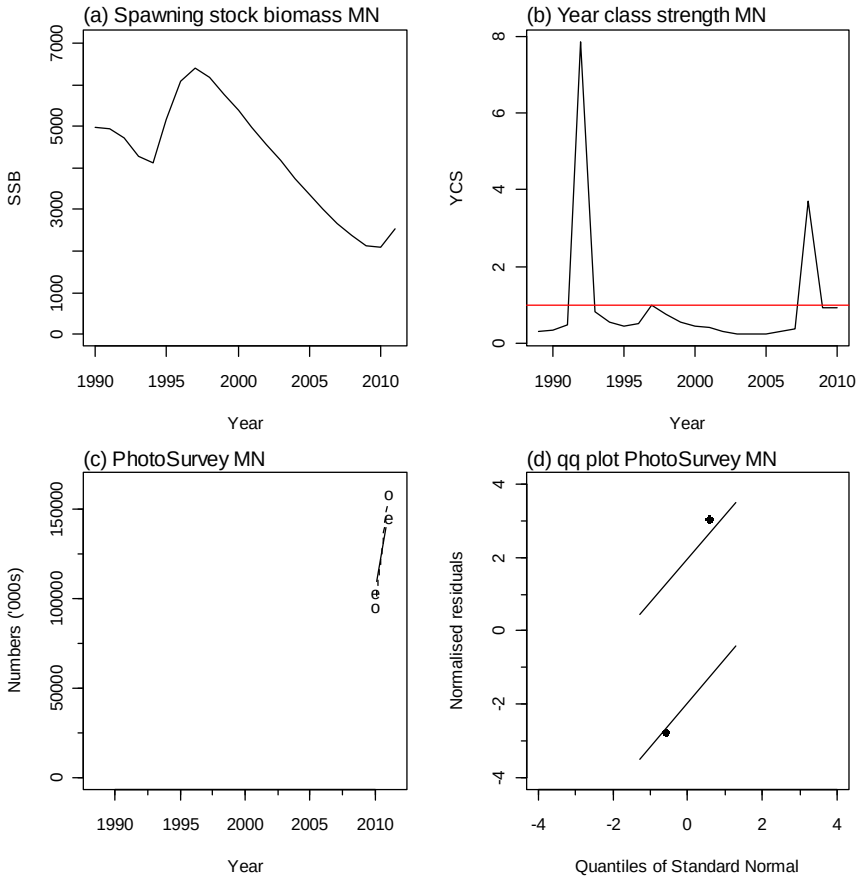

A3. 1: Spawning stock biomass trajectory (a), year class strength (b) fits (c) and q-q diagnostic plots (d) to photo survey abundance index for SCI 3 subarea MN from BASE model.

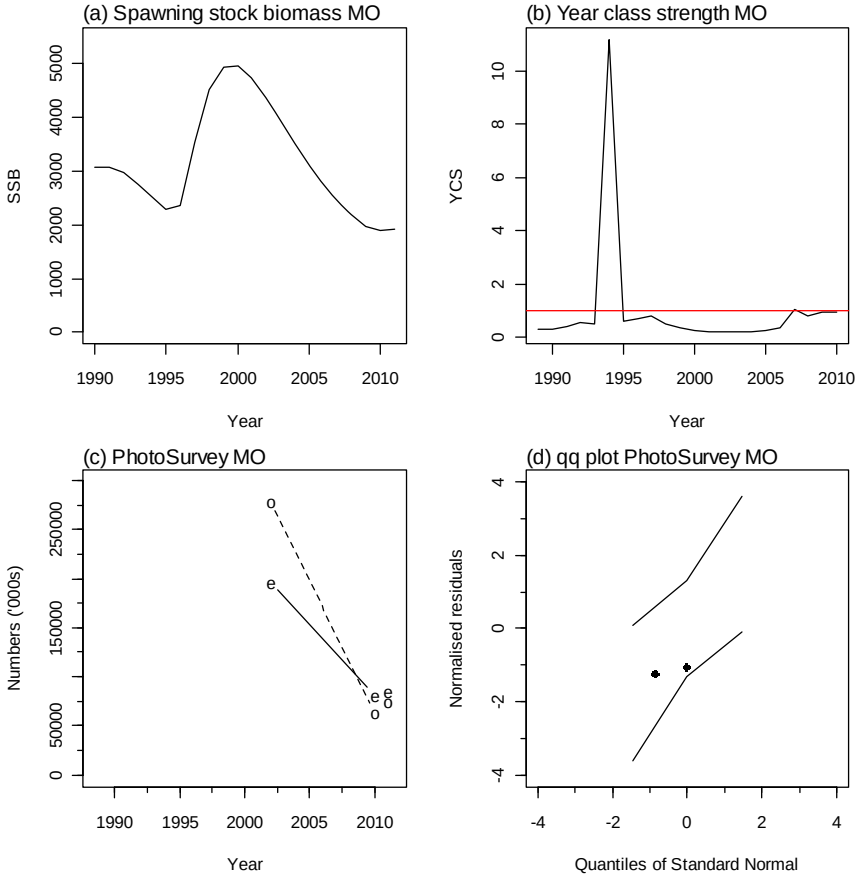

A3. 2: Spawning stock biomass trajectory (a), year class strength (b) fits (c) and q-q diagnostic plots (d) to photo survey abundance index for SCI 3 subarea MO from BASE model.

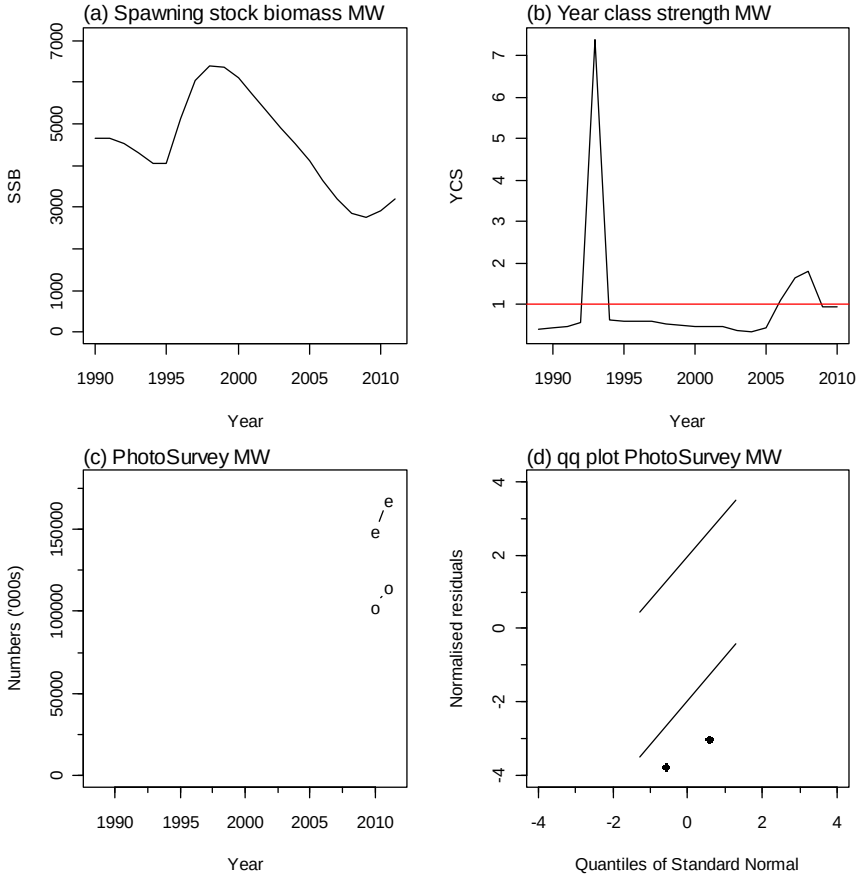

A3. 3: Spawning stock biomass trajectory (a), year class strength (b) fits (c) and q-q diagnostic plots (d) to photo survey abundance index for SCI 3 subarea MW from BASE model.

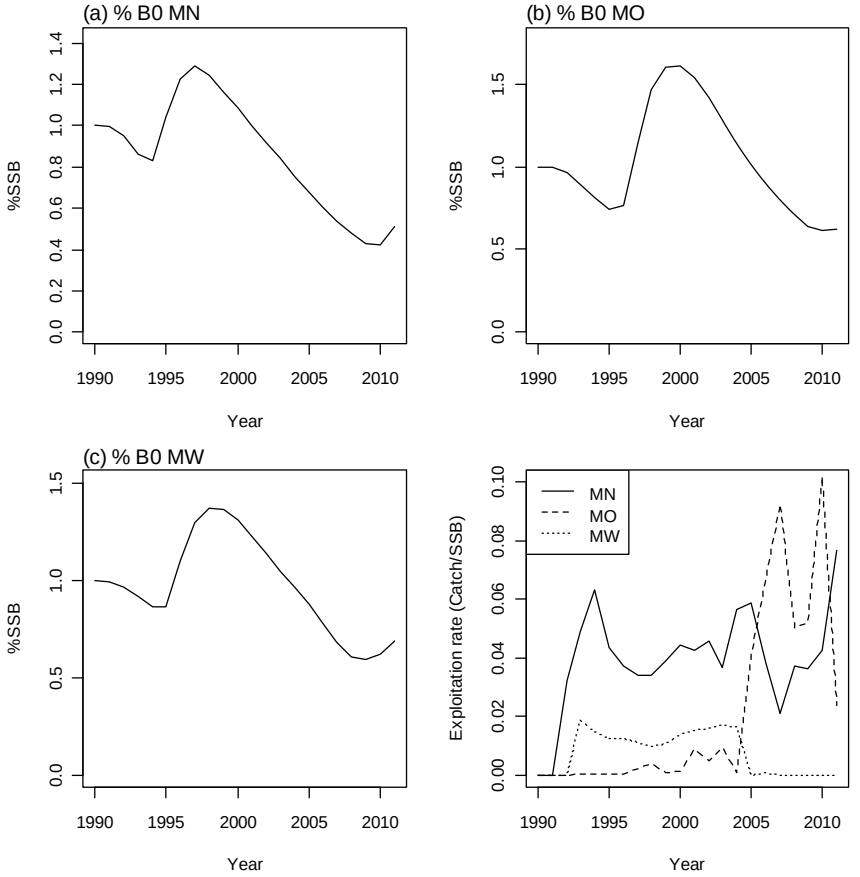

A3. 4: Trajectory of SSB as a percentage of B_0 for each subarea from the MPD fit to BASE model, and exploitation rate (catch/SSB).

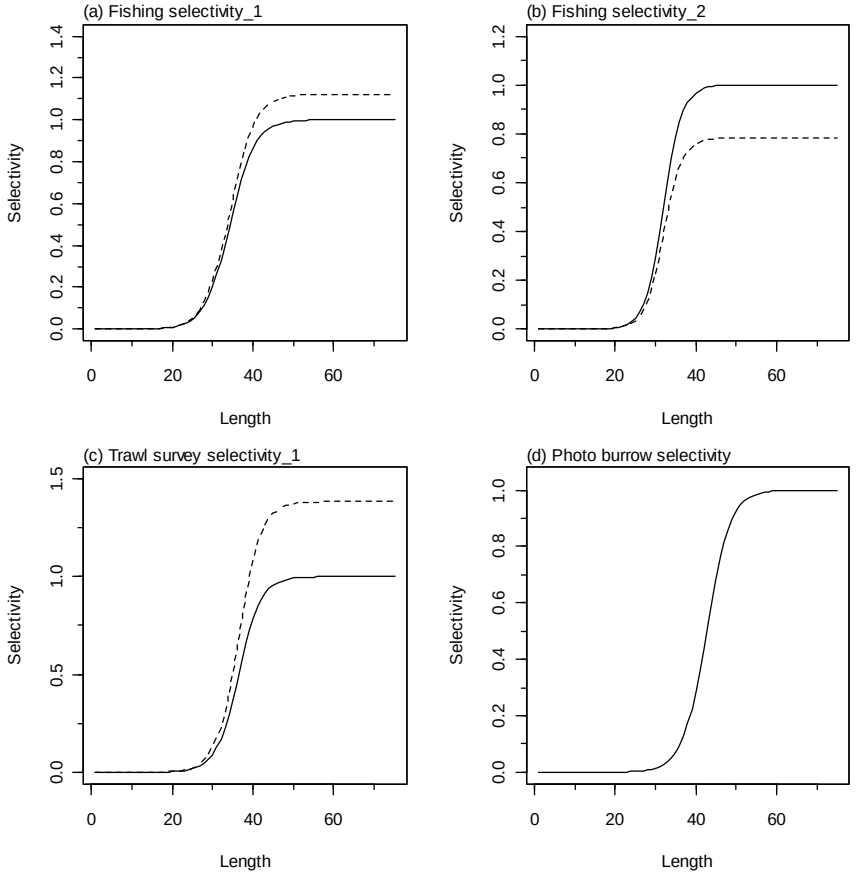

A3. 5: Fishery and survey selectivity curves. Solid line – females, dotted line – males. The scampi burrow index is not sexed, and a single selectivity applies.

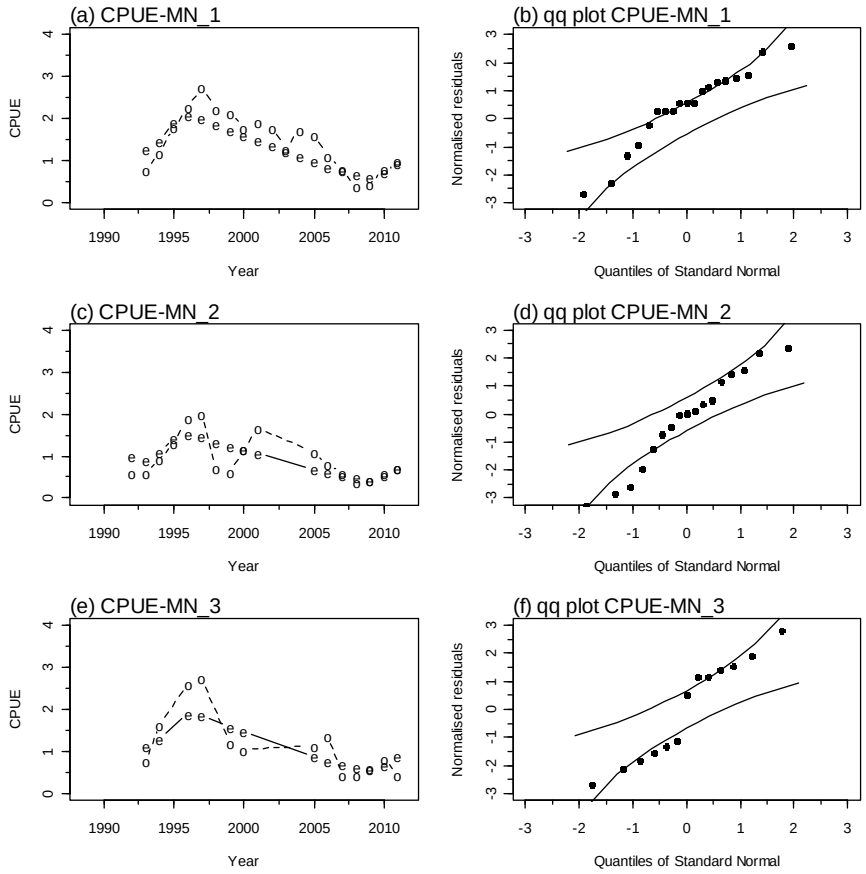

A3. 6: Fits and q-q diagnostic plots to CPUE abundance indices for MN.

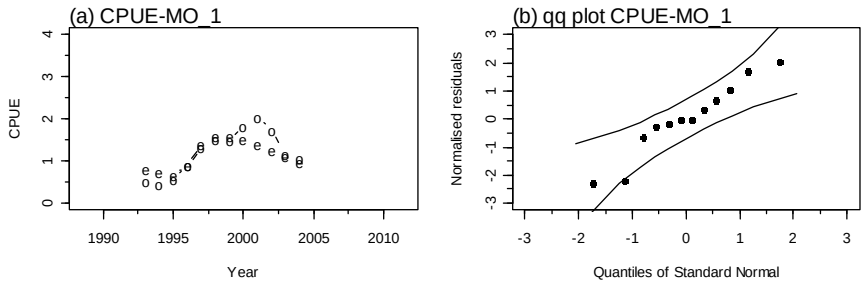

A3. 7: Fits and q-q diagnostic plots to CPUE abundance indices for MO.

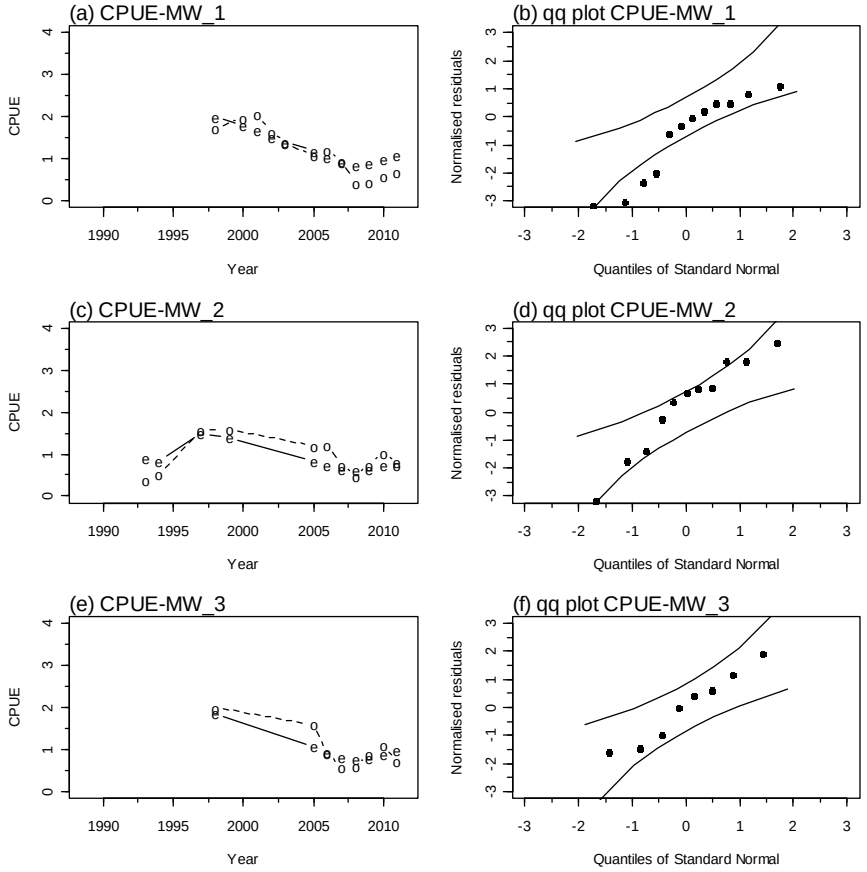

A3. 8: Fits and q-q diagnostic plots to CPUE abundance indices for MW.

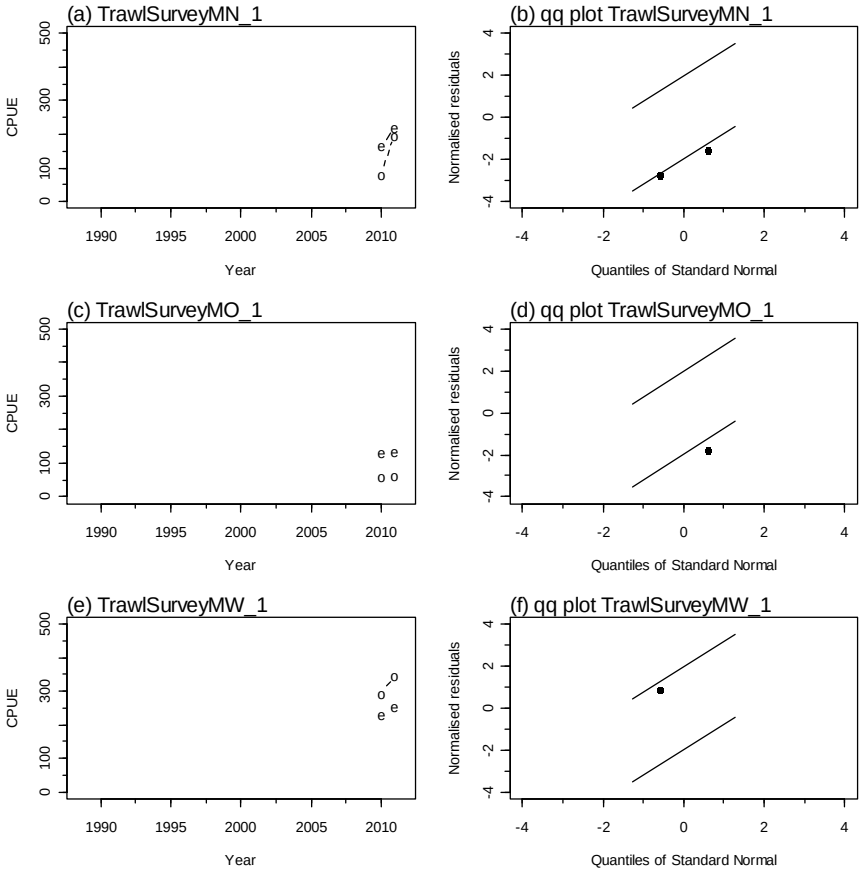

A3. 9: Fits and q-q diagnostic plots to trawl survey abundance indices.

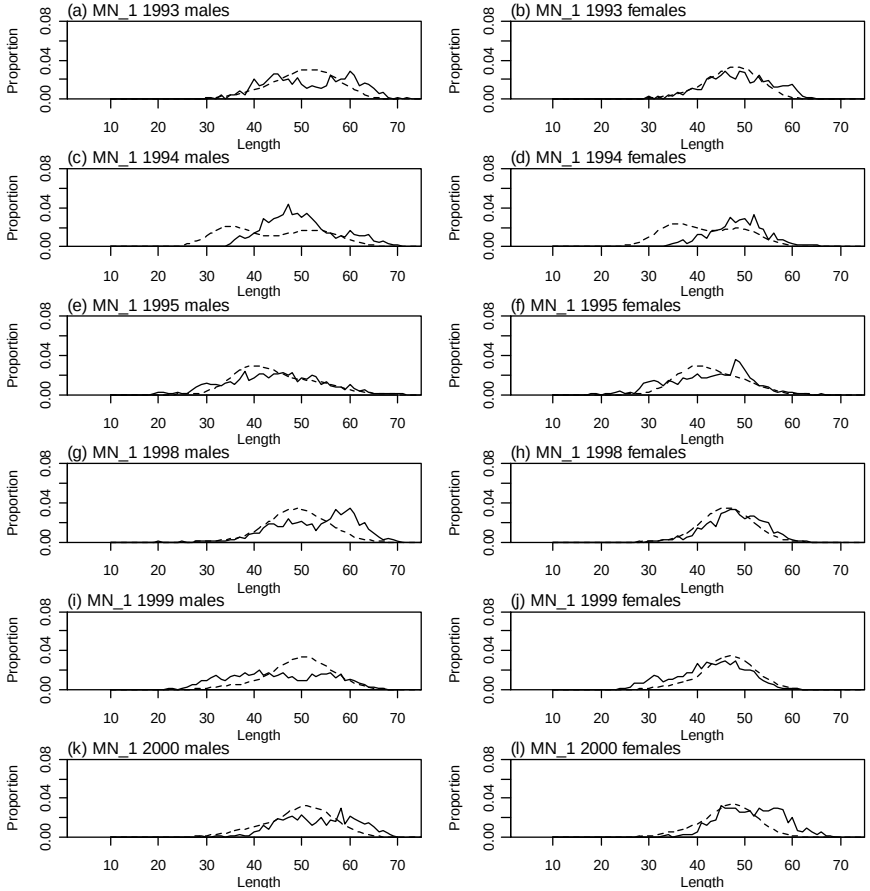

A3. 10: Observed (solid line) and fitted (dashed line) length frequency distributions for observer samples from MN, time step 1 (1993–2000).

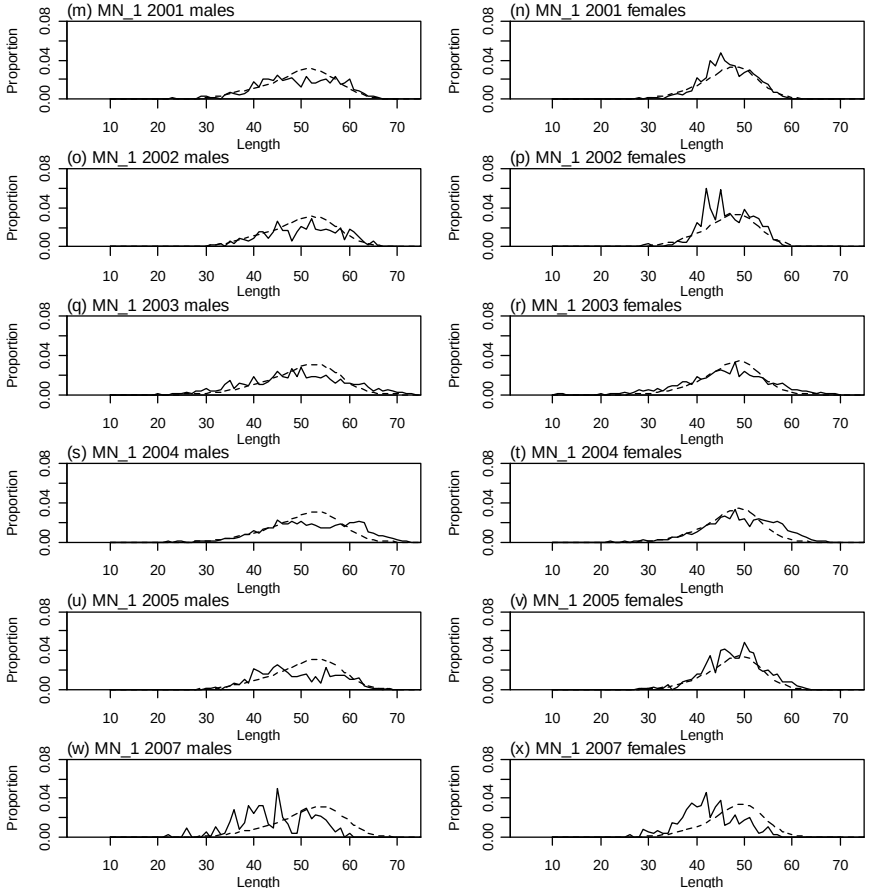

A3. 11: Observed (solid line) and fitted (dashed line) length frequency distributions for observer samples from MN, time step 1 (2001–2007).

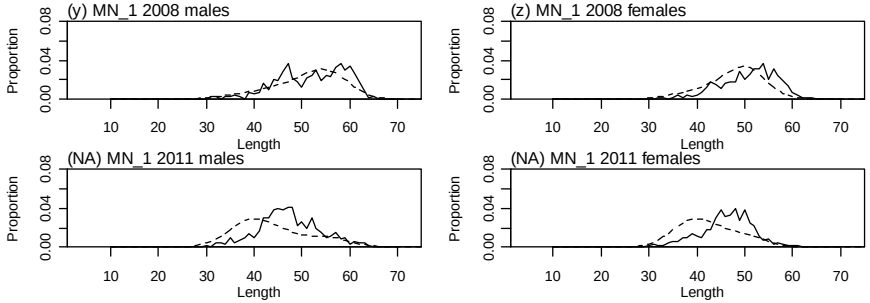

A3. 12: Observed (solid line) and fitted (dashed line) length frequency distributions for observer samples from MN, time step 1 (2008–2011).

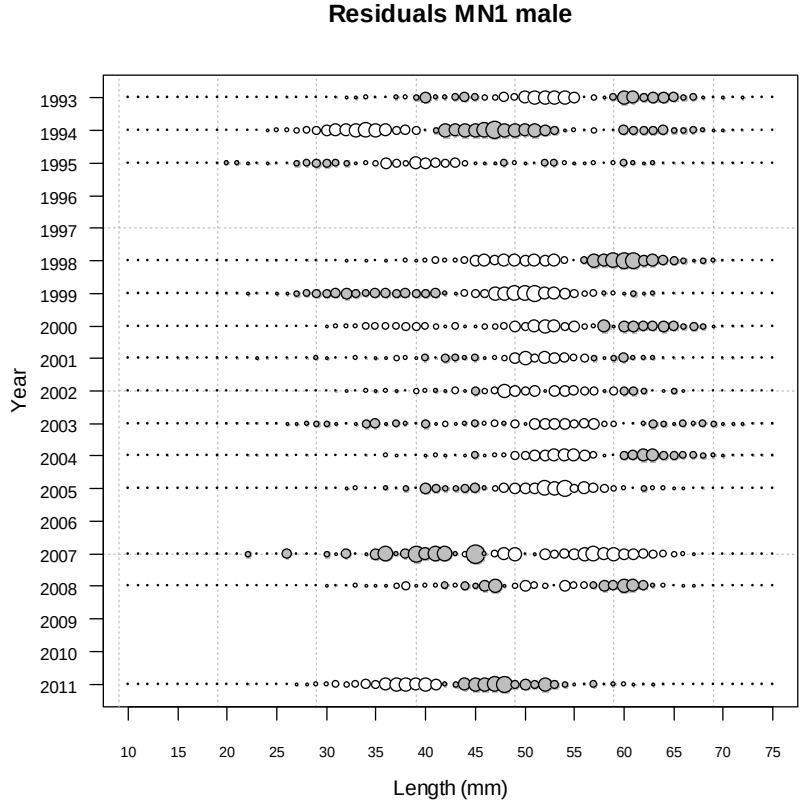

A3. 13: Bubble plots of residuals of fits to length frequency distributions for observer sampling from MN, time step 1, male.

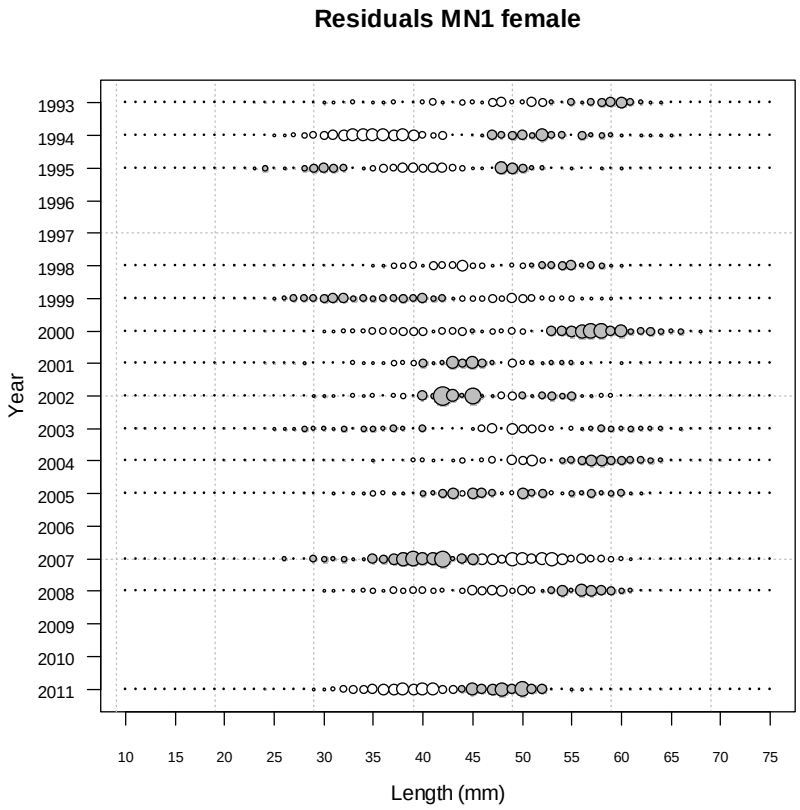

A3. 14: Bubble plots of residuals of fits to length frequency distributions for observer sampling from MN, time step 1, female.

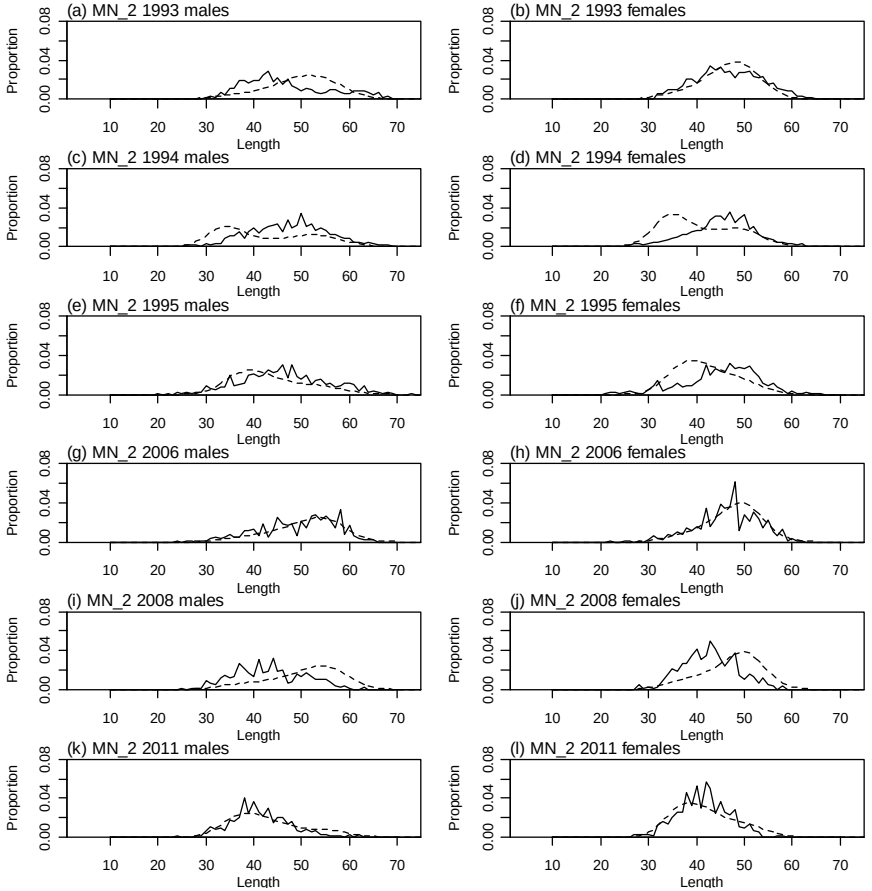

A3. 15: Observed (solid line) and fitted (dashed line) length frequency distributions for observer samples from MN, time step 2.

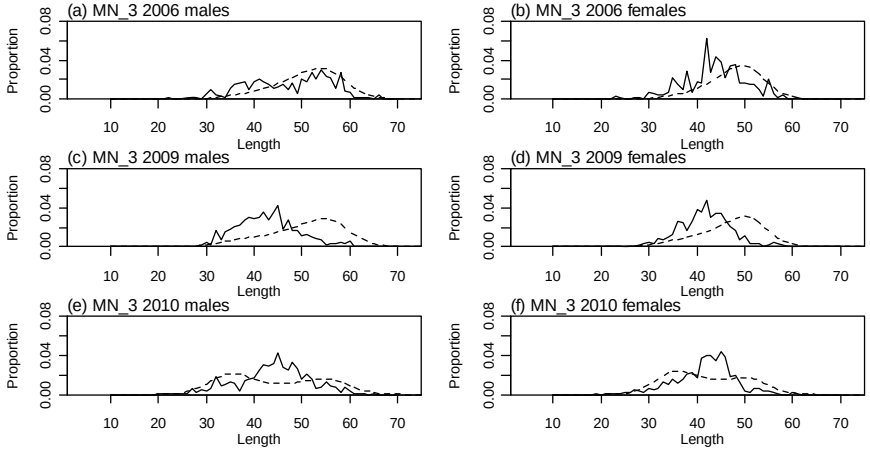

A3. 16: Observed (solid line) and fitted (dashed line) length frequency distributions for observer samples from MN, time step 3.

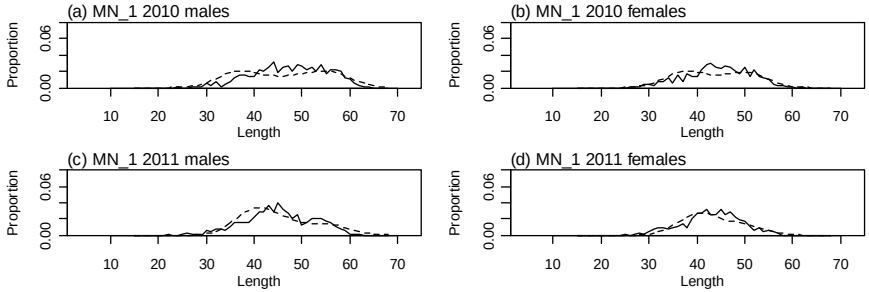

A3. 17: Observed (solid line) and fitted (dashed line) length frequency distributions for trawl survey samples from MN.

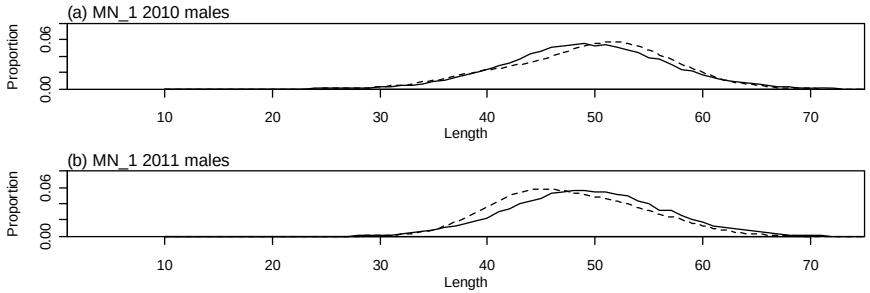

A3. 18: Observed (solid line) and fitted (dashed line) length frequency distributions for photo survey samples from MN.

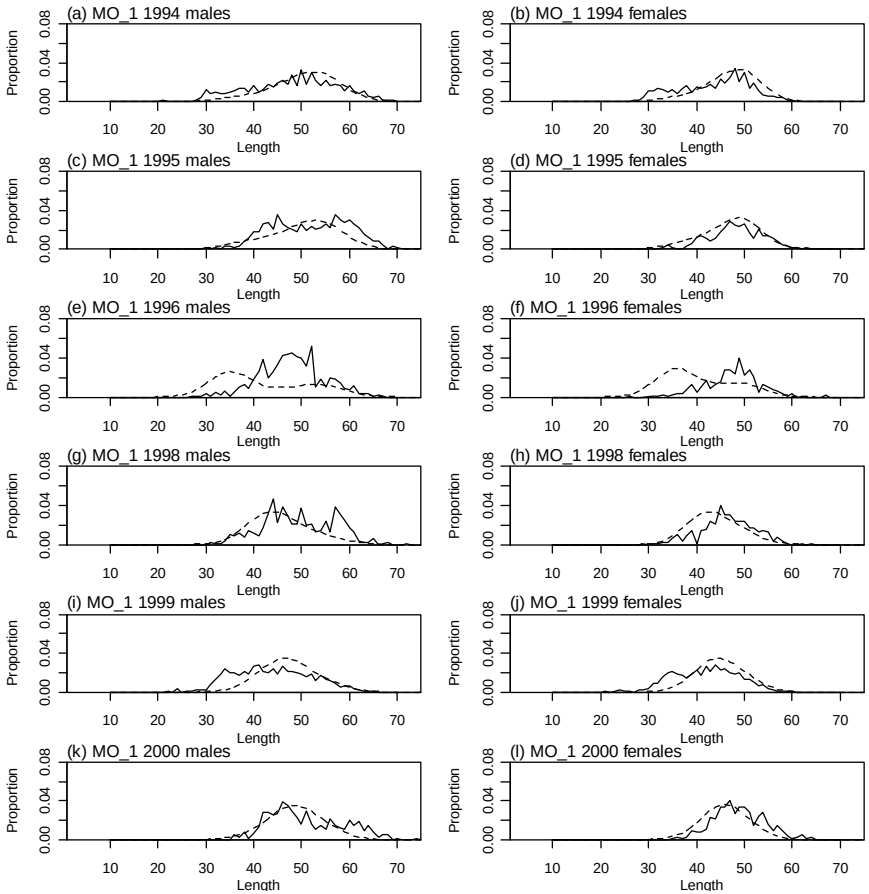

A3. 19: Observed (solid line) and fitted (dashed line) length frequency distributions for observer samples from MO, time step 1 (1994–2000).

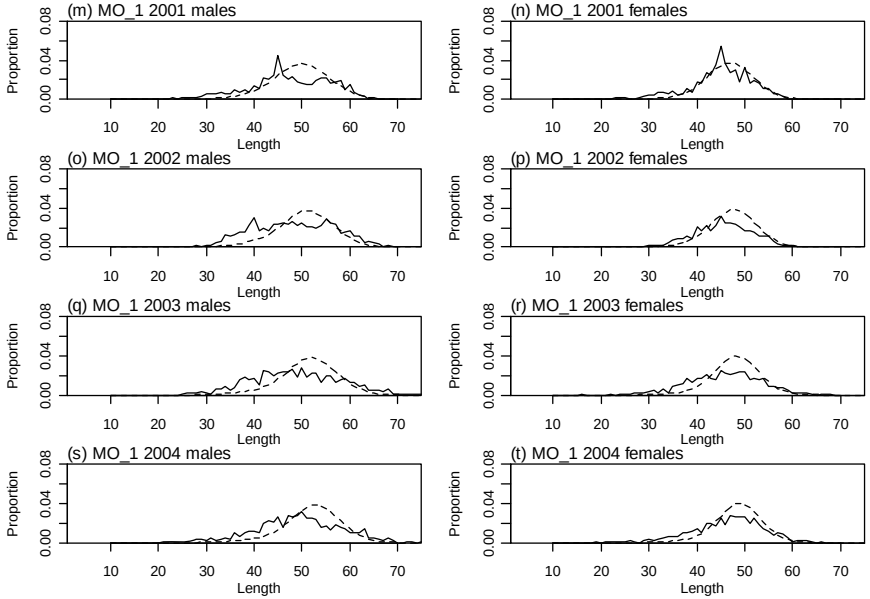

A3. 20: Observed (solid line) and fitted (dashed line) length frequency distributions for observer samples from MO, time step 1 (2001–2004).

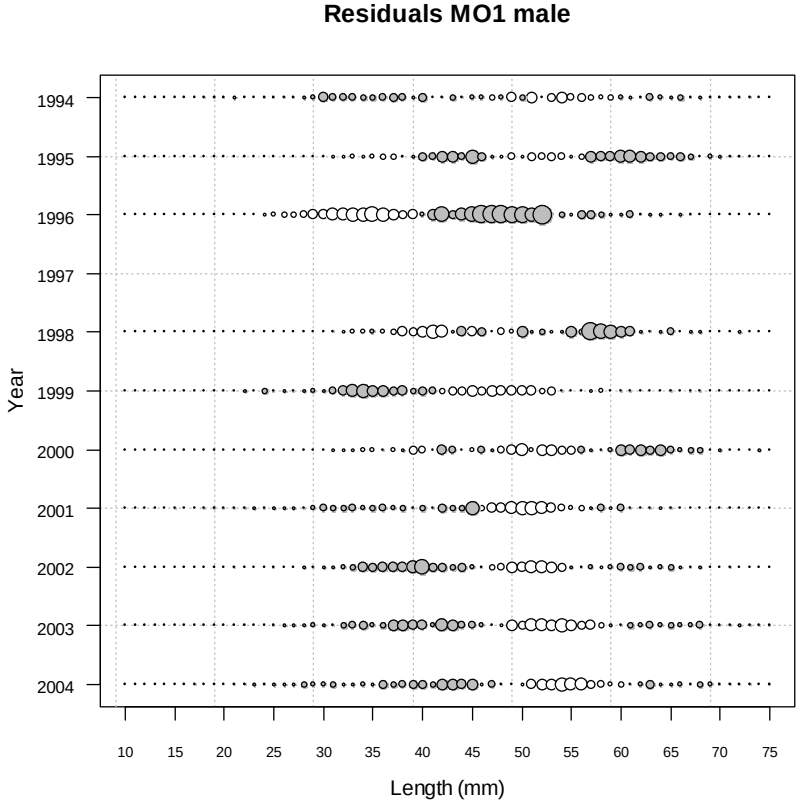

A3. 21: Bubble plots of residuals of fits to length frequency distributions for observer sampling from MO, time step 1, male.

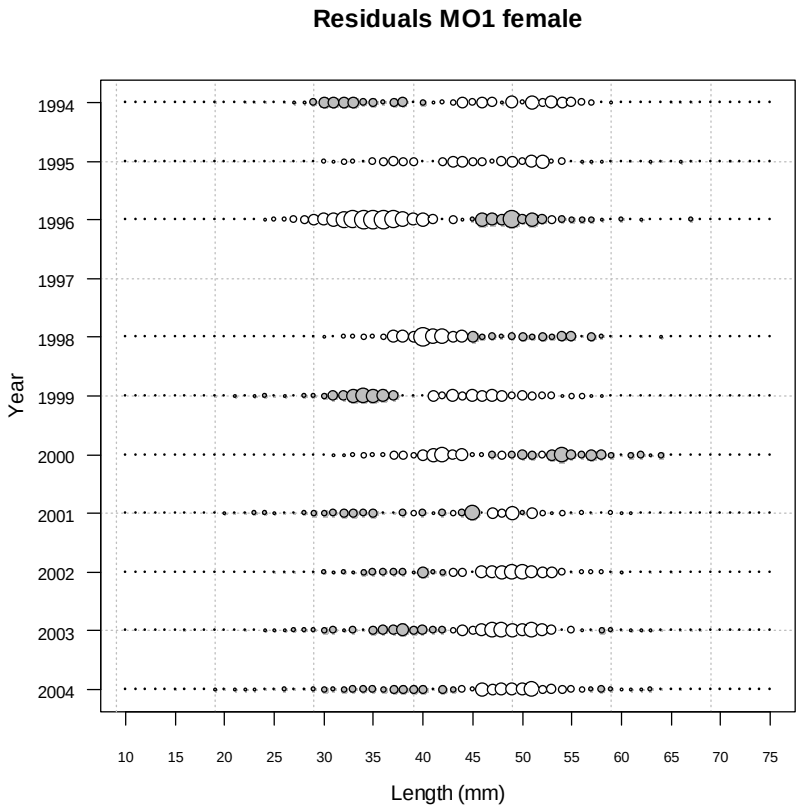

A3. 22: Bubble plots of residuals of fits to length frequency distributions for observer sampling from MO, time step 1, female.

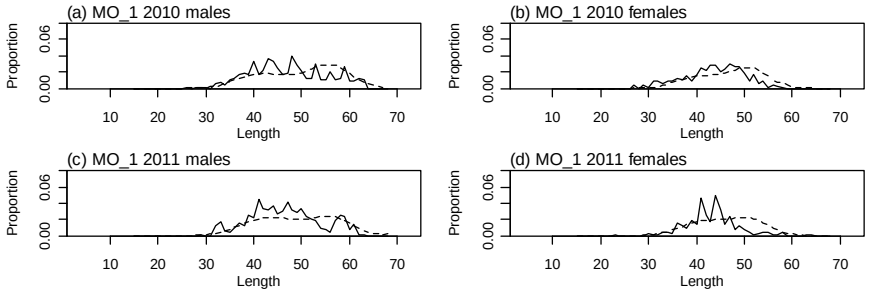

A3. 23: Observed (solid line) and fitted (dashed line) length frequency distributions for trawl survey samples from MO.

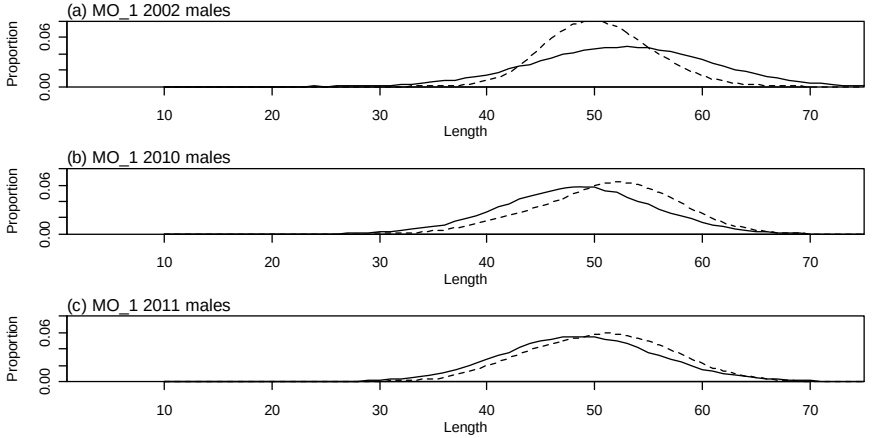

A3. 24: Observed (solid line) and fitted (dashed line) length frequency distributions for photo survey samples from MO.

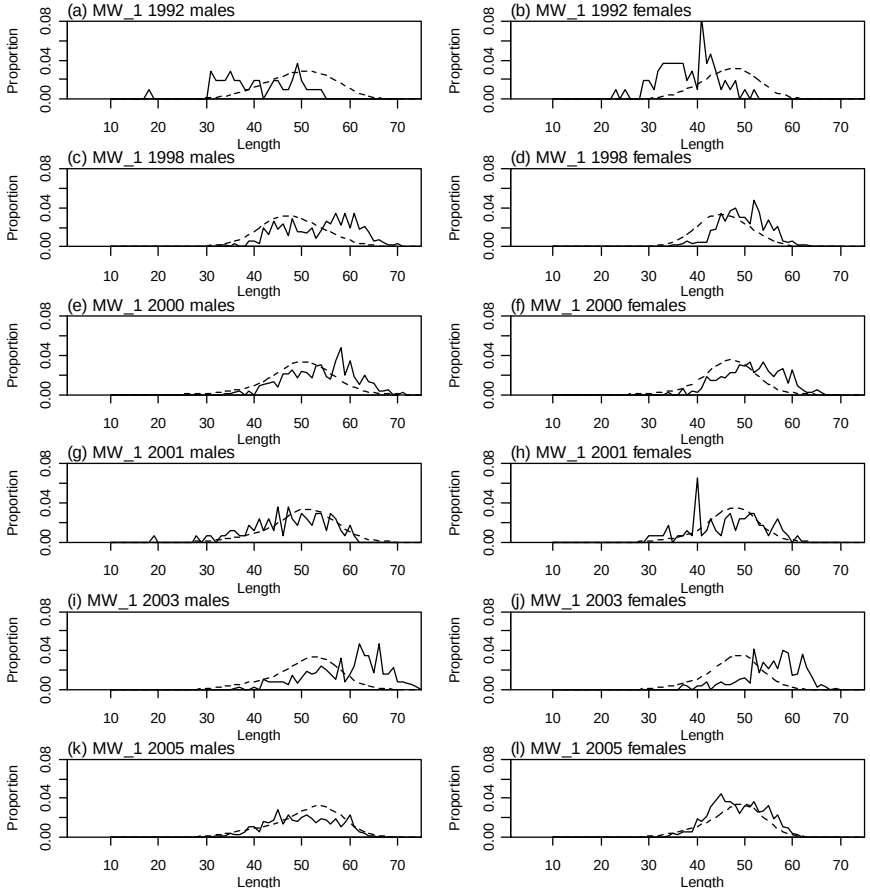

A3. 25: Observed (solid line) and fitted (dashed line) length frequency distributions for observer samples from MW, time step 1 (1992–2005).

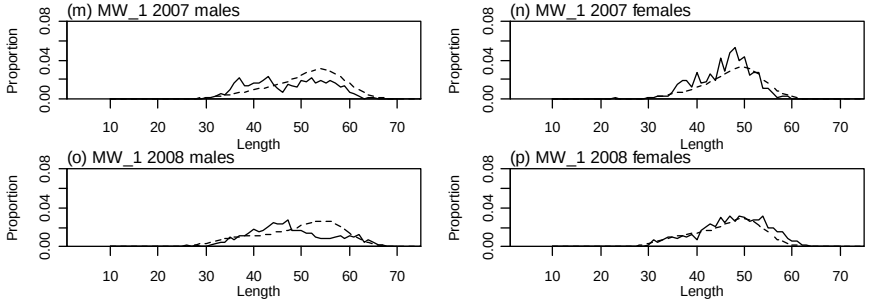

A3. 26: Observed (solid line) and fitted (dashed line) length frequency distributions for observer samples from MW, time step 1 (2007–2008).

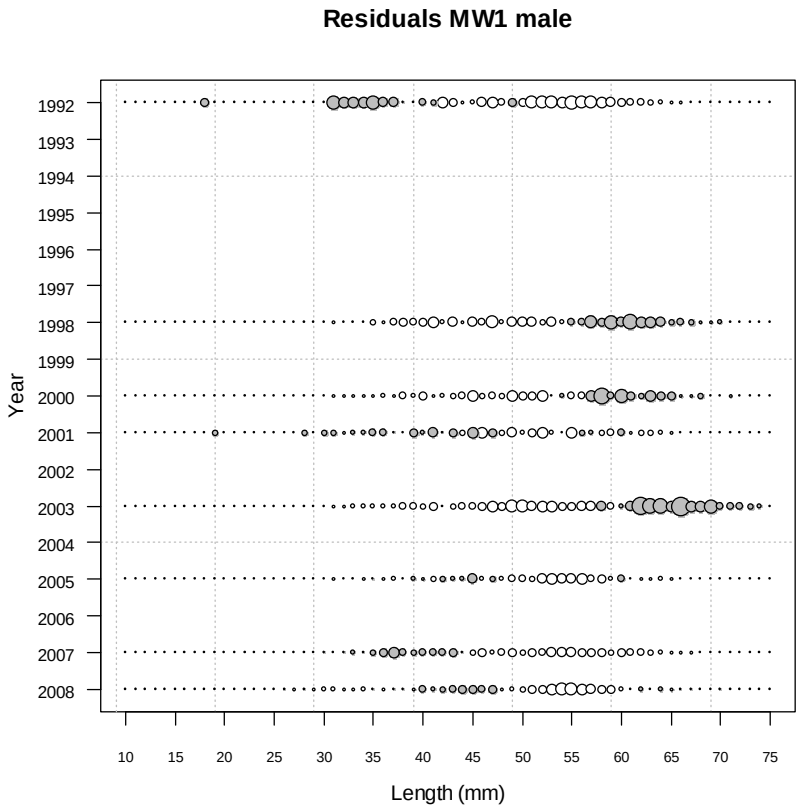

A3. 27: Bubble plots of residuals of fits to length frequency distributions for observer sampling from MW, time step 1, male.

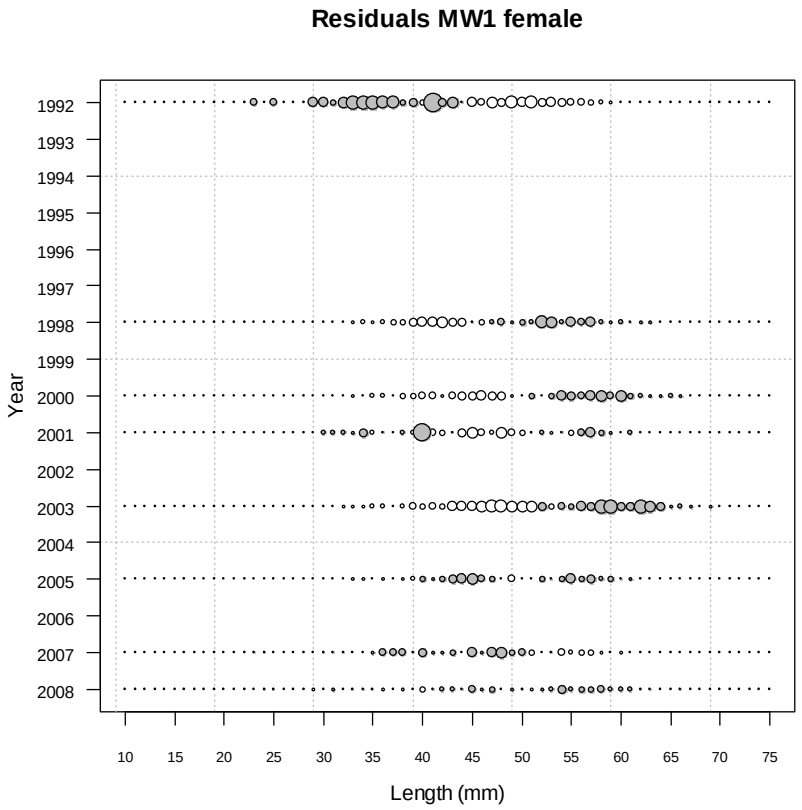

A3. 28: Bubble plots of residuals of fits to length frequency distributions for observer sampling from MW, time step 1, female.

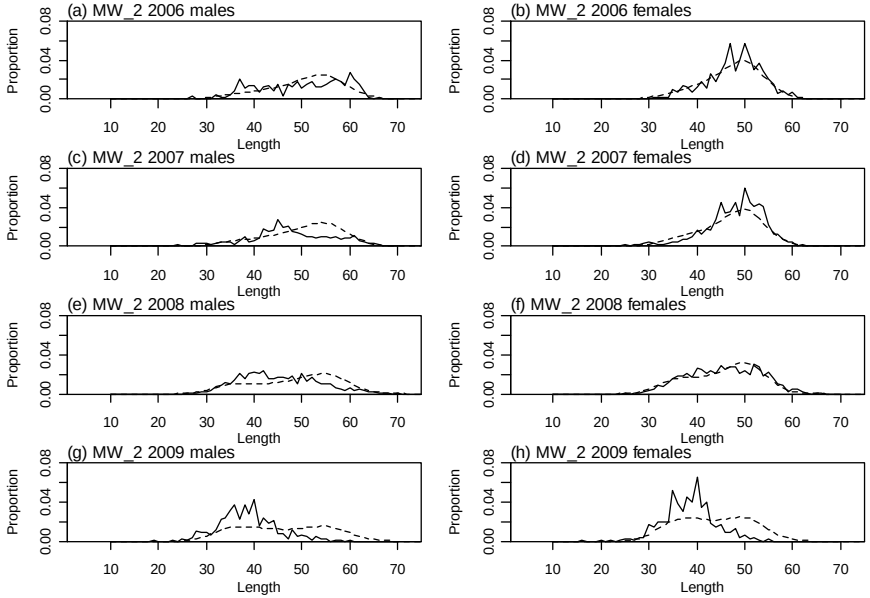

A3. 29: Observed (solid line) and fitted (dashed line) length frequency distributions for observer samples from MW, time step 2.

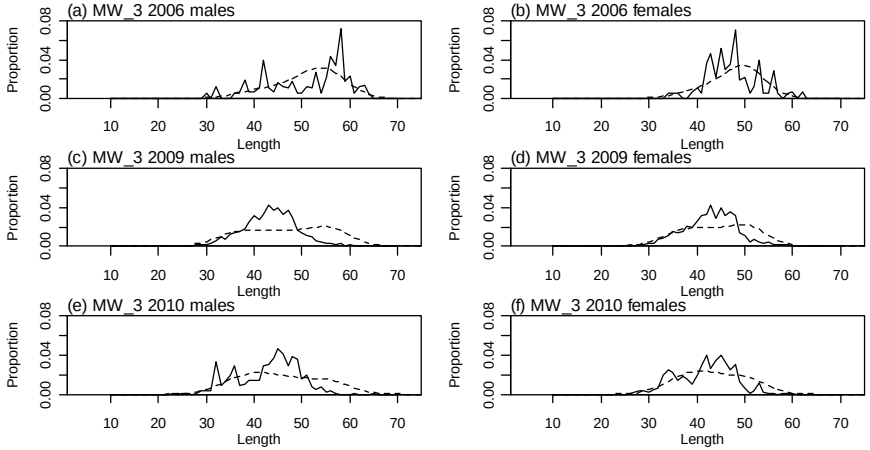

A3. 30: Observed (solid line) and fitted (dashed line) length frequency distributions for observer samples from MW, time step 3.

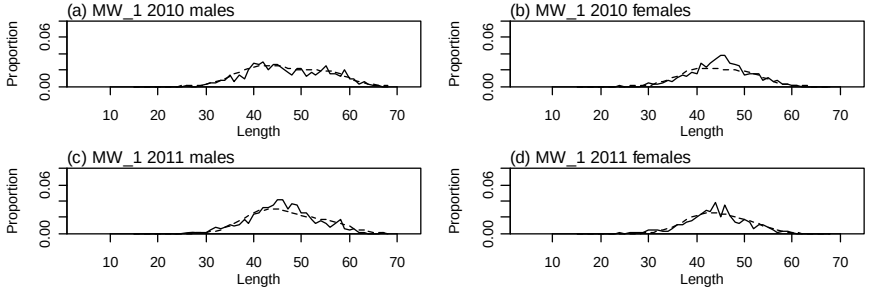

A3. 31: Observed (solid line) and fitted (dashed line) length frequency distributions for trawl survey samples from MW.

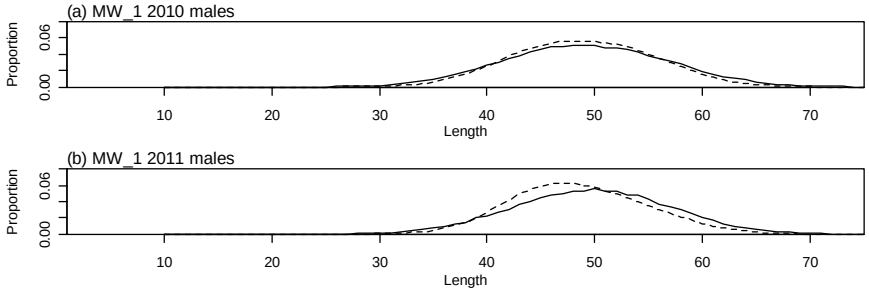

A3. 32: Observed (solid line) and fitted (dashed line) length frequency distributions for photo survey samples from MW.

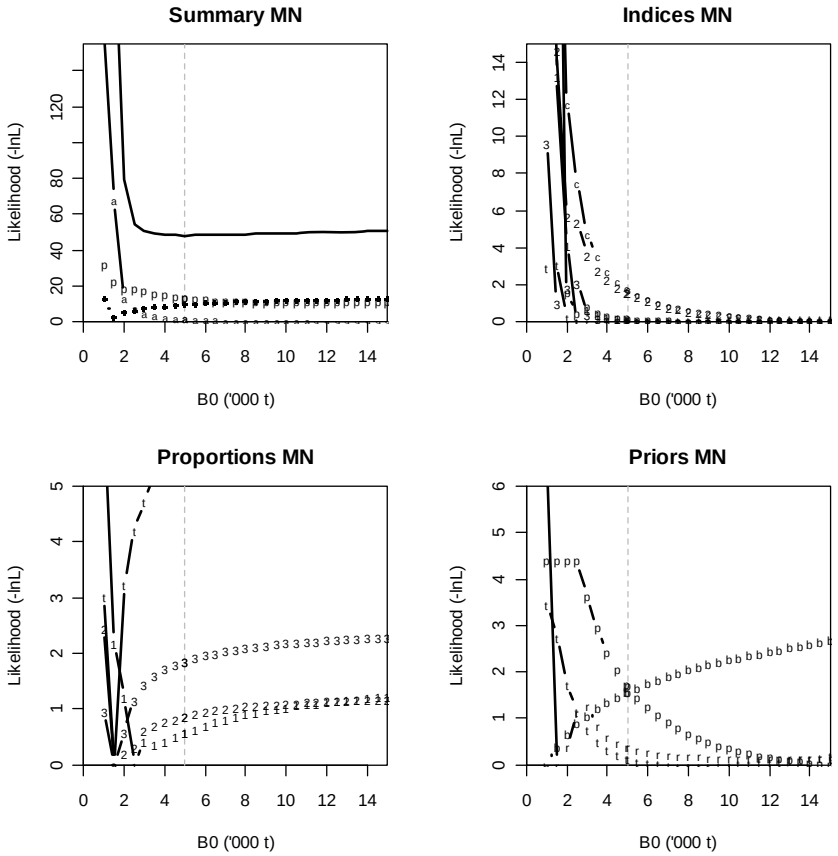

A3. 33: Likelihood profiles for model 1 when MN B_0 is fixed in the model. Figures show profiles for main priors (top left, p-priors, a – abundance indices, • – proportions at length), abundance indices (top right, t - trawl survey, 1 - CPUE time step 1, 2 - CPUE time step 2, 3 - CPUE time step 3, p – photo survey), proportion at length data (bottom left, t-trawl, 1 – observer time step 1, 2 – observer time step 2, 3 – observer time step 3) and priors (bottom right, b- B_0, YCS - r, p- *q-Photo*, t – *q-Trawl*).

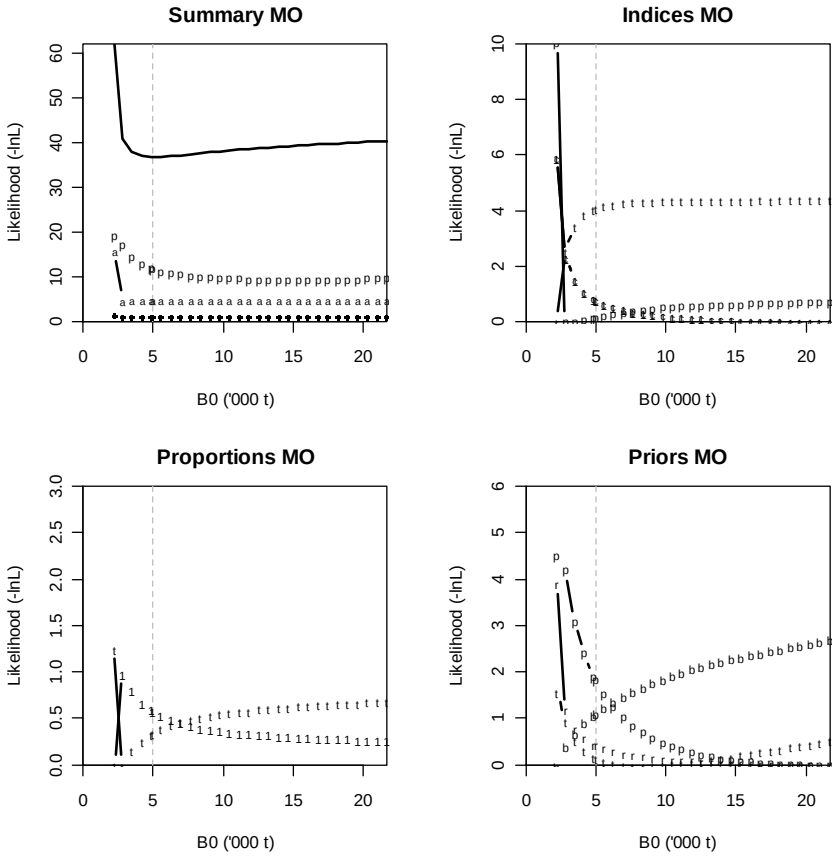

A3. 34: Likelihood profiles for model 1 when MO B_0 is fixed in the model. Figures show profiles for main priors (top left, p-priors, a – abundance indices, • – proportions at length), abundance indices (top right, t - trawl survey, 1 - CPUE time step 1, 2 - CPUE time step 2, 3 - CPUE time step 3, p – photo survey), proportion at length data (bottom left, t-trawl, 1 – observer time step 1, 2 – observer time step 2, 3 – observer time step 3) and priors (bottom right, b- B_0, YCS - r, p- *q-Photo*, t – *q-Trawl*).

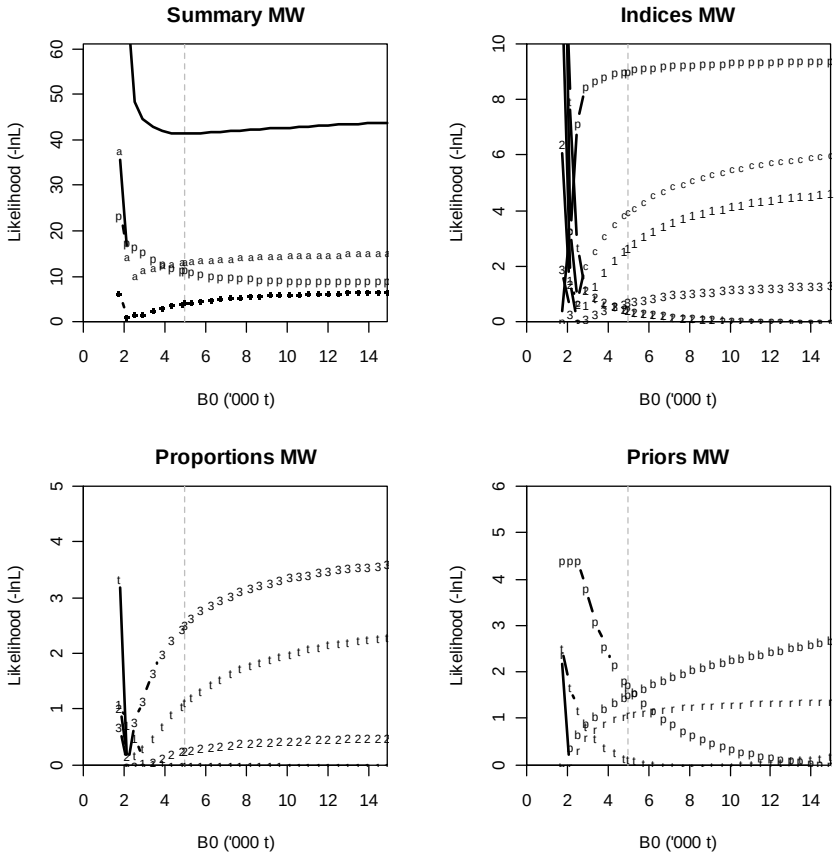

A3. 35: Likelihood profiles for model 1 when MW B_0 is fixed in the model. Figures show profiles for main priors (top left, p-priors, a – abundance indices, • – proportions at length), abundance indices (top right, t - trawl survey, 1 - CPUE time step 1, 2 - CPUE time step 2, 3 - CPUE time step 3, p – photo survey), proportion at length data (bottom left, t-trawl, 1 – observer time step 1, 2 – observer time step 2, 3 – observer time step 3) and priors (bottom right, b- B_0, YCS - r, p- *q-Photo*, t – *q-Trawl*).

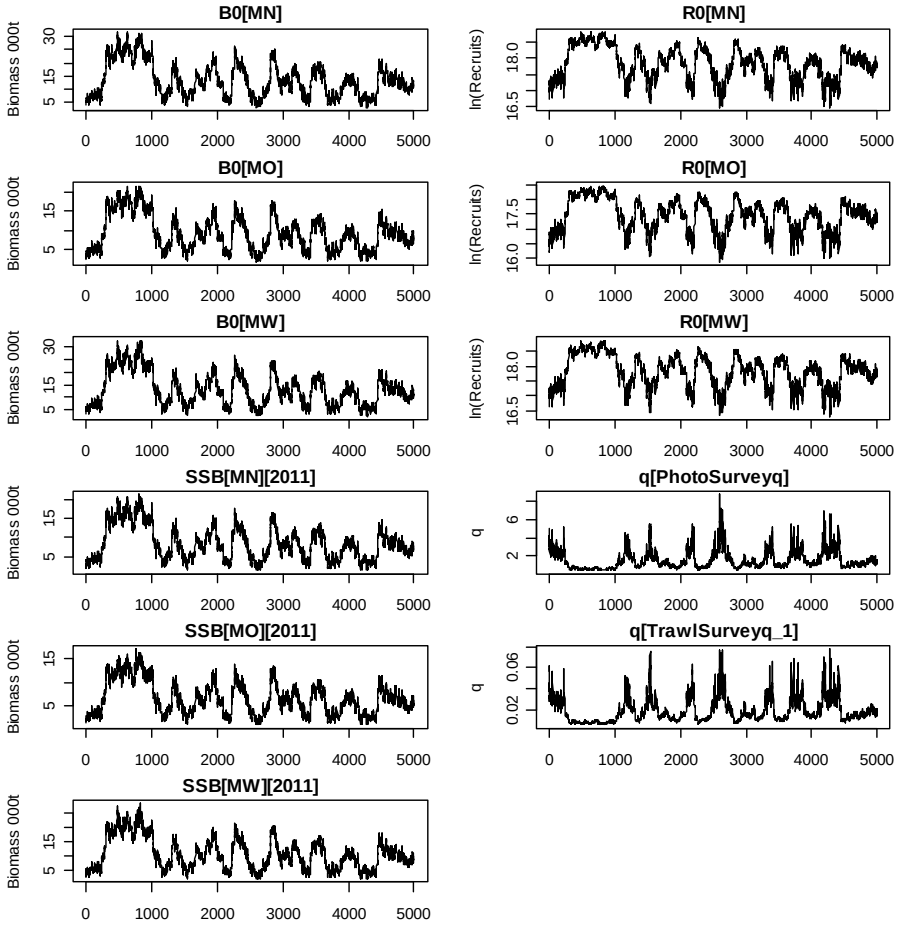

A3. 36: MCMC traces for B_0, SSB_{2011}, R_0 and *q* terms for the BASE model.

11. APPENDIX 4. BASE-015 model plots

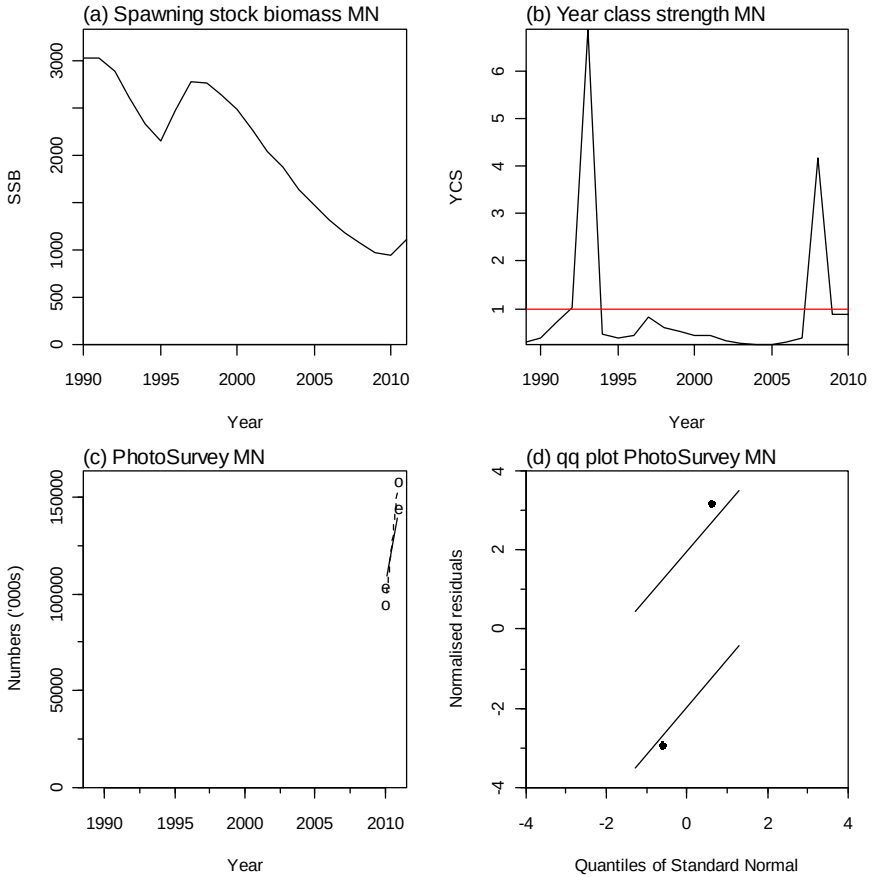

A4. 1: Spawning stock biomass trajectory (a), year class strength (b) fits (c) and q-q diagnostic plots (d) to photo survey abundance index for SCI 3 subarea MN from BASE-015 model.

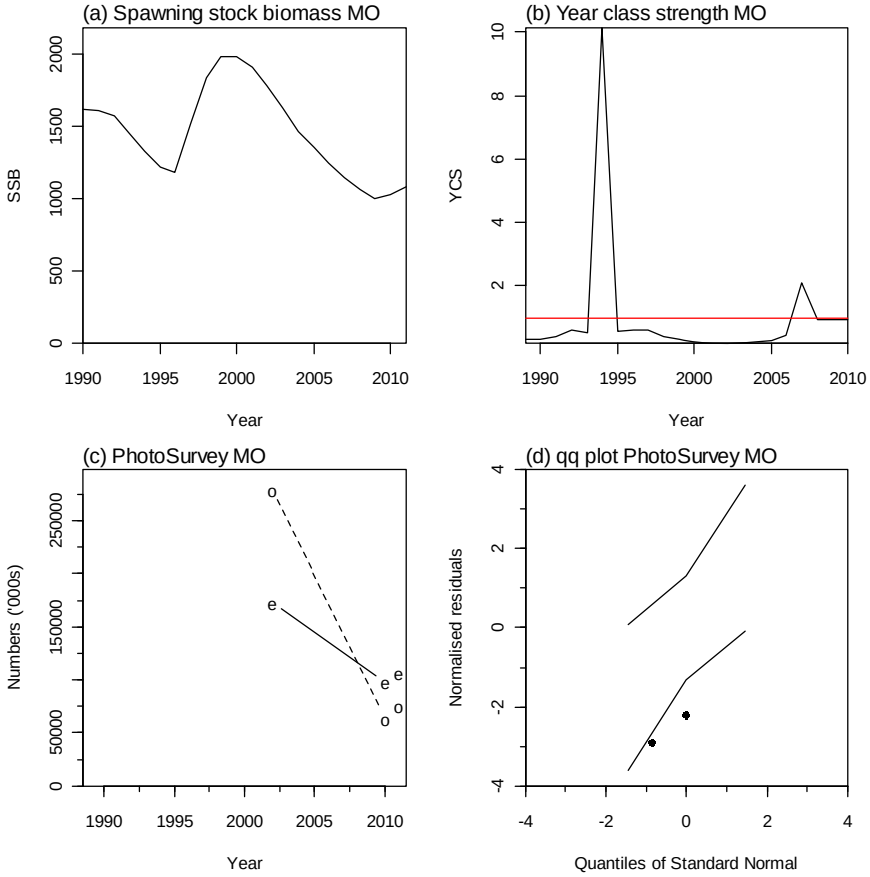

A4. 2: Spawning stock biomass trajectory (a), year class strength (b) fits (c) and q-q diagnostic plots (d) to photo survey abundance index for SCI 3 subarea MO from BASE-015 model.

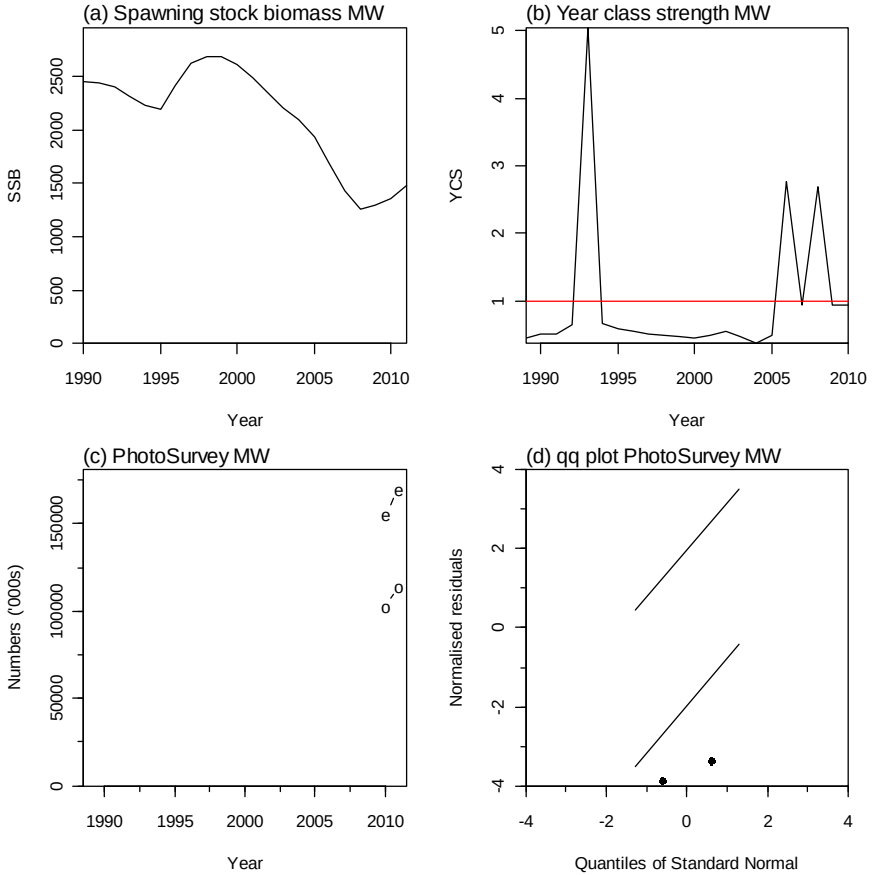

A4. 3: Spawning stock biomass trajectory (a), year class strength (b) fits (c) and q-q diagnostic plots (d) to photo survey abundance index for SCI 3 subarea MW from BASE-015 model.

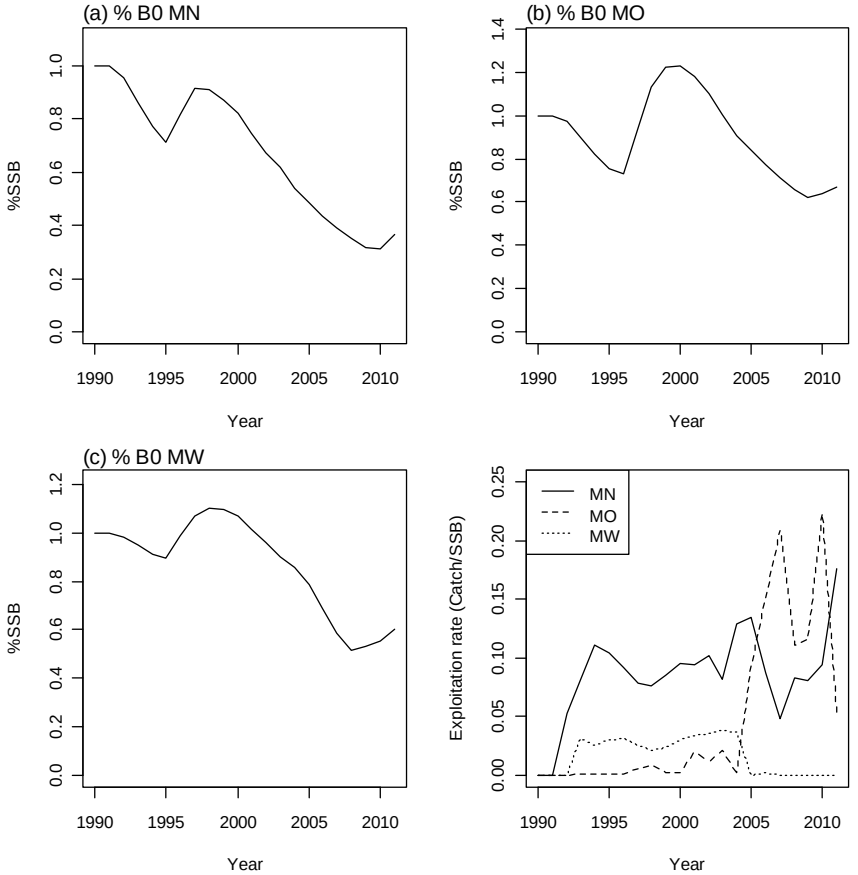

A4. 4: Trajectory of SSB as a percentage of B_0 for each subarea from the MPD fit to BASE-g-est model, and exploitation rate (catch/SSB).

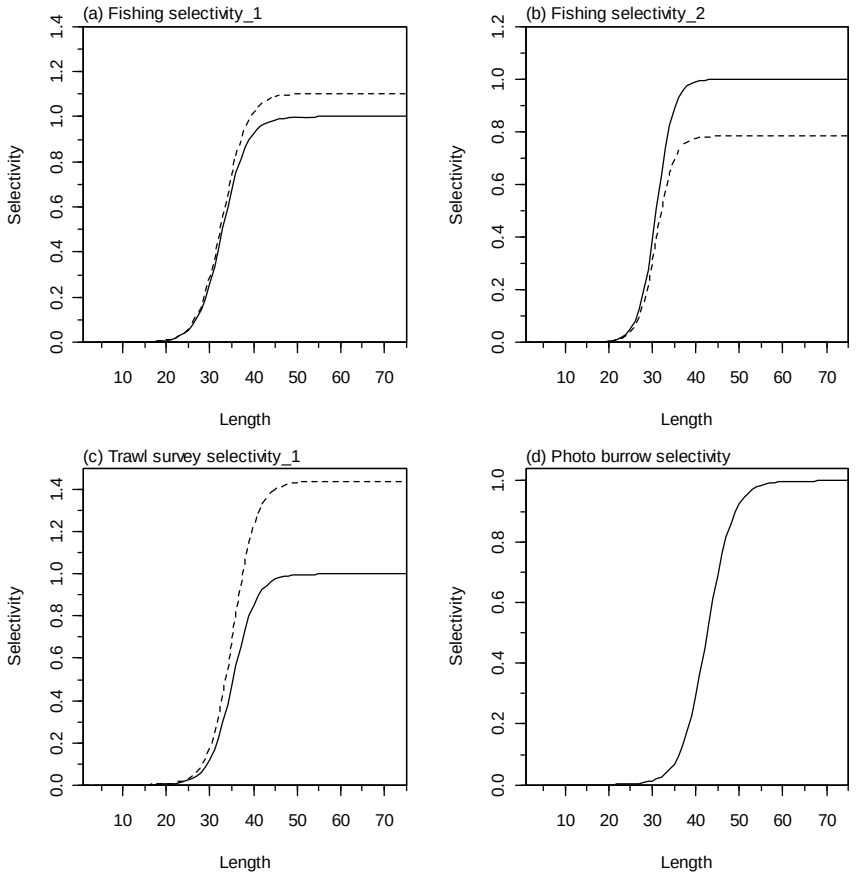

A4. 5: Fishery and survey selectivity curves. Solid line – females, dotted line – males. The scampi burrow index is not sexed, and a single selectivity applies.

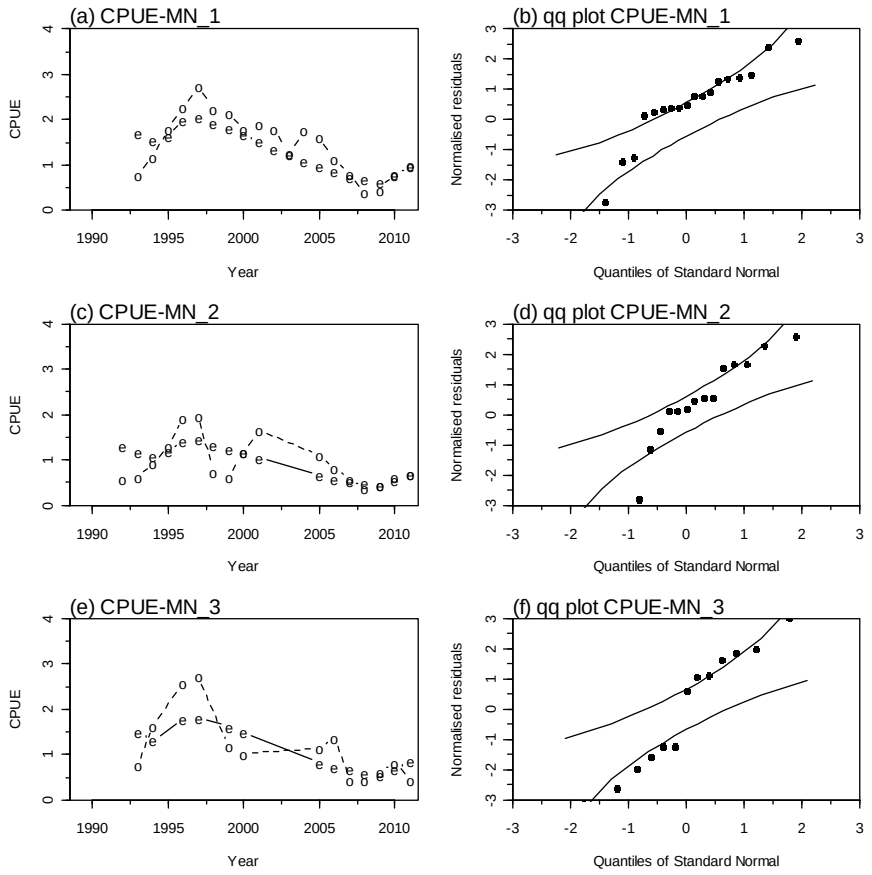

A4. 6: Fits and q-q diagnostic plots to CPUE abundance indices for MN.

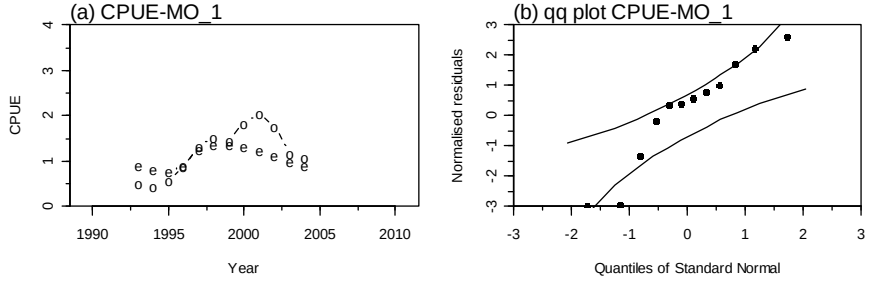

A4. 7: Fits and q-q diagnostic plots to CPUE abundance indices for MO.

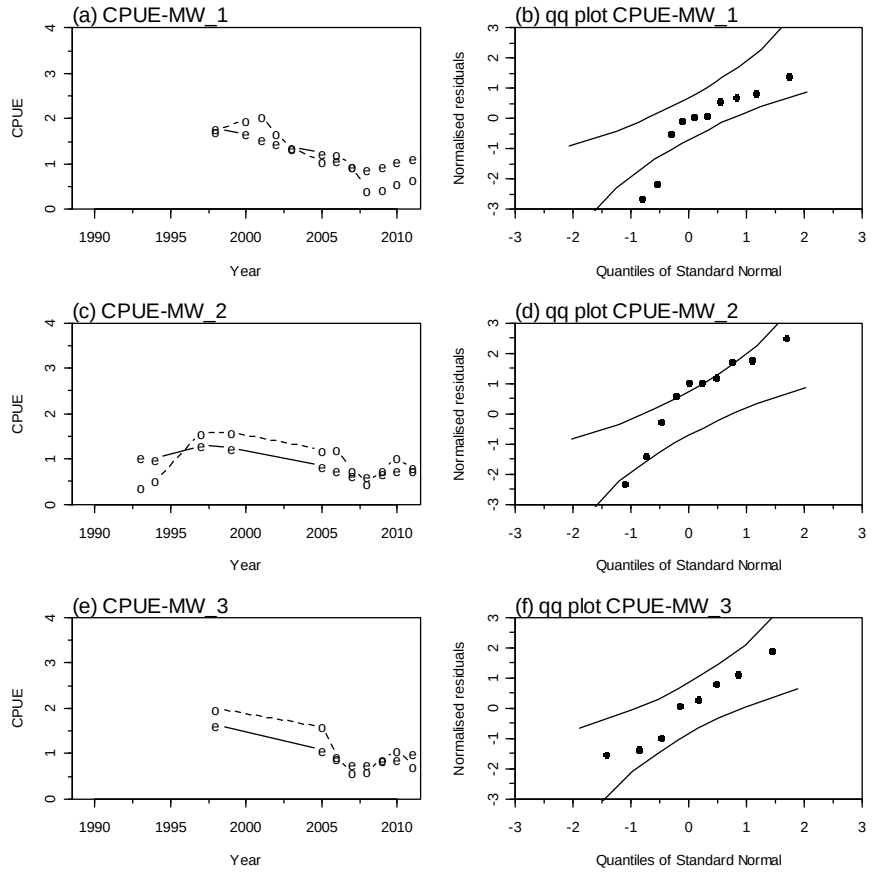

A4. 8: Fits and q-q diagnostic plots to CPUE abundance indices for MW.

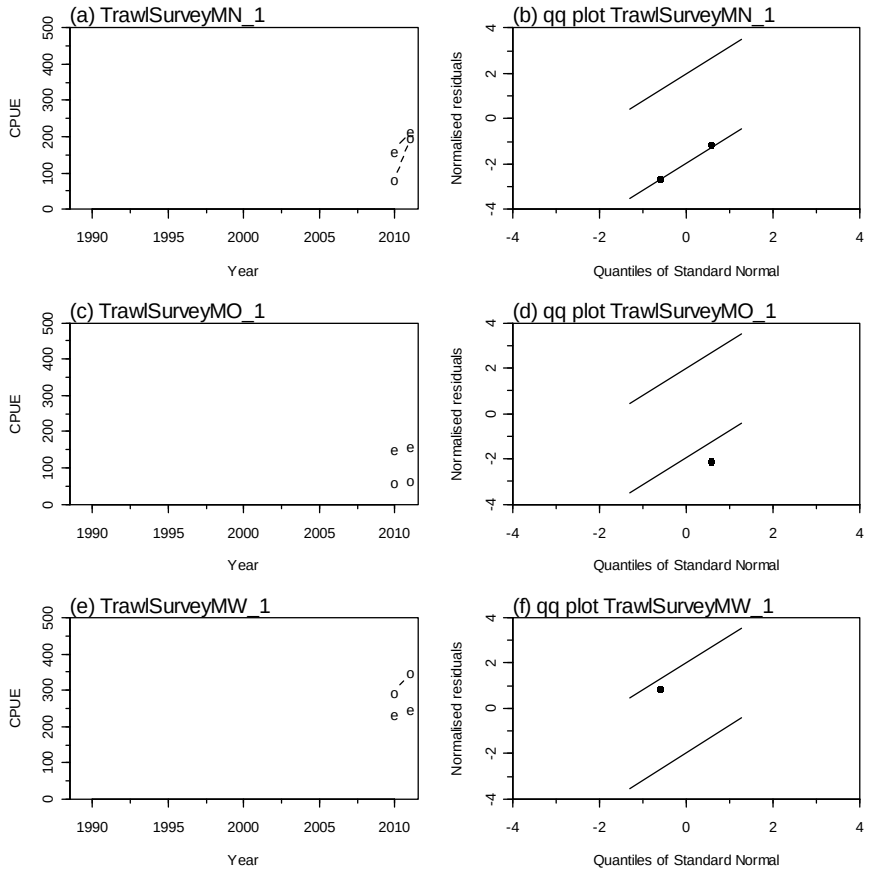

A4. 9: Fits and q-q diagnostic plots to trawl survey abundance indices.

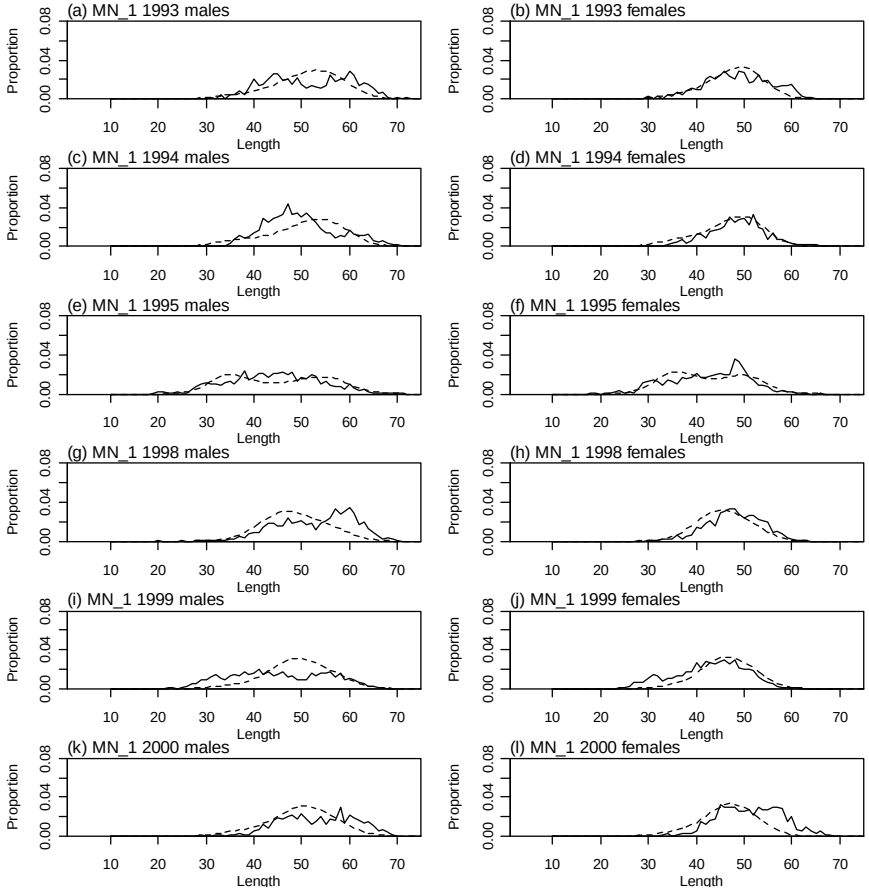

A4. 10: Observed (solid line) and fitted (dashed line) length frequency distributions for observer samples from MN, time step 1 (1993–2000).

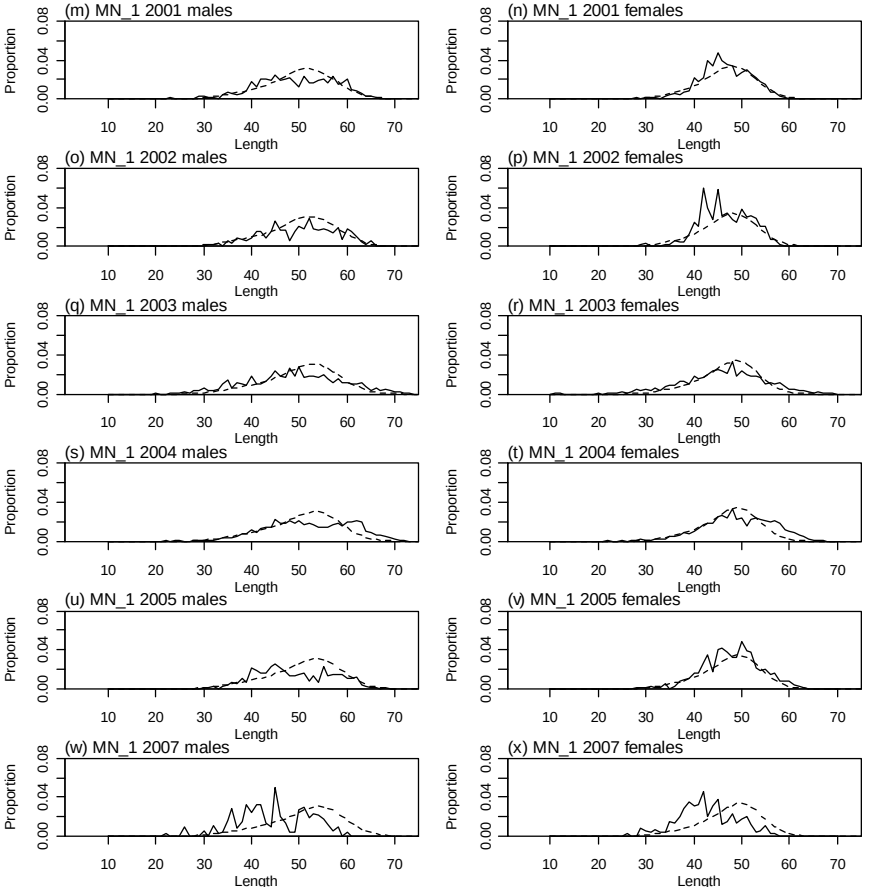

A4. 11: Observed (solid line) and fitted (dashed line) length frequency distributions for observer samples from MN, time step 1 (2001–2007).

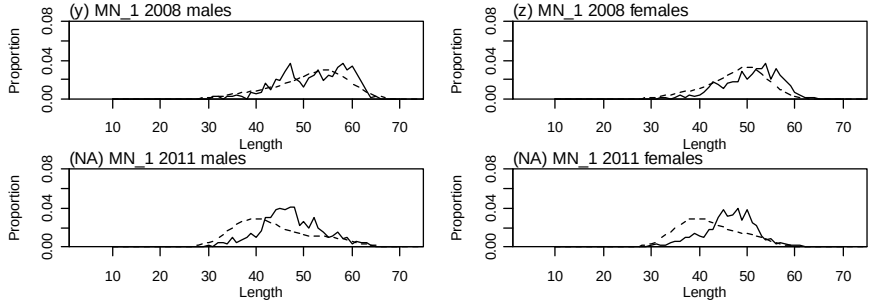

A4. 12: Observed (solid line) and fitted (dashed line) length frequency distributions for observer samples from MN, time step 1 (2008–2011).

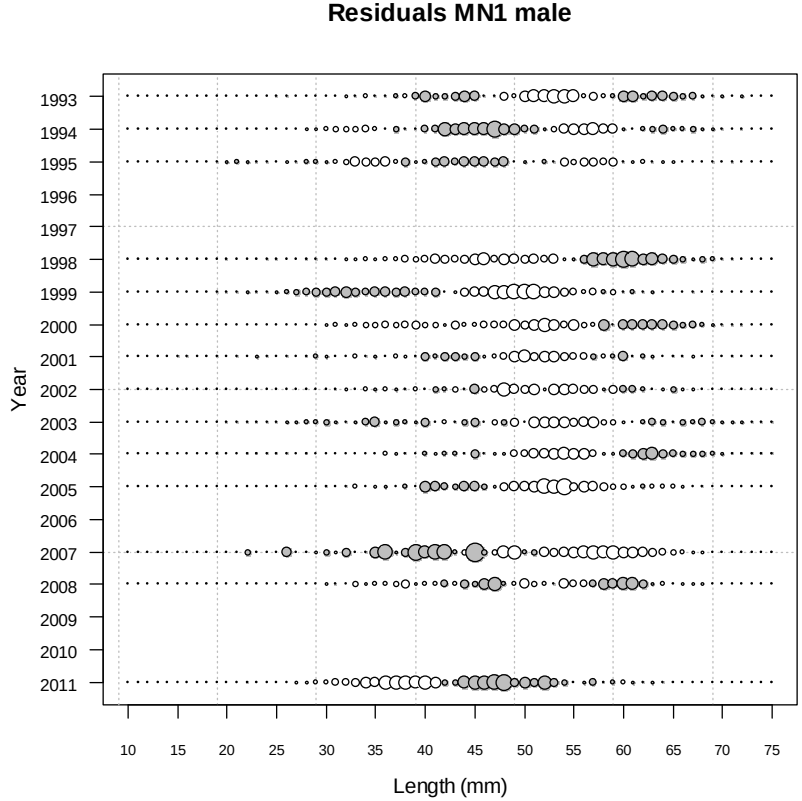

A4. 13: Bubble plots of residuals of fits to length frequency distributions for observer sampling from MN, time step 1, male.

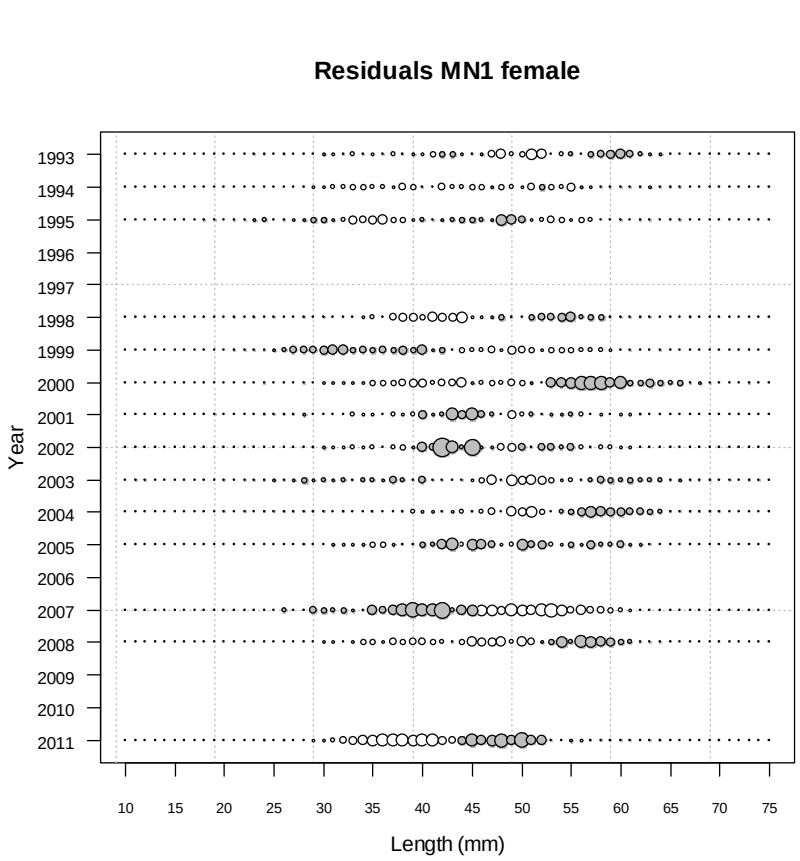

A4. 14: Bubble plots of residuals of fits to length frequency distributions for observer sampling from MN, time step 1, female.

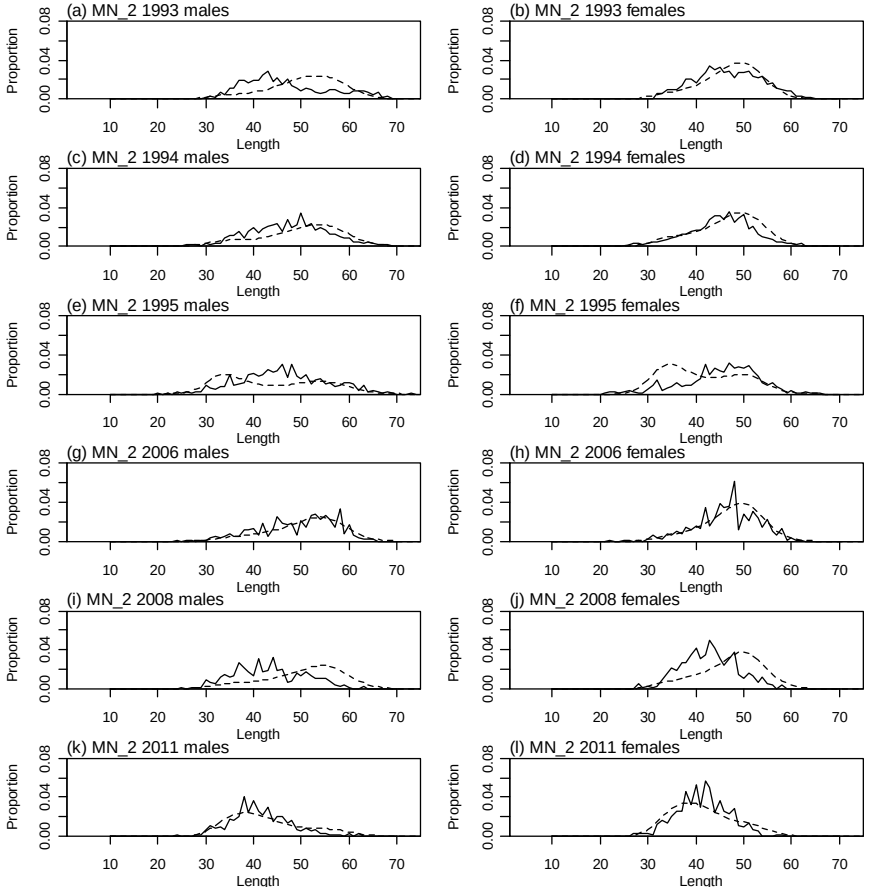

A4. 15: Observed (solid line) and fitted (dashed line) length frequency distributions for observer samples from MN, time step 2.

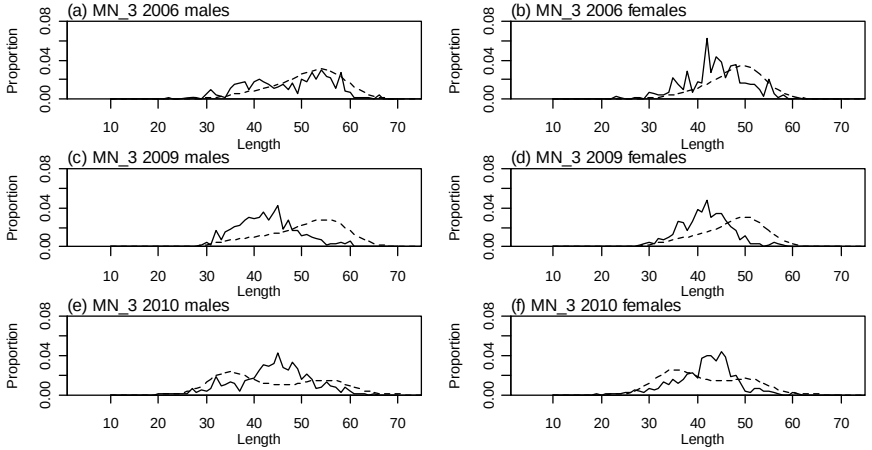

A4. 16: Observed (solid line) and fitted (dashed line) length frequency distributions for observer samples from MN, time step 3.

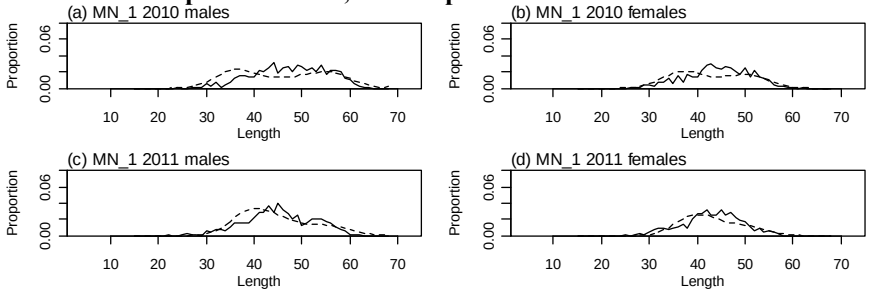

A4. 17: Observed (solid line) and fitted (dashed line) length frequency distributions for trawl survey samples from MN.

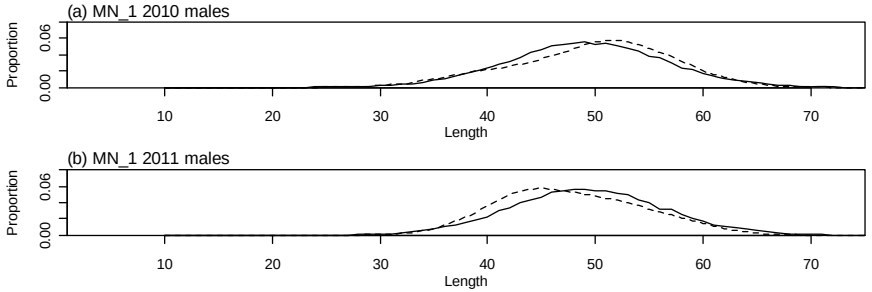

A4. 18: Observed (solid line) and fitted (dashed line) length frequency distributions for photo survey samples from MN.

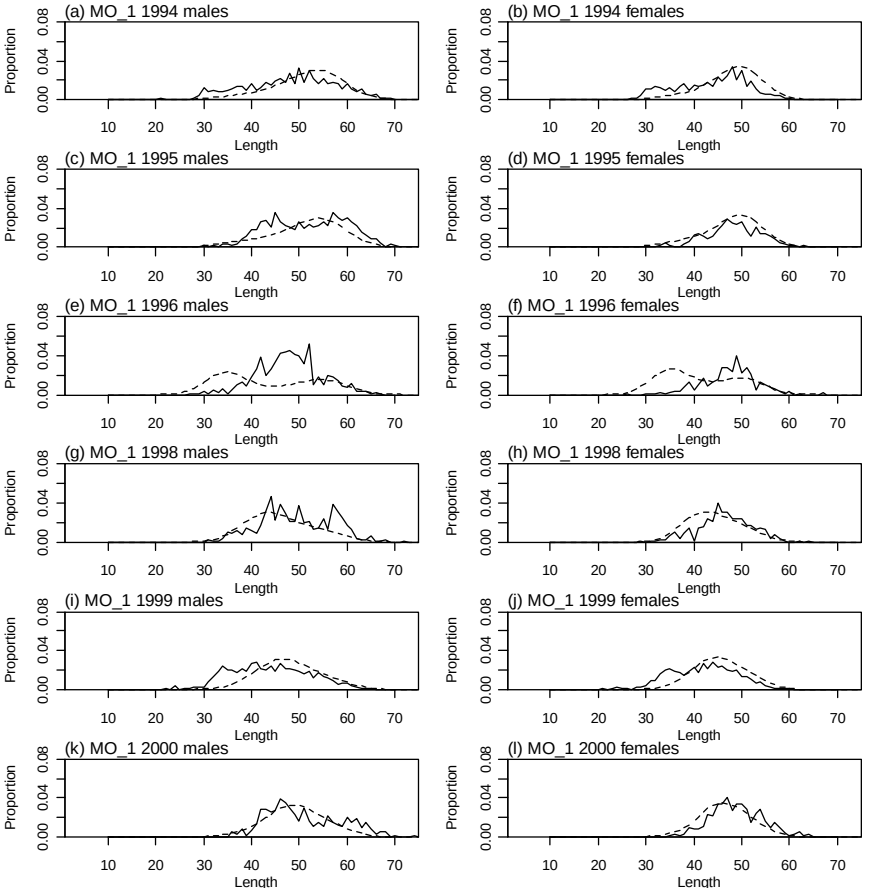

A4. 19: Observed (solid line) and fitted (dashed line) length frequency distributions for observer samples from MO, time step 1 (1994–2000).

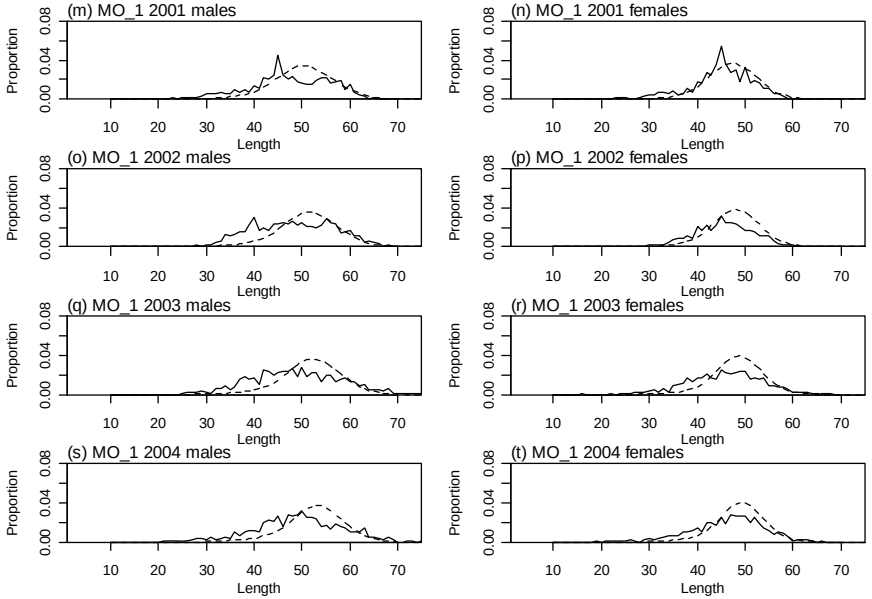

A4. 20: Observed (solid line) and fitted (dashed line) length frequency distributions for observer samples from MO, time step 1 (2001–2004).

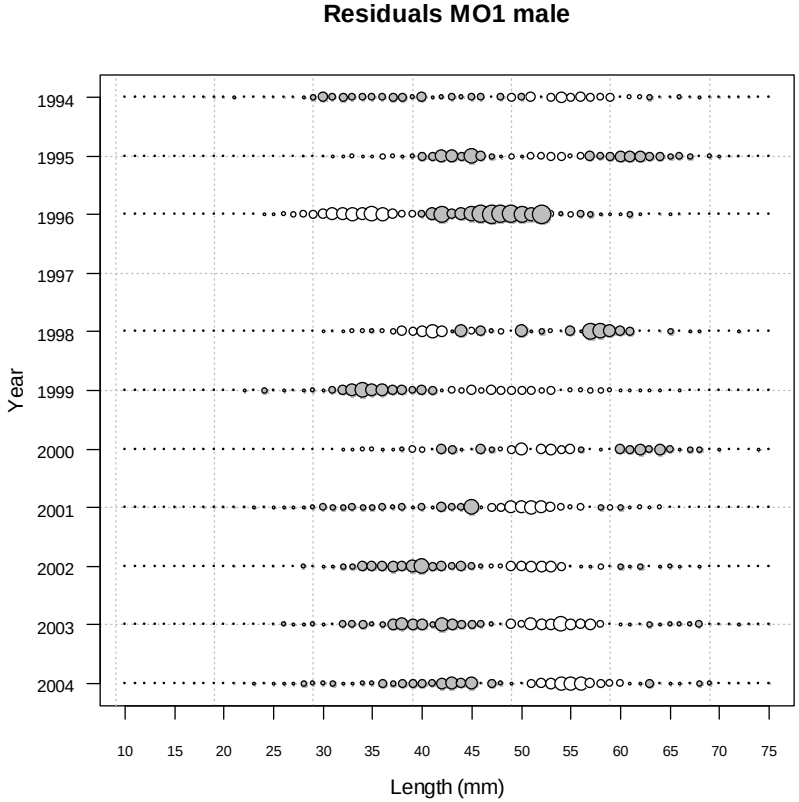

A4. 21: Bubble plots of residuals of fits to length frequency distributions for observer sampling from MO, time step 1, male.

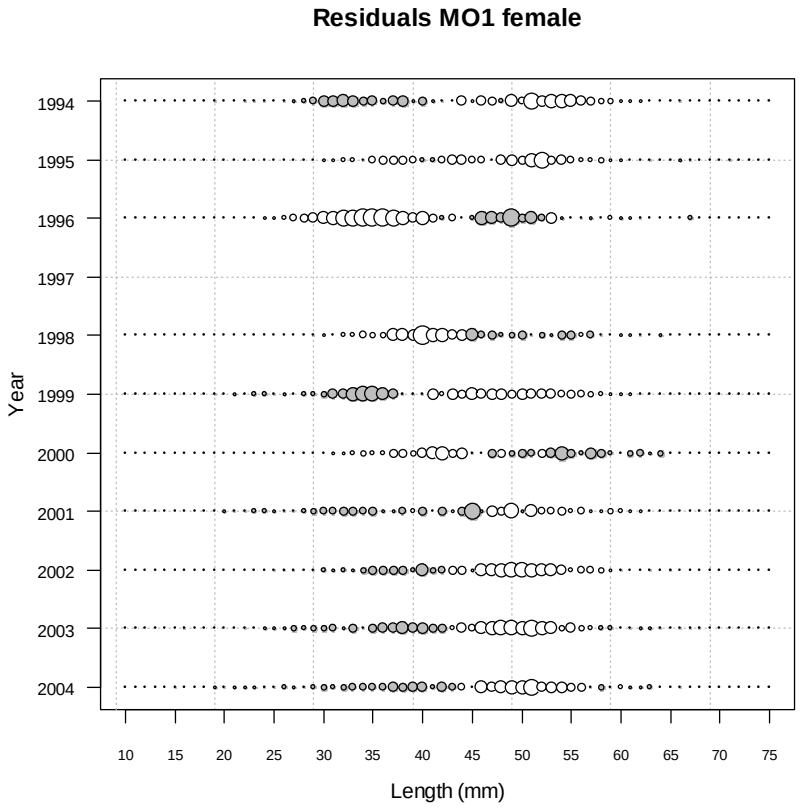

A4. 22: Bubble plots of residuals of fits to length frequency distributions for observer sampling from MO, time step 1, female.

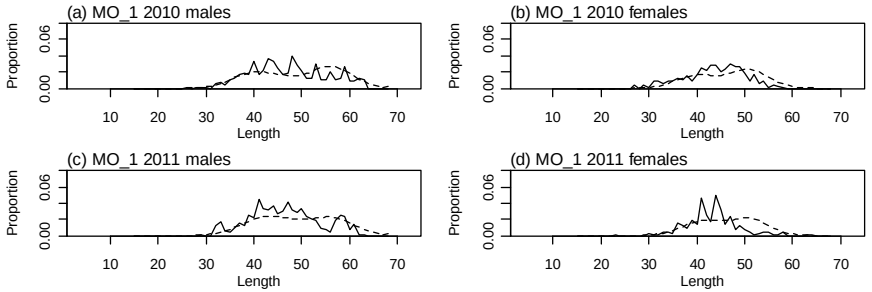

A4. 23: Observed (solid line) and fitted (dashed line) length frequency distributions for trawl survey samples from MO.

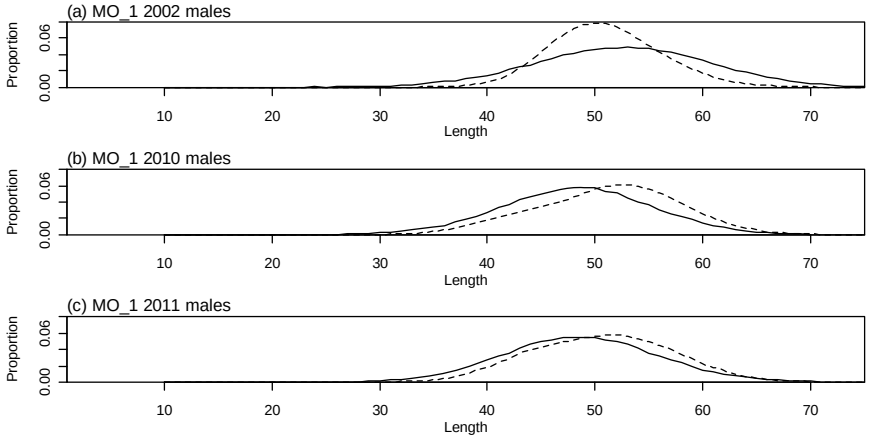

A4. 24: Observed (solid line) and fitted (dashed line) length frequency distributions for photo survey samples from MO.

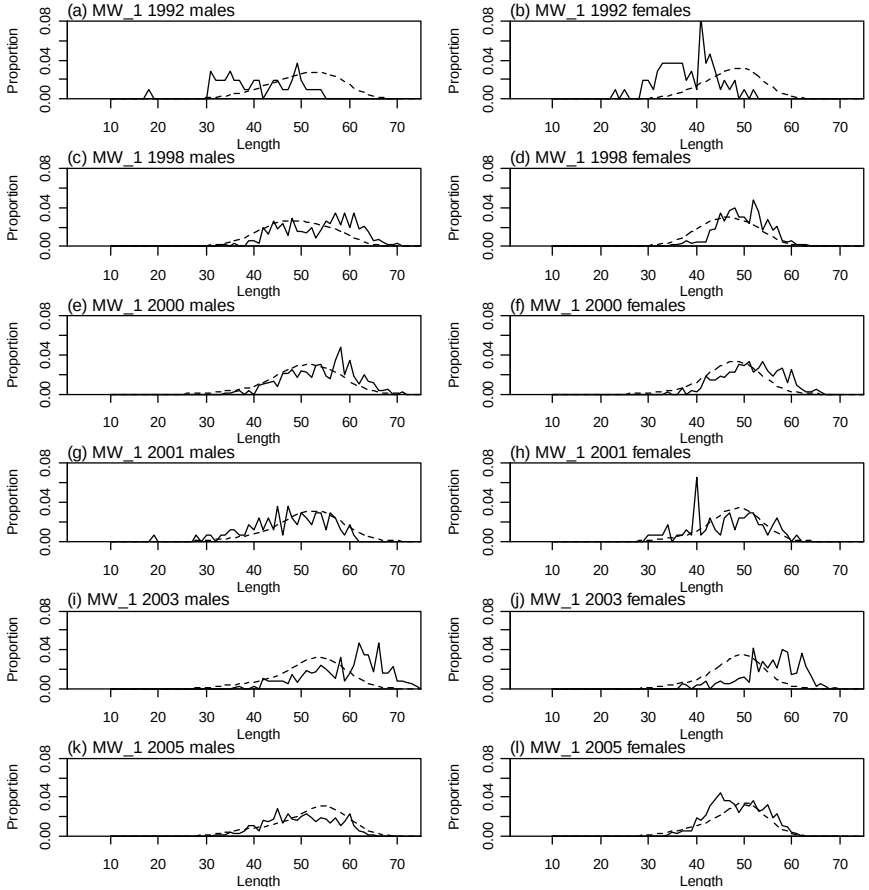

A4. 25: Observed (solid line) and fitted (dashed line) length frequency distributions for observer samples from MW, time step 1 (1992–2005).

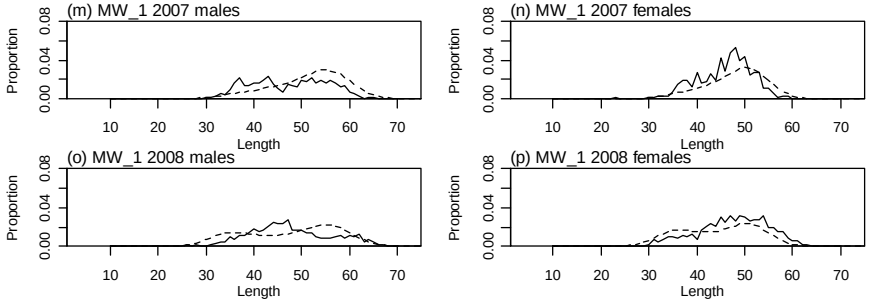

A4. 26: Observed (solid line) and fitted (dashed line) length frequency distributions for observer samples from MW, time step 1 (2007–2008).

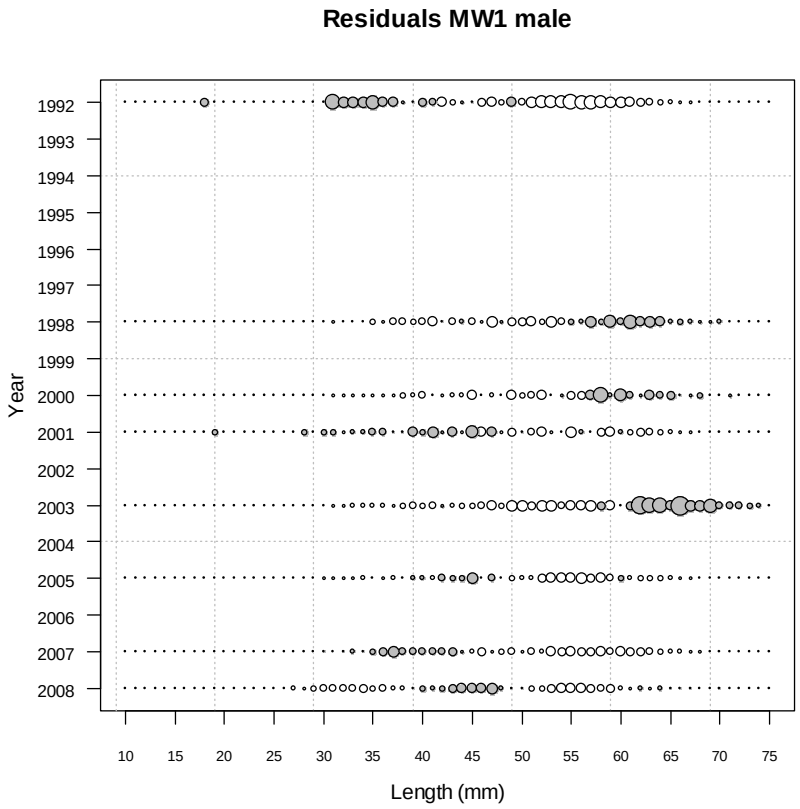

A4. 27: Bubble plots of residuals of fits to length frequency distributions for observer sampling from MW, time step 1, male.

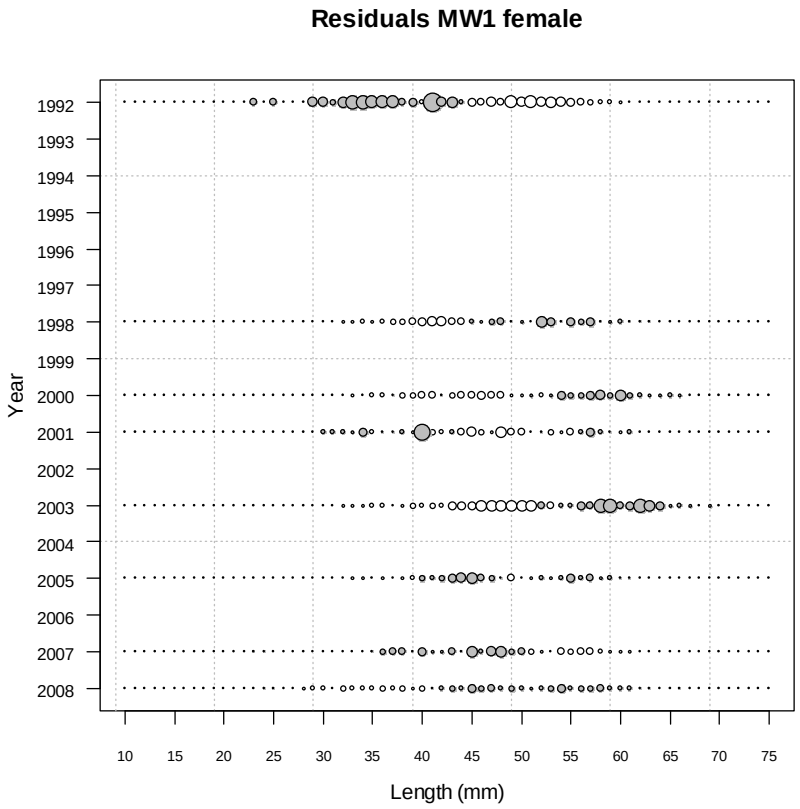

A4. 28: Bubble plots of residuals of fits to length frequency distributions for observer sampling from MW, time step 1, female.

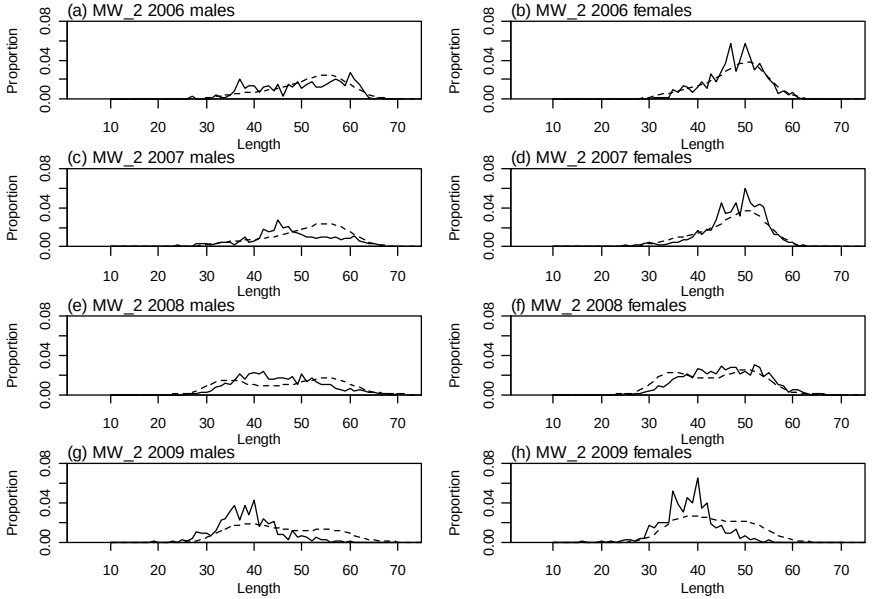

A4. 29: Observed (solid line) and fitted (dashed line) length frequency distributions for observer samples from MW, time step 2.

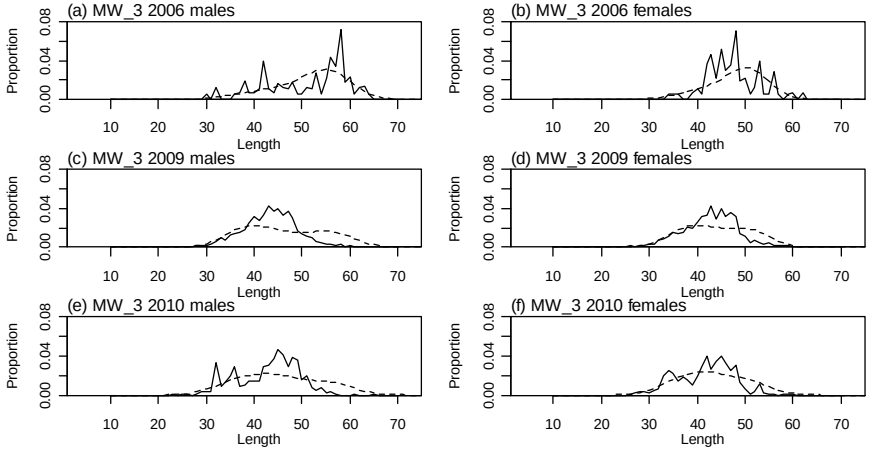

A4. 30: Observed (solid line) and fitted (dashed line) length frequency distributions for observer samples from MW, time step 3.

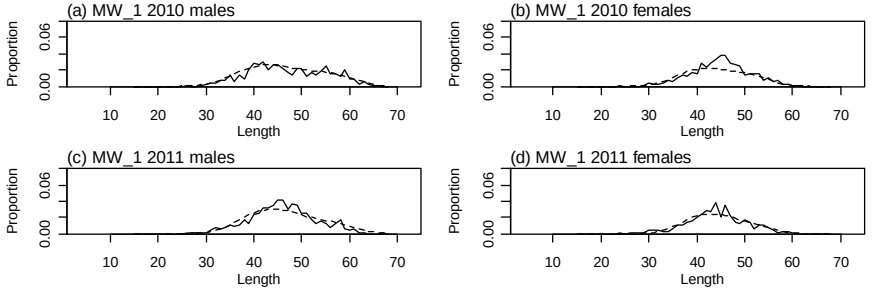

A4. 31: Observed (solid line) and fitted (dashed line) length frequency distributions for trawl survey samples from MW.

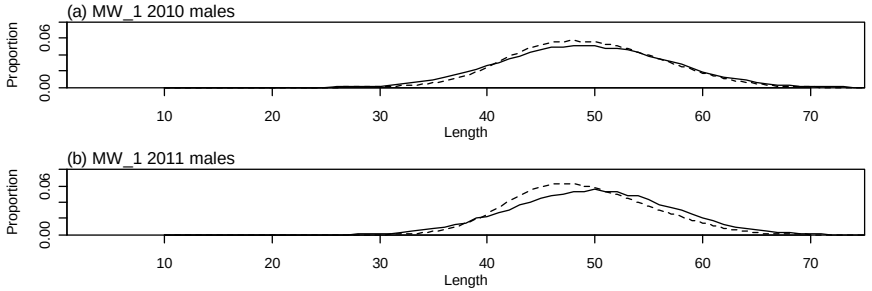

A4. 32: Observed (solid line) and fitted (dashed line) length frequency distributions for photo survey samples from MW.

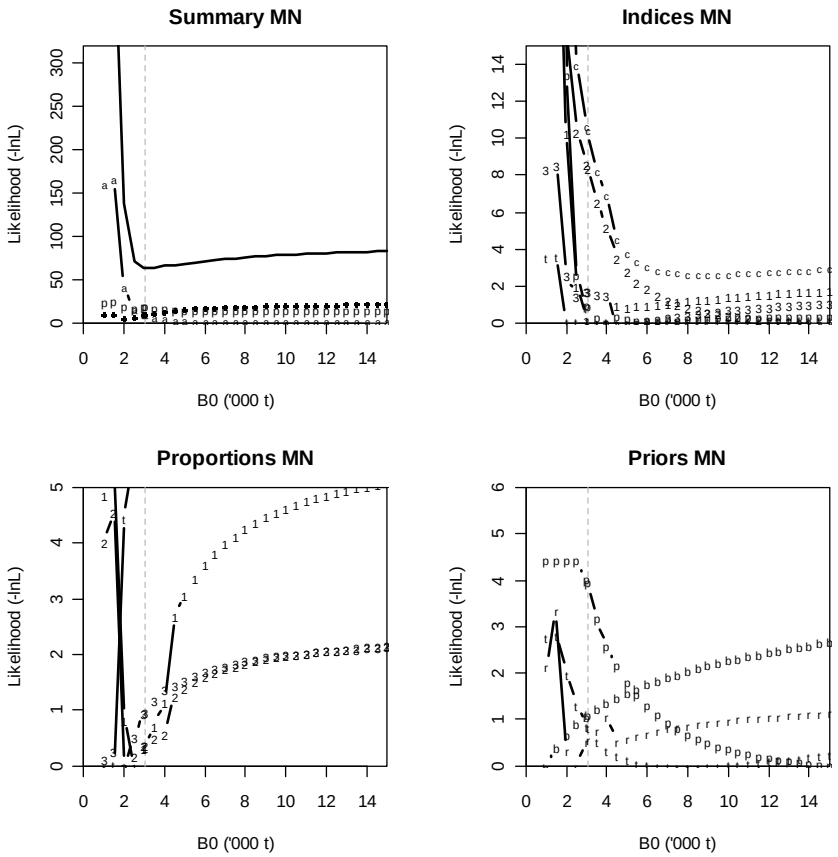

A4. 33: Likelihood profiles for model 1 when MN B_0 is fixed in the model. Figures show profiles for main priors (top left, p-priors, a – abundance indices, • – proportions at length), abundance indices (top right, t - trawl survey, 1 - CPUE time step 1, 2 - CPUE time step 2, 3 - CPUE time step 3, p – photo survey), proportion at length data (bottom left, t-trawl, 1 – observer time step 1, 2 – observer time step 2, 3 – observer time step 3) and priors (bottom right, b- B_0, YCS - r, p- *q-Photo*, t – *q-Trawl*).

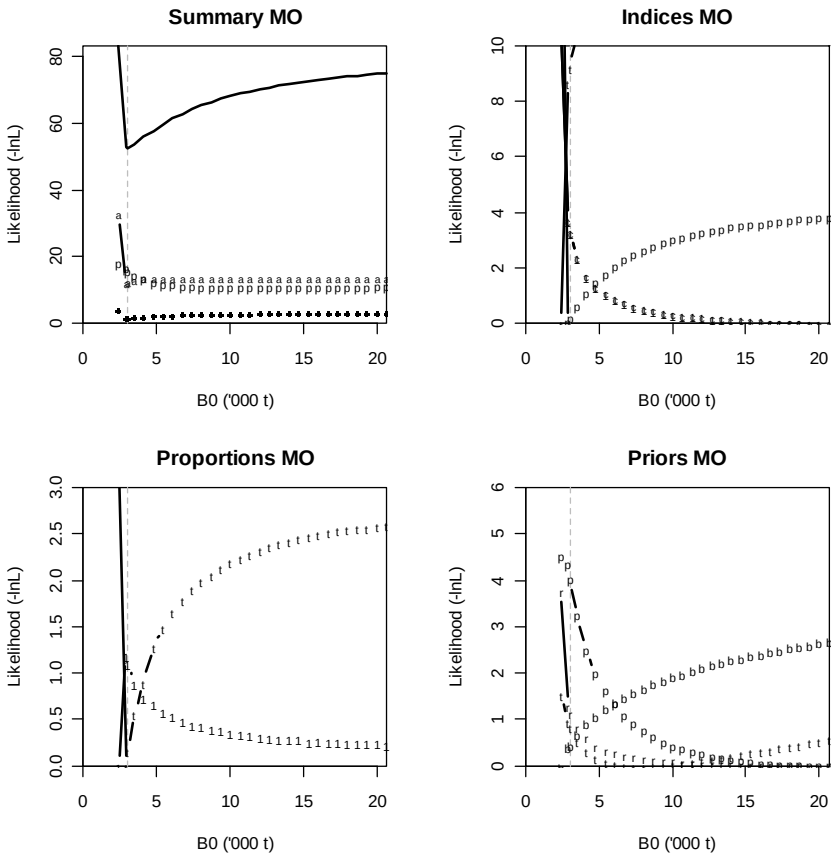

A4. 34: Likelihood profiles for model 1 when MO B_0 is fixed in the model. Figures show profiles for main priors (top left, p-priors, a – abundance indices, • – proportions at length), abundance indices (top right, t - trawl survey, 1 - CPUE time step 1, 2 - CPUE time step 2, 3 - CPUE time step 3, p – photo survey), proportion at length data (bottom left, t-trawl, 1 – observer time step 1, 2 – observer time step 2, 3 – observer time step 3) and priors (bottom right, b- B_0, YCS - r, p- *q-Photo*, t – *q-Trawl*).

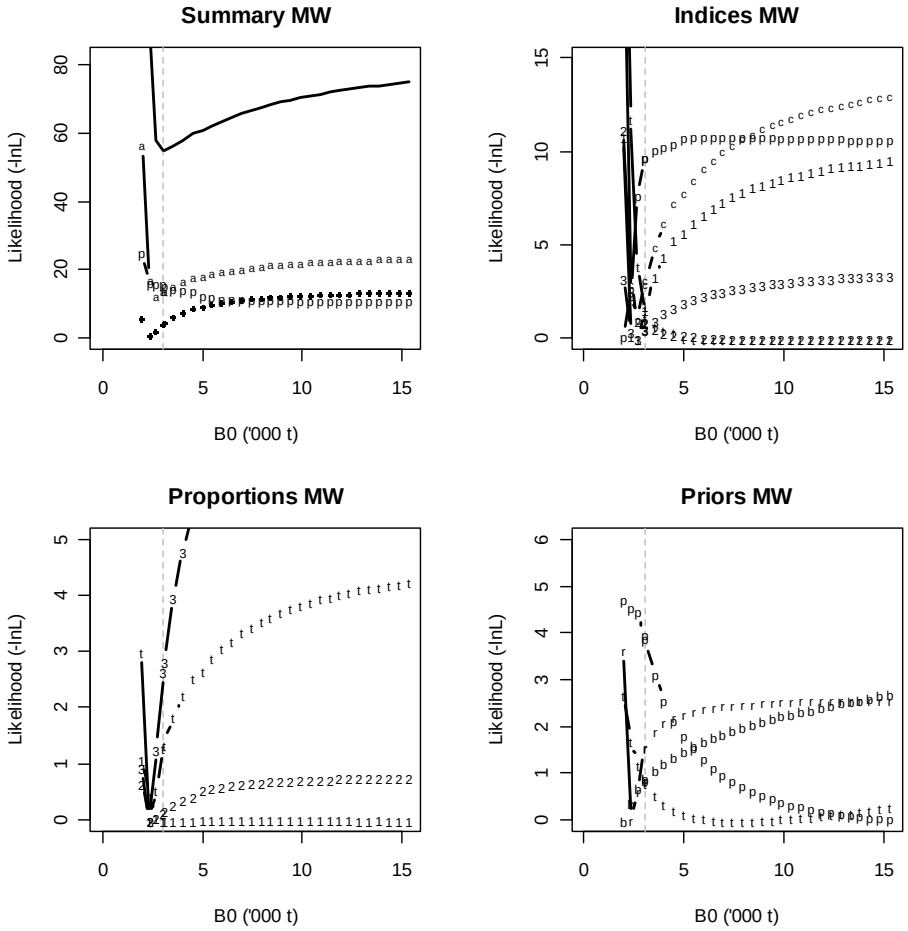

A4. 35: Likelihood profiles for model 1 when MW B_0 is fixed in the model. Figures show profiles for main priors (top left, p-priors, a – abundance indices, • – proportions at length), abundance indices (top right, t - trawl survey, 1 - CPUE time step 1, 2 - CPUE time step 2, 3 - CPUE time step 3, p – photo survey), proportion at length data (bottom left, t-trawl, 1 – observer time step 1, 2 – observer time step 2, 3 – observer time step 3) and priors (bottom right, b- B_0, YCS - r, p- *q-Photo*, t – *q-Trawl*).

12. APPENDIX 5. BASE-030 model plots

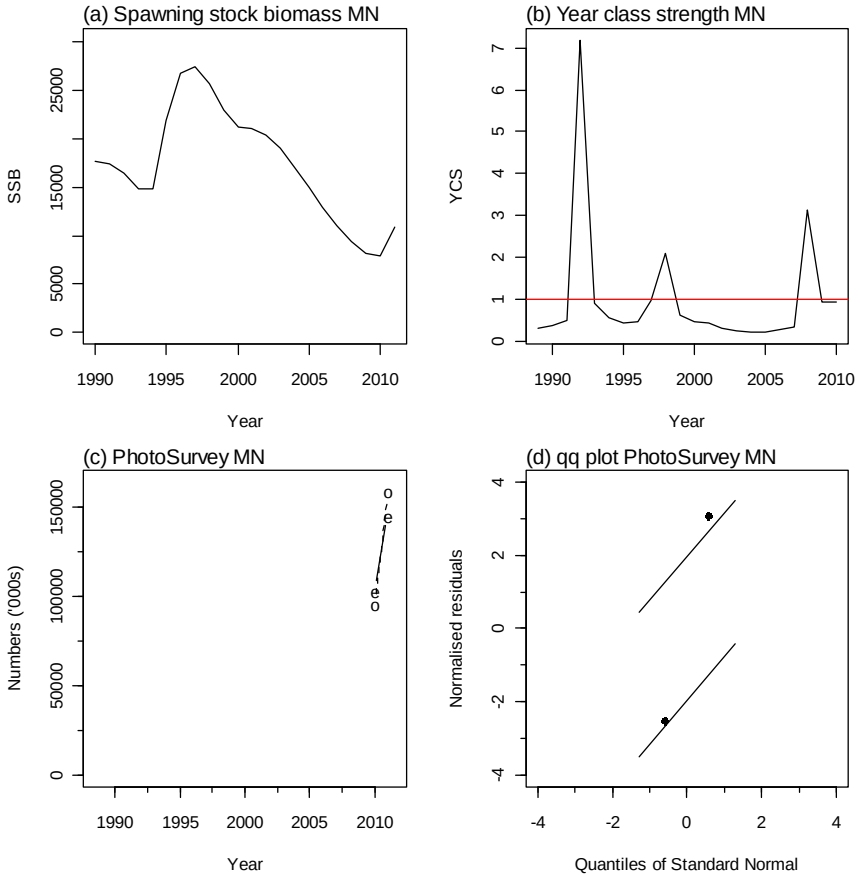

A5. 1: Spawning stock biomass trajectory (a), year class strength (b) fits (c) and q-q diagnostic plots (d) to photo survey abundance index for SCI 3 subarea MN from BASE-030 model.

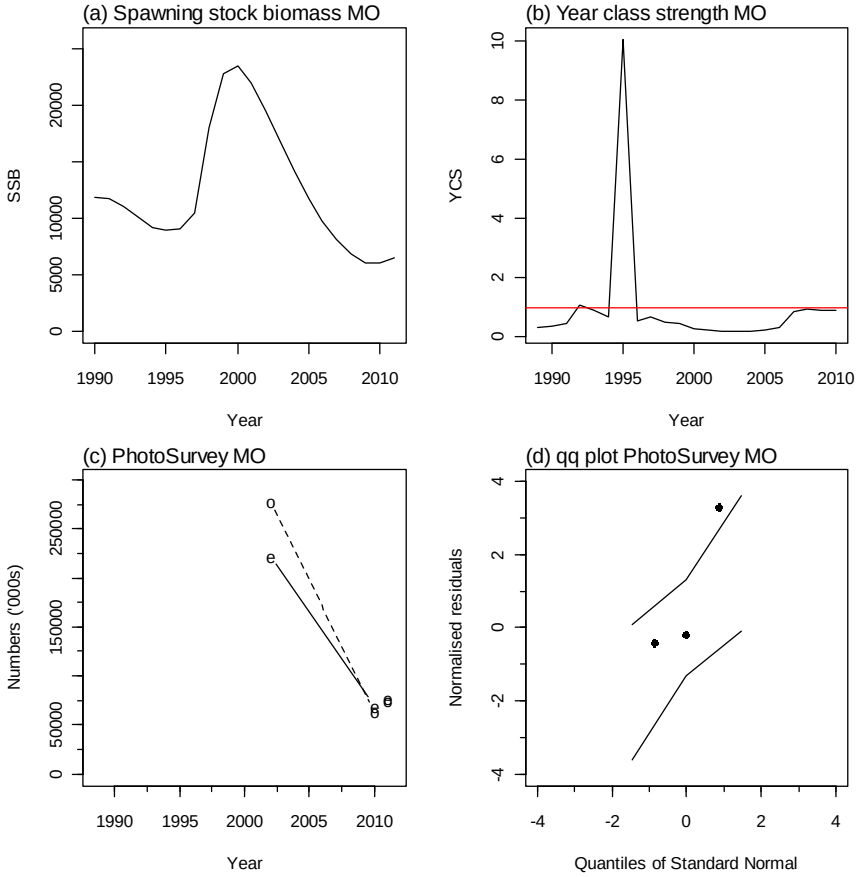

A5. 2: Spawning stock biomass trajectory (a), year class strength (b) fits (c) and q-q diagnostic plots (d) to photo survey abundance index for SCI 3 subarea MO from BASE-030 model.

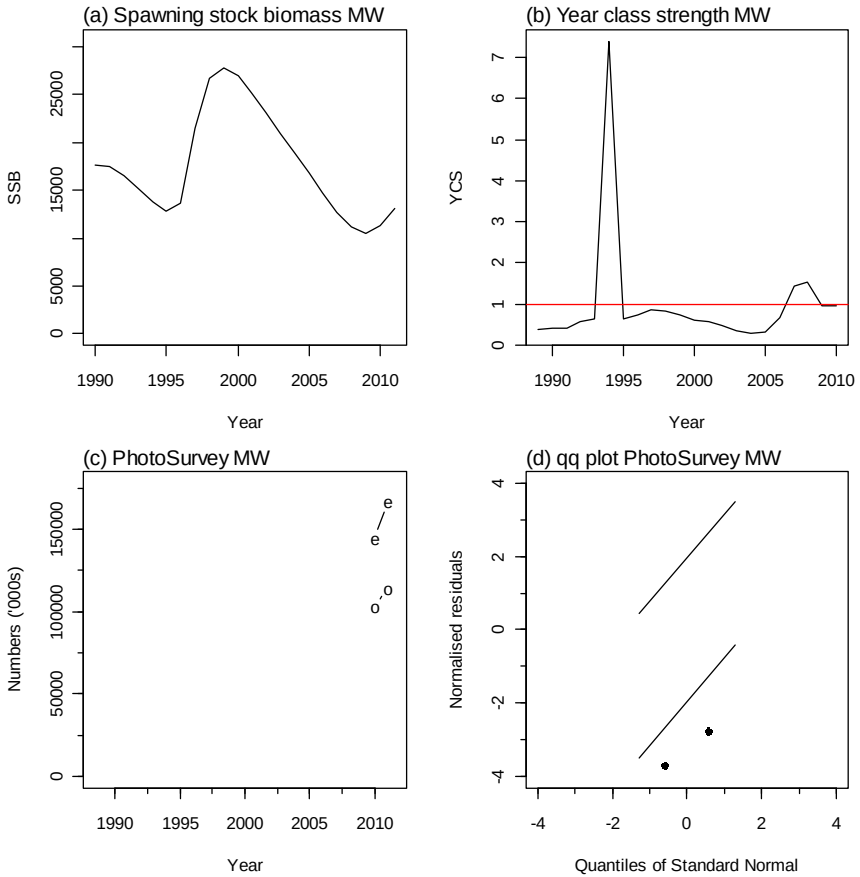

A5. 3: Spawning stock biomass trajectory (a), year class strength (b) fits (c) and q-q diagnostic plots (d) to photo survey abundance index for SCI 3 subarea MW from BASE-030 model.

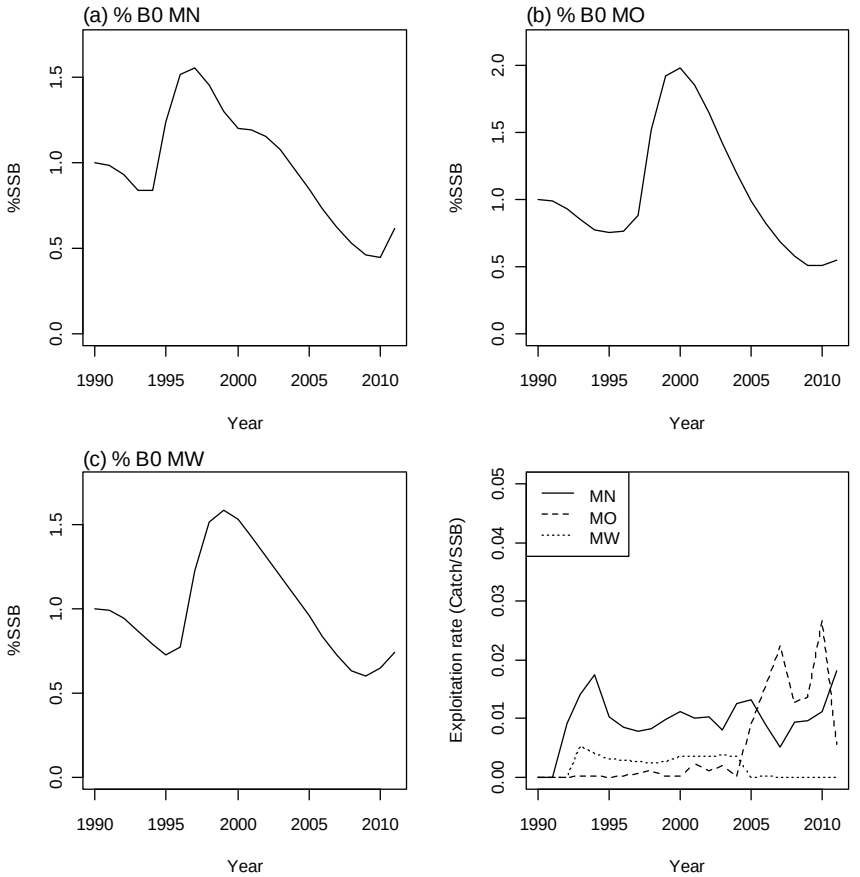

A5. 4: Trajectory of SSB as a percentage of B_0 for each subarea from the MPD fit to BASE-030 model, and exploitation rate (catch/SSB).

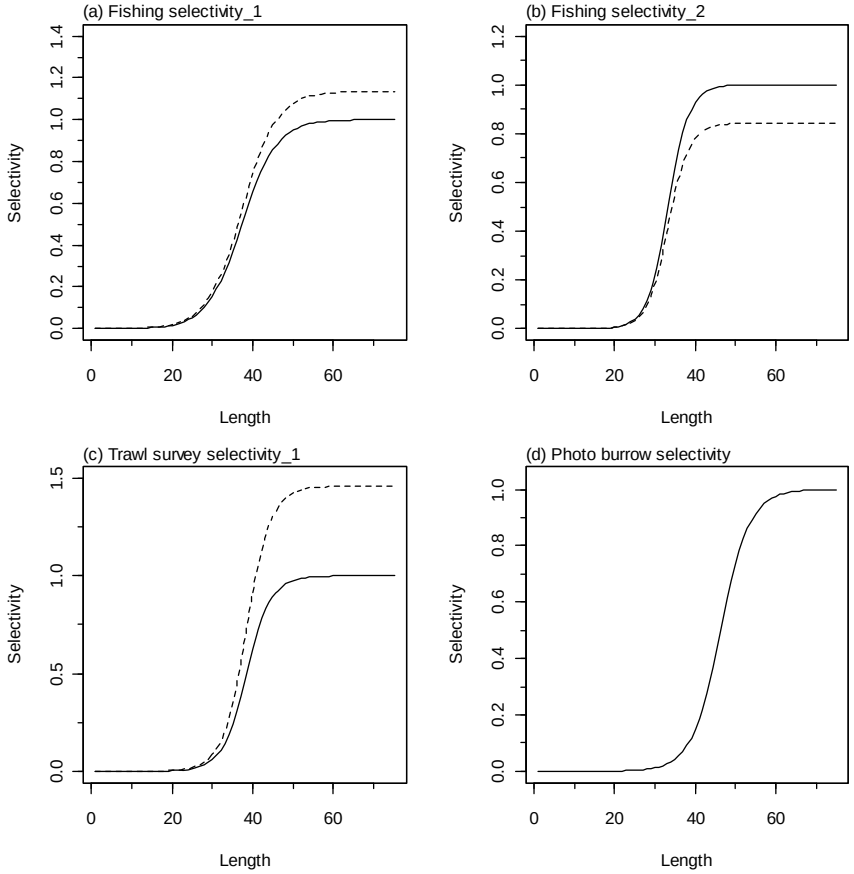

A5. 5: Fishery and survey selectivity curves. Solid line – females, dotted line – males. The scampi burrow index is not sexed, and a single selectivity applies.

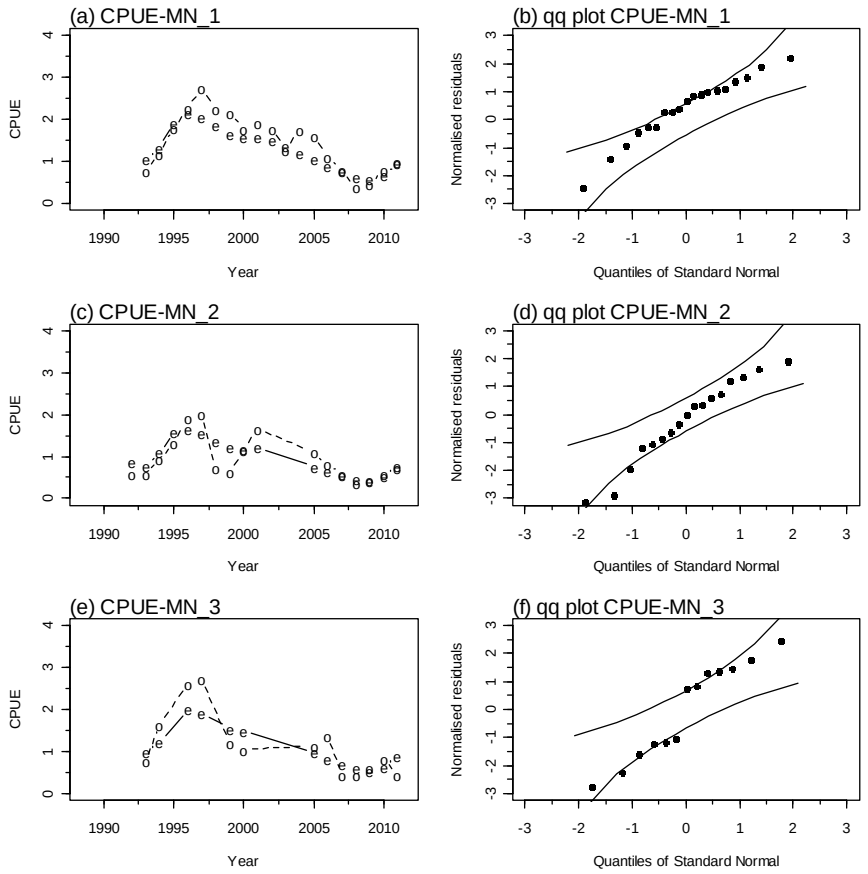

A5. 6: Fits and q-q diagnostic plots to CPUE abundance indices for MN.

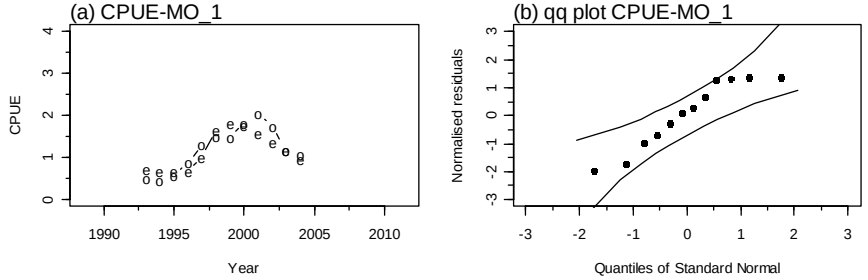

A5. 7: Fits and q-q diagnostic plots to CPUE abundance indices for MO.

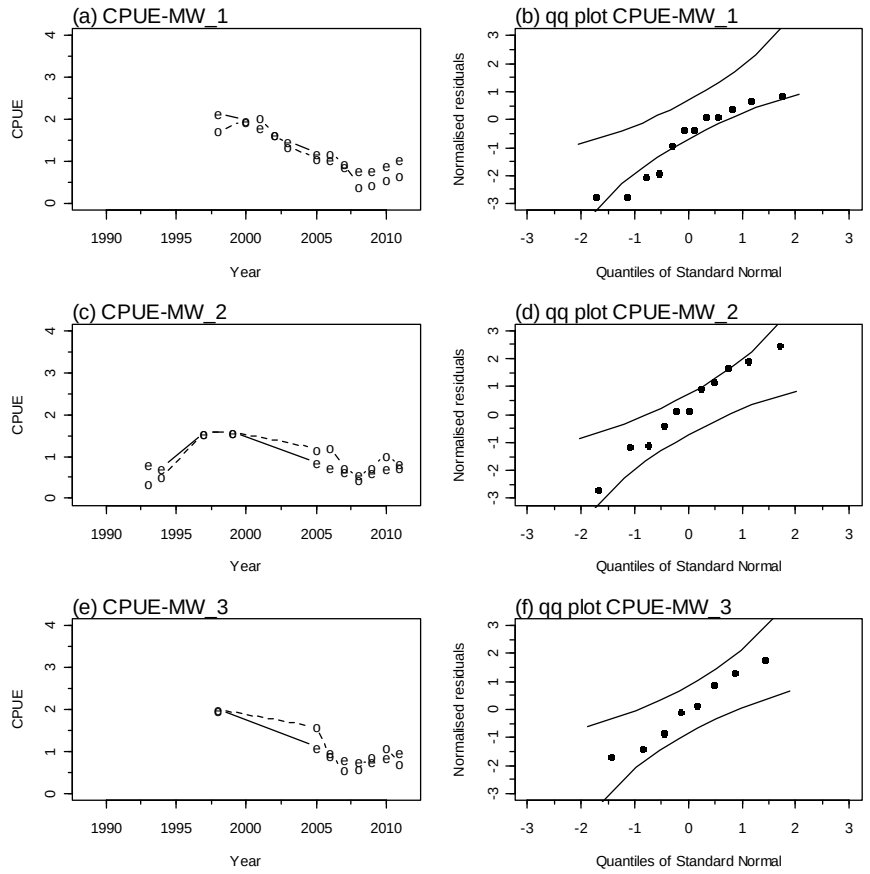

A5. 8: Fits and q-q diagnostic plots to CPUE abundance indices for MW.

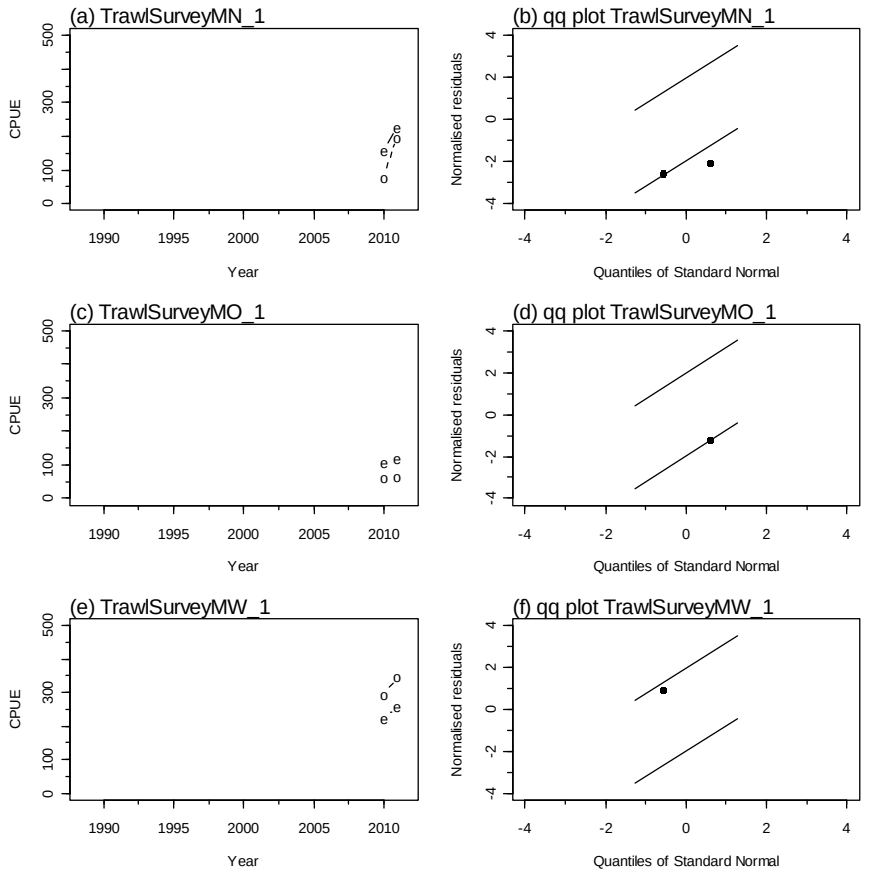

A5. 9: Fits and q-q diagnostic plots to trawl survey abundance indices.

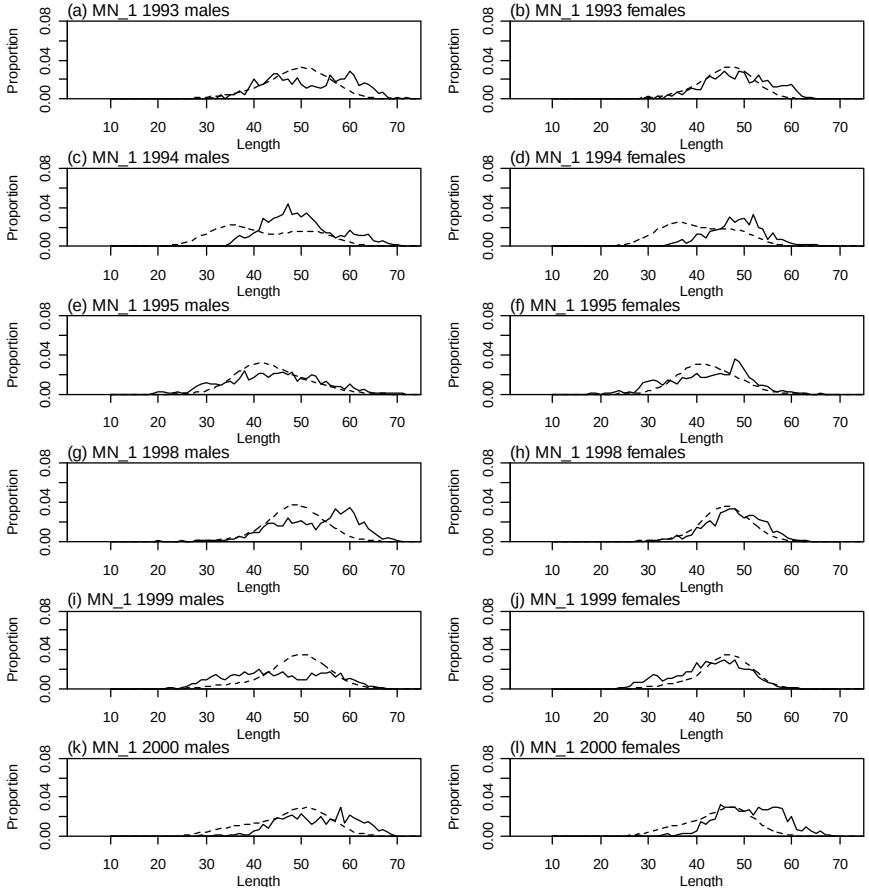

A5. 10: Observed (solid line) and fitted (dashed line) length frequency distributions for observer samples from MN, time step 1 (1993–2000).

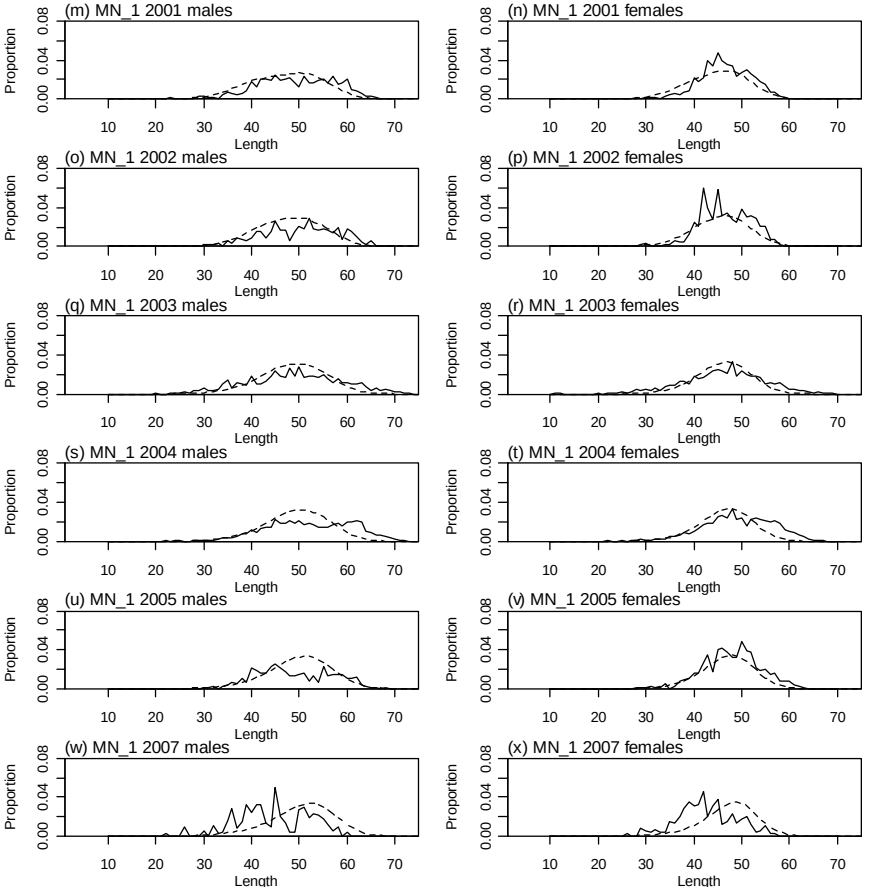

A5. 11: Observed (solid line) and fitted (dashed line) length frequency distributions for observer samples from MN, time step 1 (2001–2007).

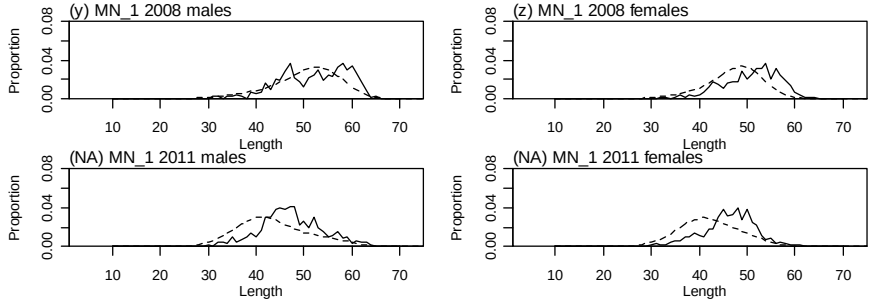

A5. 12: Observed (solid line) and fitted (dashed line) length frequency distributions for observer samples from MN, time step 1 (2008–2011).

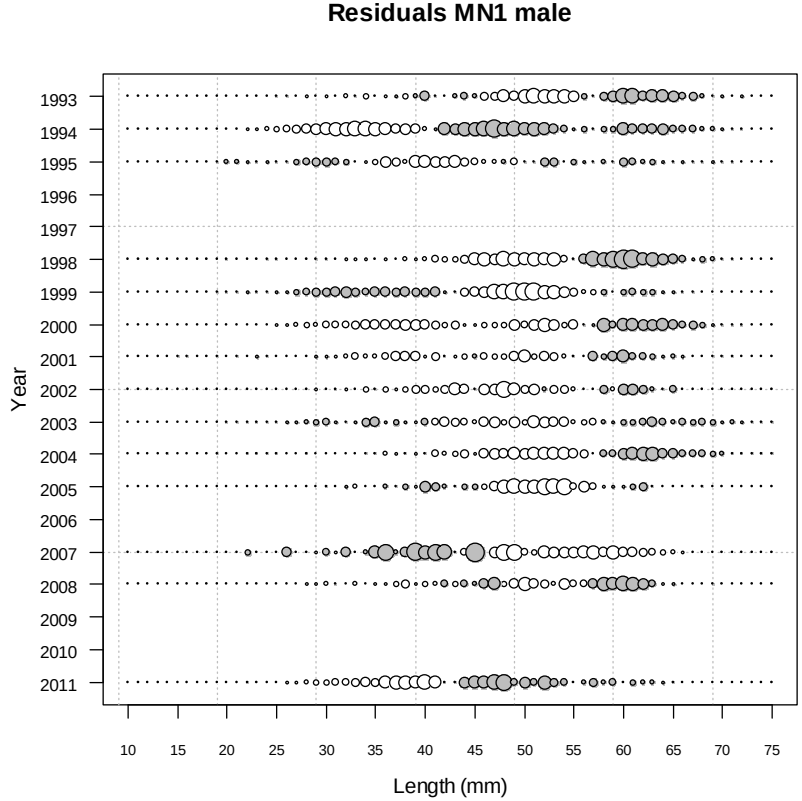

A5. 13: Bubble plots of residuals of fits to length frequency distributions for observer sampling from MN, time step 1, male.

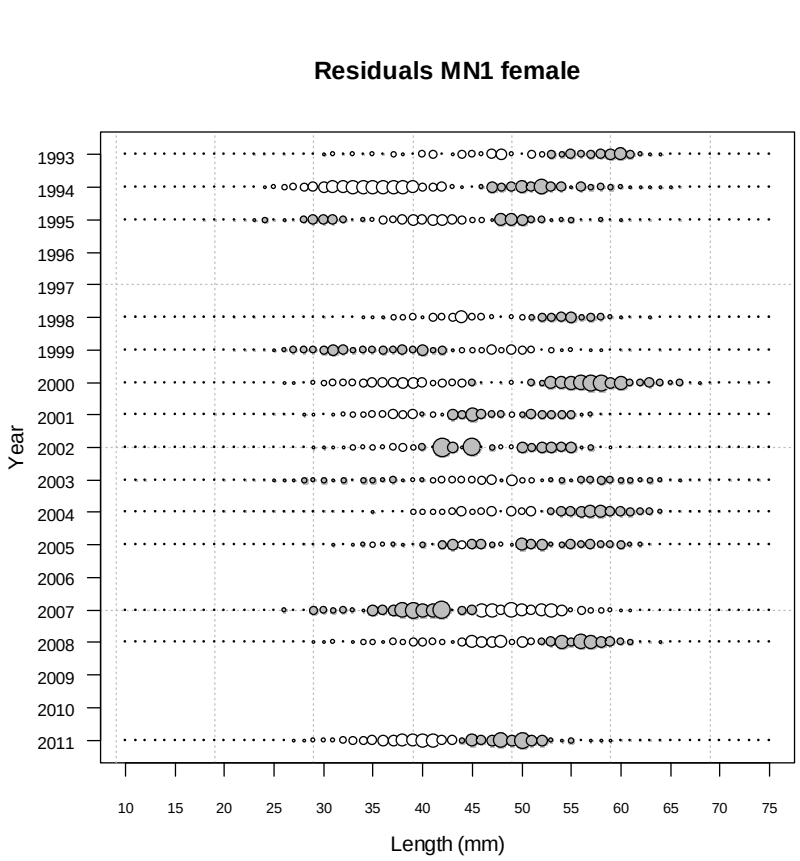

A5. 14: Bubble plots of residuals of fits to length frequency distributions for observer sampling from MN, time step 1, female.

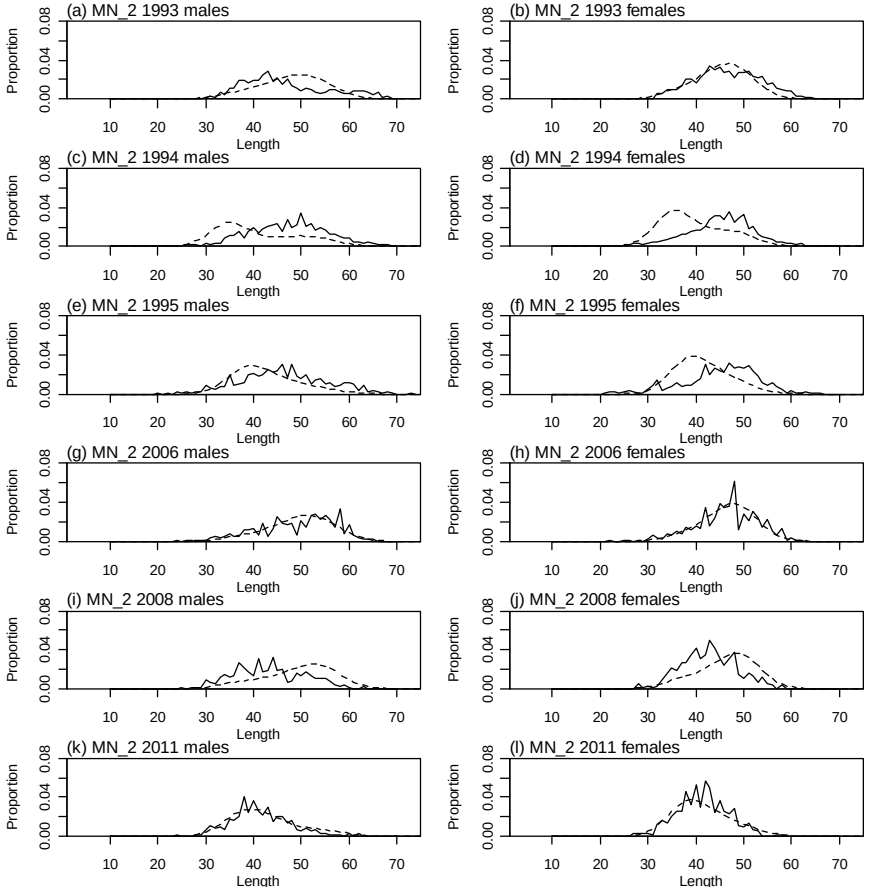

A5. 15: Observed (solid line) and fitted (dashed line) length frequency distributions for observer samples from MN, time step 2.

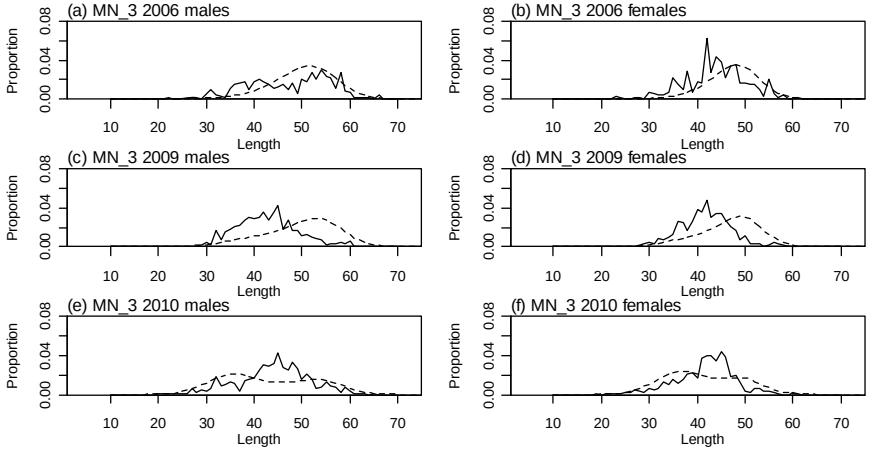

A5. 16: Observed (solid line) and fitted (dashed line) length frequency distributions for observer samples from MN, time step 3.

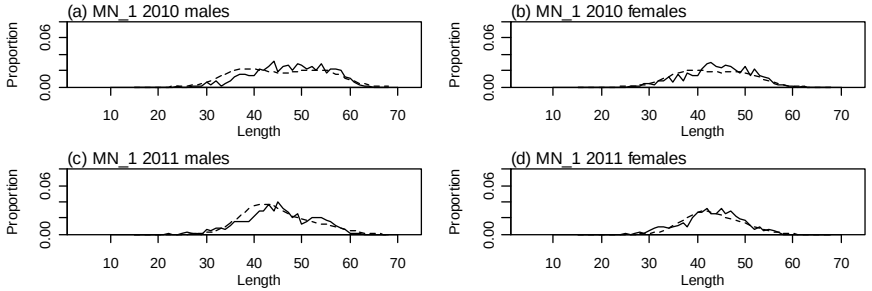

A5. 17: Observed (solid line) and fitted (dashed line) length frequency distributions for trawl survey samples from MN.

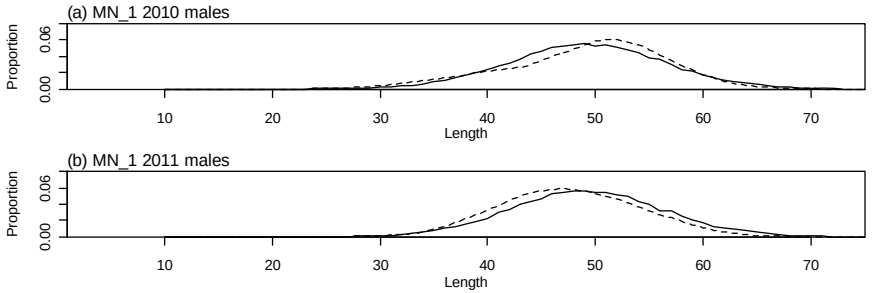

A5. 18: Observed (solid line) and fitted (dashed line) length frequency distributions for photo survey samples from MN.

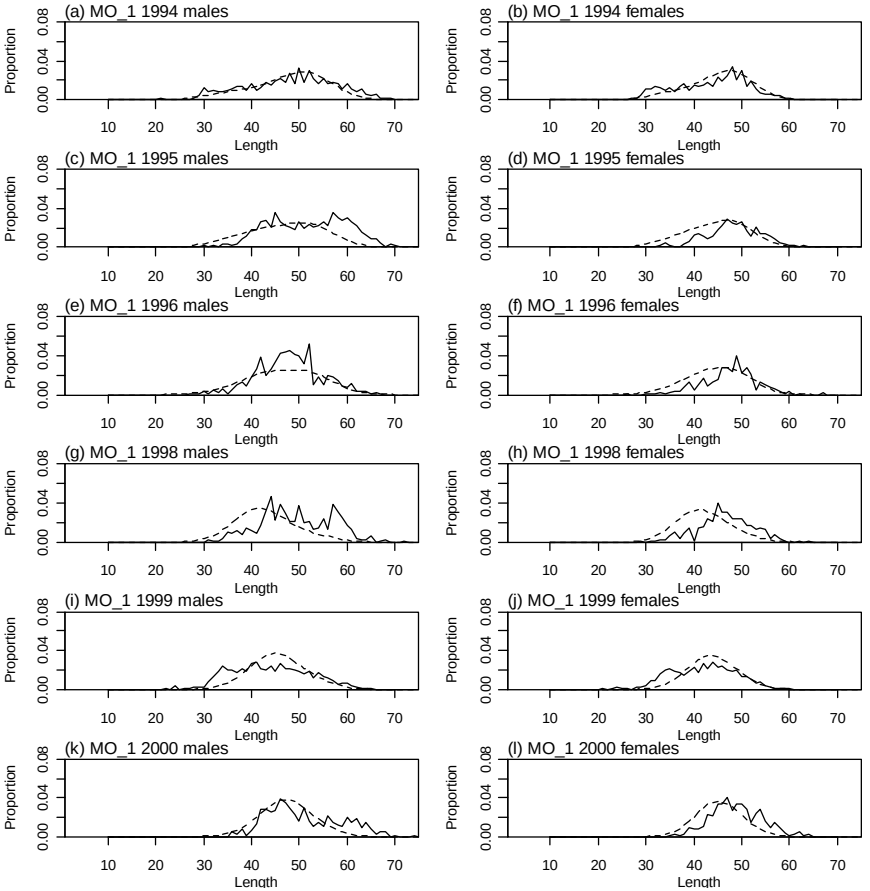

A5. 19: Observed (solid line) and fitted (dashed line) length frequency distributions for observer samples from MO, time step 1 (1994–2000).

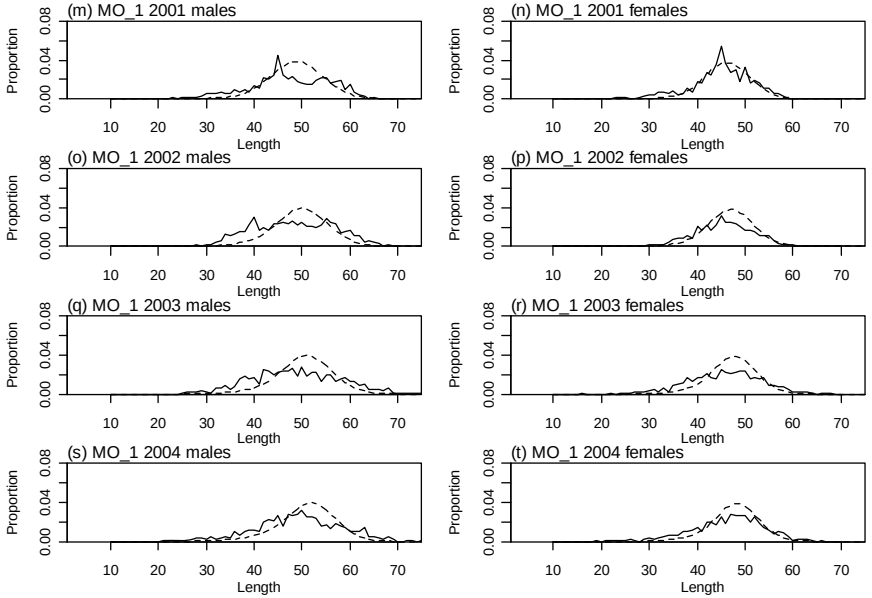

A5. 20: Observed (solid line) and fitted (dashed line) length frequency distributions for observer samples from MO, time step 1 (2001–2004).

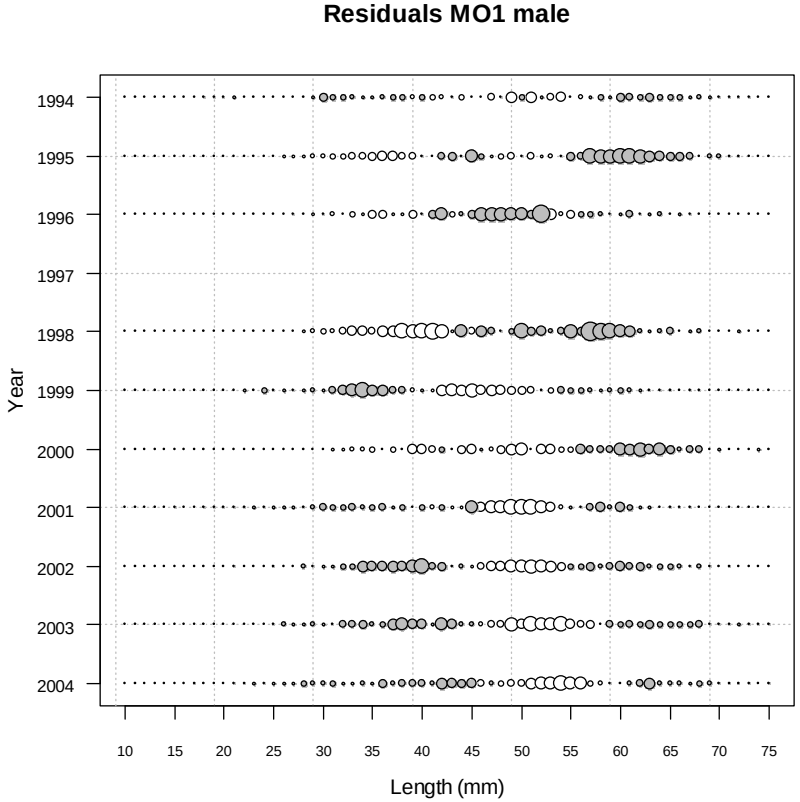

A5. 21: Bubble plots of residuals of fits to length frequency distributions for observer sampling from MO, time step 1, male.

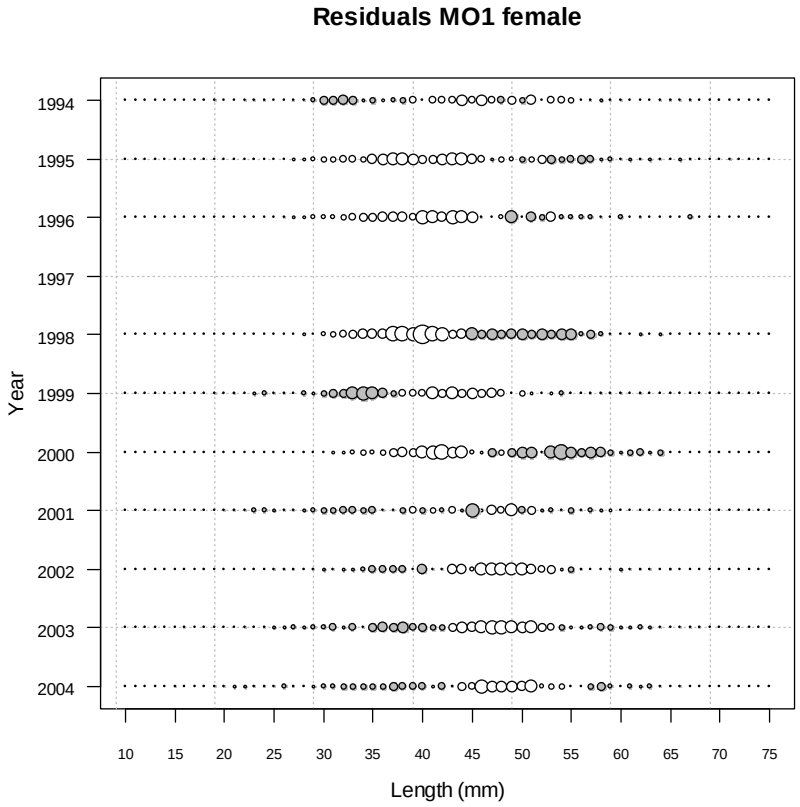

A5. 22: Bubble plots of residuals of fits to length frequency distributions for observer sampling from MO, time step 1, female.

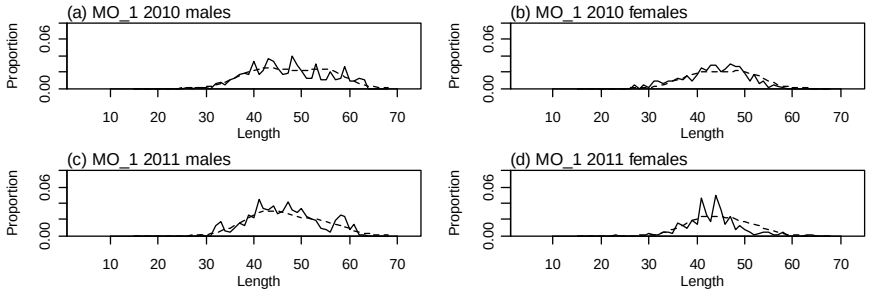

A5. 23: Observed (solid line) and fitted (dashed line) length frequency distributions for trawl survey samples from MO.

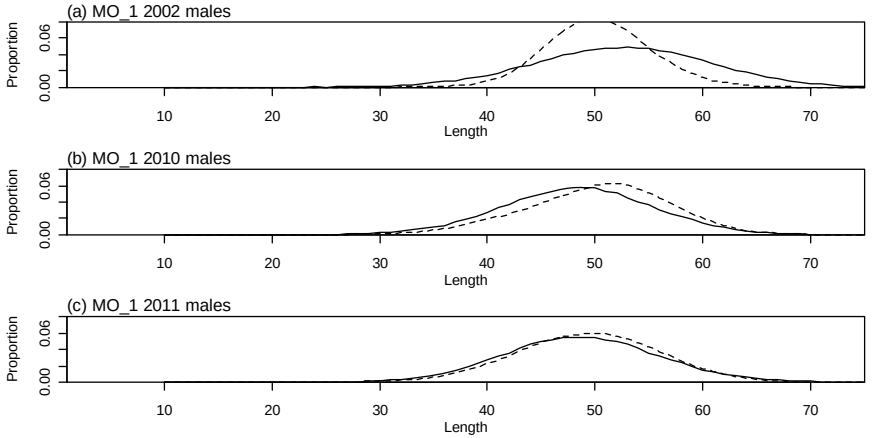

A5. 24: Observed (solid line) and fitted (dashed line) length frequency distributions for photo survey samples from MO.

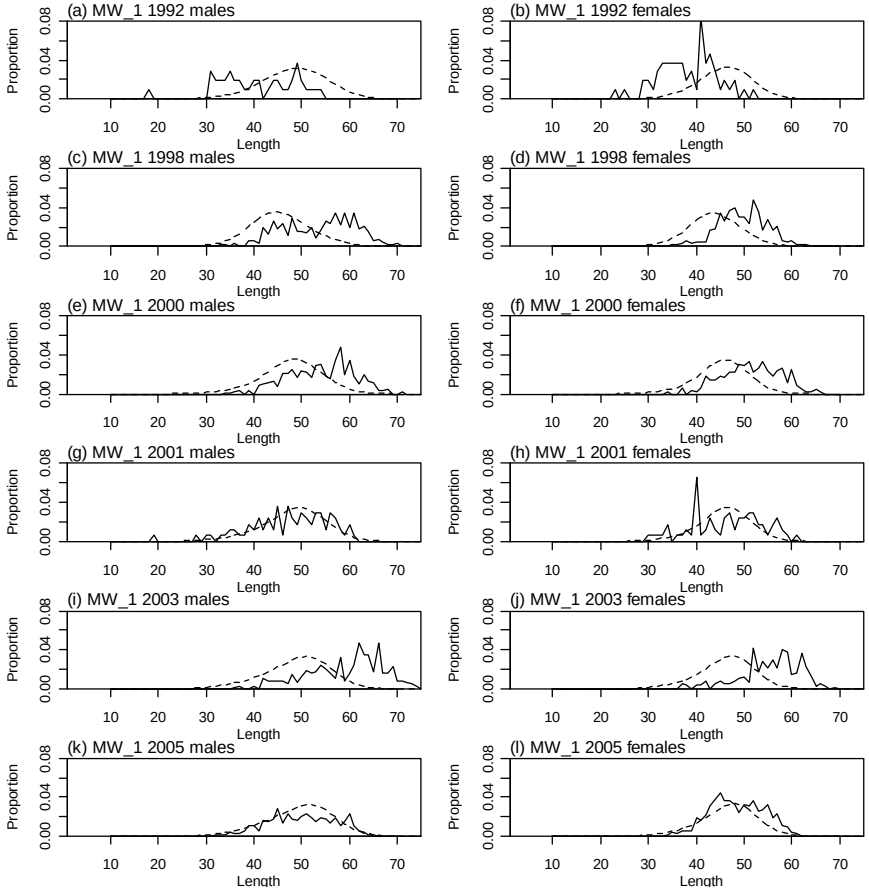

A5. 25: Observed (solid line) and fitted (dashed line) length frequency distributions for observer samples from MW, time step 1 (1992–2005).

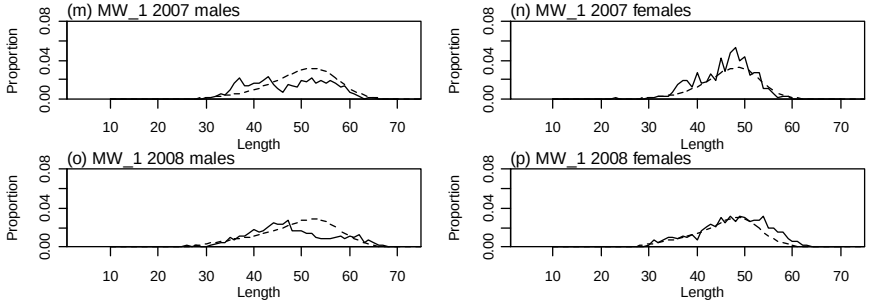

A5. 26: Observed (solid line) and fitted (dashed line) length frequency distributions for observer samples from MW, time step 1 (2007–2008).

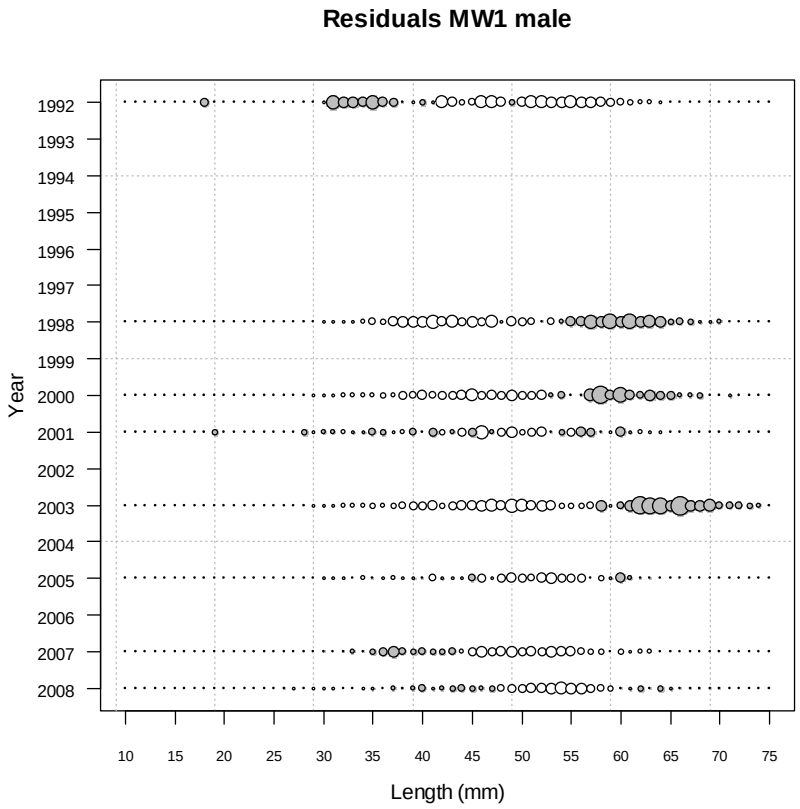

A5. 27: Bubble plots of residuals of fits to length frequency distributions for observer sampling from MW, time step 1, male.

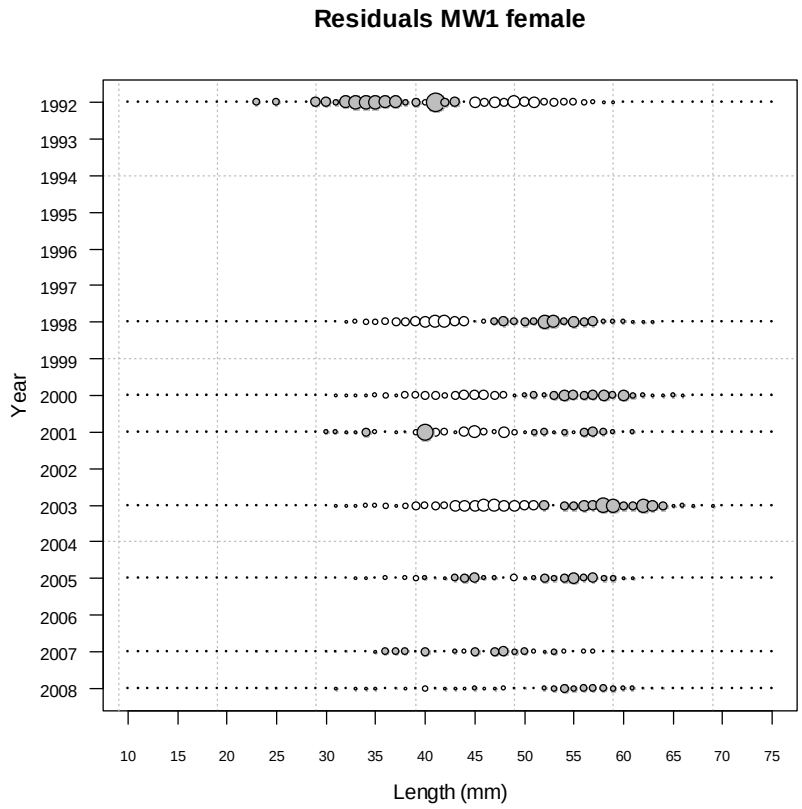

A5. 28: Bubble plots of residuals of fits to length frequency distributions for observer sampling from MW, time step 1, female.

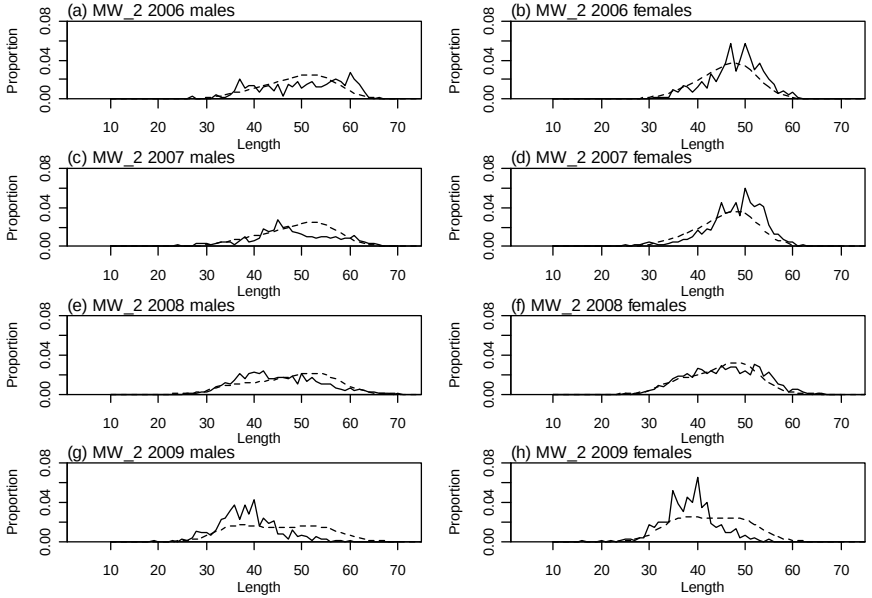

A5. 29: Observed (solid line) and fitted (dashed line) length frequency distributions for observer samples from MW, time step 2.

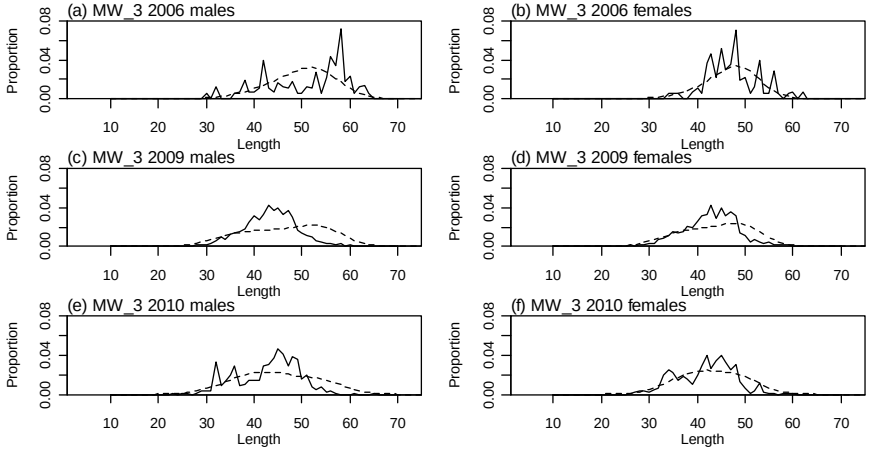

A5. 30: Observed (solid line) and fitted (dashed line) length frequency distributions for observer samples from MW, time step 3.

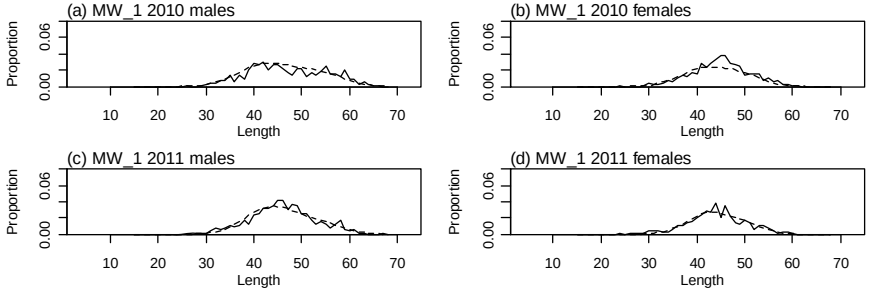

A5. 31: Observed (solid line) and fitted (dashed line) length frequency distributions for trawl survey samples from MW.

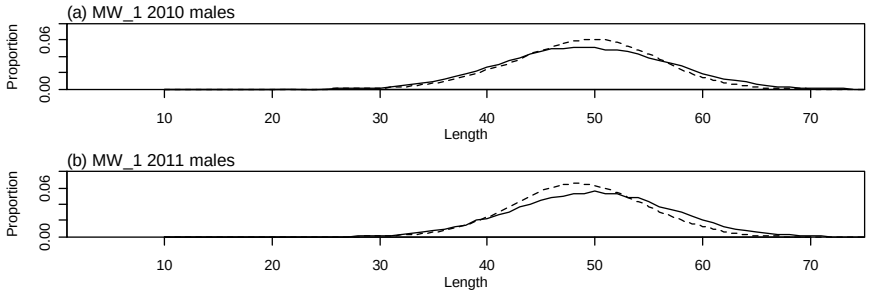

A5. 32: Observed (solid line) and fitted (dashed line) length frequency distributions for photo survey samples from MW.

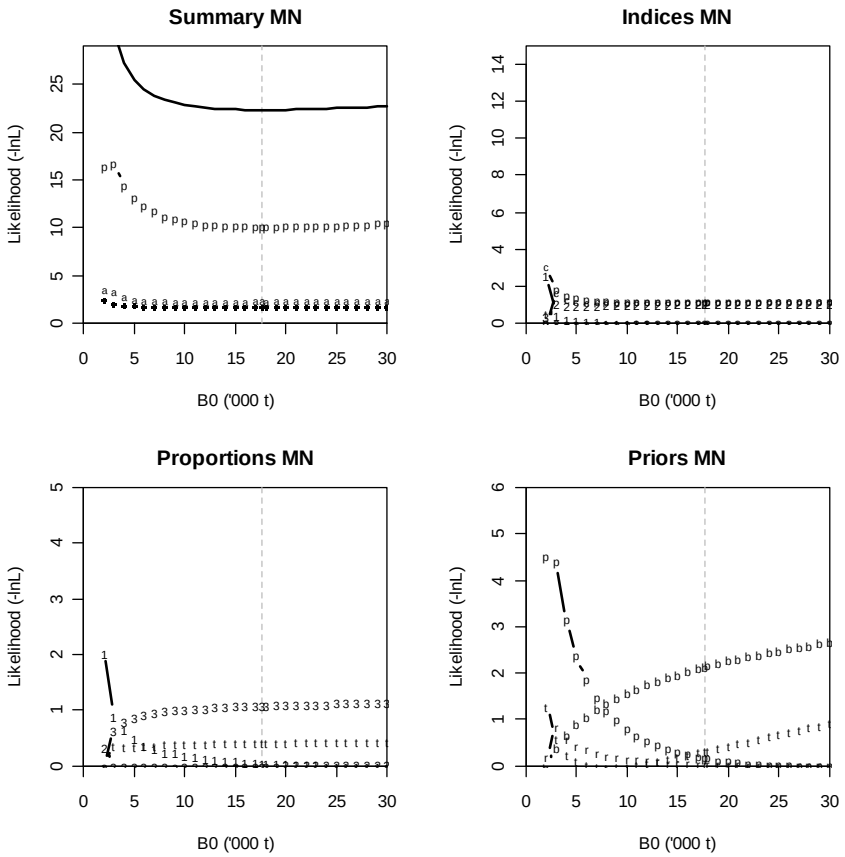

A5. 33: Likelihood profiles for model 1 when MN B_0 is fixed in the model. Figures show profiles for main priors (top left, p-priors, a – abundance indices, • – proportions at length), abundance indices (top right, t - trawl survey, 1 - CPUE time step 1, 2 - CPUE time step 2, 3 - CPUE time step 3, p – photo survey), proportion at length data (bottom left, t-trawl, 1 – observer time step 1, 2 – observer time step 2, 3 – observer time step 3) and priors (bottom right, b- B_0, YCS - r, p- *q-Photo*, t – *q-Trawl*).

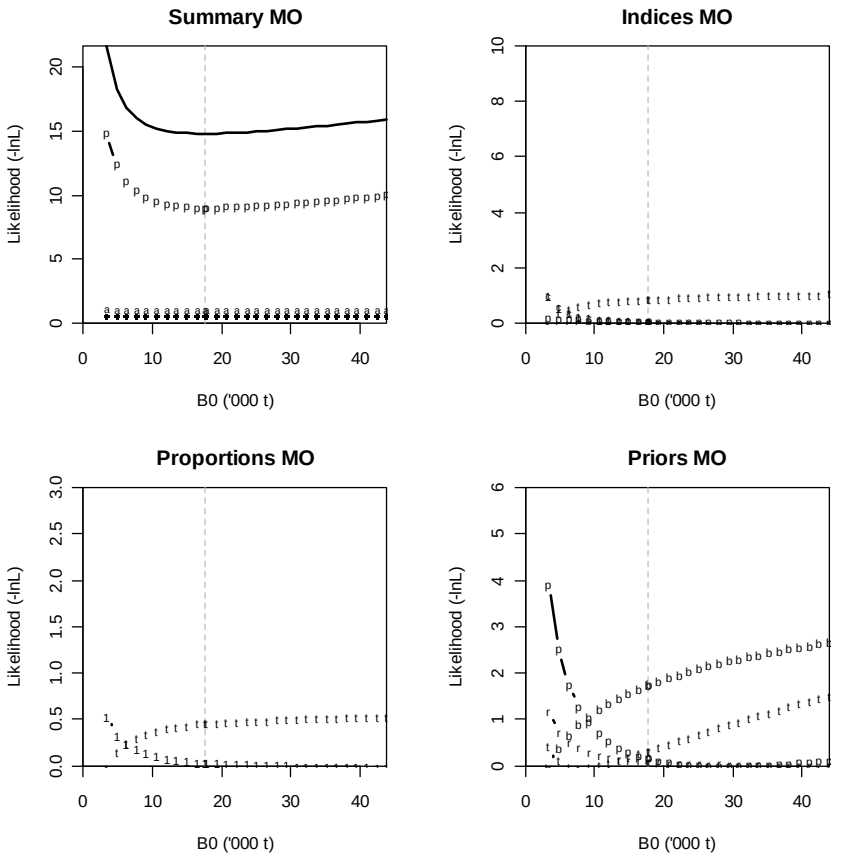

A5. 34: Likelihood profiles for model 1 when MO B_0 is fixed in the model. Figures show profiles for main priors (top left, p-priors, a – abundance indices, • – proportions at length), abundance indices (top right, t - trawl survey, 1 - CPUE time step 1, 2 - CPUE time step 2, 3 - CPUE time step 3, p – photo survey), proportion at length data (bottom left, t-trawl, 1 – observer time step 1, 2 – observer time step 2, 3 – observer time step 3) and priors (bottom right, b- B_0, YCS - r, p- *q-Photo*, t – *q-Trawl*).

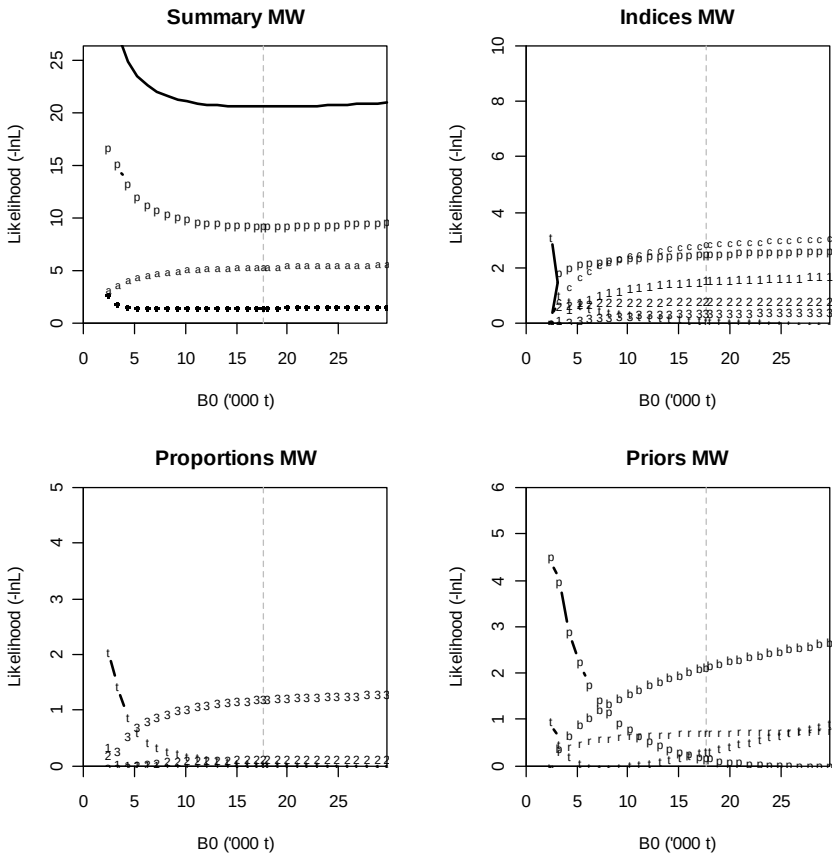

A5. 35: Likelihood profiles for model 1 when MW B_0 is fixed in the model. Figures show profiles for main priors (top left, p-priors, a – abundance indices, • – proportions at length), abundance indices (top right, t - trawl survey, 1 - CPUE time step 1, 2 - CPUE time step 2, 3 - CPUE time step 3, p – photo survey), proportion at length data (bottom left, t-trawl, 1 – observer time step 1, 2 – observer time step 2, 3 – observer time step 3) and priors (bottom right, b- B_0, YCS - r, p- *q-Photo*, t – *q-Trawl*).

13. APPENDIX 6. BASE-FAST model plots

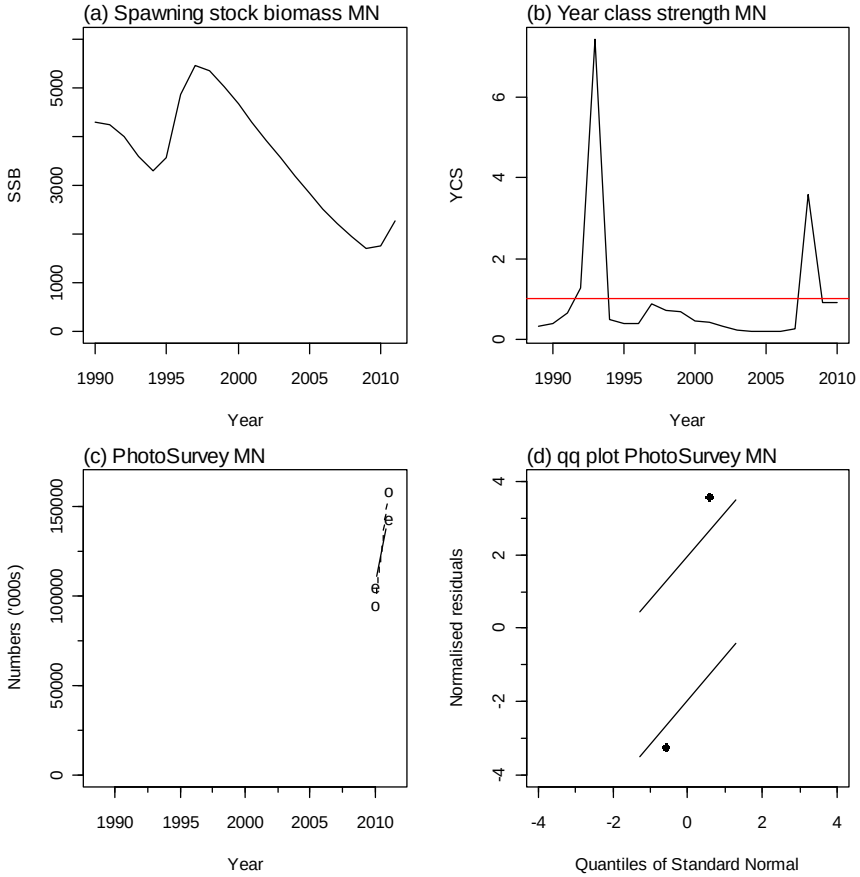

A6. 1: Spawning stock biomass trajectory (a), year class strength (b) fits (c) and q-q diagnostic plots (d) to photo survey abundance index for SCI 3 subarea MN from BASE-fast model.

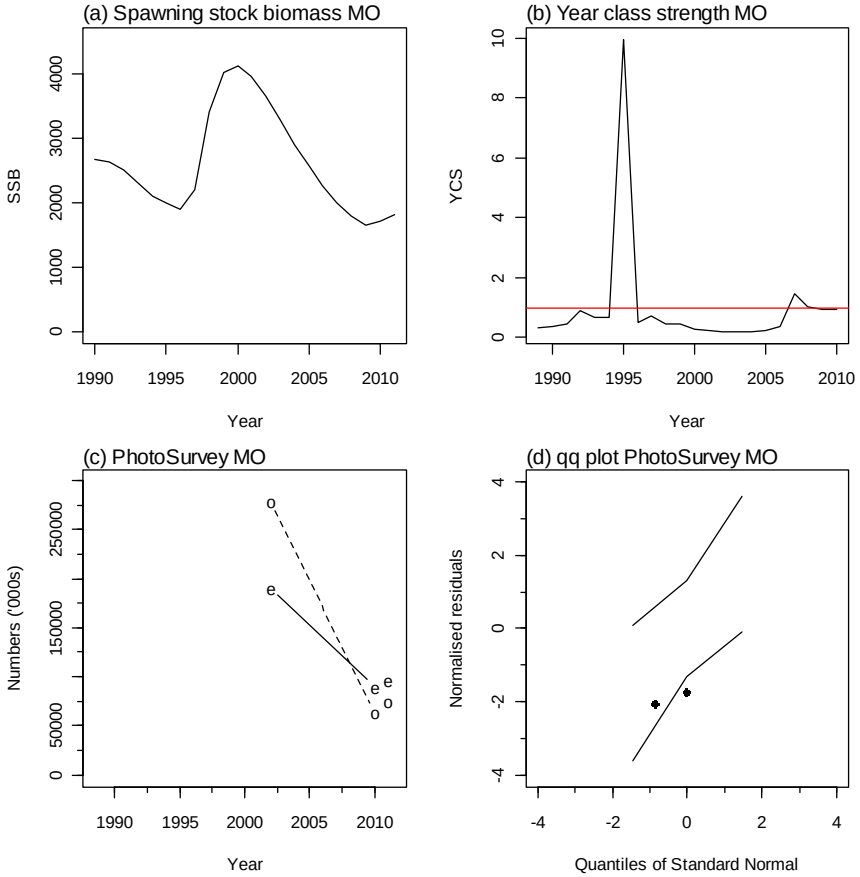

A6. 2: Spawning stock biomass trajectory (a), year class strength (b) fits (c) and q-q diagnostic plots (d) to photo survey abundance index for SCI 3 subarea MO from BASE-fast model.

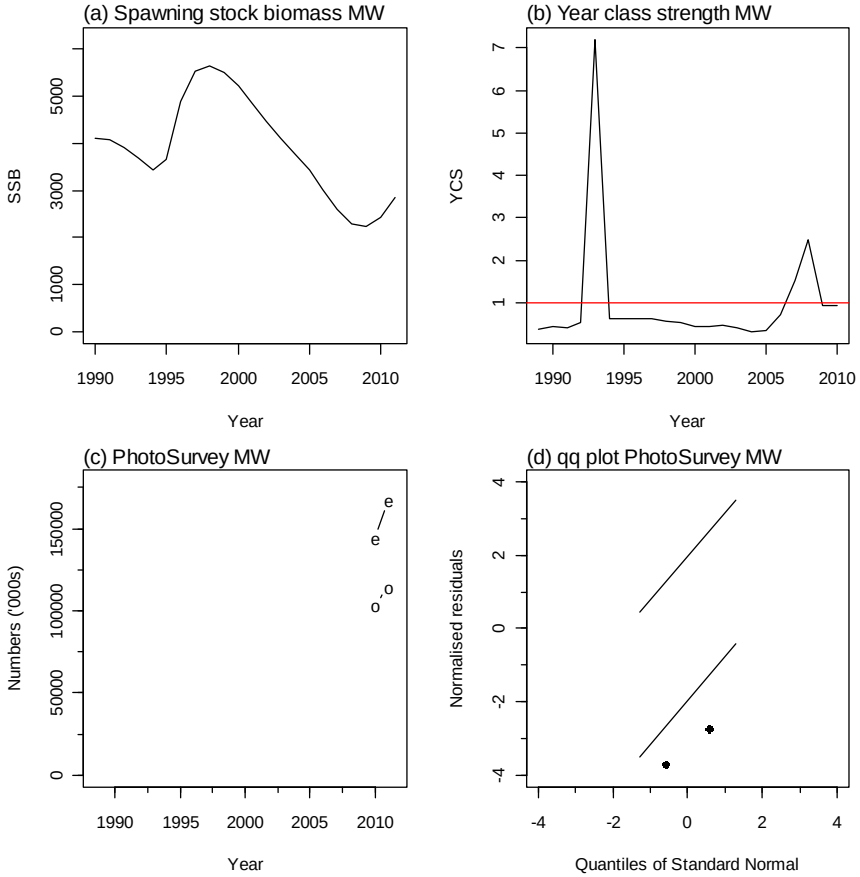

A6. 3: Spawning stock biomass trajectory (a), year class strength (b) fits (c) and q-q diagnostic plots (d) to photo survey abundance index for SCI 3 subarea MW from BASE-fast model.

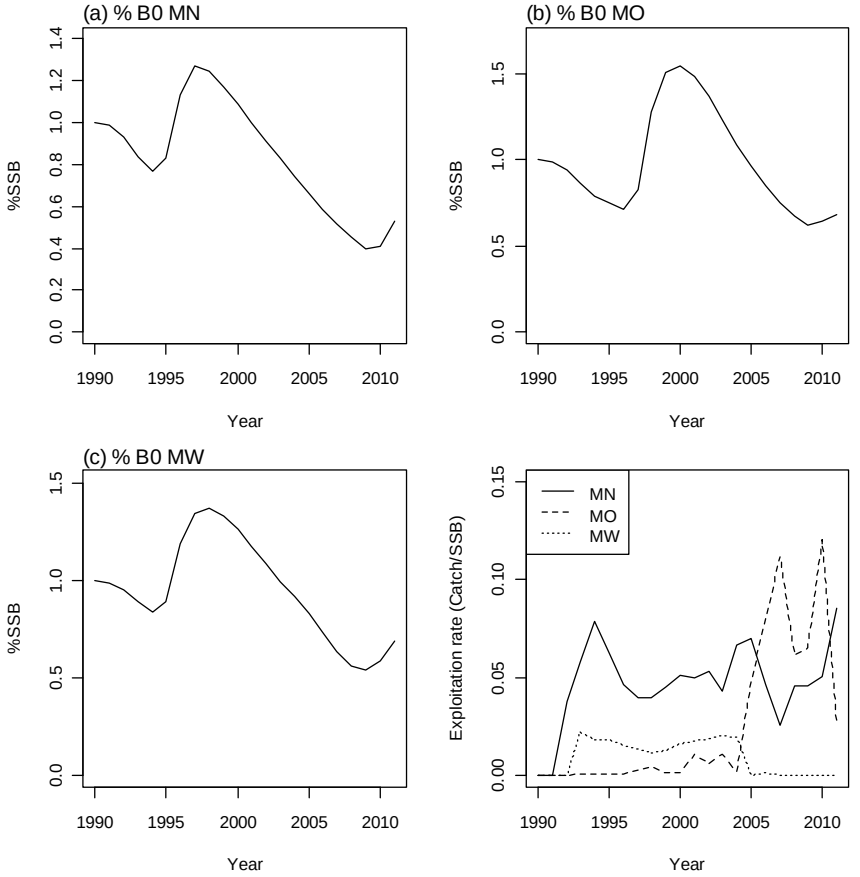

A6. 4: Trajectory of SSB as a percentage of B_0 for each subarea from the MPD fit to BASE-fast model, and exploitation rate (catch/SSB).

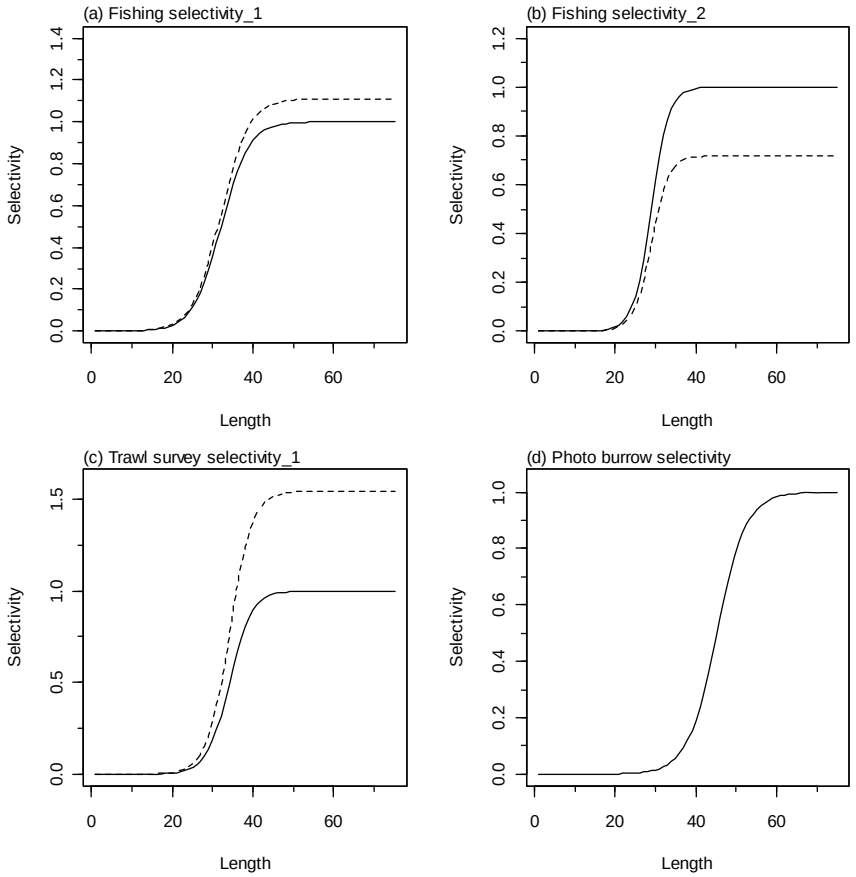

A6. 5: Fishery and survey selectivity curves. Solid line – females, dotted line – males. The scampi burrow index is not sexed, and a single selectivity applies.

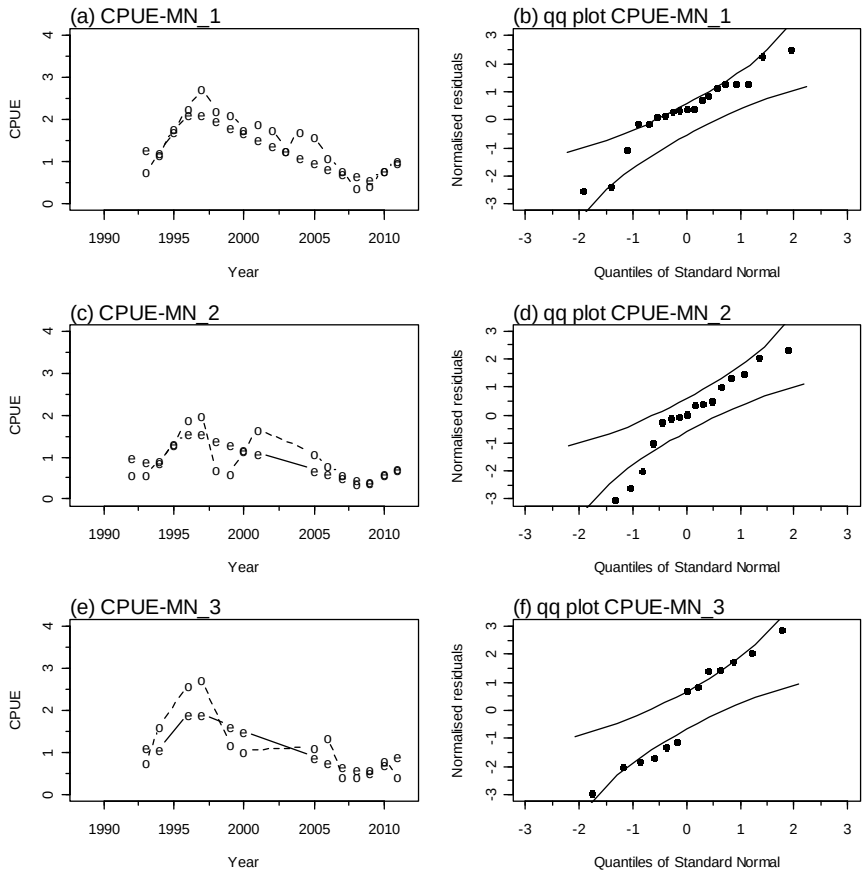

A6. 6: Fits and q-q diagnostic plots to CPUE abundance indices for MN.

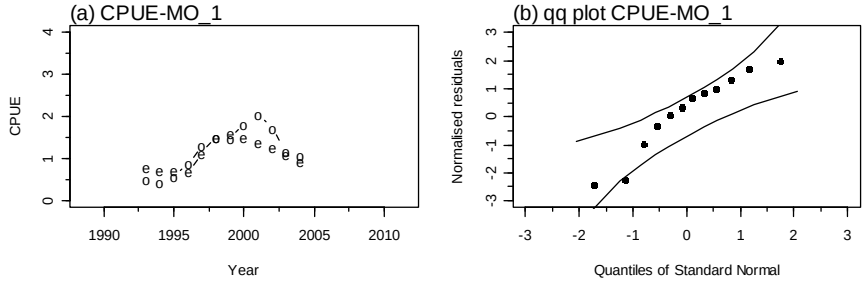

A6. 7: Fits and q-q diagnostic plots to CPUE abundance indices for MO.

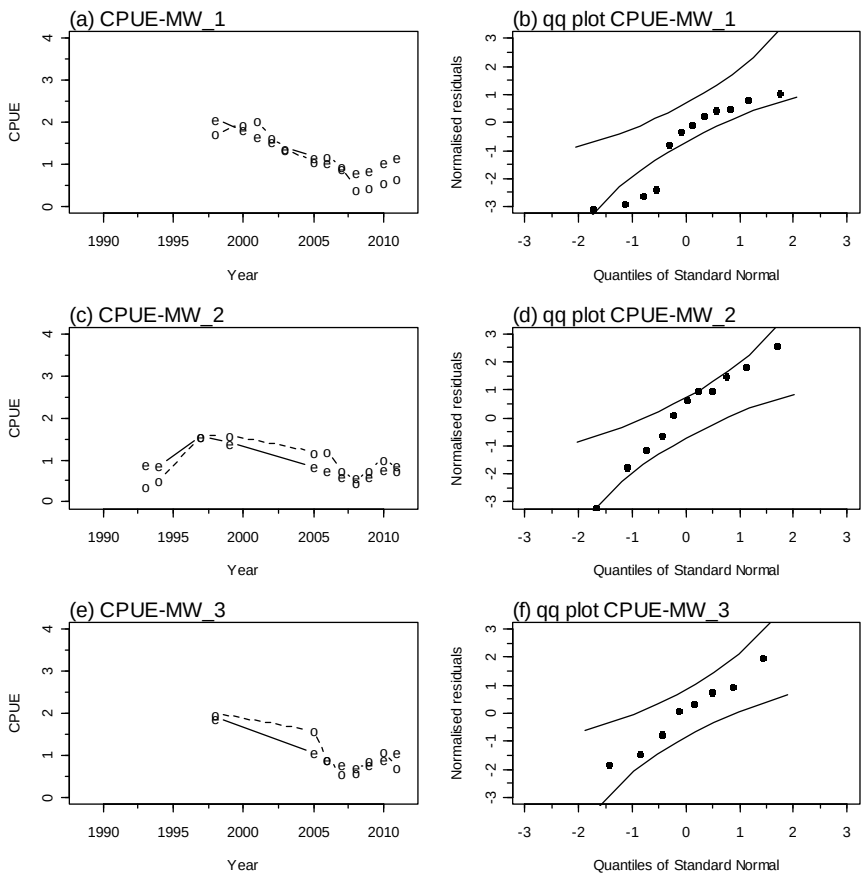

A6. 8: Fits and q-q diagnostic plots to CPUE abundance indices for MW.

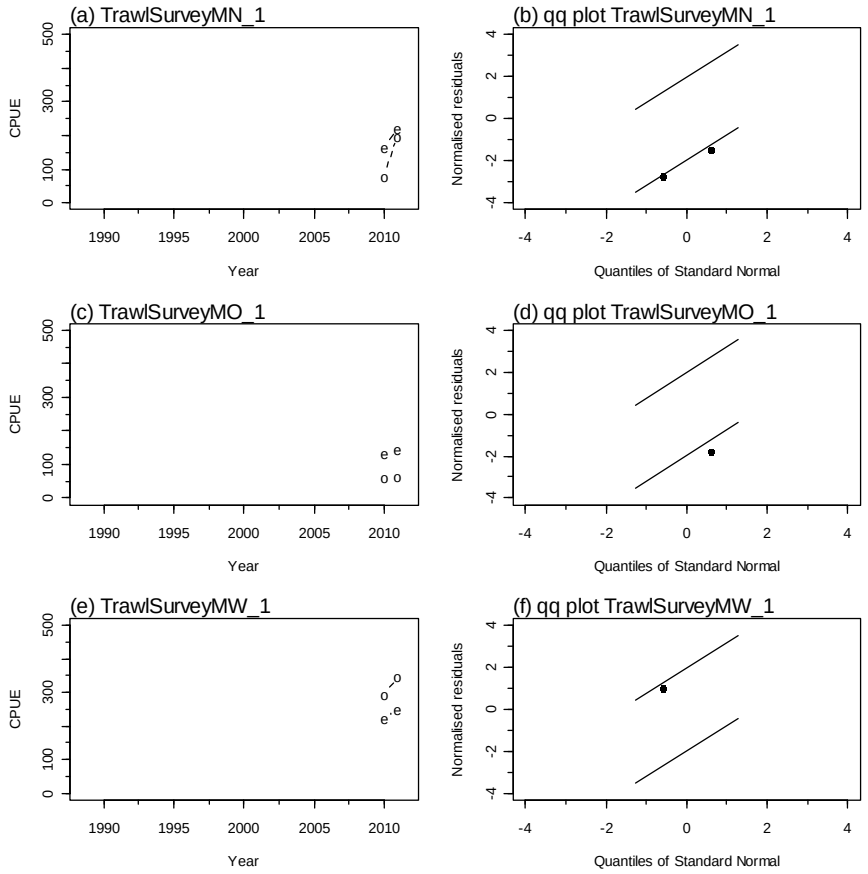

A6. 9: Fits and q-q diagnostic plots to trawl survey abundance indices.

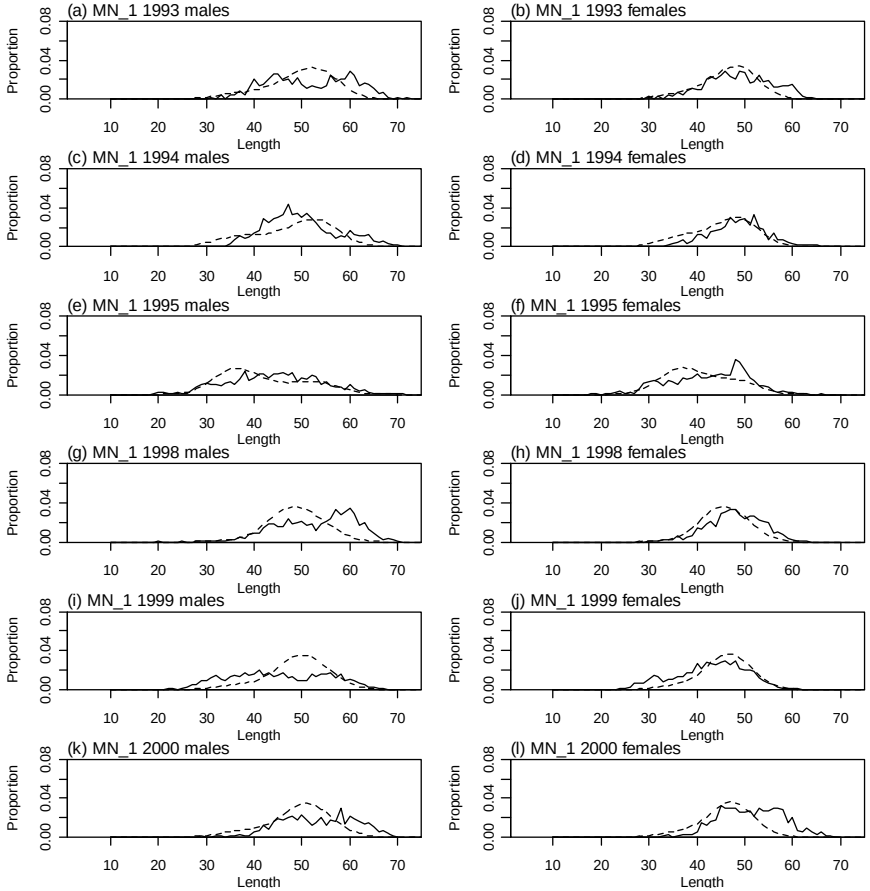

A6. 10: Observed (solid line) and fitted (dashed line) length frequency distributions for observer samples from MN, time step 1 (1993–2000).

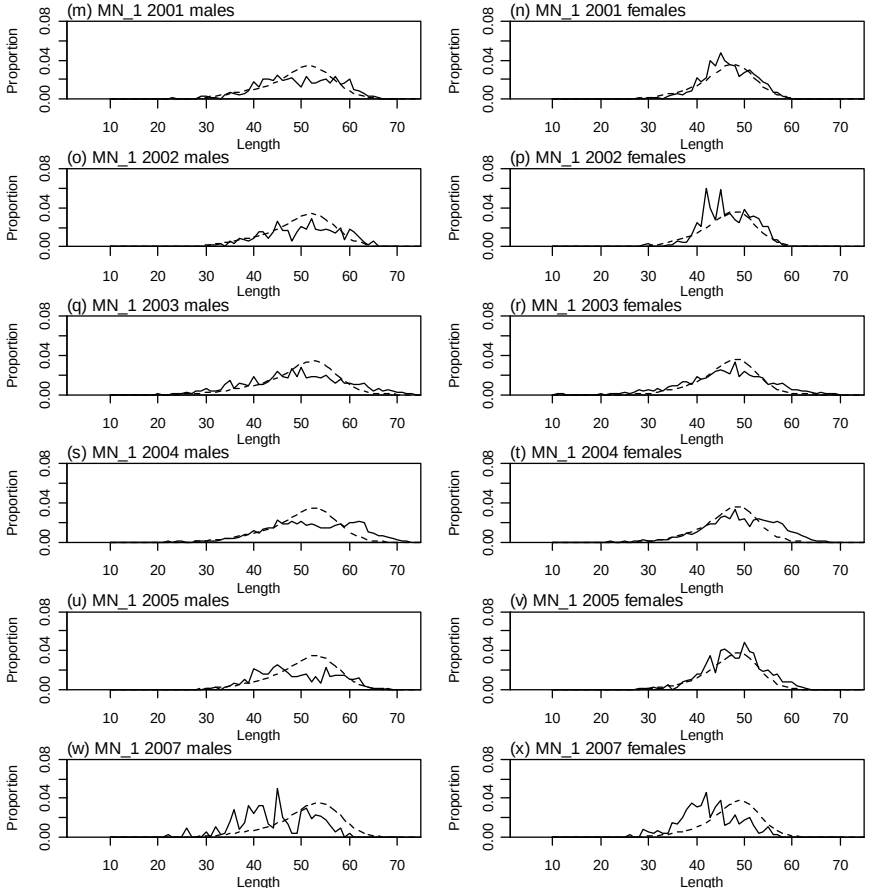

A6. 11: Observed (solid line) and fitted (dashed line) length frequency distributions for observer samples from MN, time step 1 (2001–2007).

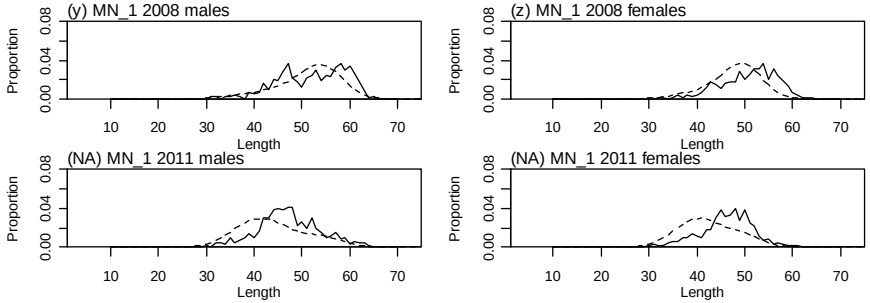

A6. 12: Observed (solid line) and fitted (dashed line) length frequency distributions for observer samples from MN, time step 1 (2008–2011).

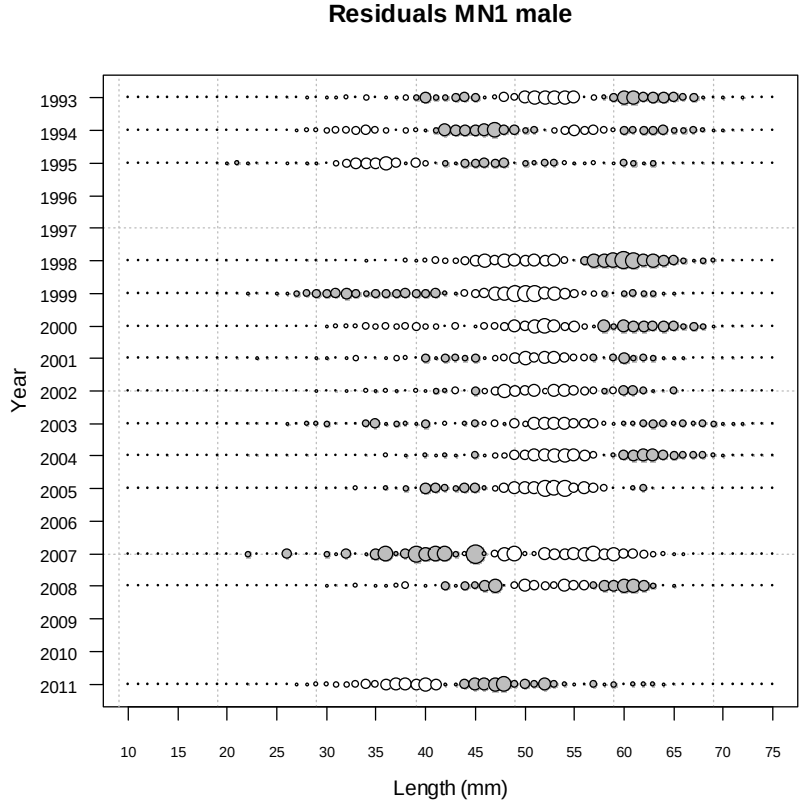

A6. 13: Bubble plots of residuals for fits to length frequency distributions for observer sampling from MN, time step 1, male.

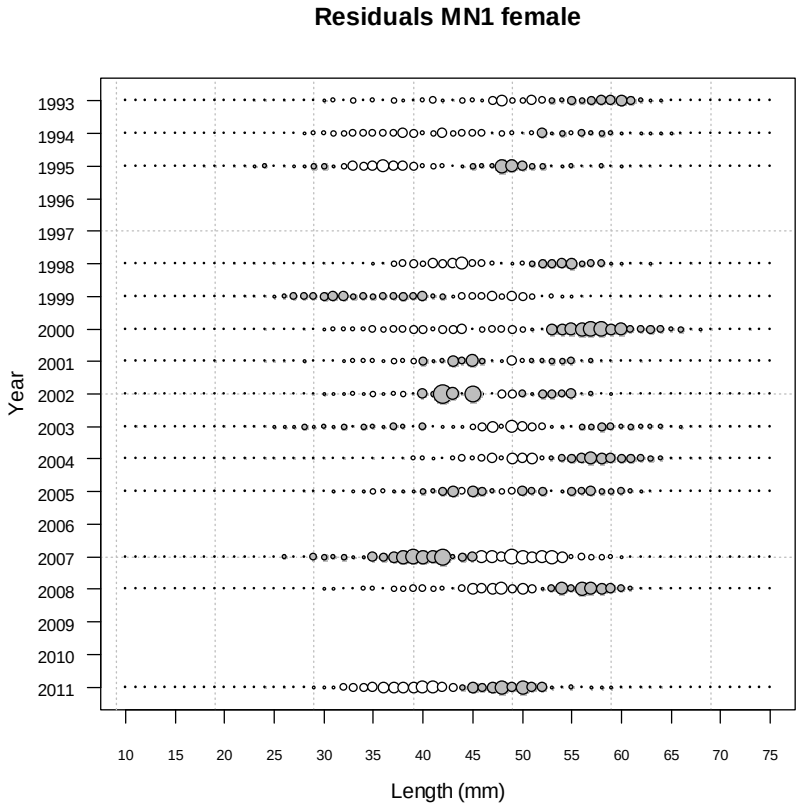

A6. 14: Bubble plots of residuals for fits to length frequency distributions for observer sampling from MN, time step 1, female.

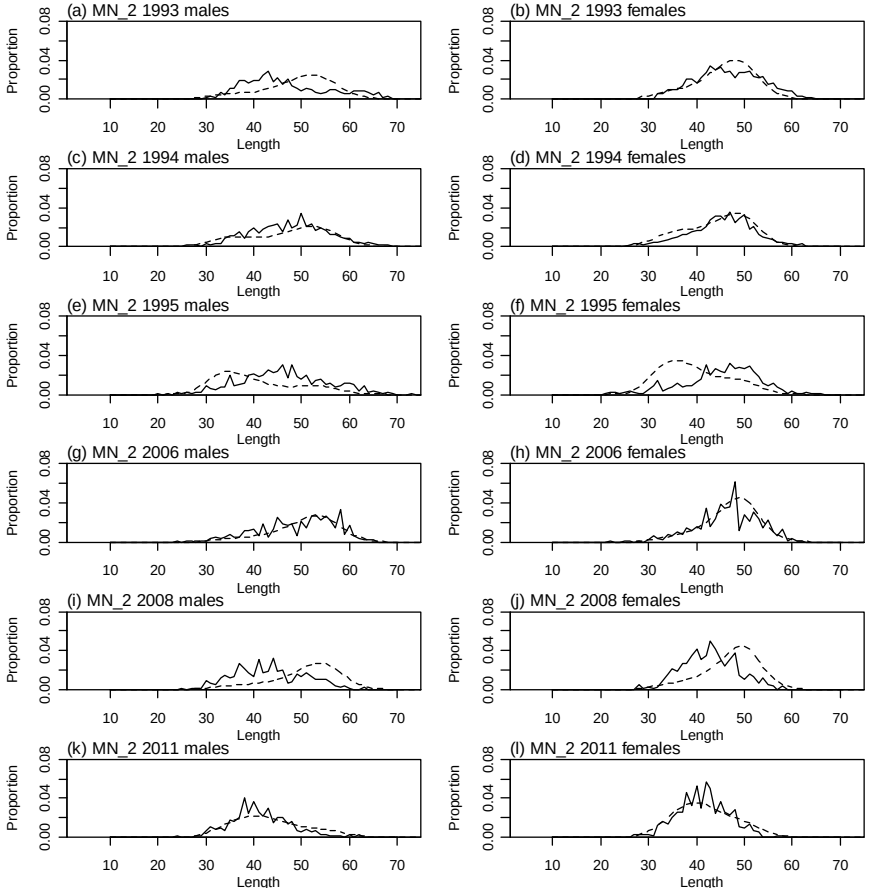

A6. 15: Observed (solid line) and fitted (dashed line) length frequency distributions for observer samples from MN, time step 2.

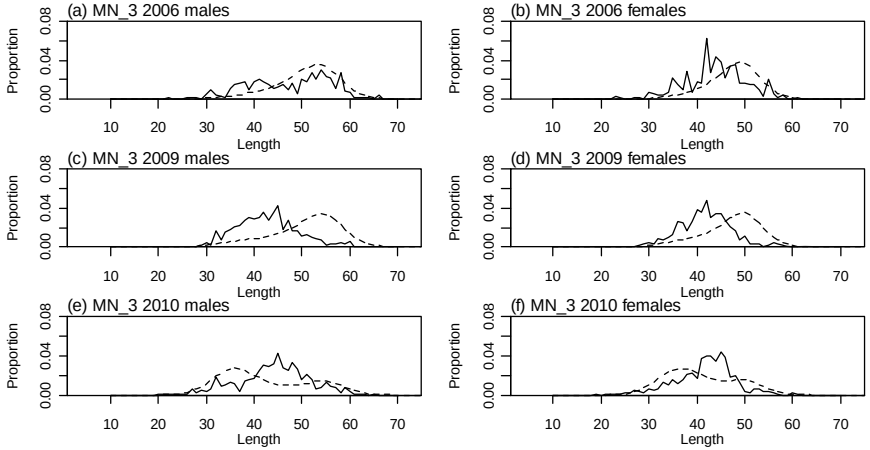

A6. 16: Observed (solid line) and fitted (dashed line) length frequency distributions for observer samples from MN, time step 3.

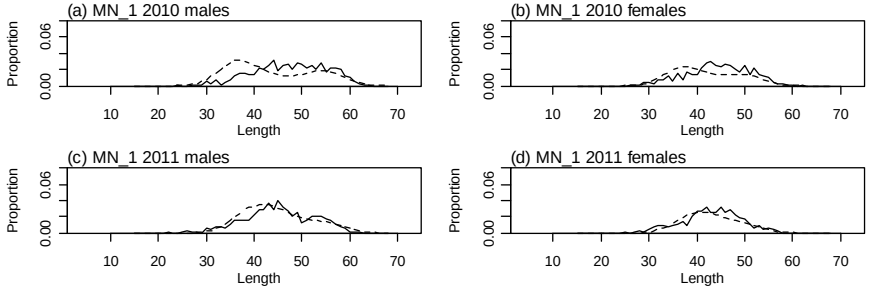

A6. 17: Observed (solid line) and fitted (dashed line) length frequency distributions for trawl survey samples from MN.

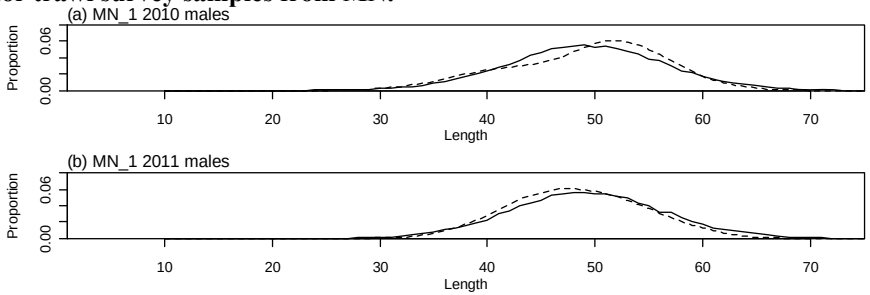

A6. 18: Observed (solid line) and fitted (dashed line) length frequency distributions for photo survey samples from MN.

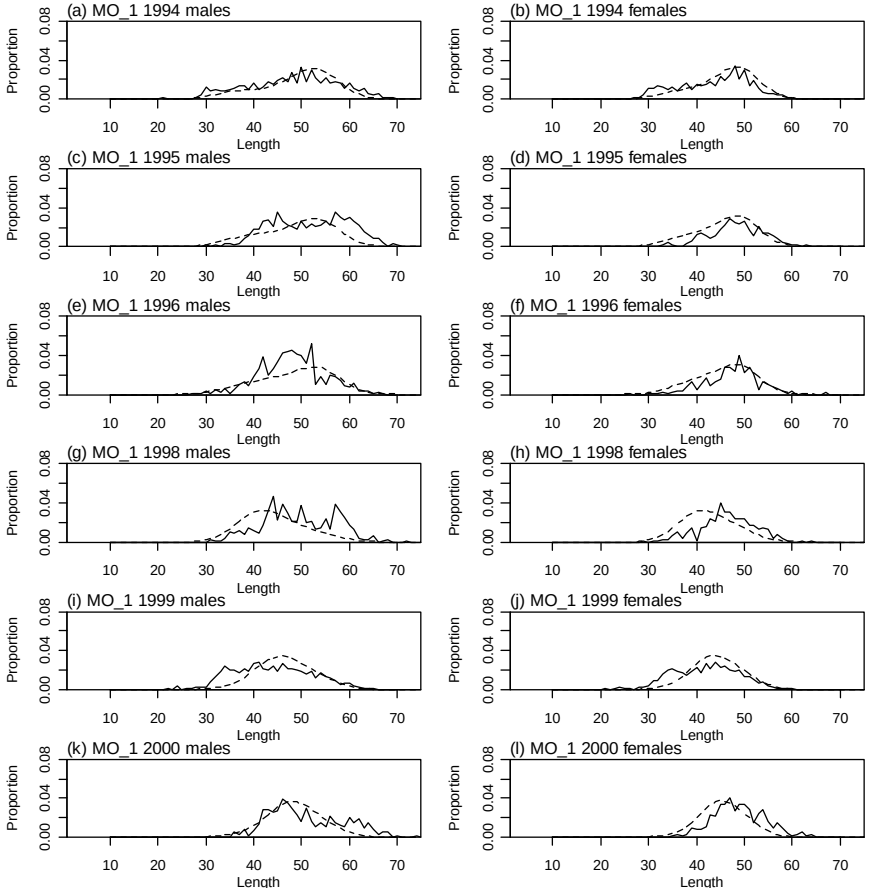

A6. 19: Observed (solid line) and fitted (dashed line) length frequency distributions for observer samples from MO, time step 1 (1994–2000).

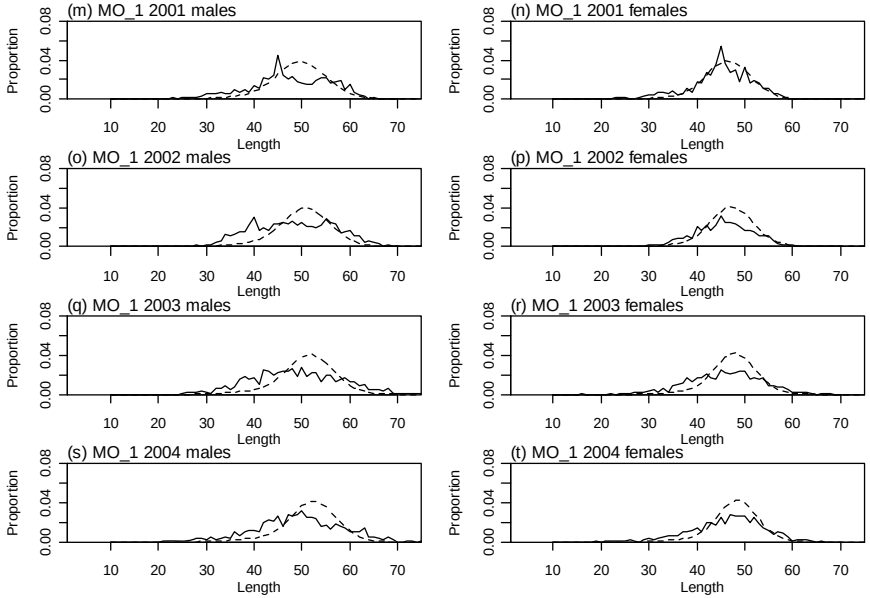

A6. 20: Observed (solid line) and fitted (dashed line) length frequency distributions for observer samples from MO, time step 1 (2001–2004).

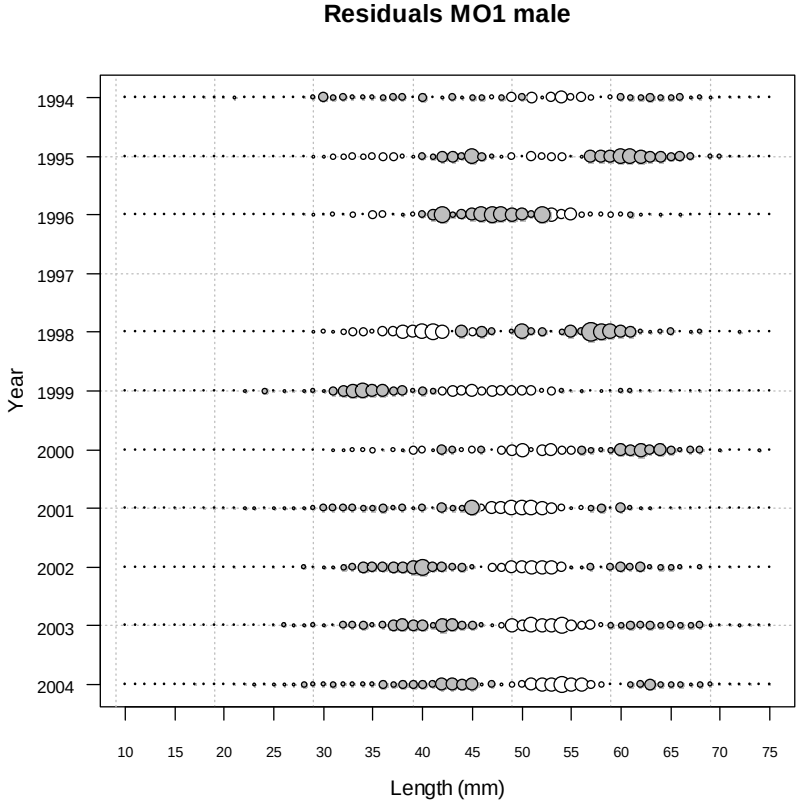

A6. 21: Bubble plots of residuals for fits to length frequency distributions for observer sampling from MO, time step 1, male.

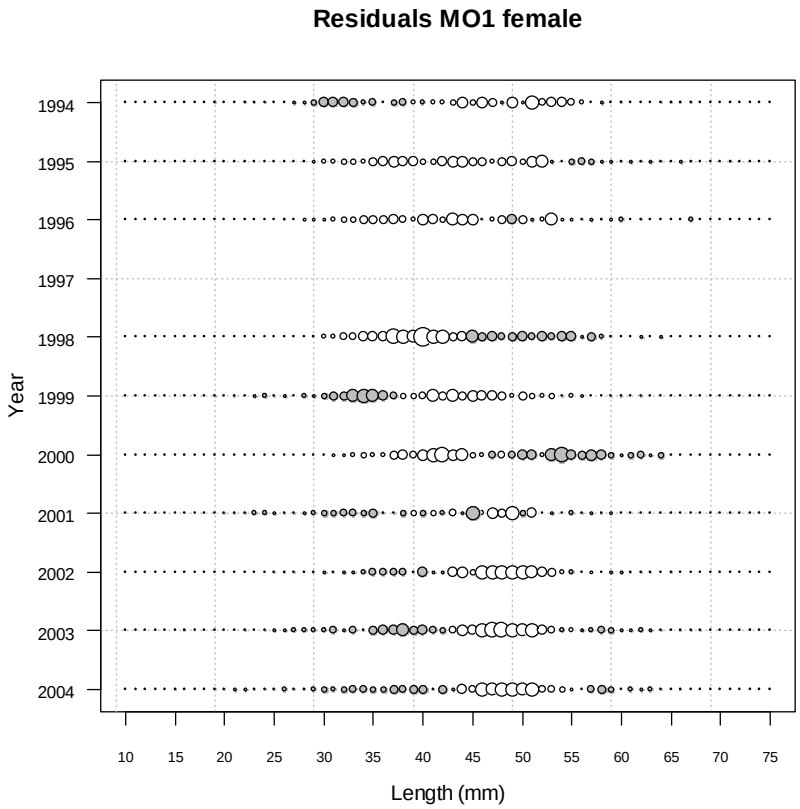

A6. 22: Bubble plots of residuals for fits to length frequency distributions for observer sampling from MO, time step 1, female.

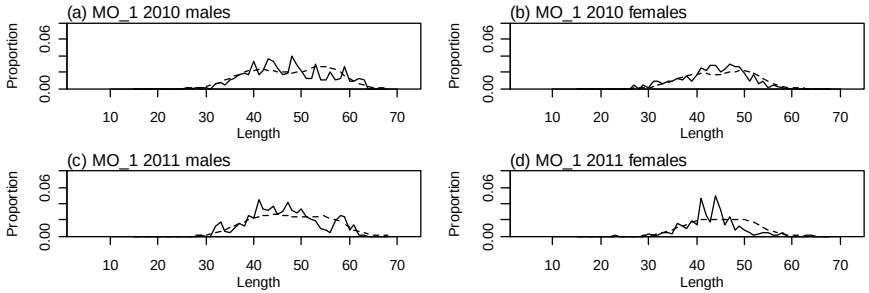

A6. 23: Observed (solid line) and fitted (dashed line) length frequency distributions for trawl survey samples from MO.

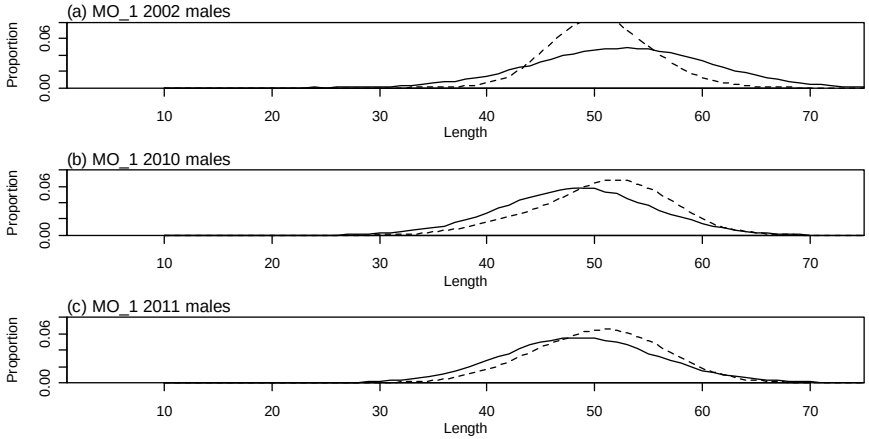

A6. 24: Observed (solid line) and fitted (dashed line) length frequency distributions for photo survey samples from MO.

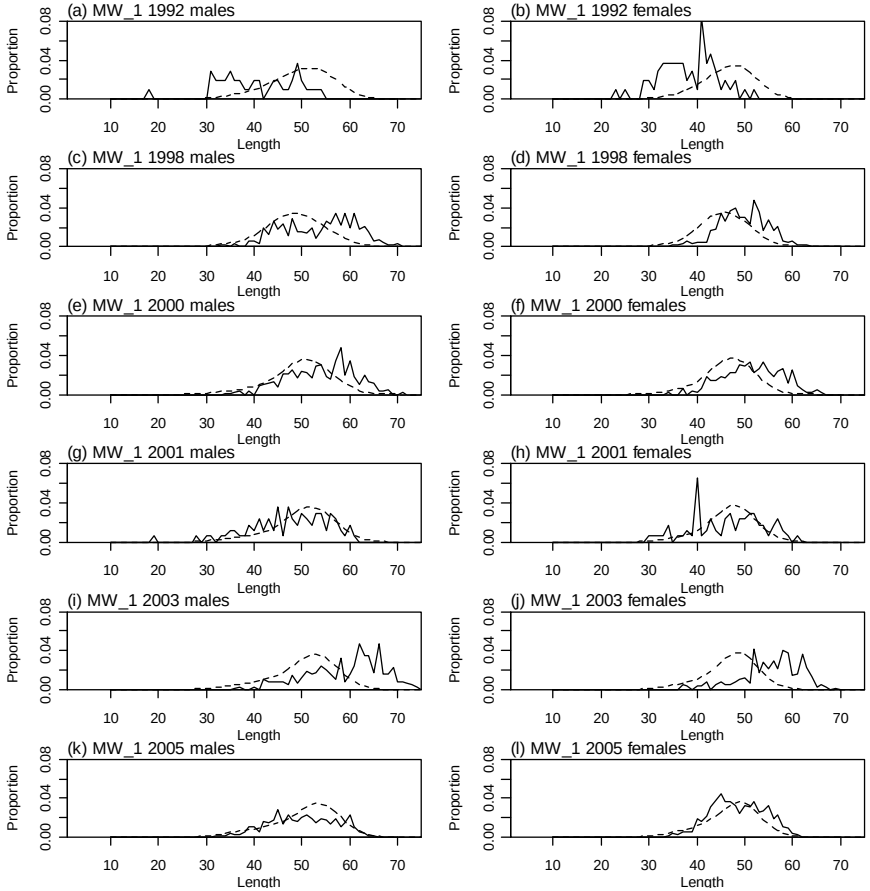

A6. 25: Observed (solid line) and fitted (dashed line) length frequency distributions for observer samples from MW, time step 1 (1992–2005).

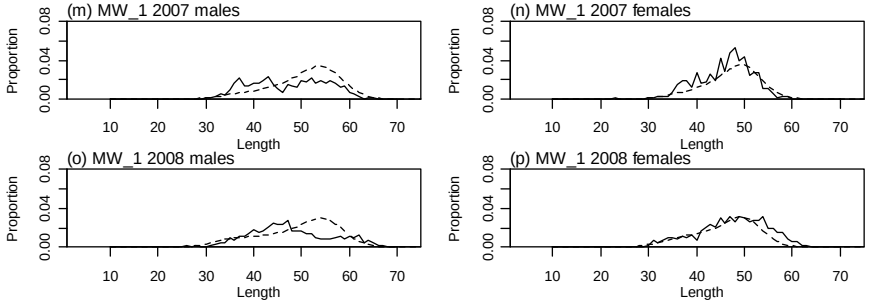

A6. 26: Observed (solid line) and fitted (dashed line) length frequency distributions for observer samples from MW, time step 1 (2007–2008).

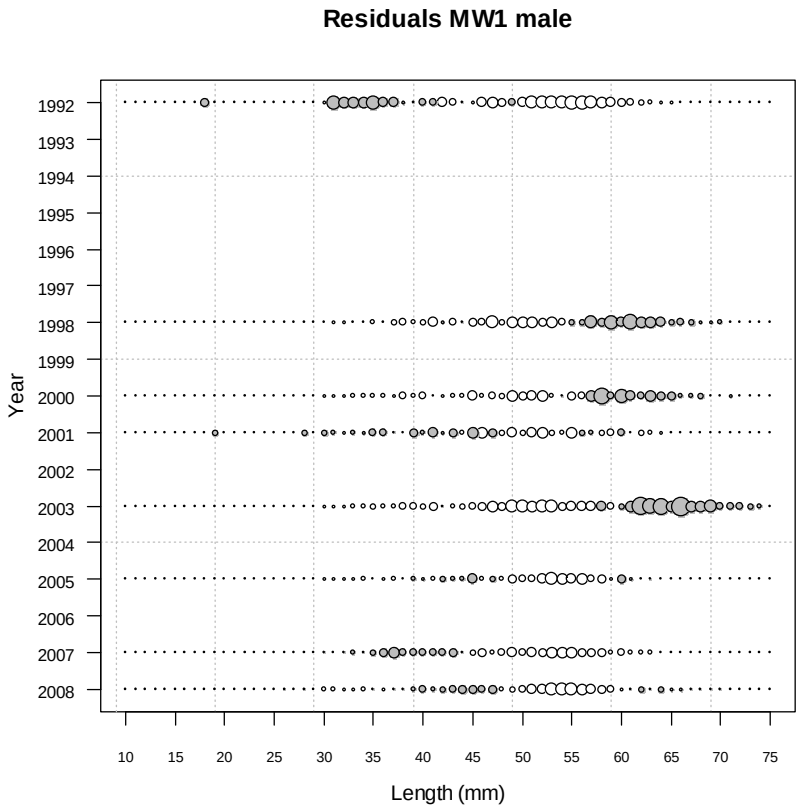

A6. 27: Bubble plots of residuals for fits to length frequency distributions for observer sampling from MW, time step 1, male.

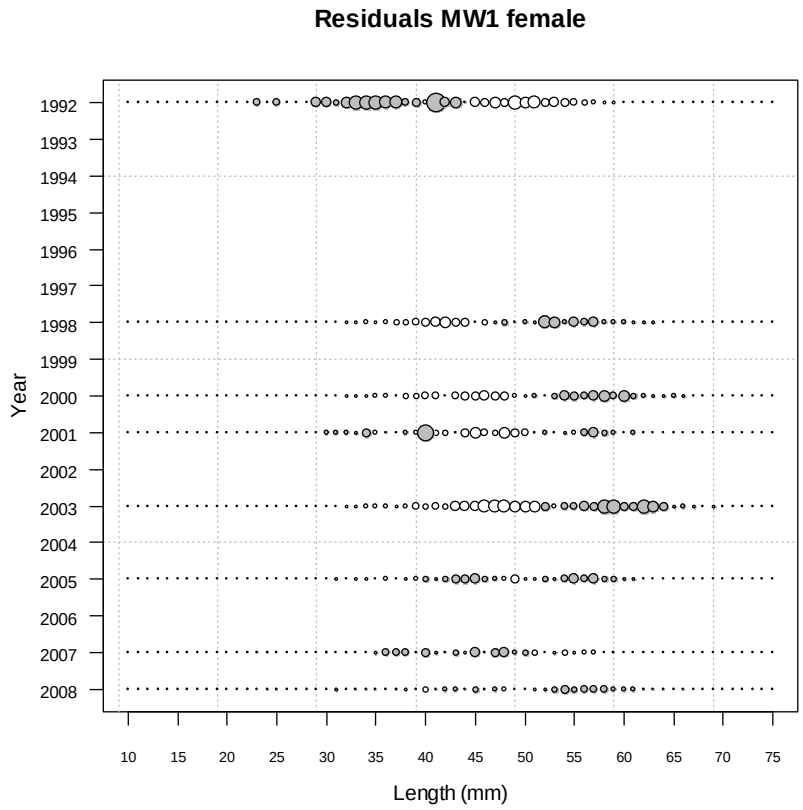

A6. 28: Bubble plots of residuals for fits to length frequency distributions for observer sampling from MW, time step 1, female.

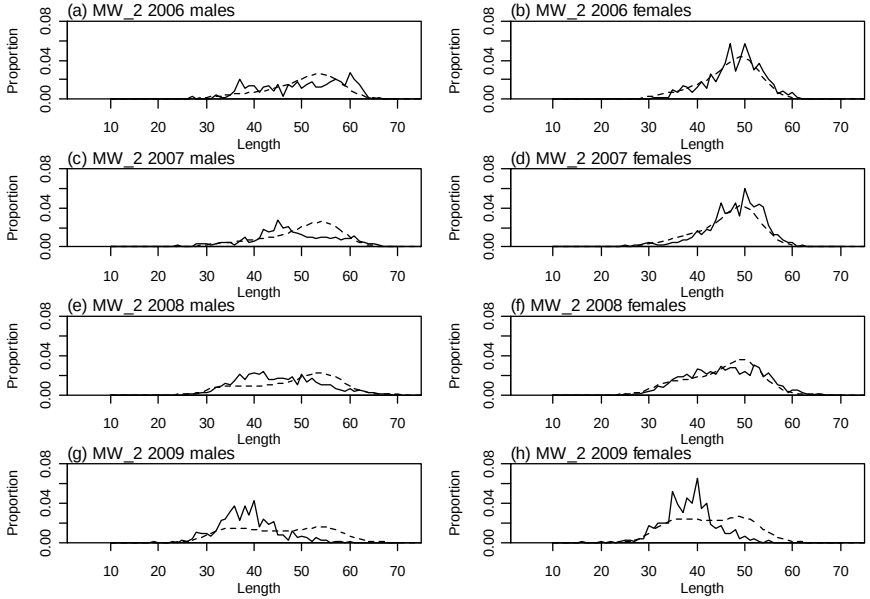

A6. 29: Observed (solid line) and fitted (dashed line) length frequency distributions for observer samples from MW, time step 2.

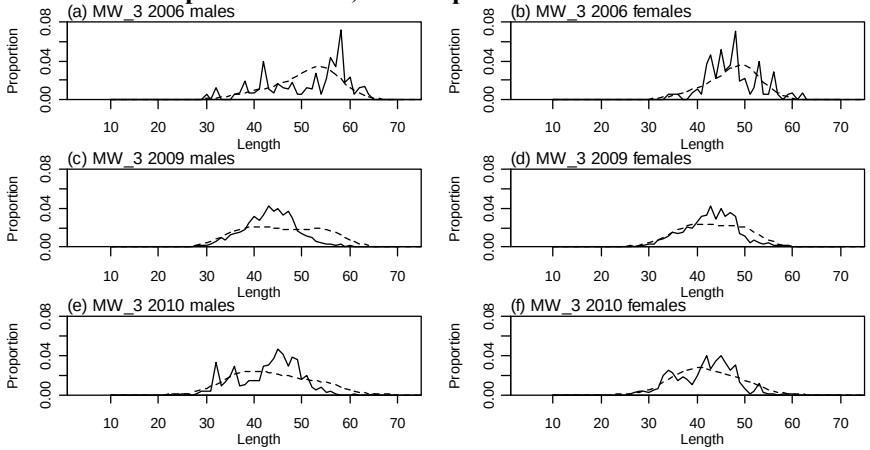

A6. 30: Observed (solid line) and fitted (dashed line) length frequency distributions for observer samples from MW, time step 2.

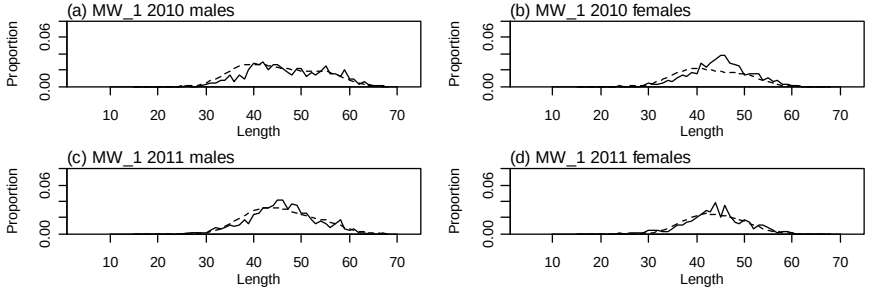

A6. 31: Observed (solid line) and fitted (dashed line) length frequency distributions for observer samples from MW, time step 3.

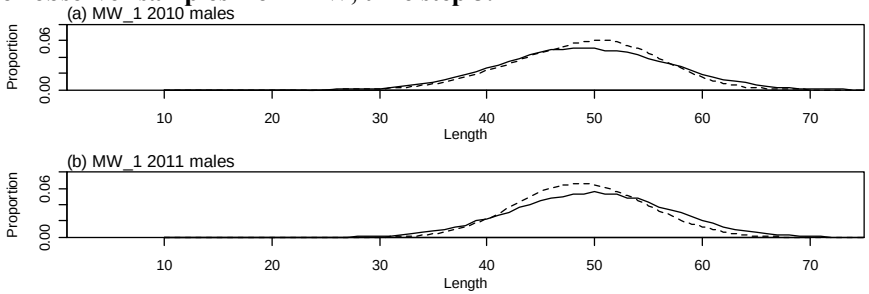

A6. 32: Observed (solid line) and fitted (dashed line) length frequency distributions for trawl survey samples from MW.

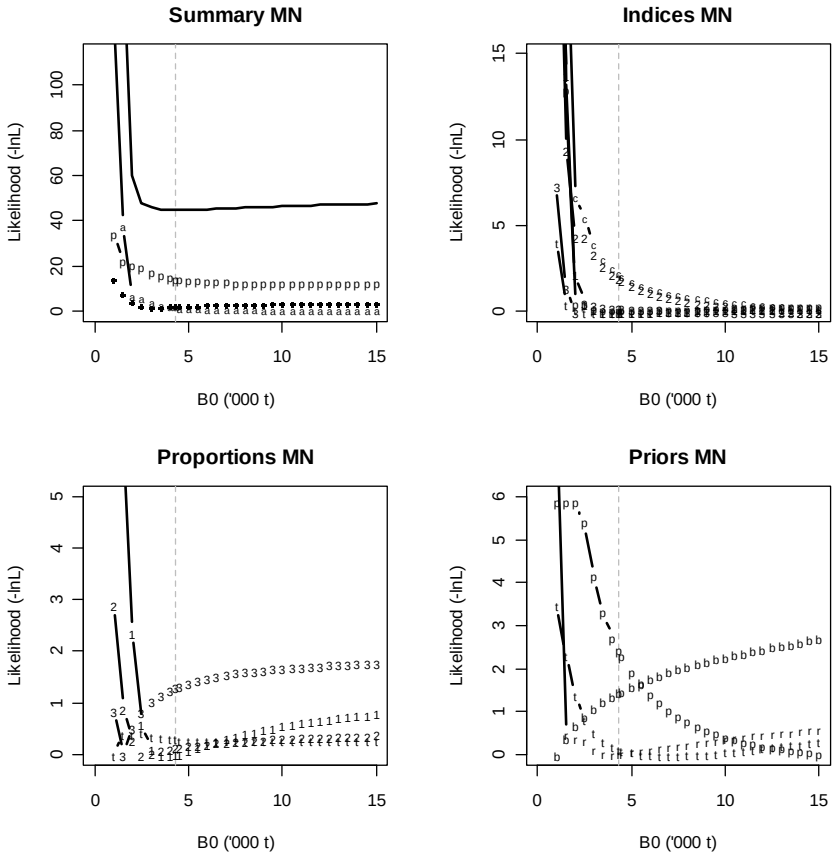

A6. 33: Likelihood profiles for model 1 when MN B_0 is fixed in the model. Figures show profiles for main priors (top left, p-priors, a – abundance indices, • – proportions at length), abundance indices (top right, t - trawl survey, 1 - CPUE time step 1, 2 - CPUE time step 2, 3 - CPUE time step 3, p – photo survey), proportion at length data (bottom left, t-trawl, 1 – observer time step 1, 2 – observer time step 2, 3 – observer time step 3) and priors (bottom right, b- B_0, YCS - r, p- *q-Photo*, t – *q-Trawl*).

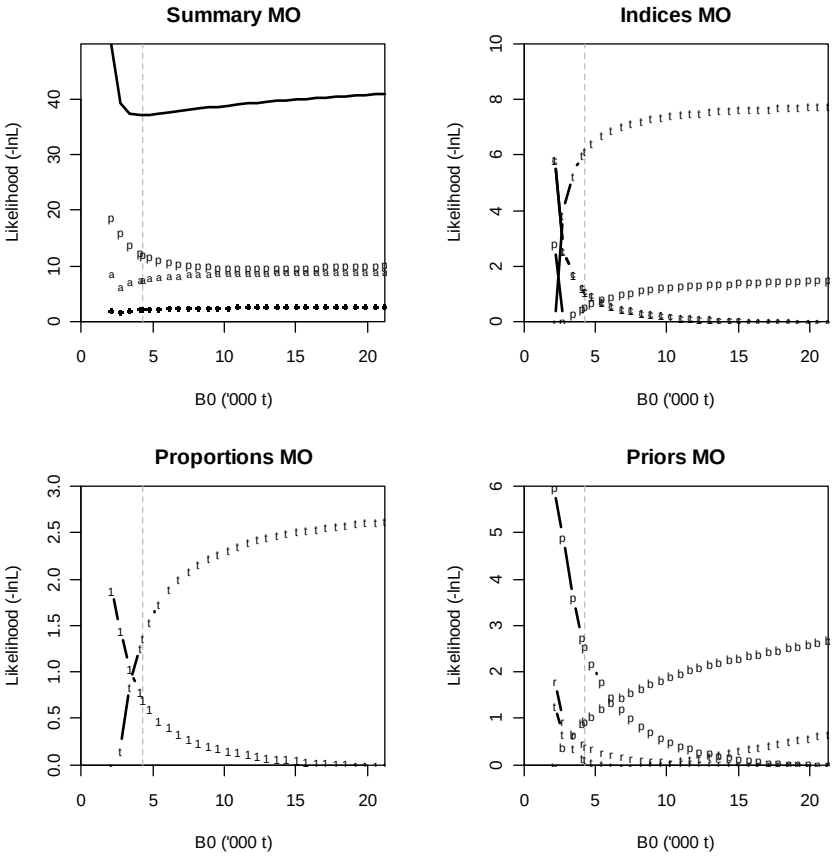

A6. 34: Likelihood profiles for model 1 when MO B_0 is fixed in the model. Figures show profiles for main priors (top left, p-priors, a – abundance indices, • – proportions at length), abundance indices (top right, t - trawl survey, 1 - CPUE time step 1, 2 - CPUE time step 2, 3 - CPUE time step 3, p – photo survey), proportion at length data (bottom left, t-trawl, 1 – observer time step 1, 2 – observer time step 2, 3 – observer time step 3) and priors (bottom right, b- B_0, YCS - r, p- *q-Photo*, t – *q-Trawl*).

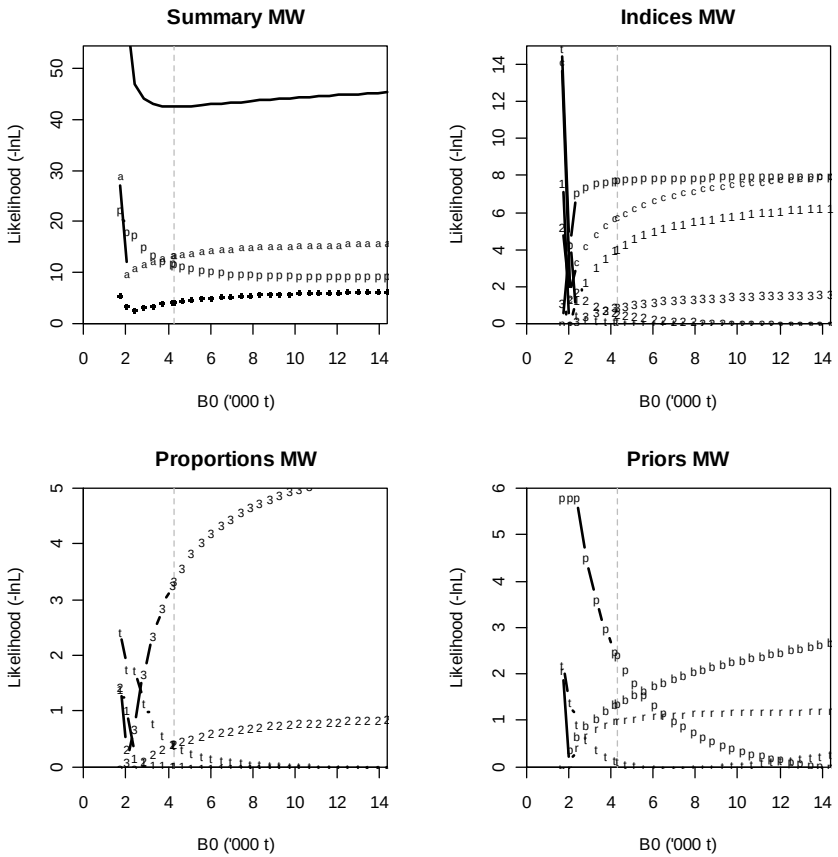

A6. 35: Likelihood profiles for model 1 when MW B_0 is fixed in the model. Figures show profiles for main priors (top left, p-priors, a – abundance indices, • – proportions at length), abundance indices (top right, t - trawl survey, 1 - CPUE time step 1, 2 - CPUE time step 2, 3 - CPUE time step 3, p – photo survey), proportion at length data (bottom left, t-trawl, 1 – observer time step 1, 2 – observer time step 2, 3 – observer time step 3) and priors (bottom right, b- B_0, YCS - r, p- *q-Photo*, t – *q-Trawl*).

14. APPENDIX 7. BASE-SLOW model plots

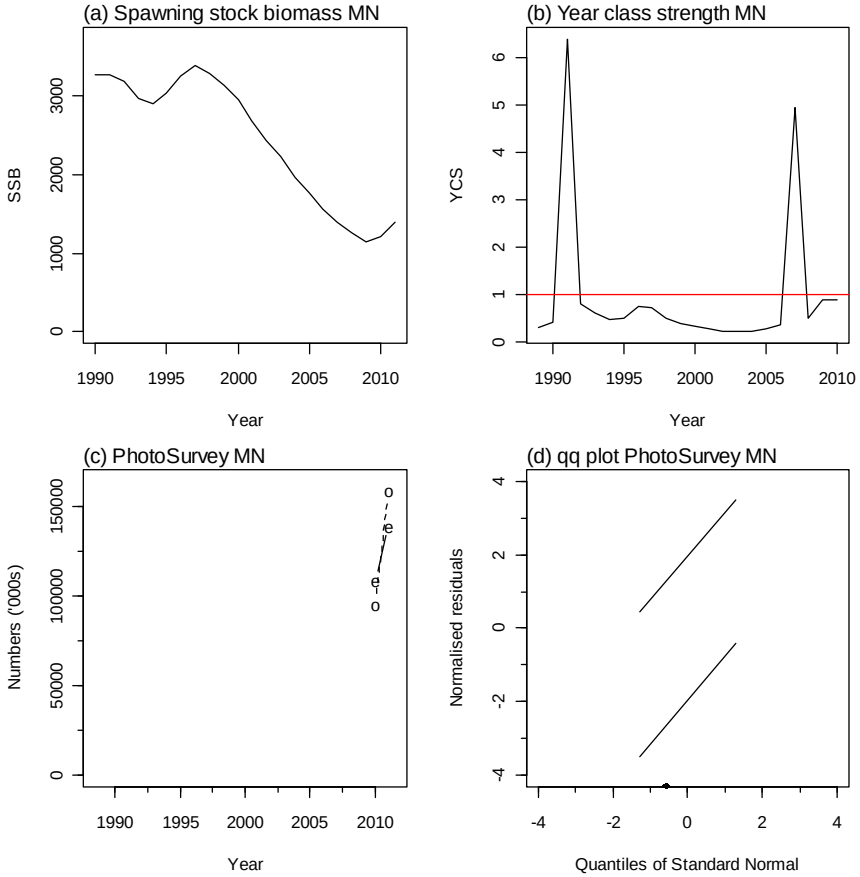

A7. 1: Spawning stock biomass trajectory (a), year class strength (b) fits (c) and q-q diagnostic plots (d) to photo survey abundance index for SCI 3 subarea MN from BASE-SLOW model.

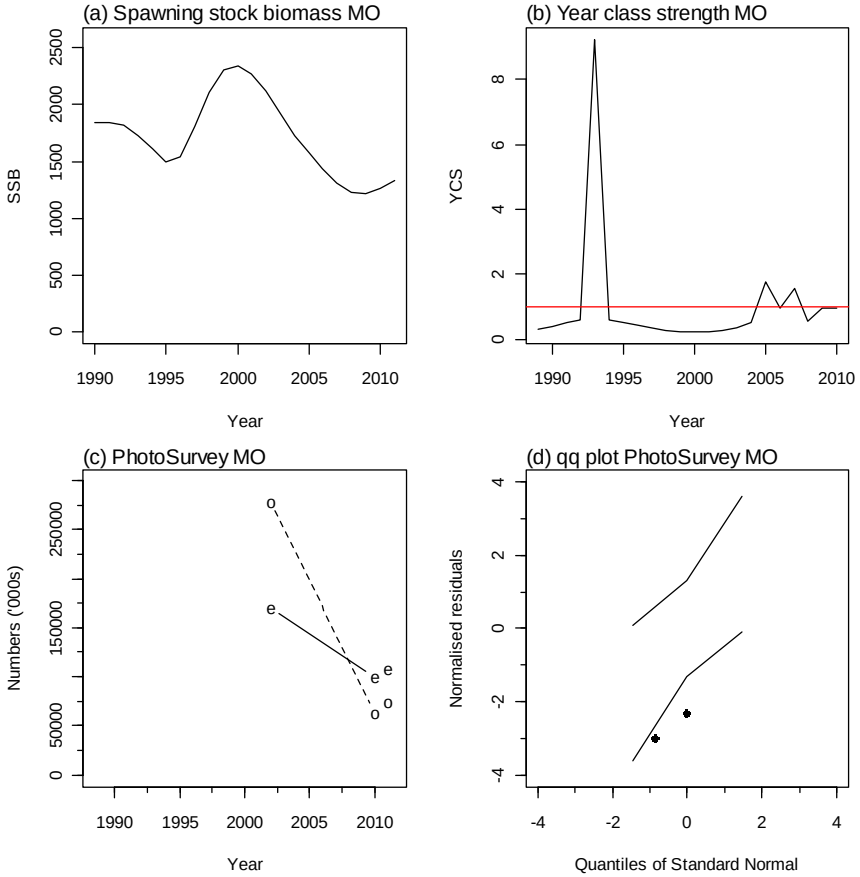

A7. 2: Spawning stock biomass trajectory (a), year class strength (b) fits (c) and q-q diagnostic plots (d) to photo survey abundance index for SCI 3 subarea MO from BASE-SLOW model.

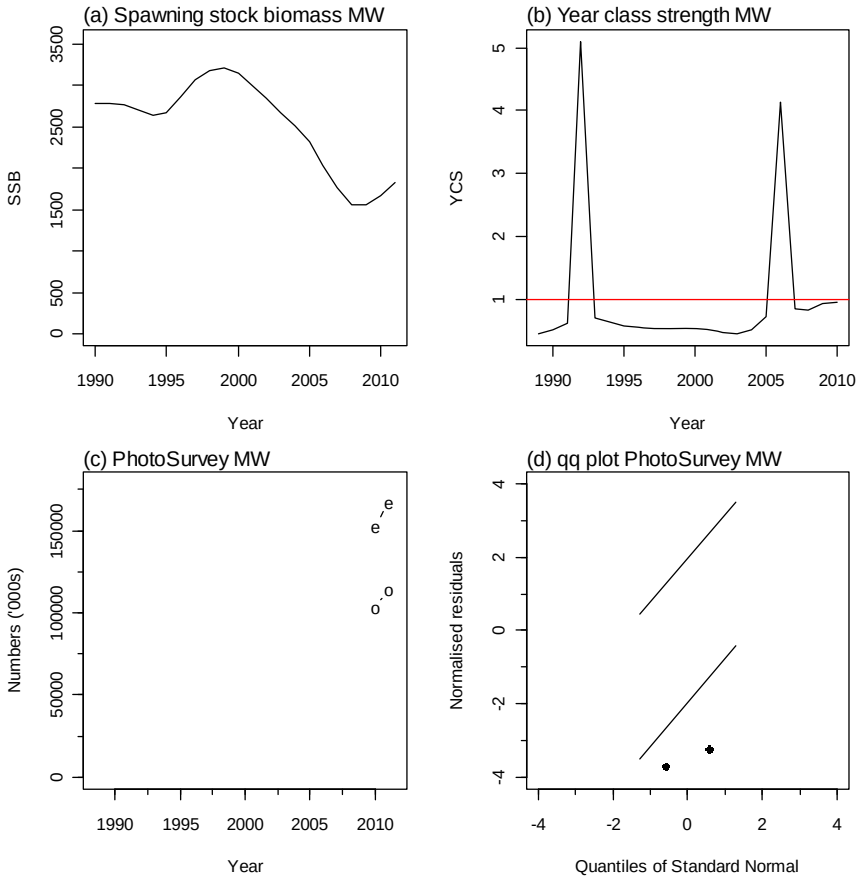

A7. 3: Spawning stock biomass trajectory (a), year class strength (b) fits (c) and q-q diagnostic plots (d) to photo survey abundance index for SCI 3 subarea MW from BASE-SLOW model.

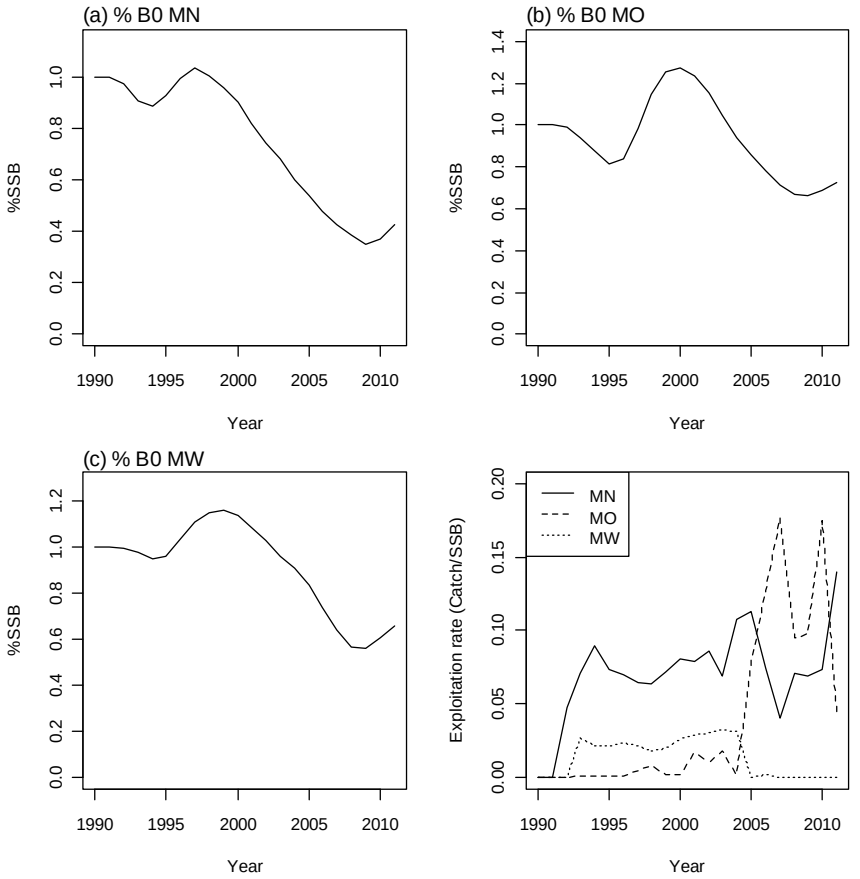

A7. 4: Trajectory of SSB as a percentage of B_0 for each subarea from the MPD fit to BASE-SLOW model, and exploitation rate (catch/SSB).

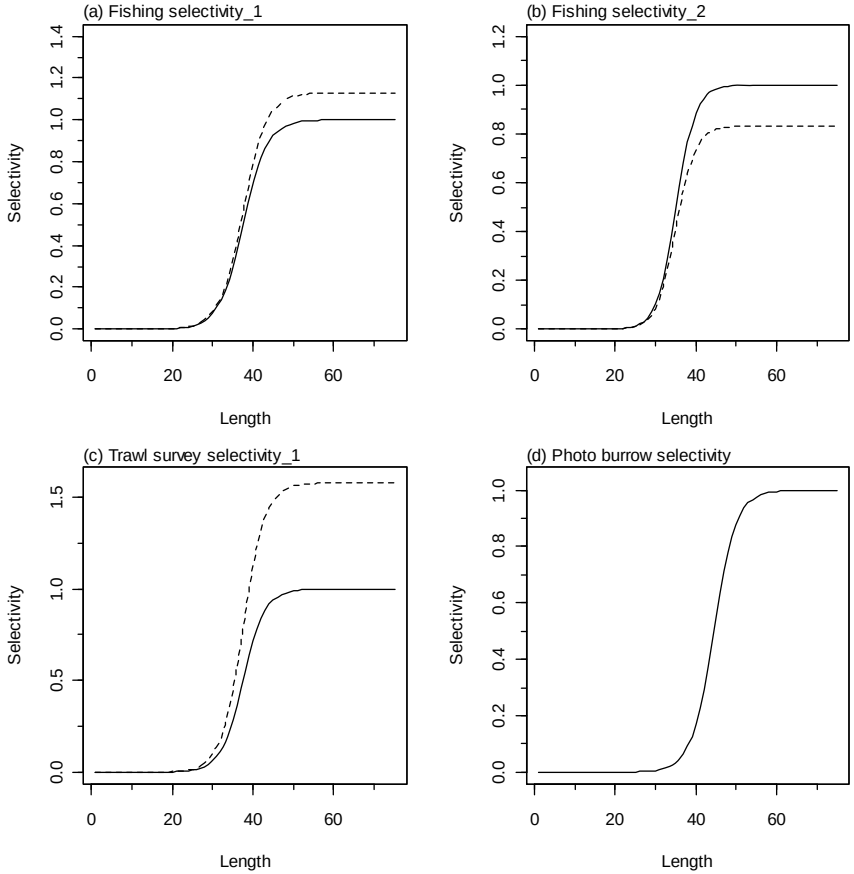

A7. 5: Fishery and survey selectivity curves. Solid line – females, dotted line – males. The scampi burrow index is not sexed, and a single selectivity applies.

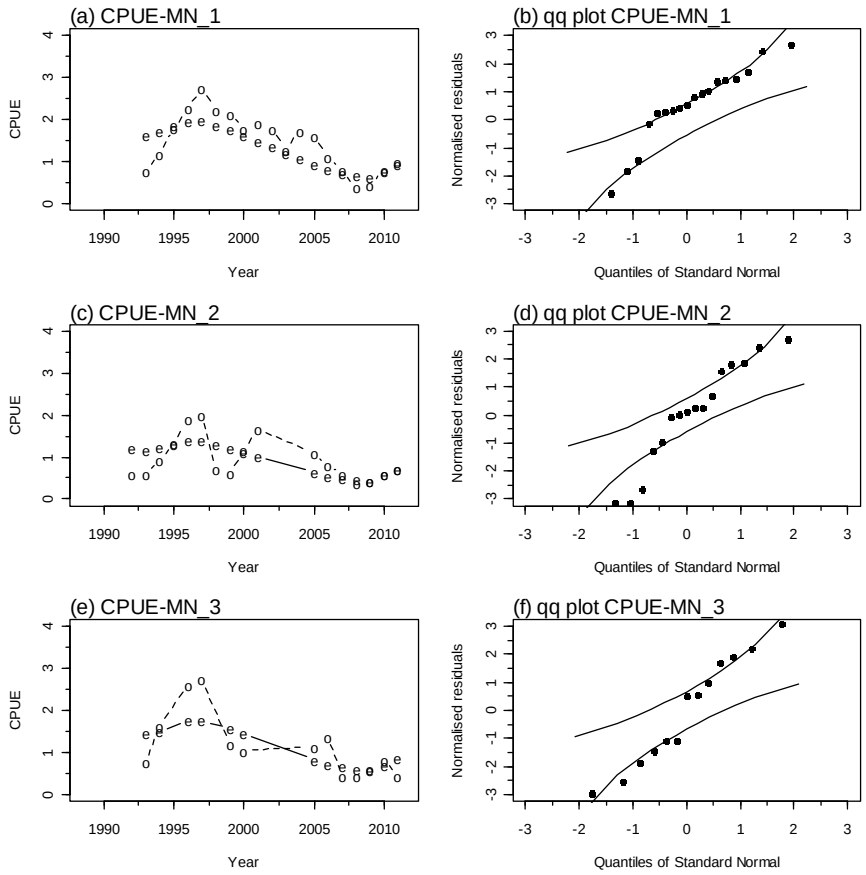

A7. 6: Fits and q-q diagnostic plots to CPUE abundance indices for MN.

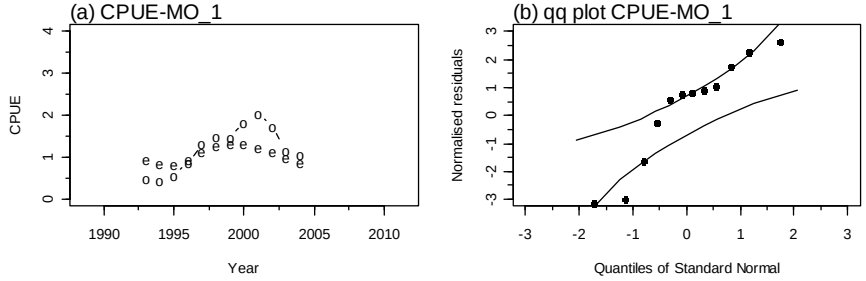

A7. 7: Fits and q-q diagnostic plots to CPUE abundance indices for MO.

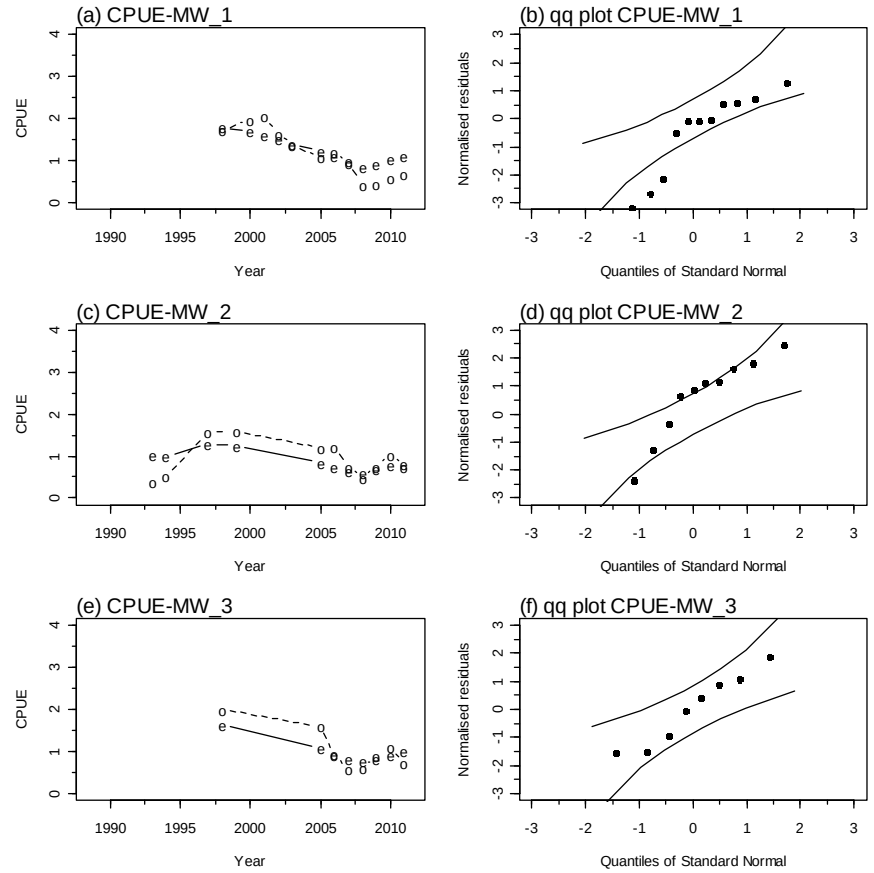

A7. 8: Fits and q-q diagnostic plots to CPUE abundance indices for MW.

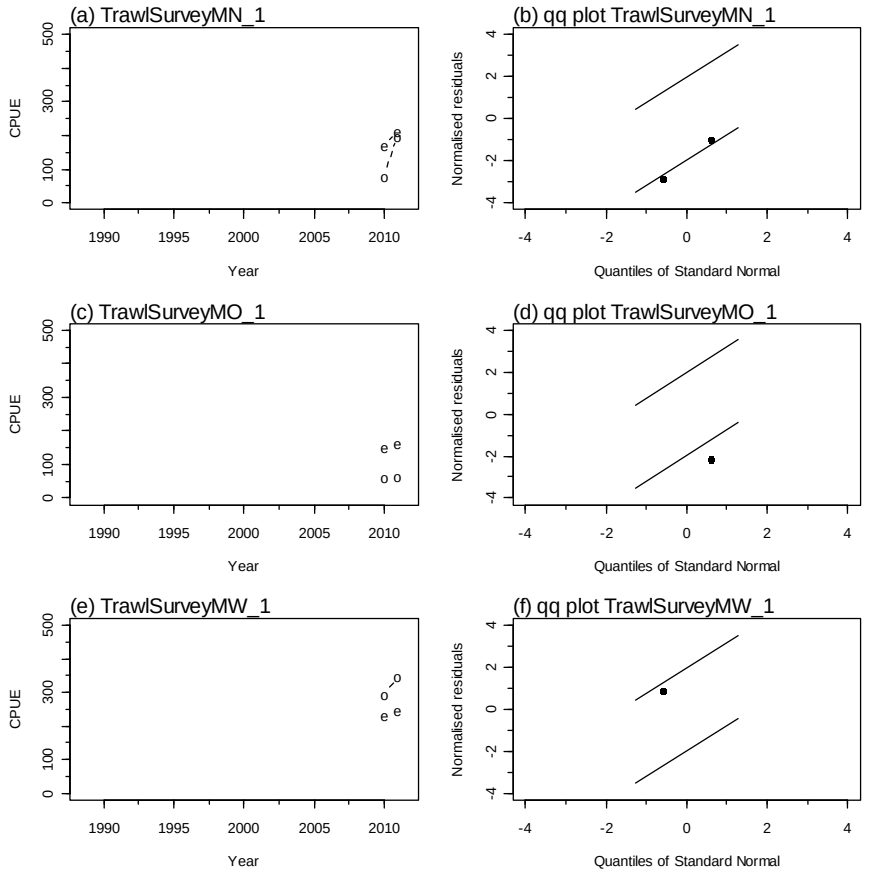

A7. 9: Fits and q-q diagnostic plots to trawl survey abundance indices.

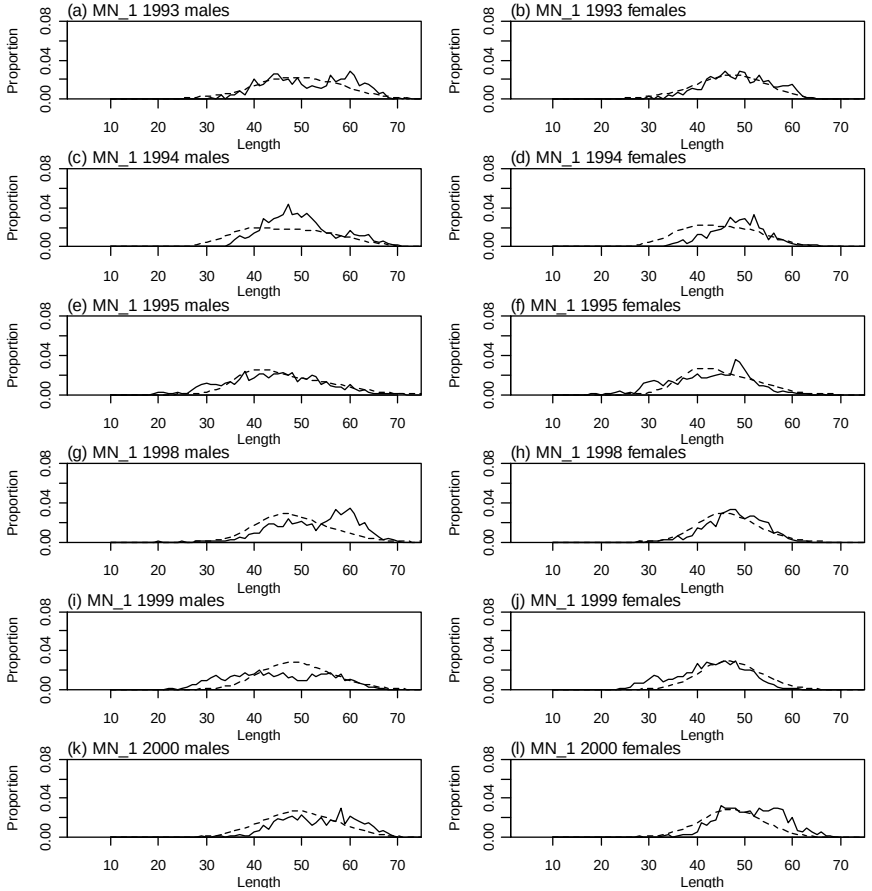

A7. 10: Observed (solid line) and fitted (dashed line) length frequency distributions for observer samples from MN, time step 1 (1993–2000).

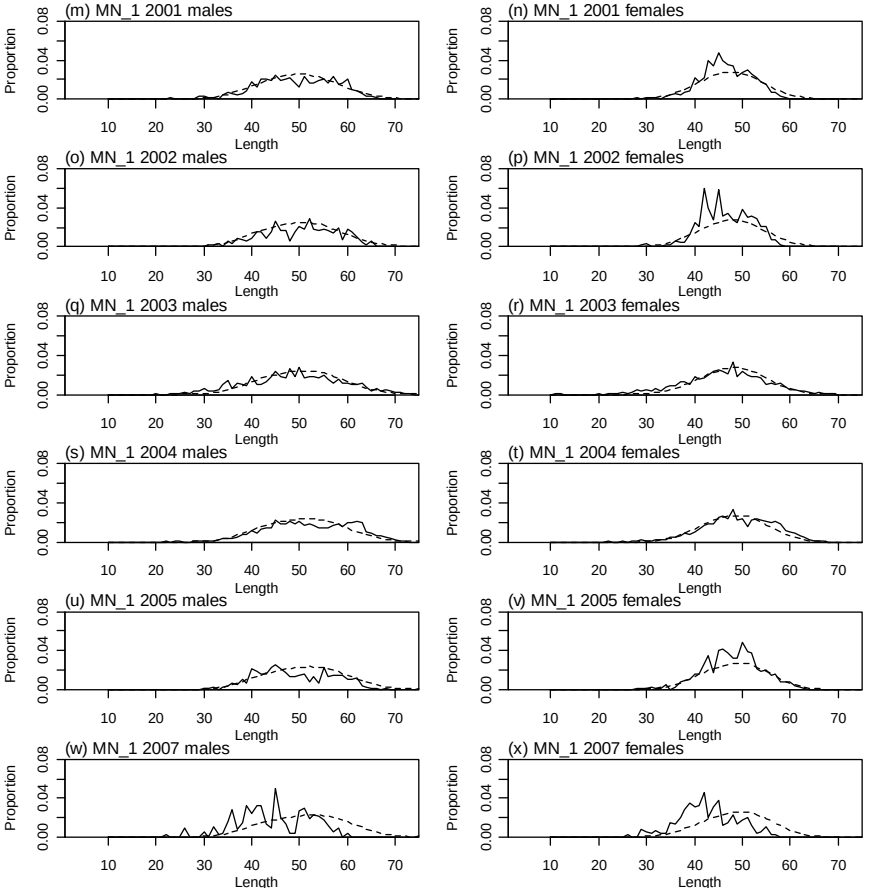

A7. 11: Observed (solid line) and fitted (dashed line) length frequency distributions for observer samples from MN, time step 1 (2001–2007).

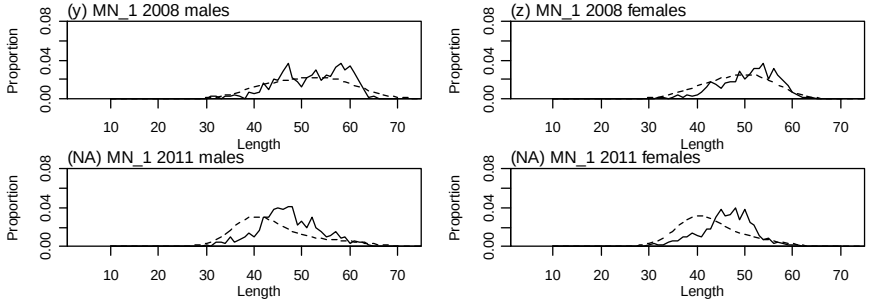

A7. 12: Observed (solid line) and fitted (dashed line) length frequency distributions for observer samples from MN, time step 1 (2008–2011).

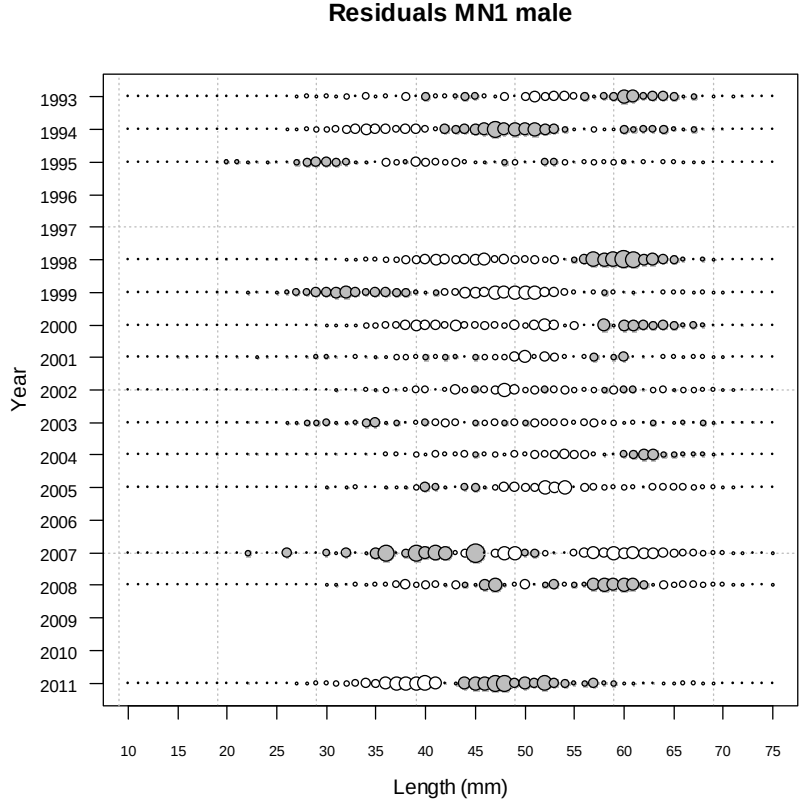

A7. 13: Bubble plots of residuals for fits to length frequency distributions for observer sampling from MN, time step 1, male.

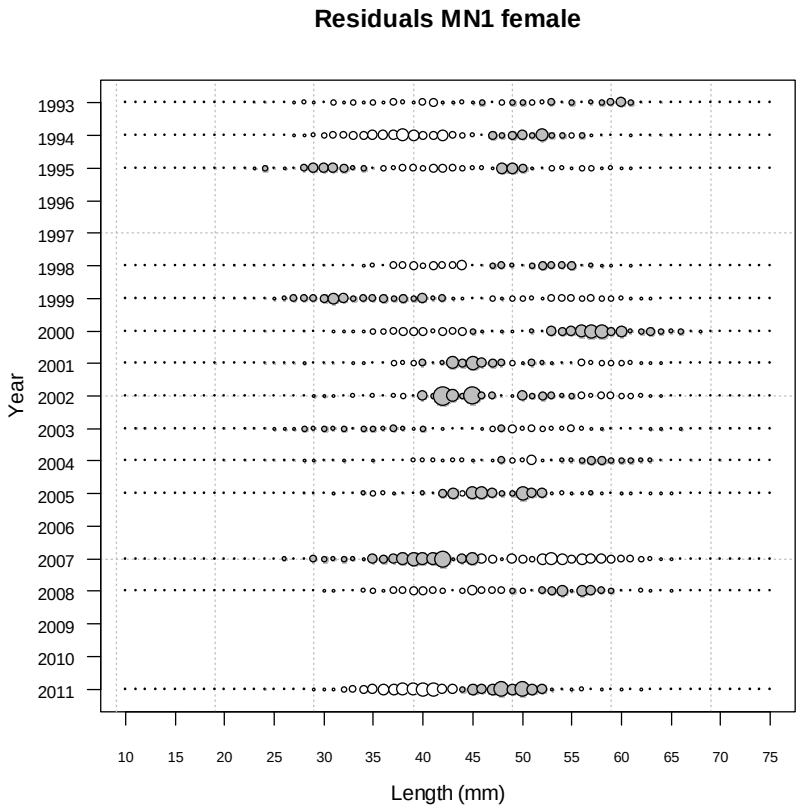

A7. 14: Bubble plots of residuals for fits to length frequency distributions for observer sampling from MN, time step 1, female.

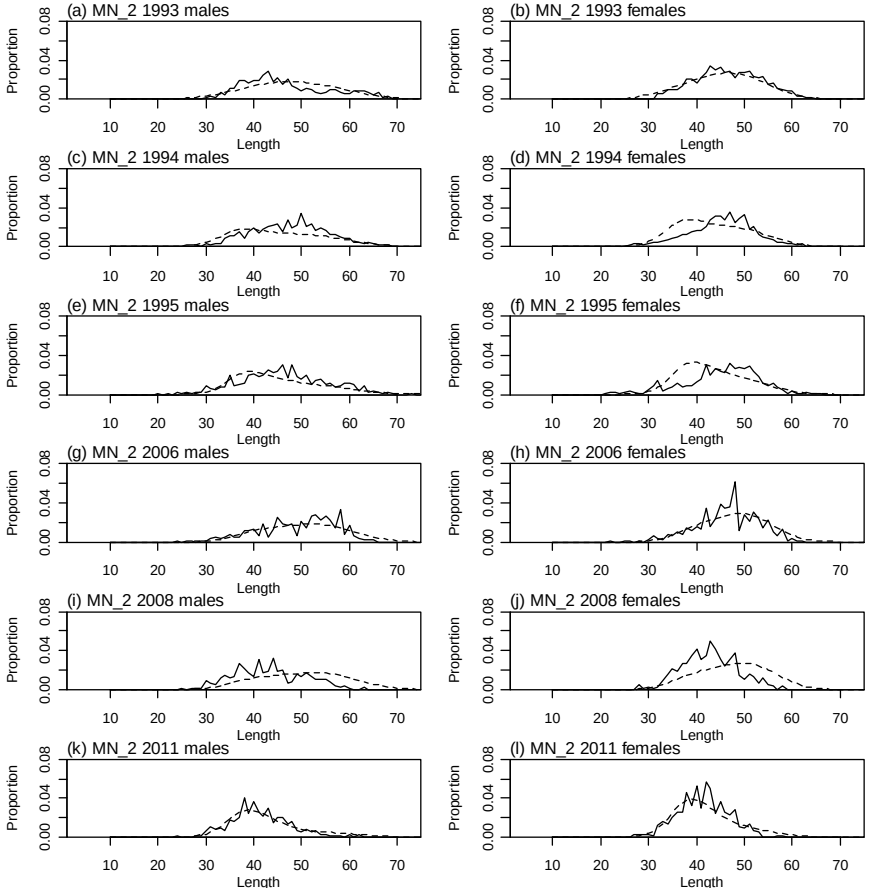

A7. 15: Observed (solid line) and fitted (dashed line) length frequency distributions for observer samples from MN, time step 2.

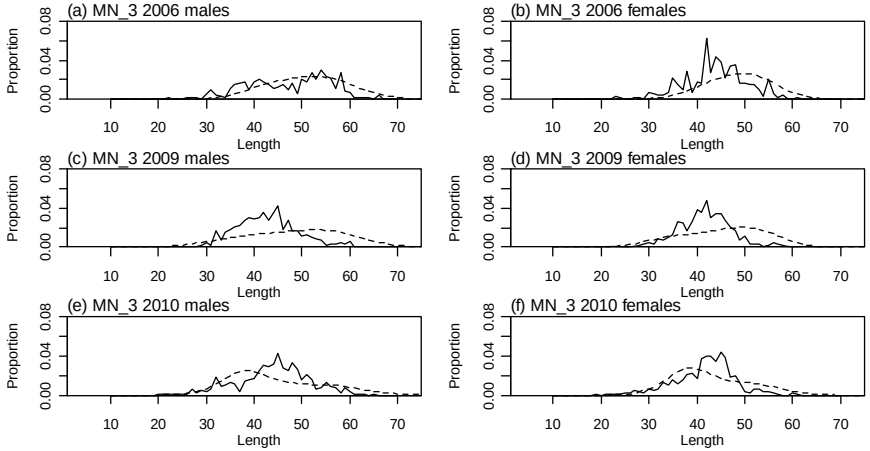

A7. 16: Observed (solid line) and fitted (dashed line) length frequency distributions for observer samples from MN, time step 3.

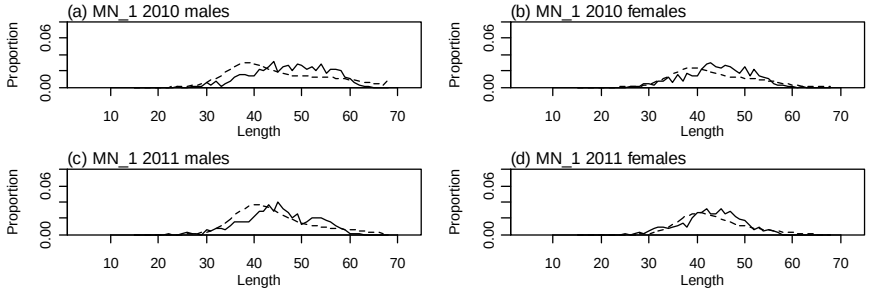

A7. 17: Observed (solid line) and fitted (dashed line) length frequency distributions for trawl survey samples from MN.

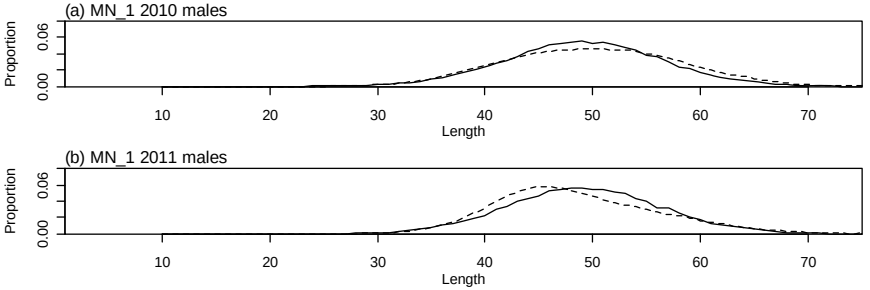

A7. 18: Observed (solid line) and fitted (dashed line) length frequency distributions for photo survey samples from MN.

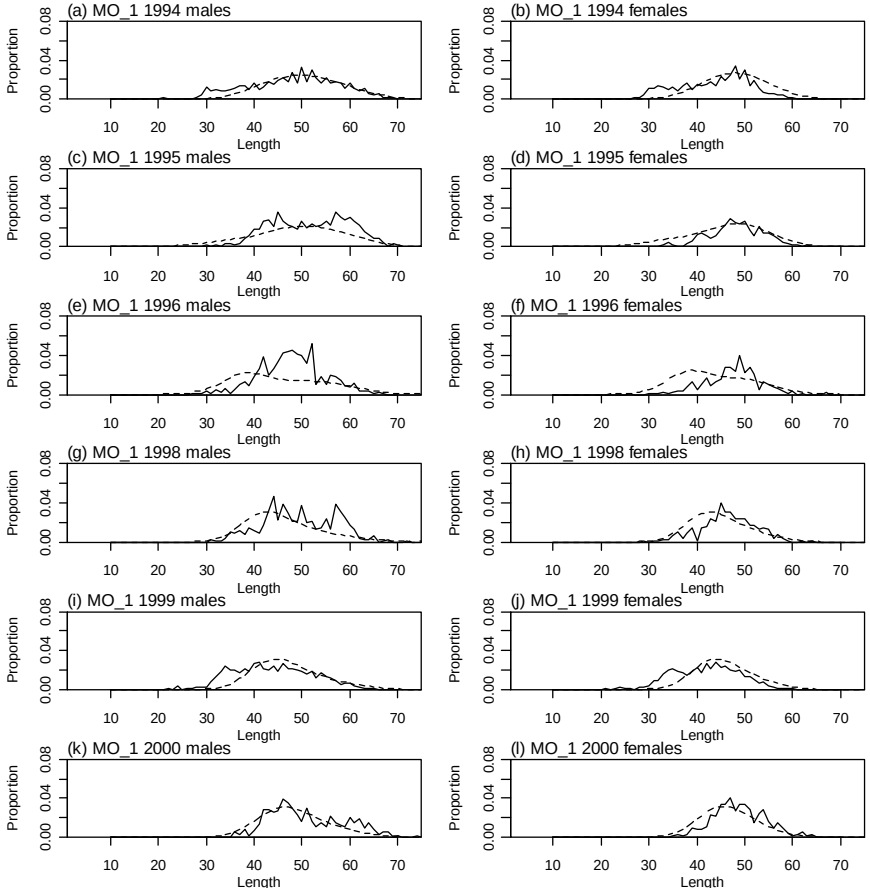

A7. 19: Observed (solid line) and fitted (dashed line) length frequency distributions for observer samples from MO, time step 1 (1994–2000).

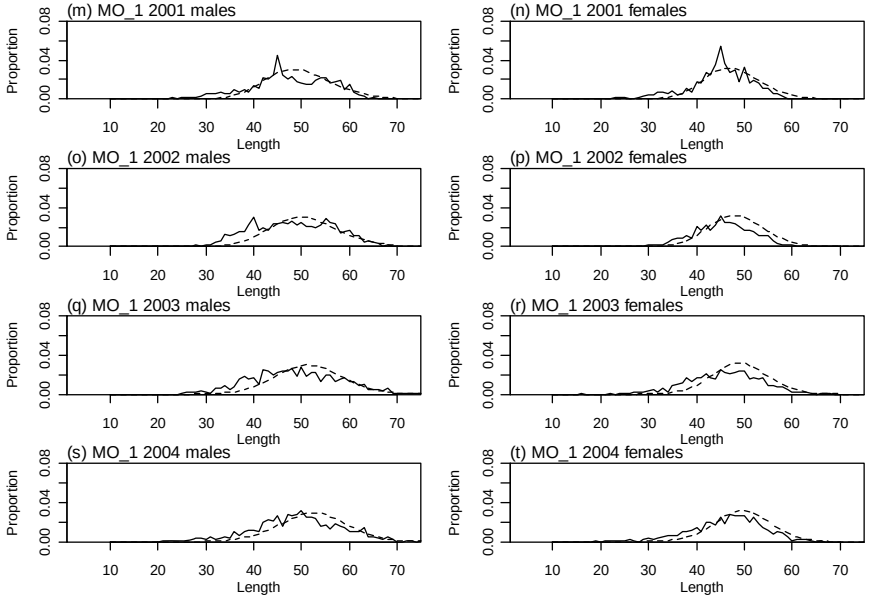

A7. 20: Observed (solid line) and fitted (dashed line) length frequency distributions for observer samples from MO, time step 1 (2001–2004).

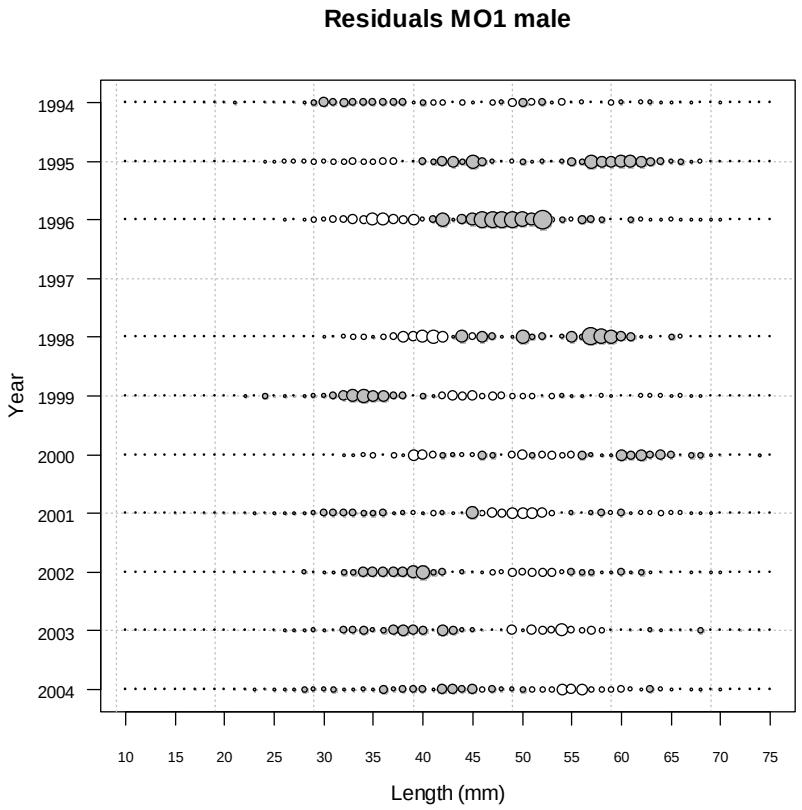

A7. 21: Bubble plots of residuals for fits to length frequency distributions for observer sampling from MO, time step 1, male.

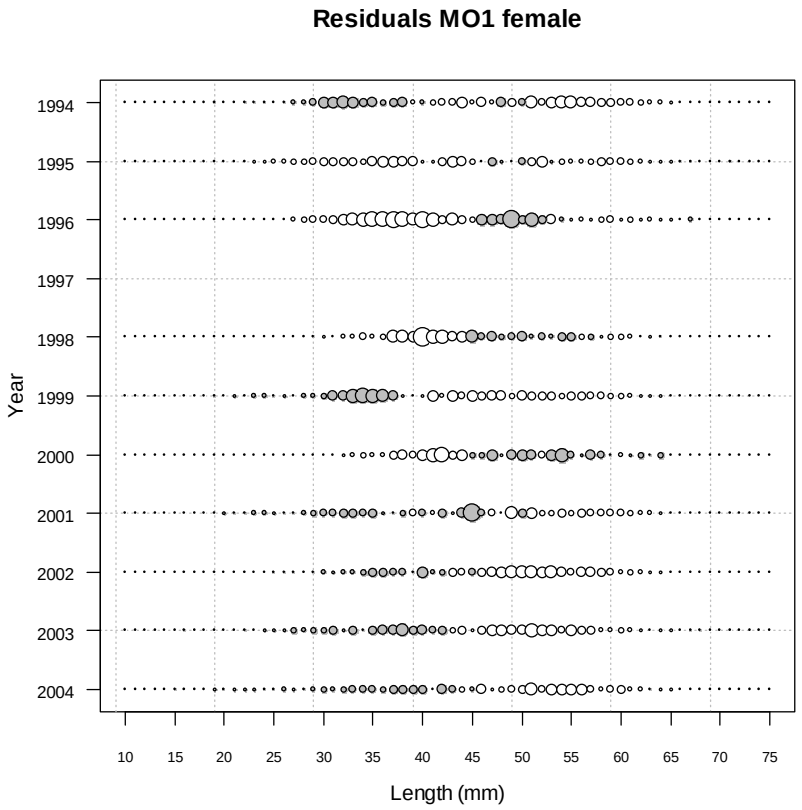

A7. 22: Bubble plots of residuals for fits to length frequency distributions for observer sampling from MO, time step 1, female.

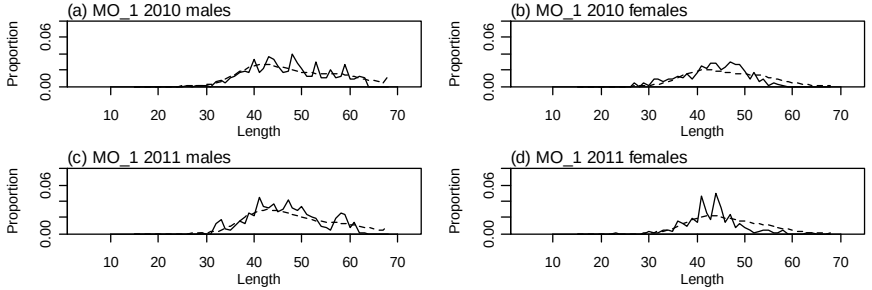

A7. 23: Observed (solid line) and fitted (dashed line) length frequency distributions for trawl survey samples from MO.

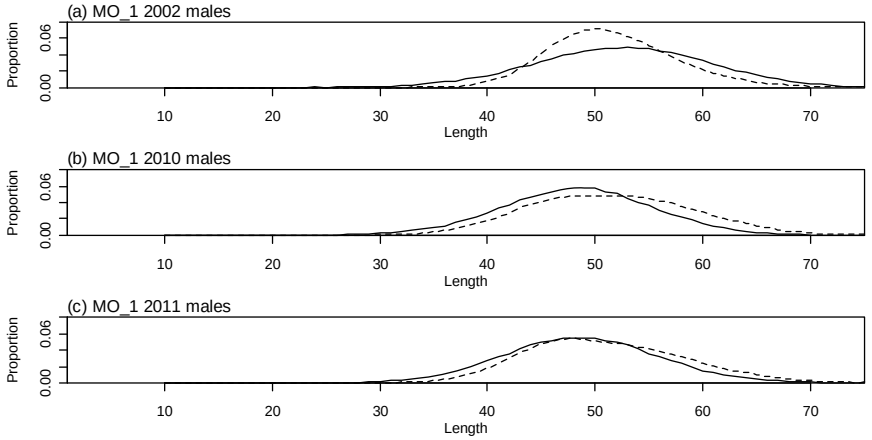

A7. 24: Observed (solid line) and fitted (dashed line) length frequency distributions for photo survey samples from MO.

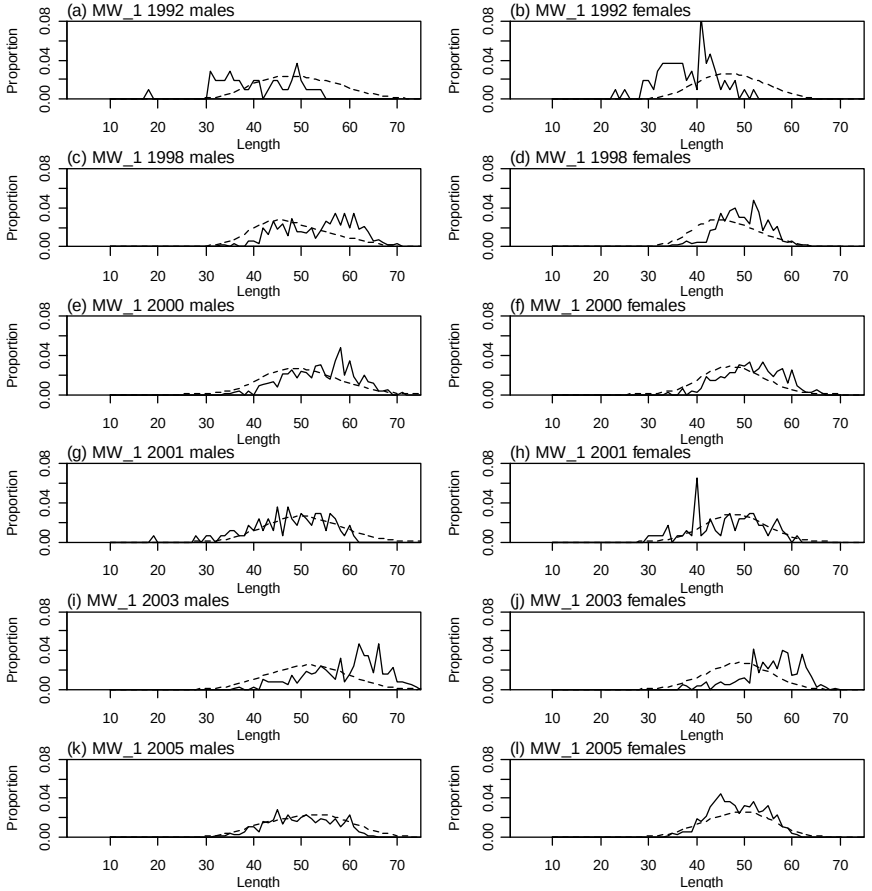

A7. 25: Observed (solid line) and fitted (dashed line) length frequency distributions for observer samples from MW, time step 1 (1992–2005).

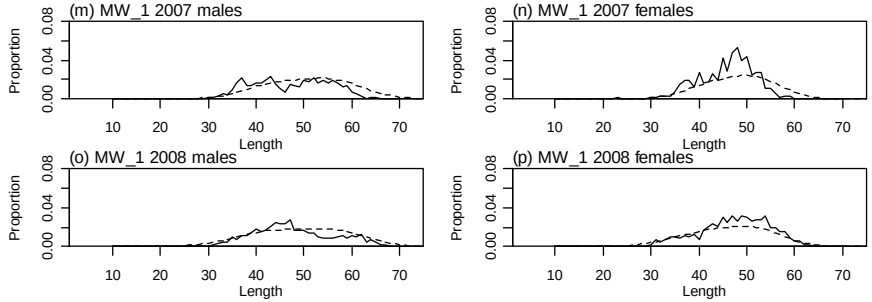

A7. 26: Observed (solid line) and fitted (dashed line) length frequency distributions for observer samples from MW, time step 1 (2007–2008).

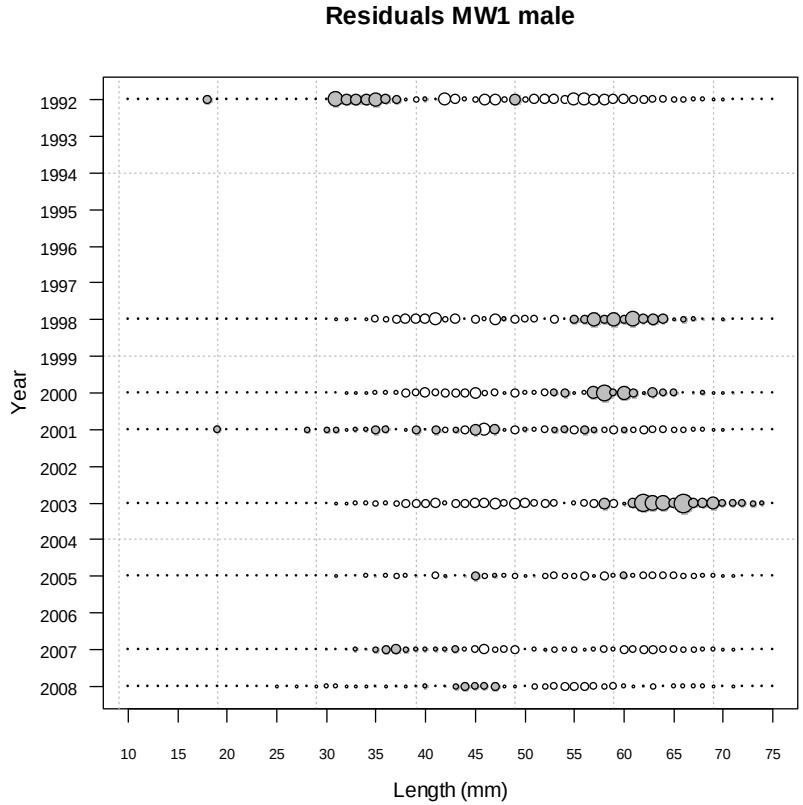

A7. 27: Bubble plots of residuals for fits to length frequency distributions for observer sampling from MW, time step 1, male.

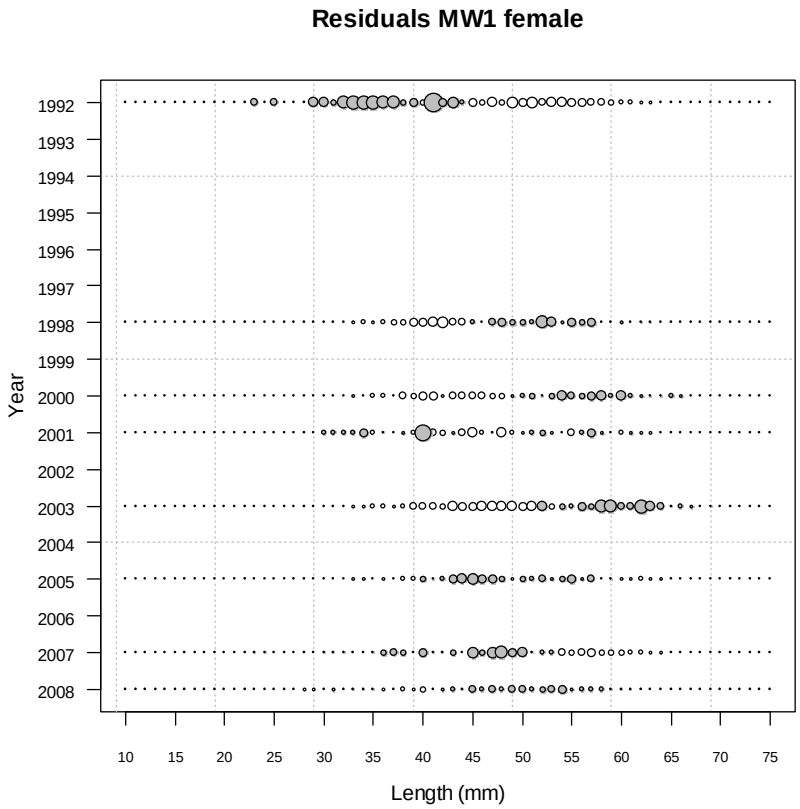

A7. 28: Bubble plots of residuals for fits to length frequency distributions for observer sampling from MW, time step 1, female.

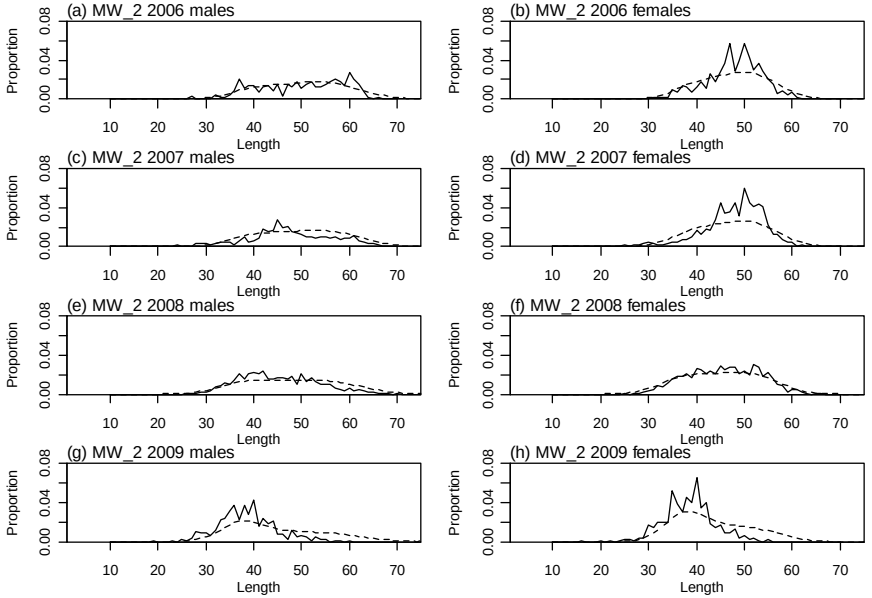

A7. 29: Observed (solid line) and fitted (dashed line) length frequency distributions for observer samples from MW, time step 2.

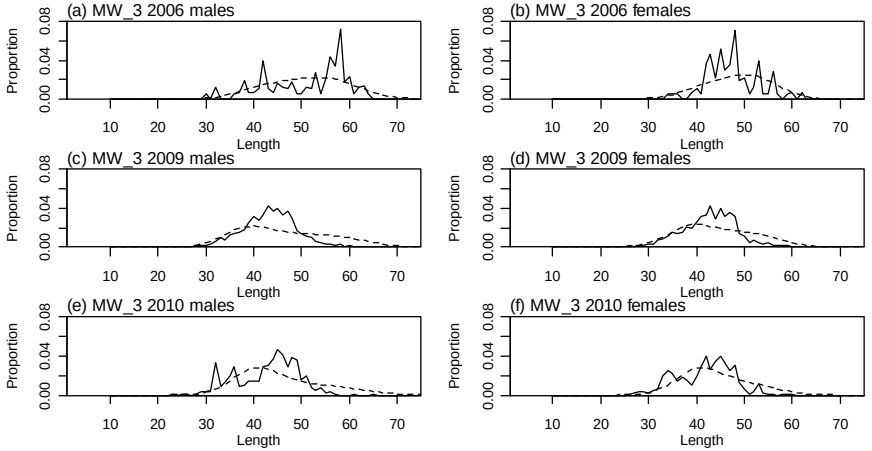

A7. 30: Observed (solid line) and fitted (dashed line) length frequency distributions for observer samples from MW, time step 3.

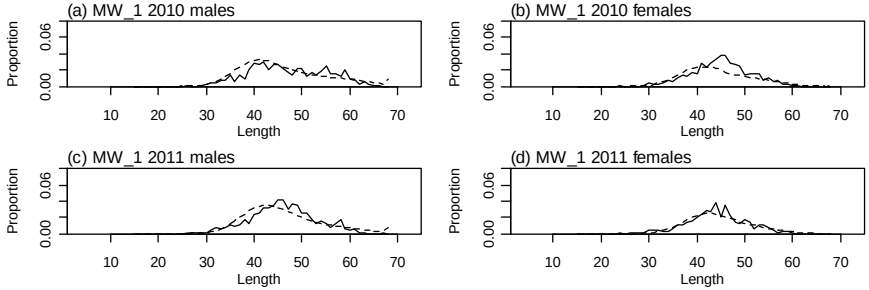

A7. 31: Observed (solid line) and fitted (dashed line) length frequency distributions for trawl survey samples from MW.

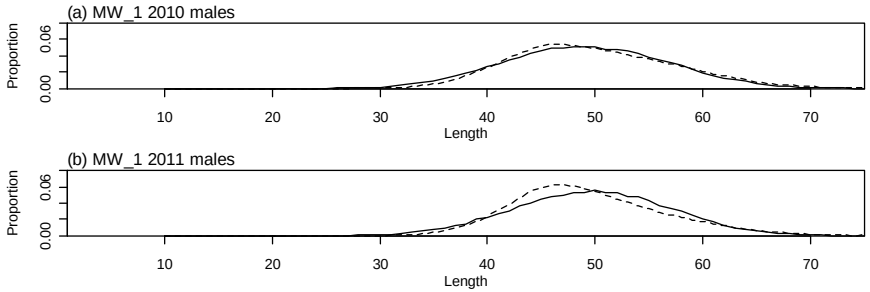

A7. 32: Observed (solid line) and fitted (dashed line) length frequency distributions for photo survey samples from MW.

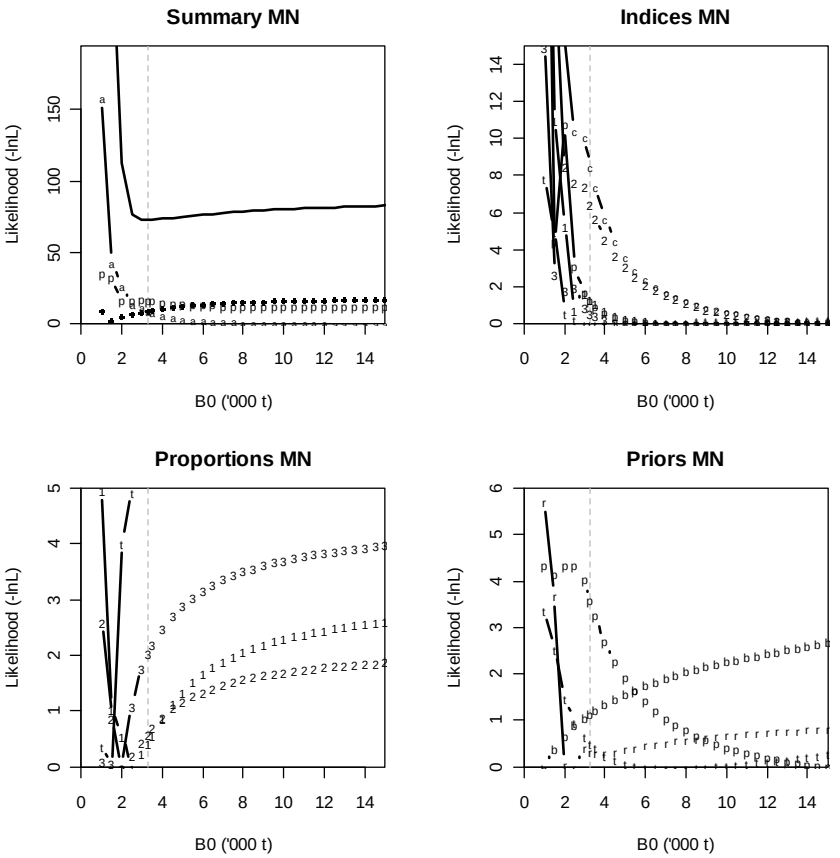

A7. 33: Likelihood profiles for model 1 when MN B_0 is fixed in the model. Figures show profiles for main priors (top left, p-priors, a – abundance indices, • – proportions at length), abundance indices (top right, t - trawl survey, 1 - CPUE time step 1, 2 - CPUE time step 2, 3 - CPUE time step 3, p – photo survey), proportion at length data (bottom left, t-trawl, 1 – observer time step 1, 2 – observer time step 2, 3 – observer time step 3) and priors (bottom right, b- B_0, YCS - r, p- *q-Photo*, t – *q-Trawl*).

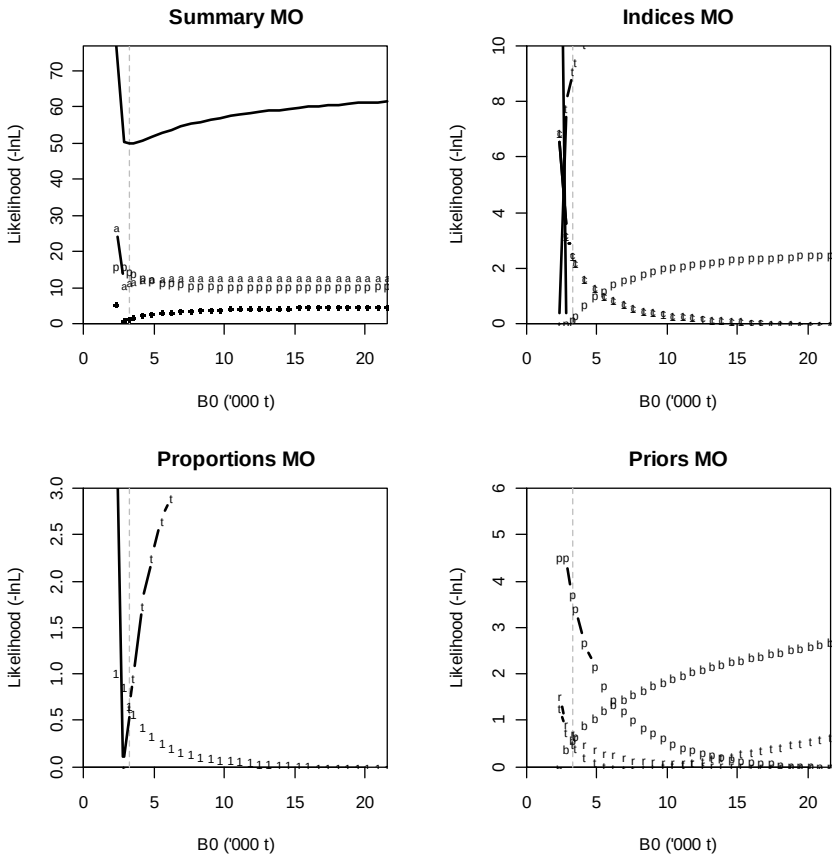

A7. 34: Likelihood profiles for model 1 when MO B_0 is fixed in the model. Figures show profiles for main priors (top left, p-priors, a – abundance indices, • – proportions at length), abundance indices (top right, t - trawl survey, 1 - CPUE time step 1, 2 - CPUE time step 2, 3 - CPUE time step 3, p – photo survey), proportion at length data (bottom left, t-trawl, 1 – observer time step 1, 2 – observer time step 2, 3 – observer time step 3) and priors (bottom right, b- B_0, YCS - r, p- *q-Photo*, t – *q-Trawl*).

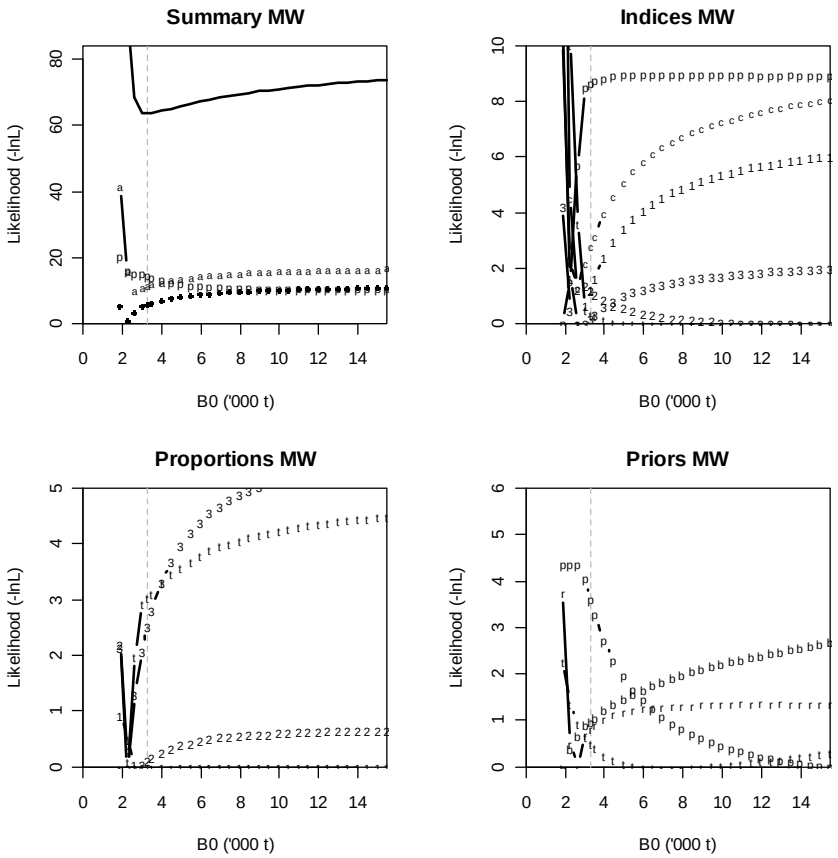

A7. 35: Likelihood profiles for model 1 when MW B_0 is fixed in the model. Figures show profiles for main priors (top left, p-priors, a – abundance indices, • – proportions at length), abundance indices (top right, t - trawl survey, 1 - CPUE time step 1, 2 - CPUE time step 2, 3 - CPUE time step 3, p – photo survey), proportion at length data (bottom left, t-trawl, 1 – observer time step 1, 2 – observer time step 2, 3 – observer time step 3) and priors (bottom right, b- B_0, YCS - r, p- *q-Photo*, t – *q-Trawl*).

15. APPENDIX 8. BASE-G-EST model plots

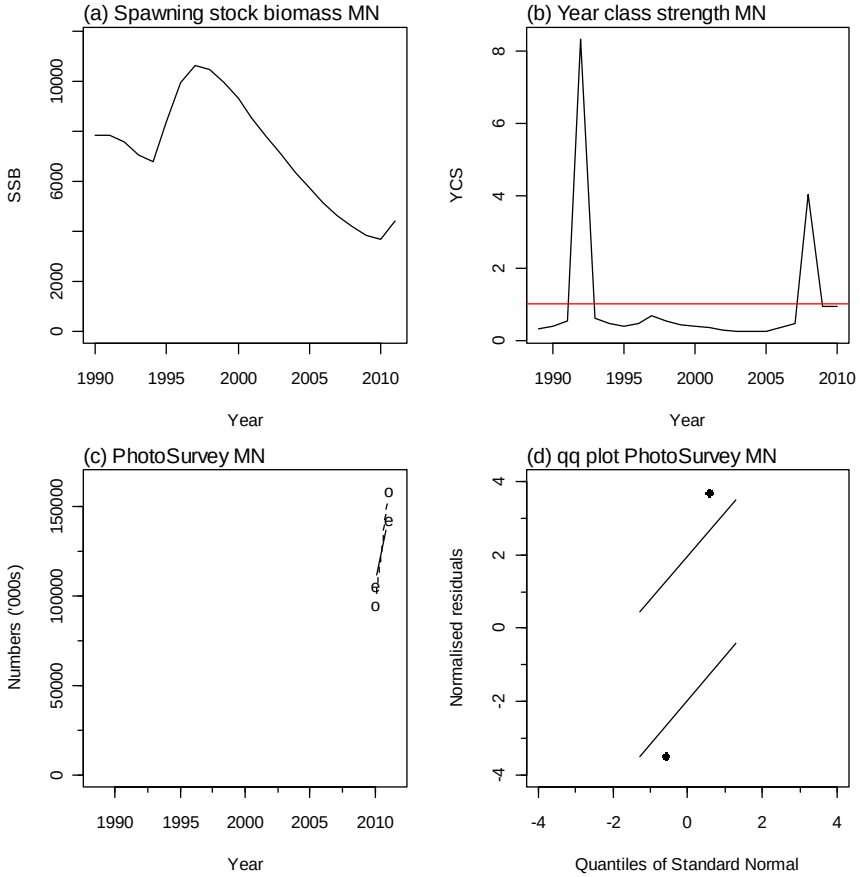

A8. 1: Spawning stock biomass trajectory (a), year class strength (b) fits (c) and q-q diagnostic plots (d) to photo survey abundance index for SCI 3 subarea MN from BASE-g-est model.

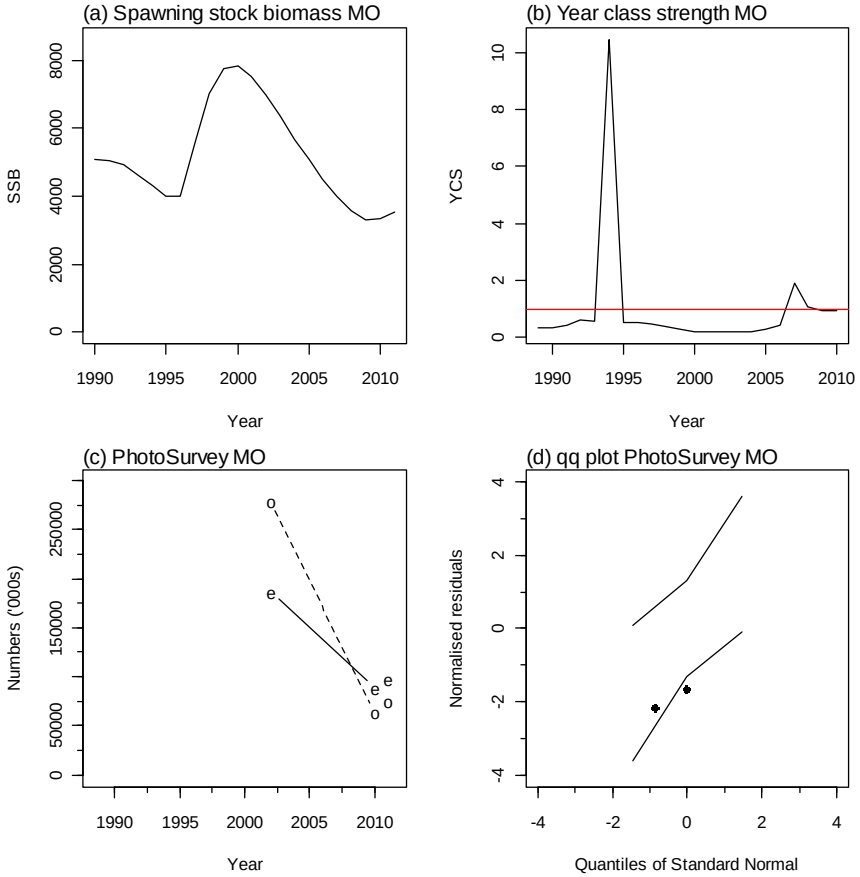

A8. 2: Spawning stock biomass trajectory (a), year class strength (b) fits (c) and q-q diagnostic plots (d) to photo survey abundance index for SCI 3 subarea MO from BASE-g-est model.

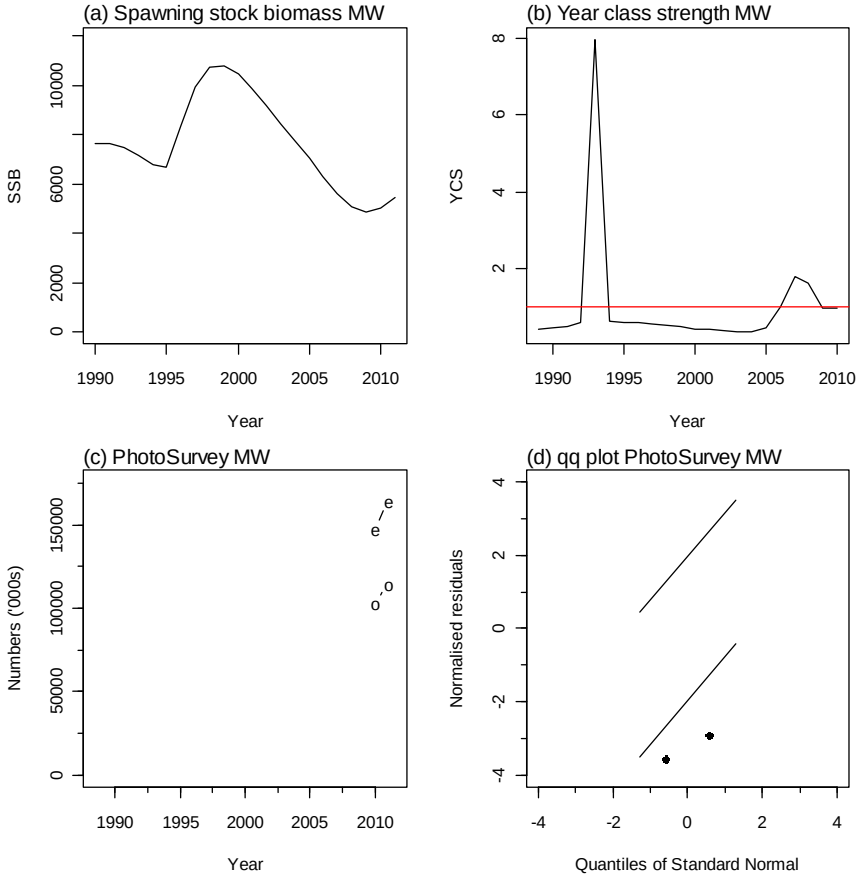

A8. 3: Spawning stock biomass trajectory (a), year class strength (b) fits (c) and q-q diagnostic plots (d) to photo survey abundance index for SCI 3 subarea MW from BASE-g-est model.

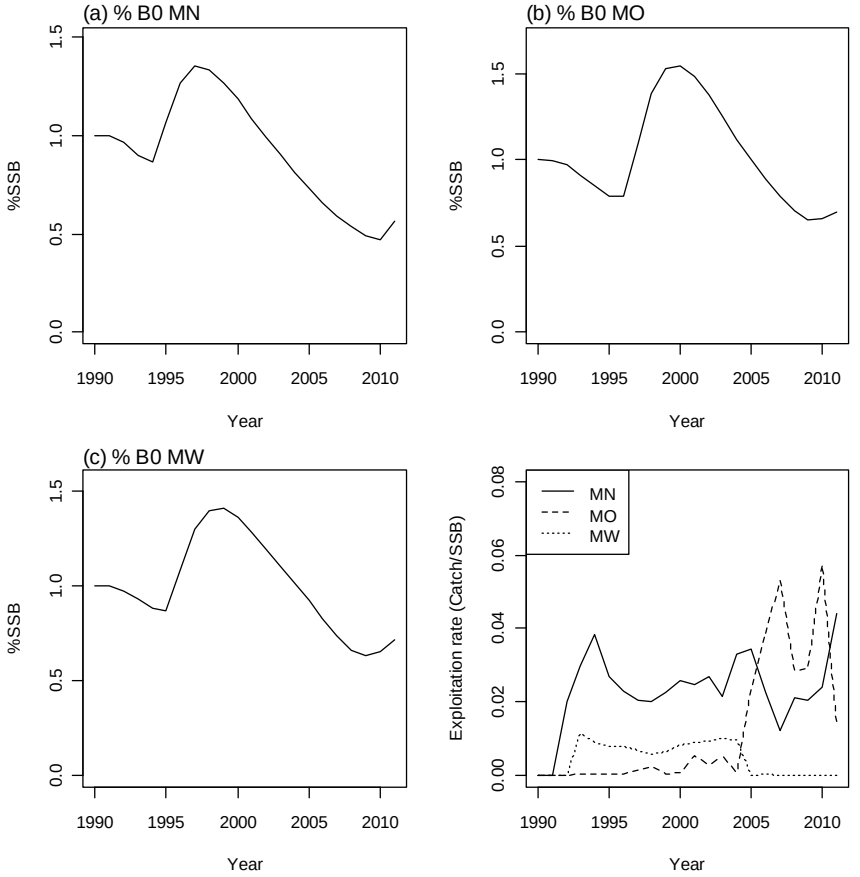

A8. 4: Trajectory of SSB as a percentage of B_0 for each subarea from the MPD fit to BASE-g-est model, and exploitation rate (catch/SSB).

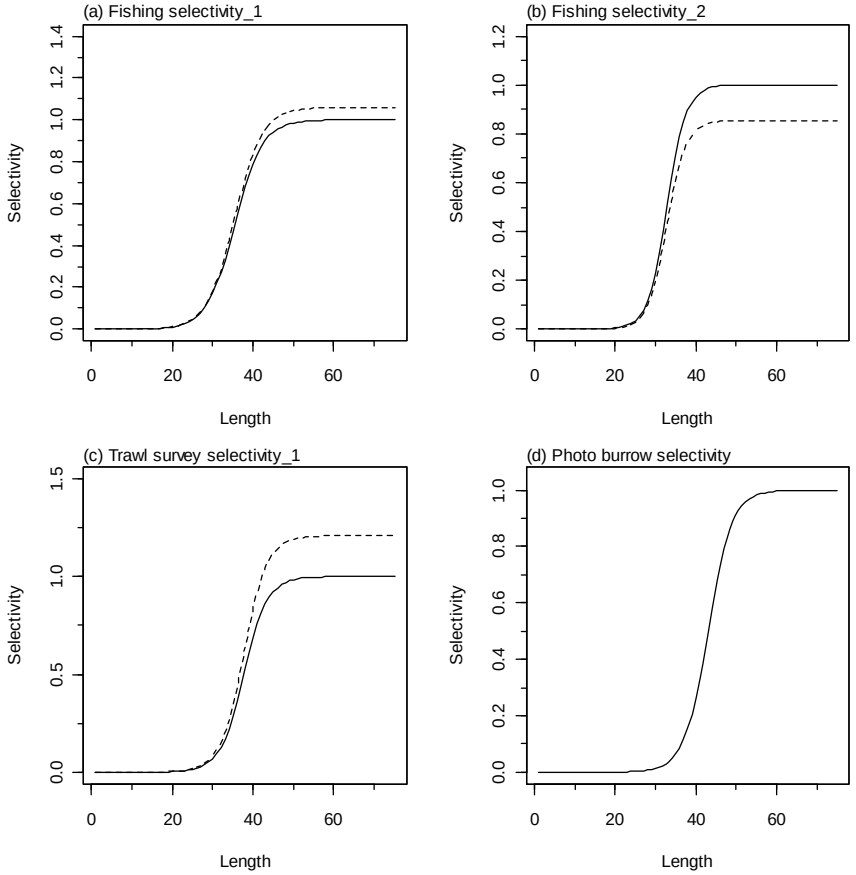

A8. 5: Fishery and survey selectivity curves. Solid line – females, dotted line – males. The scampi burrow index is not sexed, and a single selectivity applies.

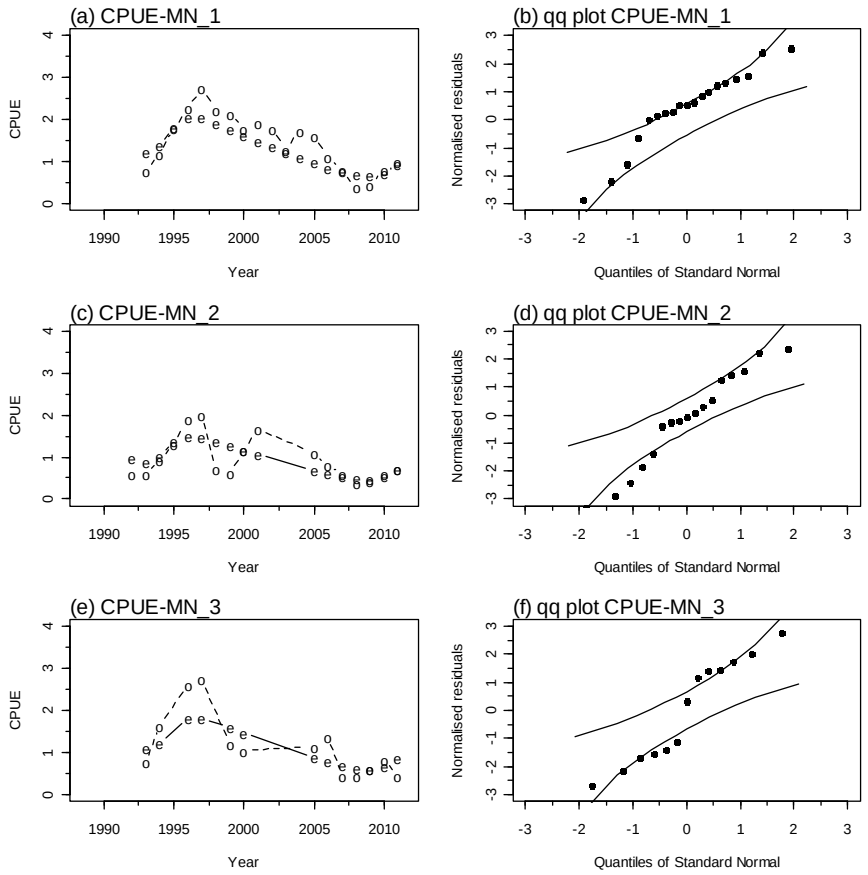

A8. 6: Fits and q-q diagnostic plots to CPUE abundance indices for MN.

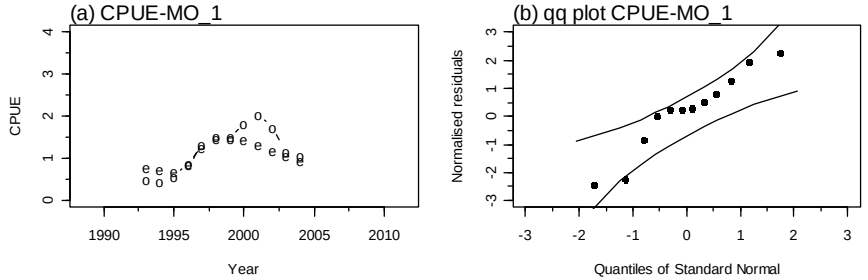

A8. 7: Fits and q-q diagnostic plots to CPUE abundance indices for MO.

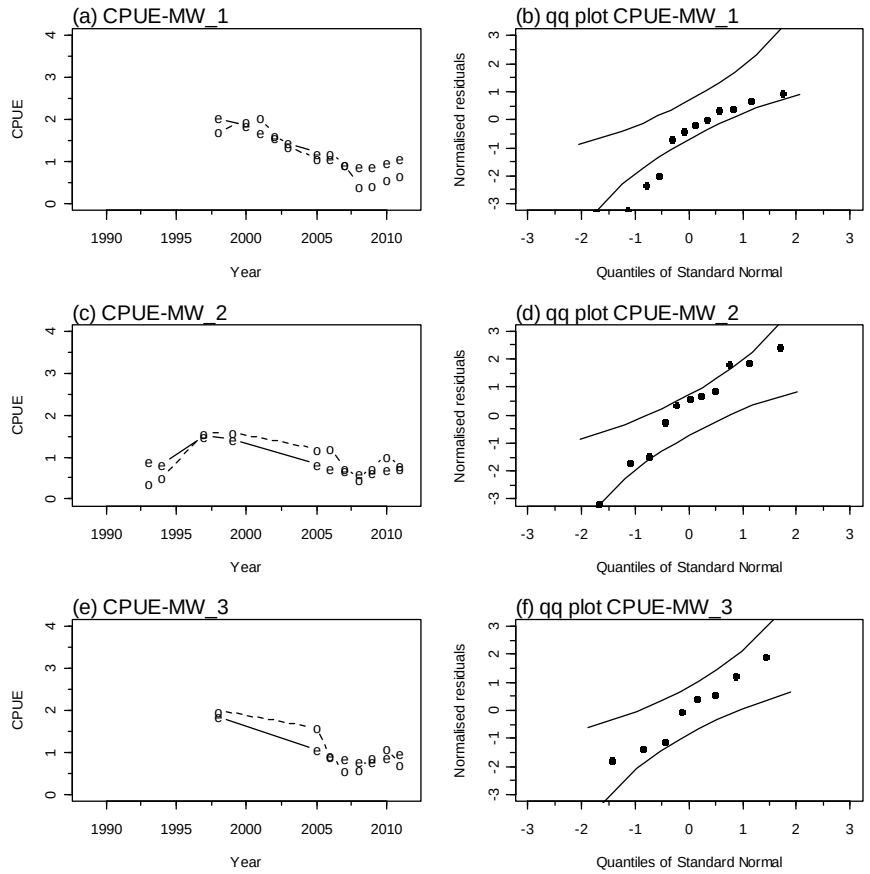

A8. 8: Fits and q-q diagnostic plots to CPUE abundance indices for MW.

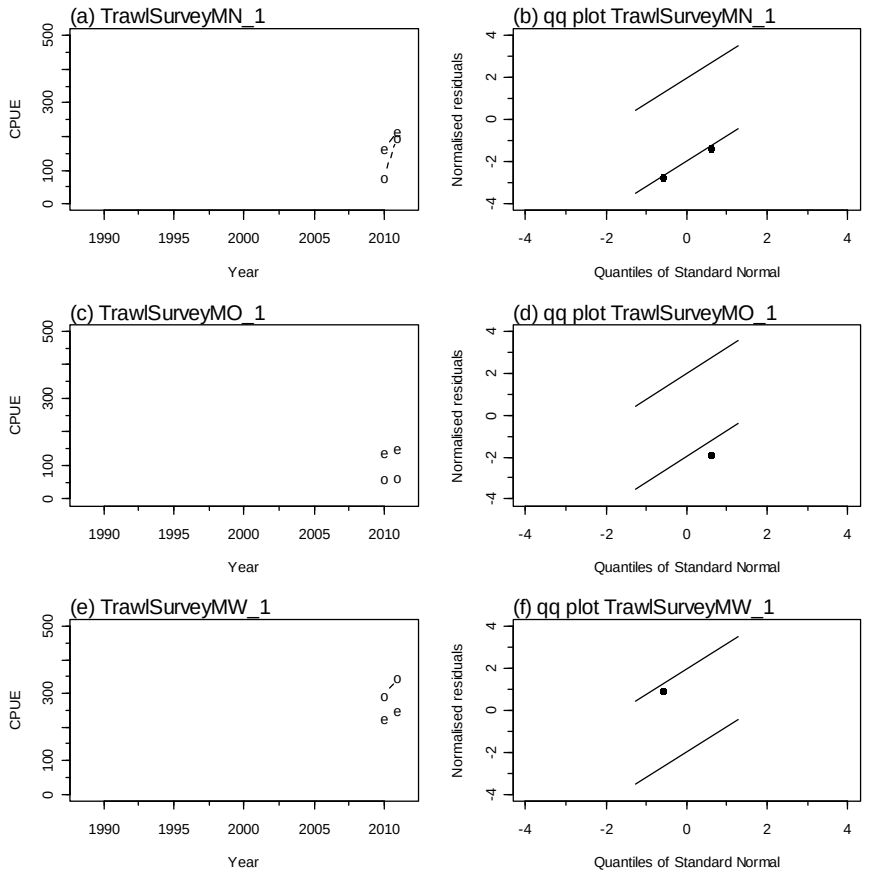

A8. 9: Fits and q-q diagnostic plots to trawl survey abundance indices.

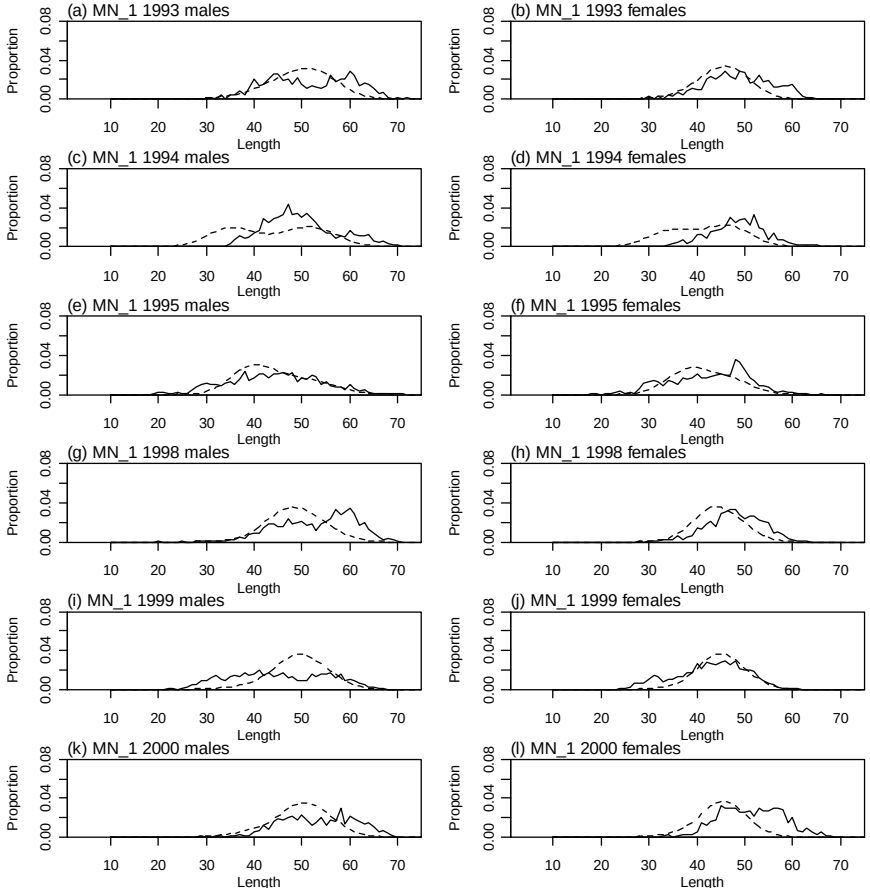

A8. 10: Observed (solid line) and fitted (dashed line) length frequency distributions for observer samples from MN, time step 1 (1993–2000).

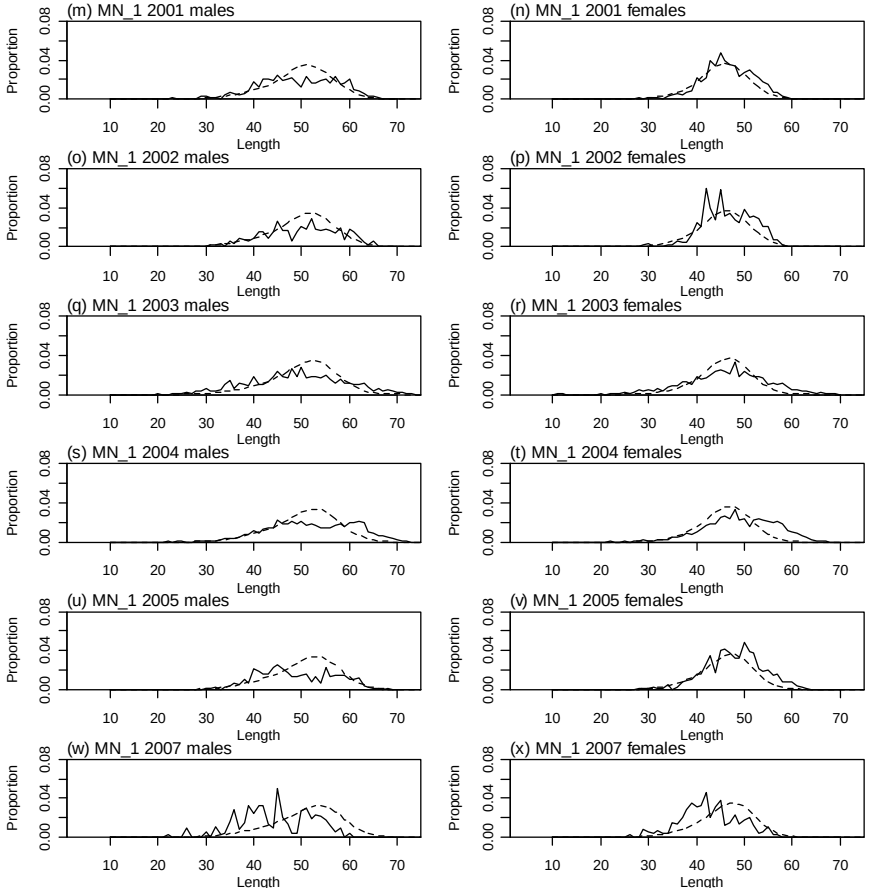

A8. 11: Observed (solid line) and fitted (dashed line) length frequency distributions for observer samples from MN, time step 1 (2001–2007).

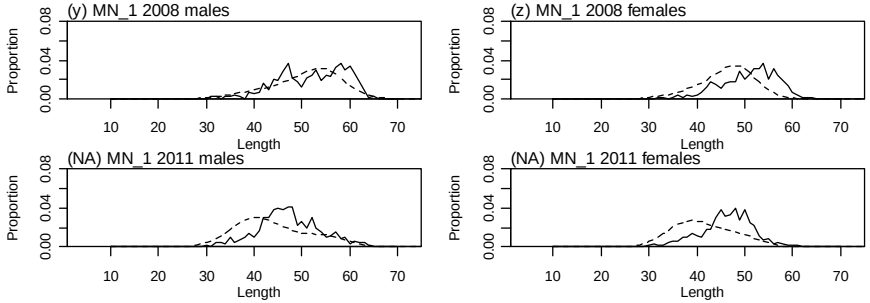

A8. 12: Observed (solid line) and fitted (dashed line) length frequency distributions for observer samples from MN, time step 1 (2008–2011).

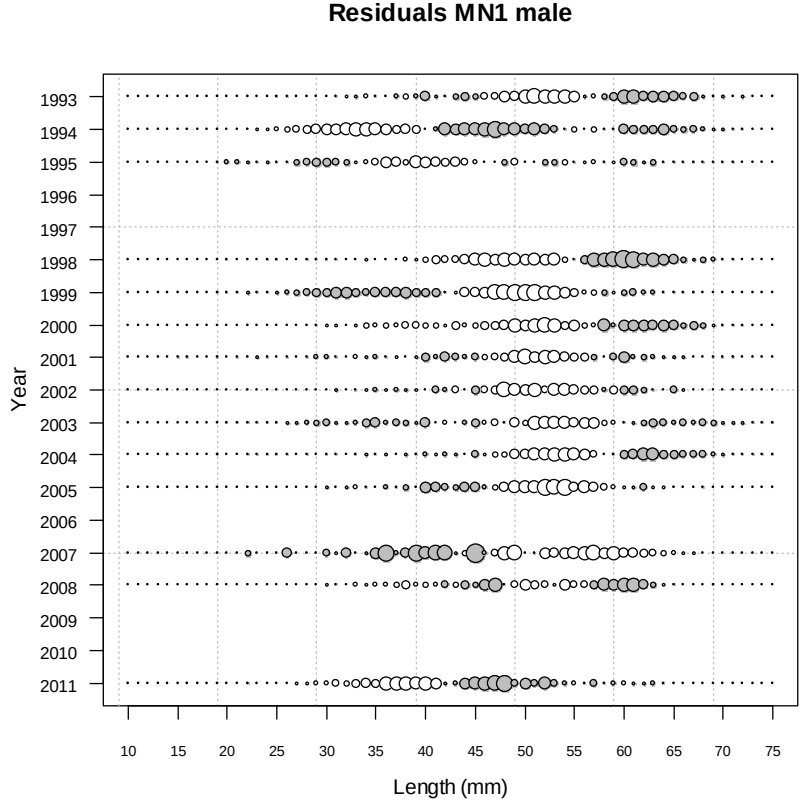

A8. 13: Bubble plots of residuals for fits to length frequency distributions for observer sampling from MN, time step 1, male.

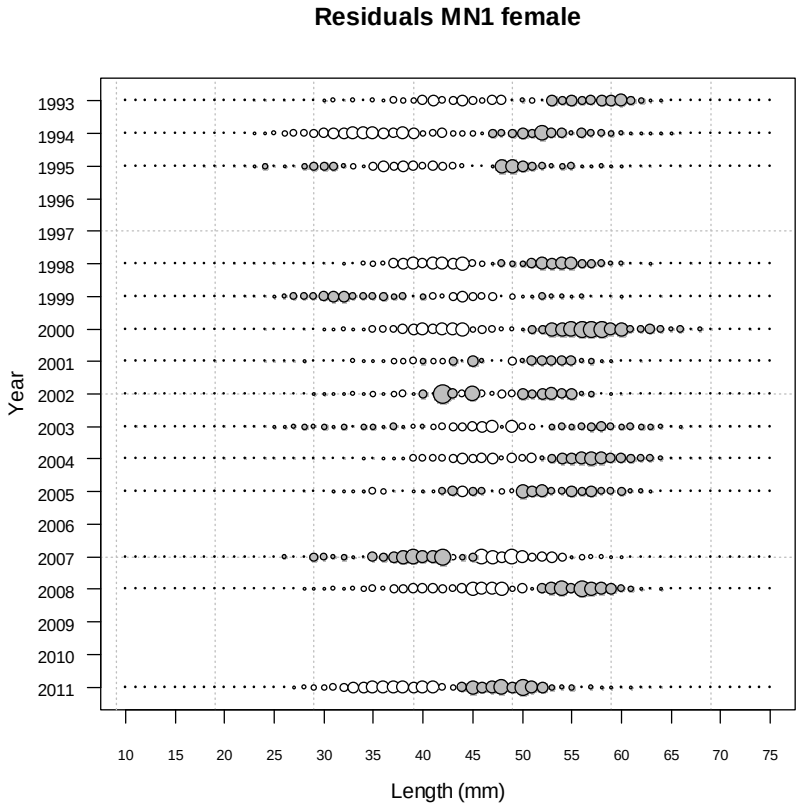

A8. 14: Bubble plots of residuals for fits to length frequency distributions for observer sampling from MN, time step 1, female.

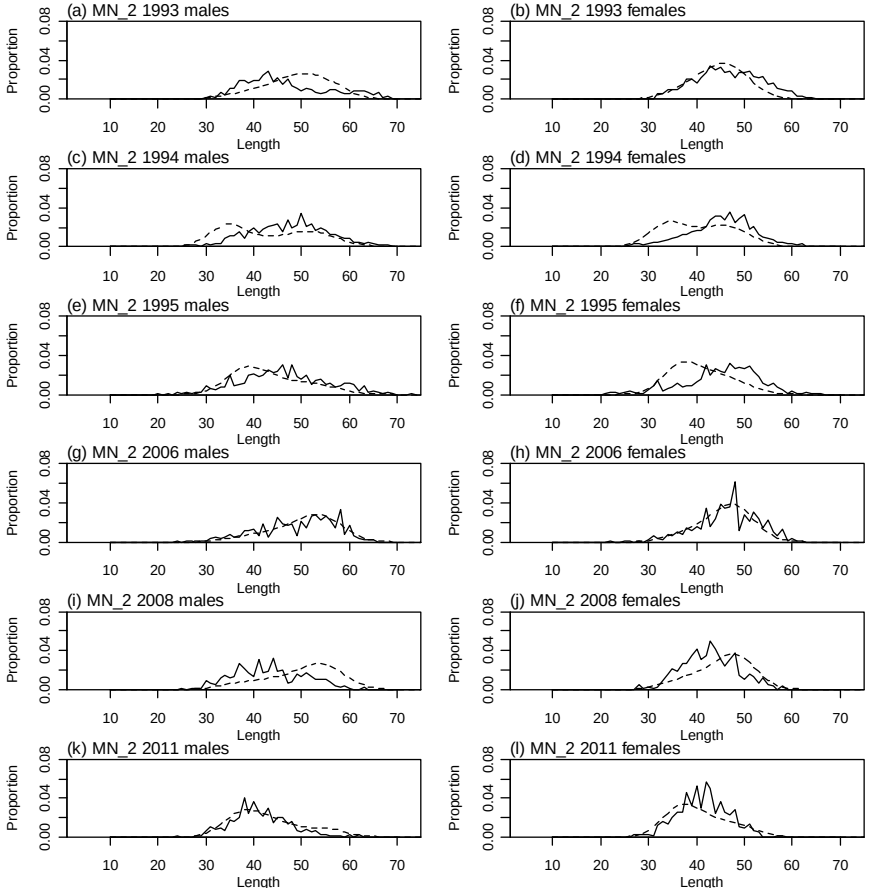

A8. 15: Observed (solid line) and fitted (dashed line) length frequency distributions for observer samples from MN, time step 2.

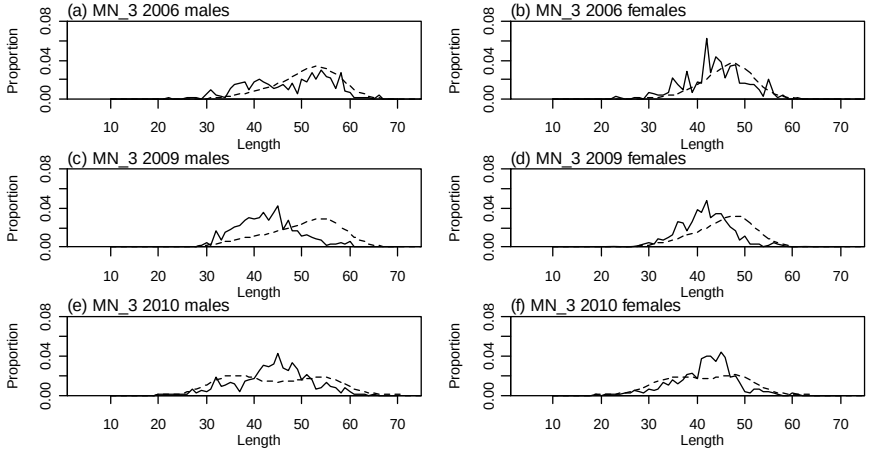

A8. 16: Observed (solid line) and fitted (dashed line) length frequency distributions for observer samples from MN, time step 3.

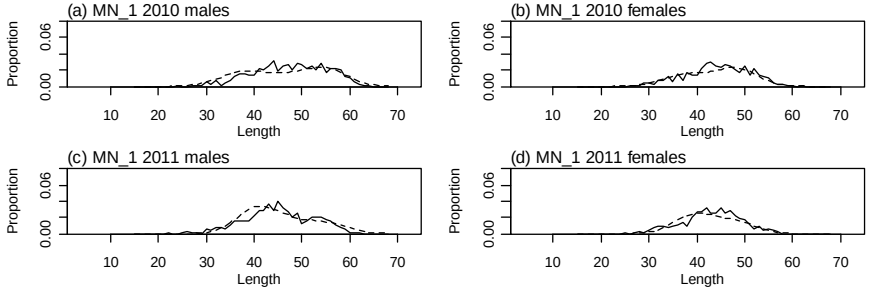

A8. 17: Observed (solid line) and fitted (dashed line) length frequency distributions for trawl survey samples from MN.

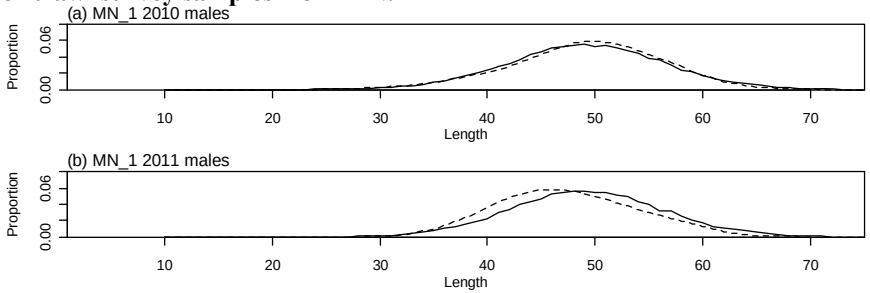

A8. 18: Observed (solid line) and fitted (dashed line) length frequency distributions for photo survey samples from MN.

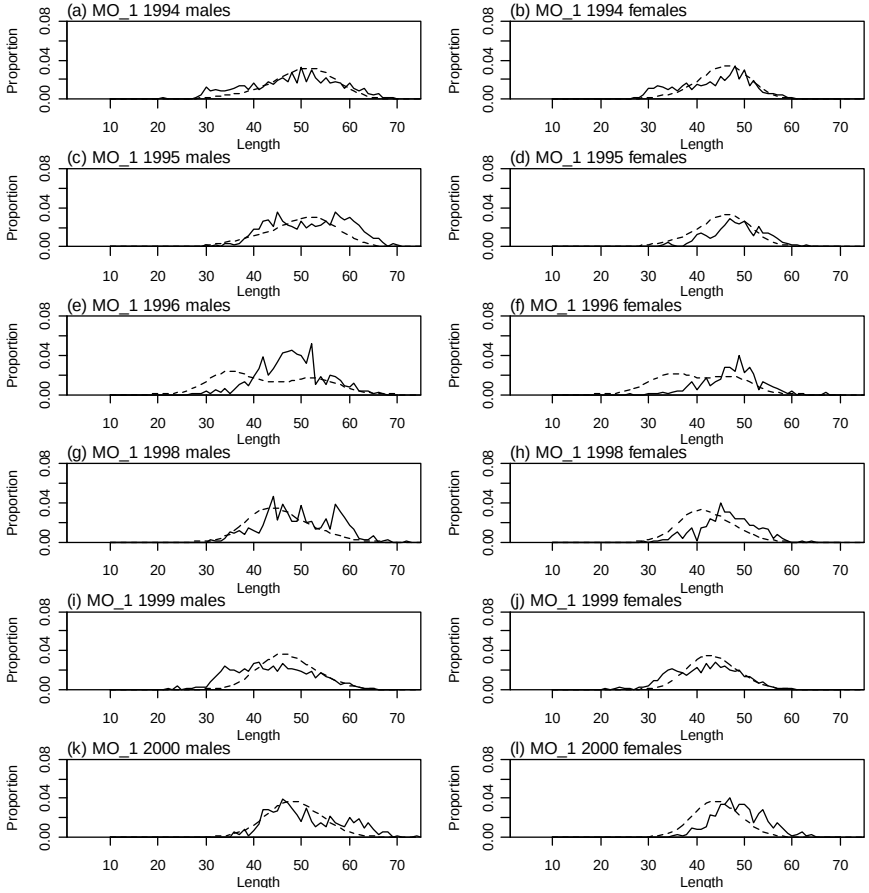

A8. 19: Observed (solid line) and fitted (dashed line) length frequency distributions for observer samples from MO, time step 1 (1994–2000).

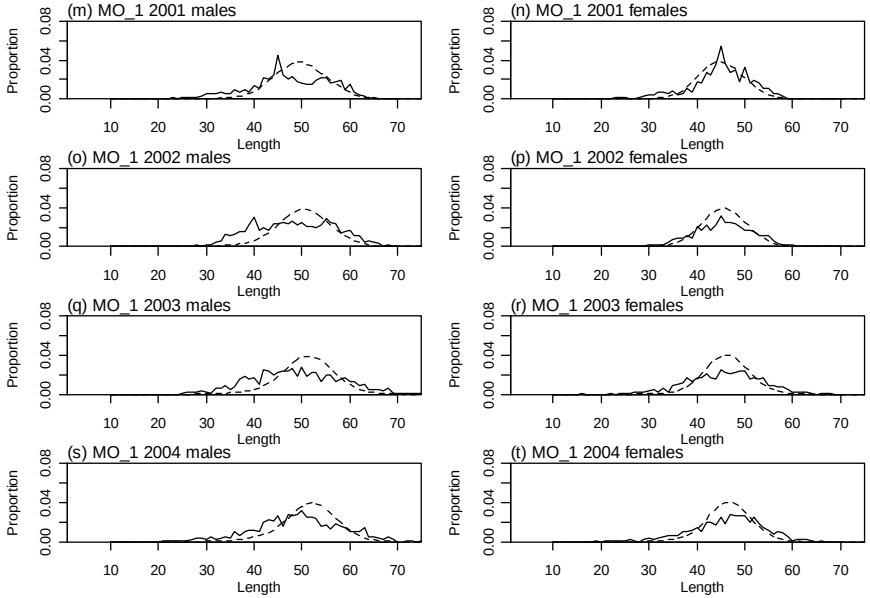

A8. 20: Observed (solid line) and fitted (dashed line) length frequency distributions for observer samples from MO, time step 1 (2001–2004).

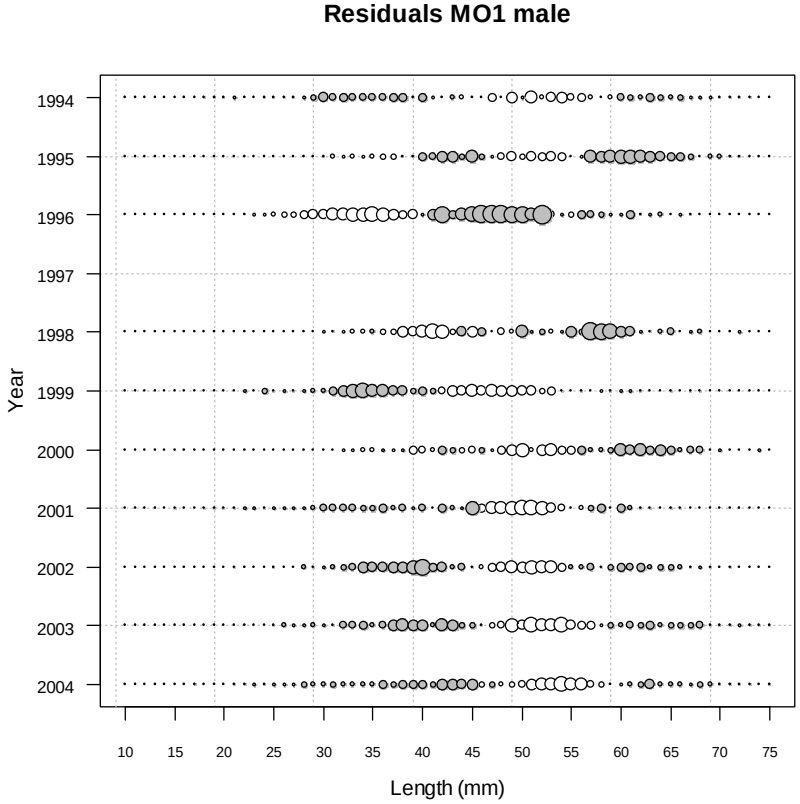

A8. 21: Bubble plots of residuals for fits to length frequency distributions for observer sampling from MO, time step 1, male.

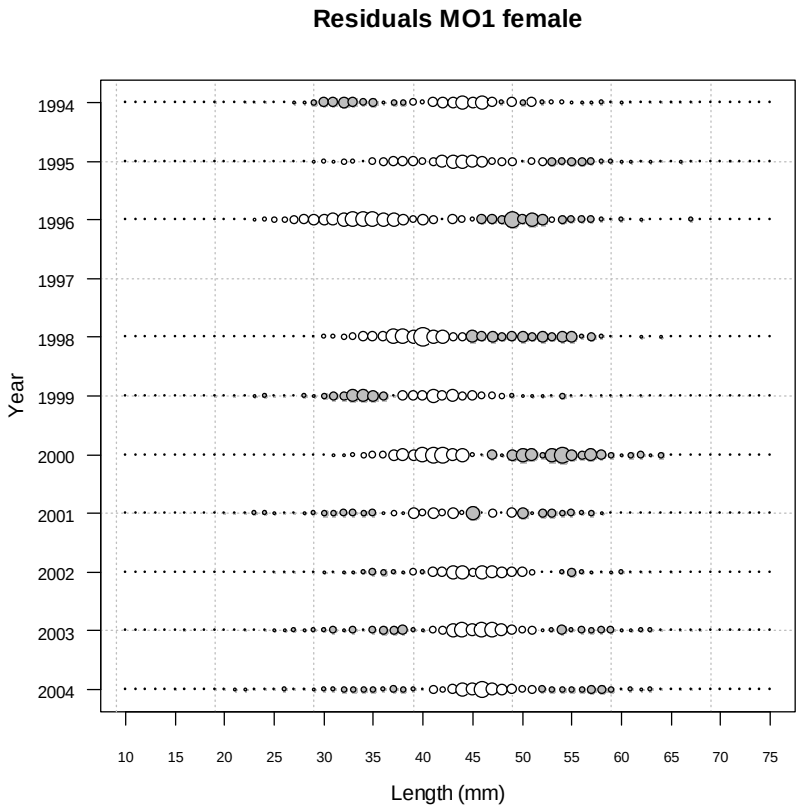

A8. 22: Bubble plots of residuals for fits to length frequency distributions for observer sampling from MO, time step 1, female.

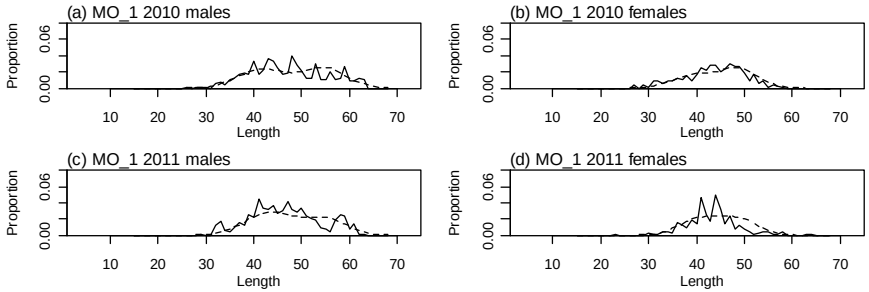

A8. 23: Observed (solid line) and fitted (dashed line) length frequency distributions for trawl survey samples from MO.

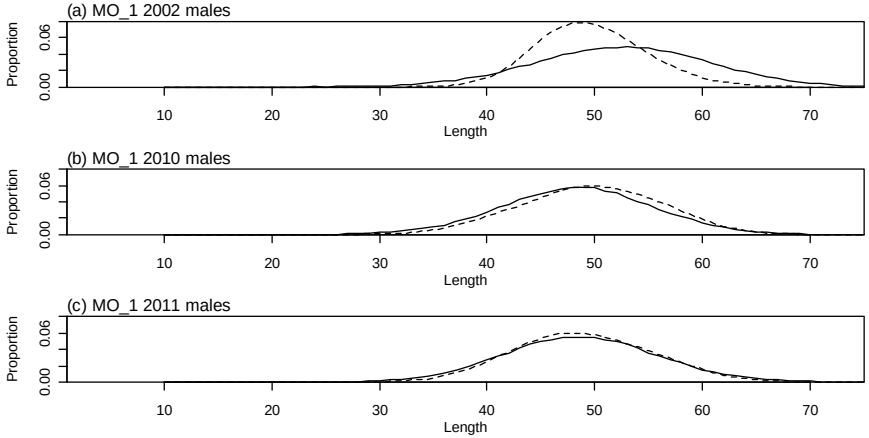

A8. 24: Observed (solid line) and fitted (dashed line) length frequency distributions for photo survey samples from MO.

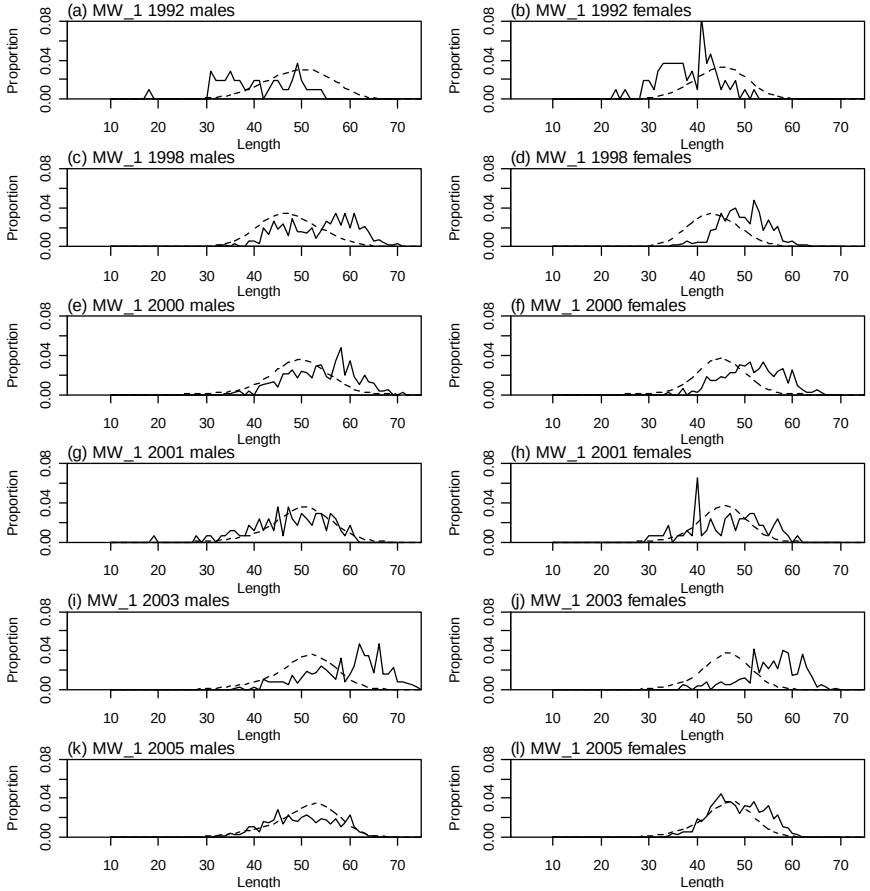

A8. 25: Observed (solid line) and fitted (dashed line) length frequency distributions for observer samples from MW, time step 1 (1992–2005).

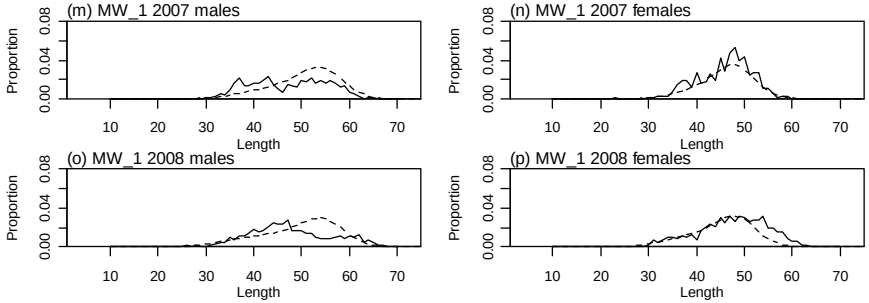

A8. 26: Observed (solid line) and fitted (dashed line) length frequency distributions for observer samples from MW, time step 1 (2007–2008).

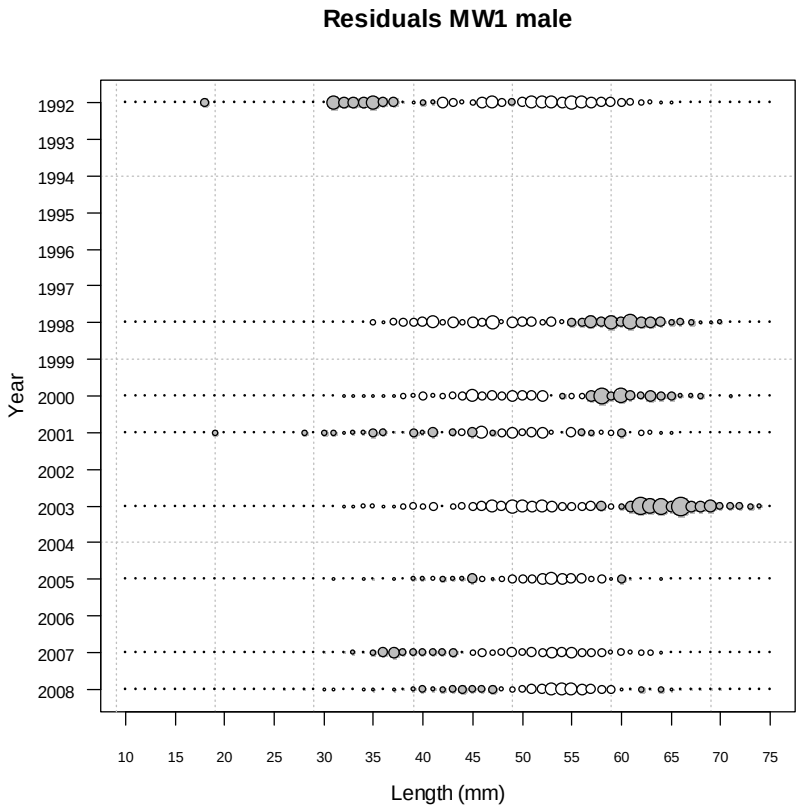

A8. 27: Bubble plots of residuals for fits to length frequency distributions for observer sampling from MW, time step 1, male.

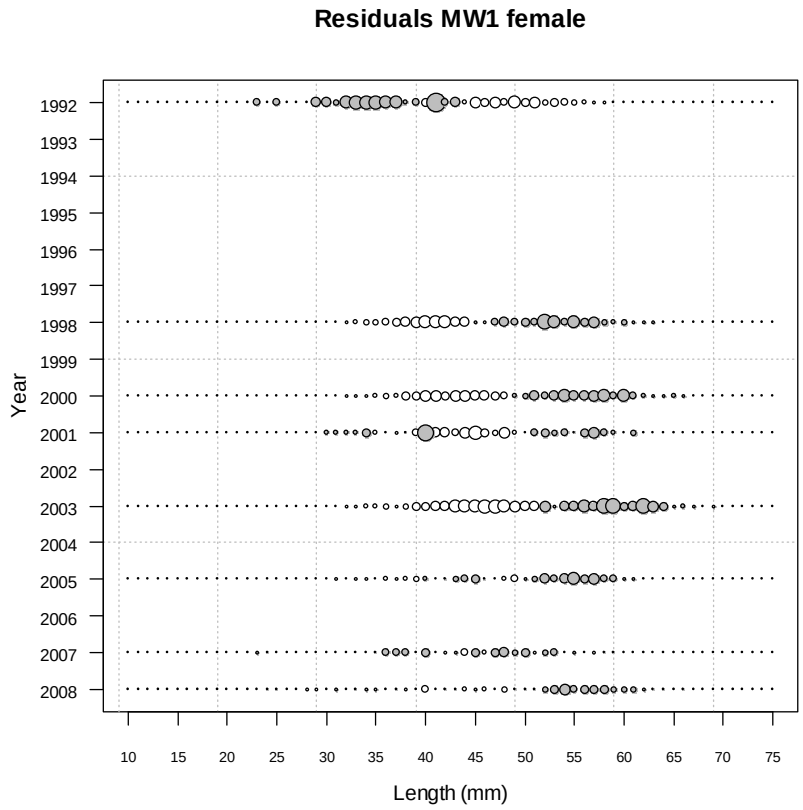

A8. 28: Bubble plots of residuals for fits to length frequency distributions for observer sampling from MW, time step 1, female.

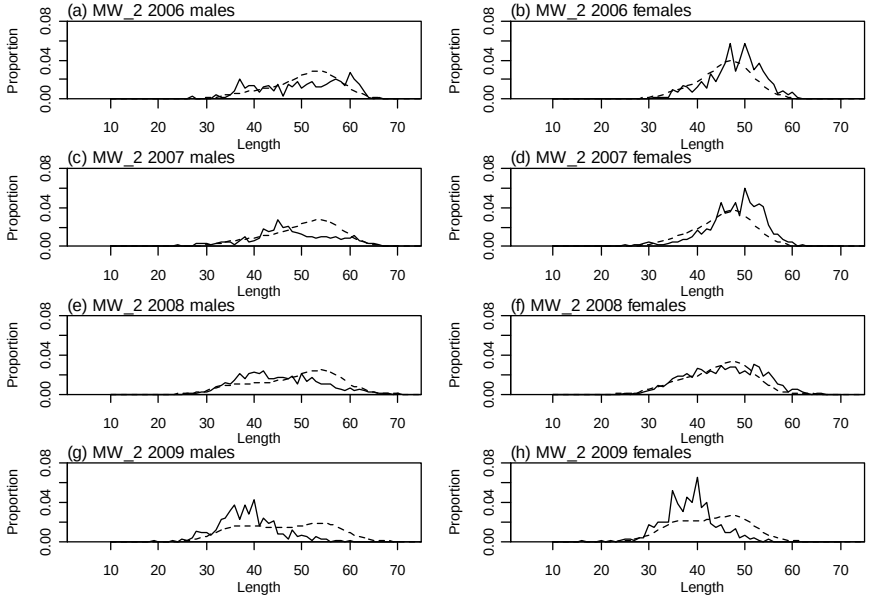

A8. 29: Observed (solid line) and fitted (dashed line) length frequency distributions for observer samples from MW, time step 2.

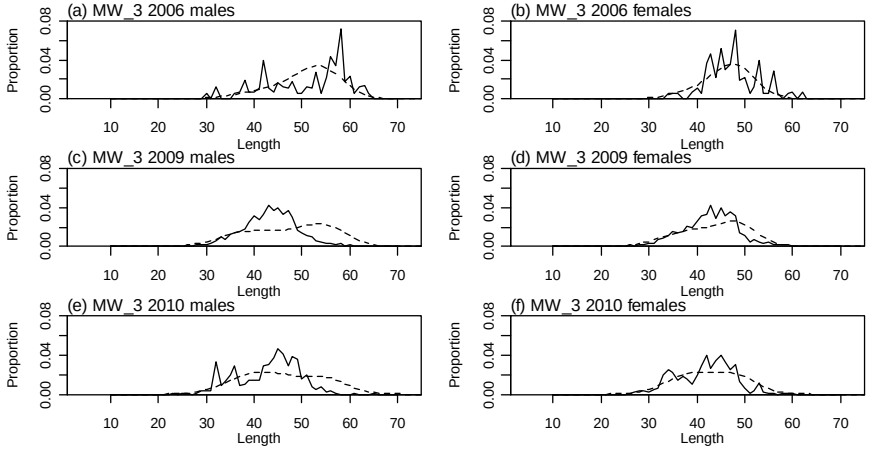

A8. 30: Observed (solid line) and fitted (dashed line) length frequency distributions for observer samples from MW, time step 3.

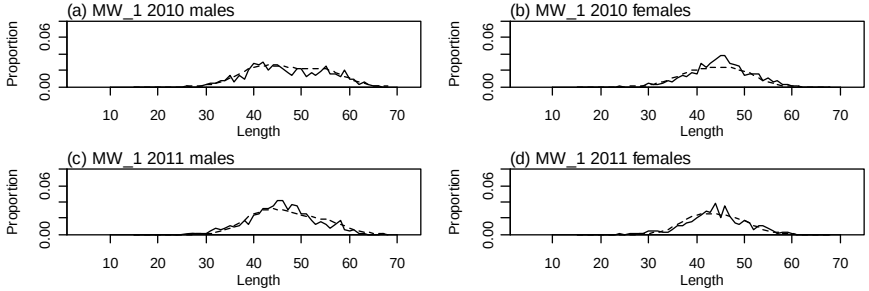

A8. 31: Observed (solid line) and fitted (dashed line) length frequency distributions for trawl survey samples from MW.

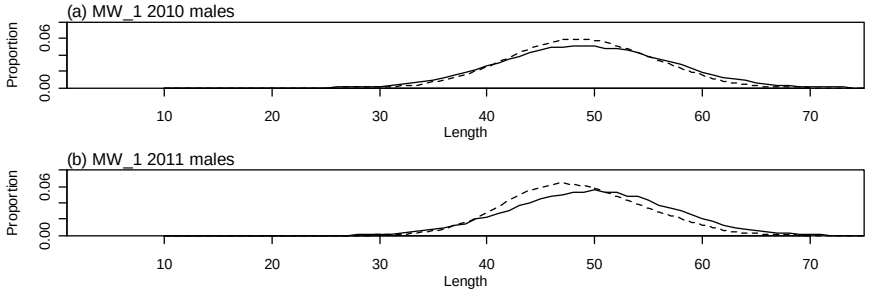

A8. 32: Observed (solid line) and fitted (dashed line) length frequency distributions for photo survey samples from MW.

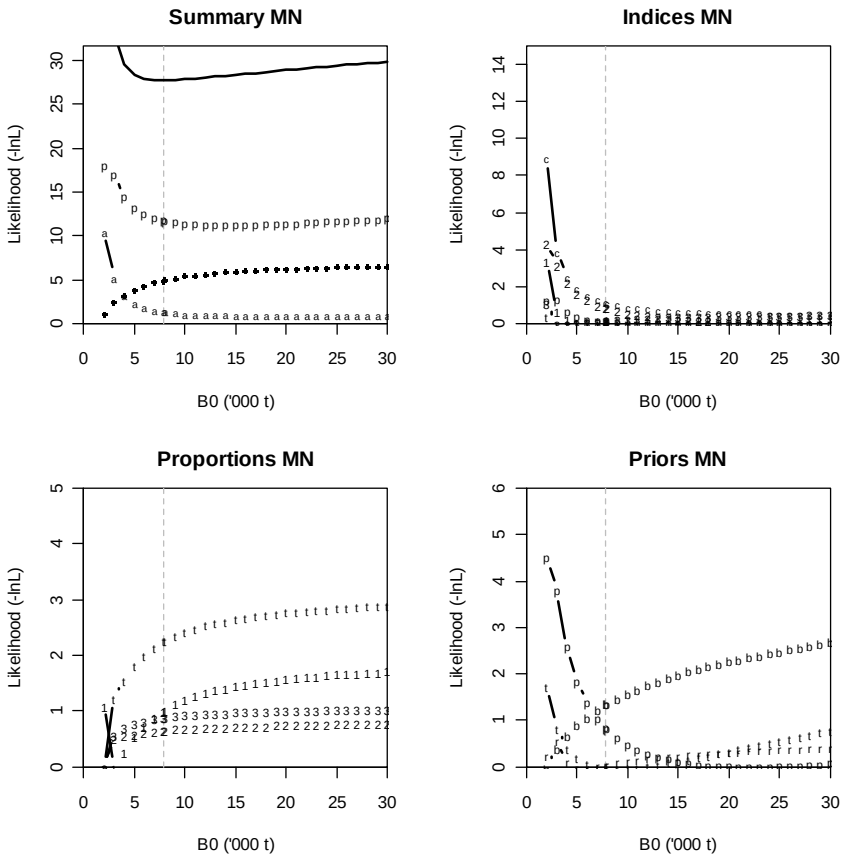

A8. 33: Likelihood profiles for model 1 when MN B_0 is fixed in the model. Figures show profiles for main priors (top left, p-priors, a – abundance indices, • – proportions at length), abundance indices (top right, t - trawl survey, 1 - CPUE time step 1, 2 - CPUE time step 2, 3 - CPUE time step 3, p – photo survey), proportion at length data (bottom left, t-trawl, 1 – observer time step 1, 2 – observer time step 2, 3 – observer time step 3) and priors (bottom right, b- B_0, YCS - r, p- *q-Photo*, t – *q-Trawl*).

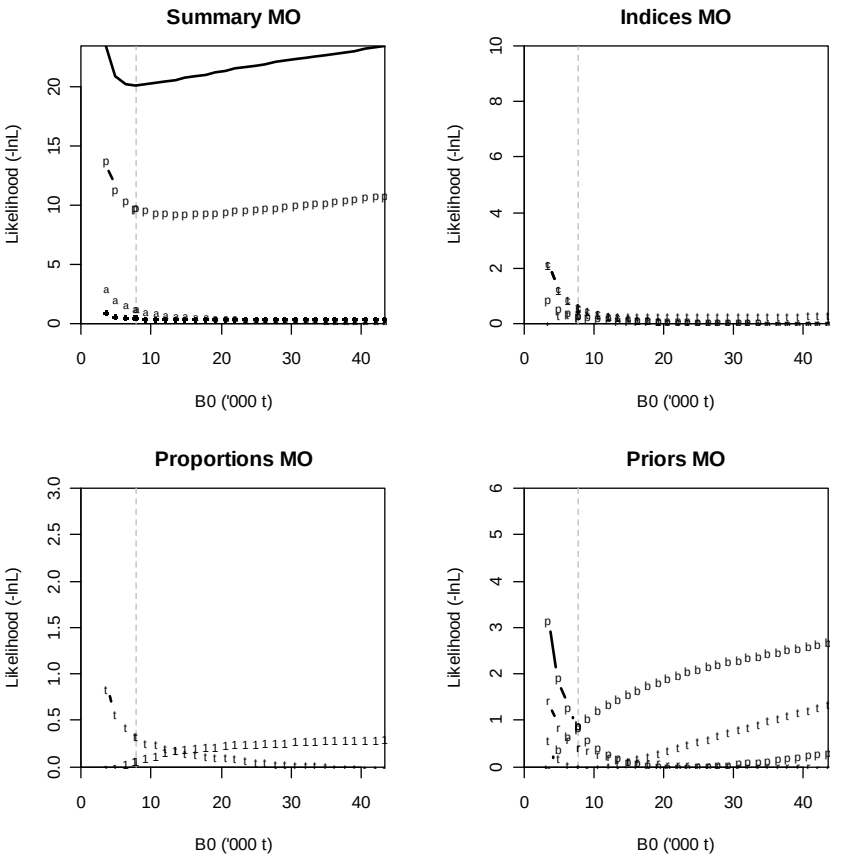

A8. 34: Likelihood profiles for model 1 when MO B_0 is fixed in the model. Figures show profiles for main priors (top left, p-priors, a – abundance indices, • – proportions at length), abundance indices (top right, t - trawl survey, 1 - CPUE time step 1, 2 - CPUE time step 2, 3 - CPUE time step 3, p – photo survey), proportion at length data (bottom left, t-trawl, 1 – observer time step 1, 2 – observer time step 2, 3 – observer time step 3) and priors (bottom right, b- B_0, YCS - r, p- *q-Photo*, t – *q-Trawl*).

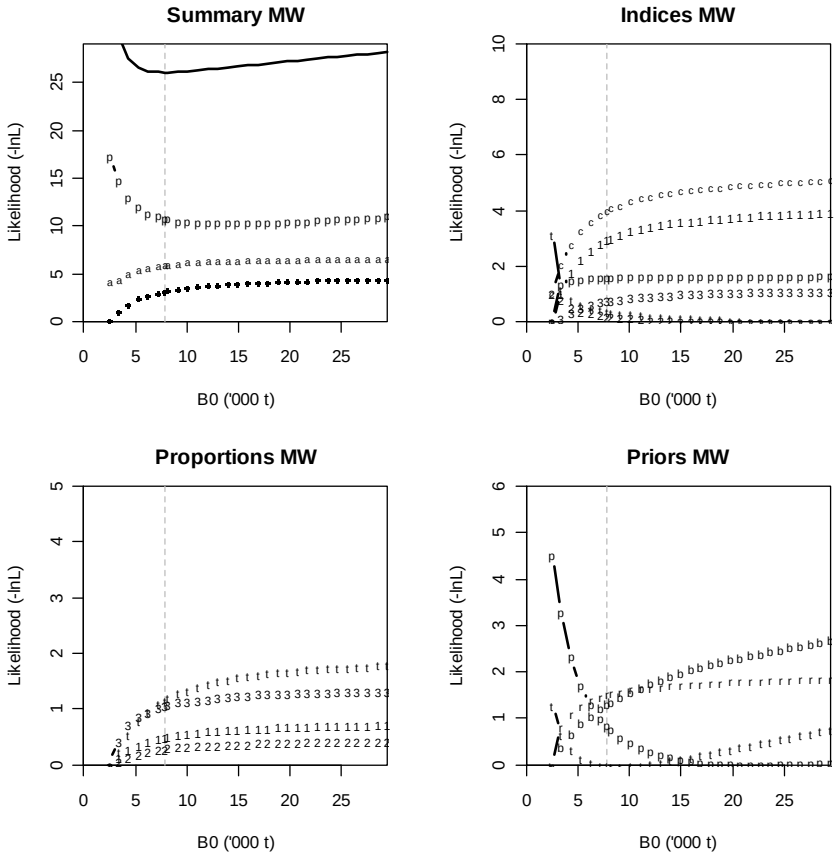

A8. 35: Likelihood profiles for model 1 when MW B_0 is fixed in the model. Figures show profiles for main priors (top left, p-priors, a – abundance indices, • – proportions at length), abundance indices (top right, t - trawl survey, 1 - CPUE time step 1, 2 - CPUE time step 2, 3 - CPUE time step 3, p – photo survey), proportion at length data (bottom left, t-trawl, 1 – observer time step 1, 2 – observer time step 2, 3 – observer time step 3) and priors (bottom right, b- B_0, YCS - r, p- *q-Photo*, t – *q-Trawl*).

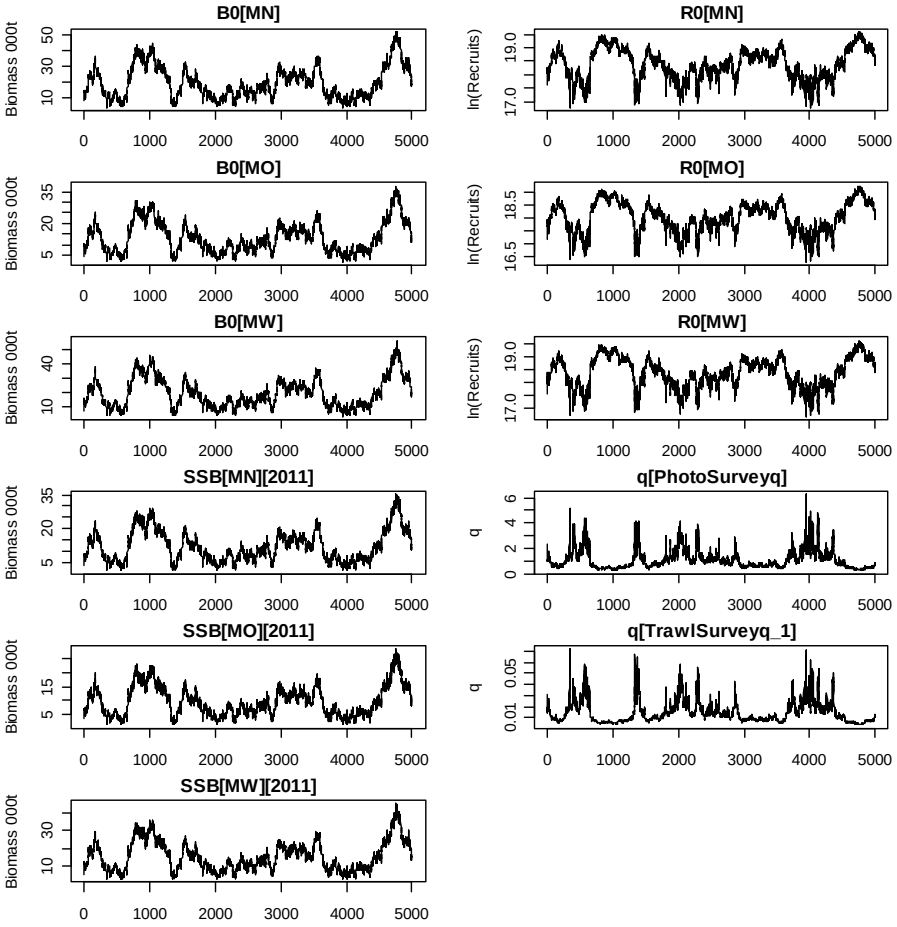

A8. 36: MCMC traces for B_0, SSB_{2011}, R_0 and *q* terms for the BASE-g-est model.